B.8 "Stress Corrosion Cracking of Carbon and Low Alloy Steels," by F. Peter Ford

Introduction

This background paper covers stress corrosion cracking of ductile carbon and low alloy steel components and their associated weldments. Stress corrosion cracking is part of a spectrum of failure mechanisms, including strain–induced cracking (SIC)[1] and corrosion fatigue. This background paper includes SIC. The topics of corrosion fatigue and stress corrosion cracking of higher strength steels used as bolting, for instance, are discussed in other background reports.

These ductile structural materials are used as pressure boundary materials in pressure vessels and piping in the RCS, ECCS, secondary water and service water systems of LWRs. The reasons for their use in LWRs are their combination of relatively low cost, good mechanical properties in thick sections and good weldability.

In components of the RCS, such as the pressure vessel, pressurizer and some piping, the carbon and low alloy steels are clad on the inside wetted surface with corrosion resistant materials such as austenitic stainless steels or nickel-base alloys. Thicker pads of alloy 182 have also been welded directly onto the pressure vessel steel in order to act as attachment points for internal structures. The higher yield strength of Alloy 182, its thicker section and its known SCC susceptibility raise special concerns for stress corrosion cracking of the underlying low alloy steel since it is possible that stress corrosion cracking or thermal fatigue of the austenitic alloy can occur such that the crack tip propagates to the interface between the austenitic and ferritic alloys. The practical questions in this case are "Will this crack propagate further into the underlying low alloy pressure vessel steel under constant load conditions?," and "What is the crack propagation rate vs. stress intensity factor (V/K) disposition relationship relevant to the material, stress and environment conditions?"

In cases where the ferritic steels are not clad, the relevant question is "Will a stress corrosion crack initiate (at, for instance, a pit), coalesce with nearby microcracks to form a primary crack, and then propagate to a significant depth?"

In general the resistance of the ferritic materials to transgranular stress corrosion cracking in LWR circuits has been very good, but isolated incidences have occurred. In order to understand the details of these observations, the mechanism of cracking and the associated corrosion system dependencies are discussed in order to (a) put this plant experience in the context of the conjoint conditions of environment, material and stress required to initiate and sustain cracking and (b) to define the predictive capabilities that are necessary in order to identify future areas of concern.

Mechanistic Understanding and Corrosion System Dependencies Governing Stress Corrosion Cracking of Carbon and Low Alloy Steels in LWRs

For a high-aspect ratio crack to advance in aqueous environments it is necessary that a mechanism exists to accelerate and focus the degradation at the strained crack tip. This degradation is generally related to localized oxidation processes at the crack tip, although historically there have been arguments that the degradation may be primarily associated with the production of hydrogen at the crack tip (which is, in turn, related to the crack tip corrosion rate) and its subsequent interaction with the microscopic deformation processes taking place there. There is a further factor, however, and that is that the crack sides must be protected by a film (oxide, salt, etc). If this latter criterion is not met then the incipient crack will degrade to a blunt notch [2-6]. Such requirements for a mechanically driven "electrochemical knife" [2] greatly limit the environmental conditions under which severe susceptibility is possible, and they provide a predictive capability for identifying the potential / pH regions where danger situations may occur in practice. For instance, cracking of carbon and low alloy steels in lower temperature aqueous environments (i.e. below 150°C) that might be representative of LWR service water or ECCS systems under faulted water chemistry conditions, is confined to potential / pH regions where a soluble species (Fe^{2+}, $HFeO_2^-$) can form when a protective magnetite, mixed oxide or salt film in hydroxide, nitrate, carbonate /bicarbonate or phosphate-containing solutions is ruptured. A relatively concentrated anionic solution is required for subsequent crack propagation to be significant under these conditions, thereby requiring precursor conditions of, for instance, crevice corrosion or localized boiling to create these high anionic activities. Thus the fact that there are these limiting criteria, indicate why transgranular stress corrosion cracking of carbon and low alloy steels in lower temperature LWR components are relatively rare. However, it should be noted that, in recent years, SCC has been observed in dilute solutions of molybdates and nitrites and in oxygenated water where the metal is cold worked in the 15-20% range or higher, and the temperature is in the range of 90-150°F and higher. As discussed below in relation to service experience, such failures have been observed in tertiary systems of nuclear plants.

In higher temperature PWR primary circuits, the oxide is protective magnetite (Fe_3O_4) but, as will be discussed below, the kinetics of crack propagation at static load of the carbon and low alloy steels under these low potential conditions will generally be low and of little practical importance. Under relatively high purity "normal water chemistry," (oxidizing), BWR water conditions the surface oxide at low temperature is less protective, and any incipient crack degrades to a non-propagating pit [5]. However at temperatures above approximately 150°C a highly protective, duplex oxide film of magnetite/hematite forms and allows the existence of a sharp crack, the propagation of which will depend on a variety of material, stress and environment conditions discussed below.

A considerable amount of attention has been focused internationally on the mechanism and kinetics of crack propagation in the carbon and low alloy steels used in, especially BWR, systems under at-power temperature and coolant chemistry conditions. Unfortunately there is a wide scatter in the stress corrosion crack propagation rate data (Figure B.8.1) [7,8], which poses a practical problem to the design or operational engineer who requires a specific life prediction or crack disposition algorithm (i.e. crack propagation rate (V) vs. stress intensity factor (K) relationship) that is technically sound and relevant to his particular plant.

The reason for the scatter in the stress corrosion data in Figure B.8.1 is associated with the fact that the crack propagation rate is controlled by interactions between various system parameters that are not always well defined or controlled in the plant or laboratory experiments. These factors include:

- Stress intensity and mode of stressing e.g., constant load, constant displacement, loading rate, periodic unloading etc.
- Test temperature
- MnS inclusion morphology and dispersion with respect to the crack plane
- Dissolved oxygen content (or, more accurately, corrosion potential as controlled by the coolant flow rate, alloy surface composition, dissolved hydrogen in the coolant, and oxidants such as oxygen, hydrogen peroxide, cupric cations, etc.)
- Solution flow rate past the crack mouth (or, more specifically, the extent to which hydrodynamic conditions permit flushing out of the internal crack environment)
- Solution conductivity (or, more accurately, anionic activity)
- Extent of crack tip constraint, i.e. plane stress vs. plane strain
- Yield stress of the material
- Testing time (and sequence of loading changes made during the test)

As a result there has evolved in the testing community a set of "quality control" criteria that can be applied to a given data set to assess their relevance to the conditions in operating Light Water Reactors. [8]

Coincident with these quality control actions, there has been a considerable international effort [7, 9-13] to develop a quantitative understanding of the mechanism of cracking, with the purpose of providing a sound basis for predicting and managing the cracking under the diverse corrosion system parameters listed above.

The hypothesis that has been most widely accepted for crack propagation in the carbon and low alloy steel /LWR water systems is the slip–oxidation mechanism. This mechanism relates crack advance to the enhanced oxidation rate that occurs at the crack tip when the thermodynamically stable and protective oxide film is ruptured by a strain increment in the underlying metal matrix. Once the protective oxide is ruptured, the crack will rapidly advance into the metal but will, within a matter of milliseconds, begin to slow down as the thermodynamically stable and protective oxide reforms at the crack tip. Continued crack advance depends, therefore, on maintaining a strain rate in the low alloy steel in the vicinity of the crack tip that will allow repeated rupture of the oxide film.

Thus the crack propagation rate, V, is governed by a relationship of the general form;

$$V = A\,(d\varepsilon/dt)_{ct}^{\ n} \qquad (1)$$

where the parameters A and n are related to the dissolution and passivation kinetics at the strained crack tip [11], and $(d\varepsilon/dt)_{ct}$ is the crack tip strain rate, which may be formulated in terms of "engineering parameters" such as stress, stress intensity, stress amplitude, loading frequency, etc. [11,12].

Both the dissolution and passivation kinetics on a bare low alloy steel surface depend critically on potential and the anionic activity in the crack tip environment [9,11,14] and these kinetics are bounded asymptotically by two limiting conditions associated [15] with the maintenance of either <20 ppb or >0.5 ppm S^{2-}. (Note that earlier investigations focussed primarily on the deleterious effect of sulfur-rich anions; more recent investigations indicate that chloride anions will also affect the crack propagation rate). This, in turn, leads to a predicted range in V vs.$(d\varepsilon/dt)_{ct}$ responses which are bounded by the "high" and "low" sulfur lines;

"High Sulfur" $V = 2.25 \times 10^{-3}\,(d\varepsilon/dt)_{ct}^{\ 0.35}$ $mm.s^{-1}$ (2)

"Low Sulfur" $V = 10^{-1}\,(d\varepsilon/dt)_{ct}^{\ 1.0}$ $mm.s^{-1}$ (3)

As can be seen in Figure B.8.2 the theoretical bounding crack propagation rates described by Eqn. 2 are not maintainable at the lower $(d\varepsilon/dt)_{ct}$ values, which are pertinent to creep rates under constant load or displacement conditions. The divergence from the maximum theoretical rates for these dissolved sulfur concentrations depends on the dissolved oxygen content and flow rate of the water. One reason for these divergences relates to the origin of the dissolved sulfur and other anions at the crack tip which can control the crack tip oxidation rate. As illustrated schematically in Figure B.8.3, the crack tip concentration of anions that originated in the bulk environment will be governed by the anionic concentration in the bulk environment and the mass transport mechanisms governed by convection, Fickian (i.e. concentration gradient) and potential gradient considerations within the crack. However, the concentration of sulfur-rich anions will be controlled not only by these specific mass transport mechanisms, but also by the rate of introduction of dissolvable MnS precipitates to the crack tip solution as the advancing crack tip exposes them to the crack tip solution. Thus it is predicted and observed that the crack propagation rate will be a sensitive function of, for example, the corrosion potential (Figure B.8.4), flow rate of the water past the crack mouth, the bulk anion concentration and, finally, the MnS size, shape and distribution. If the crack propagation rate falls below a critical value, such that a dissolved sulfur activity >0.5ppm S^{2-} cannot be maintained, then crack arrest may well occur, especially under the high water flow rate conditions expected in many plant conditions which tends to "flush" the aggressive anions out of short cracks, or in high purity water where there are no other non-OH anionic purities present.

The achievement and maintenance of crack propagation rates associated with the "high sulfur" rates depends not only on the maintenance of a high crack tip sulfur activity but also on the maintenance of a sustainable crack tip strain rate. The conjoint engineering system conditions that will achieve all these criteria will be met by combinations of:

- High sulfur content steels, mainly in the form of elongated MnS inclusions
- High corrosion potentials
- Stagnant or low flow rate water
- Highly impure water conditions, primarily chloride
- Unconstrained plane stress crack tip conditions

It is interesting therefore to note that the extremely high propagation rates that have been recorded by some laboratories [17-21] where combinations of the above system criteria have been met, are in agreement with the predicted "high-sulfur" rates (Figure B.8.1).

$$V = 9.6 \times 10^{-8} K^{1.4} \quad mm.s^{-1} \tag{4}$$

with K in units of MPa$\sqrt{m}$

These "worst case" combinations of conditions do not exist generally in operating LWRs. For PWRs (and for the majority of the pressure vessel of BWRs on hydrogen water chemistry or Noblechem^{TM}) the low corrosion potential effectively preclude stress corrosion crack growth at rates that could be of any engineering significance. Under conditions more symptomatic of BWRs operating under "normal water chemistry" the crack propagation rates are generally below the "low sulfur" line; i.e.

$$V = 3.29 \times 10^{-14} K^{4} \quad mm.s^{-1} \tag{5}$$

with K in units of MPa$\sqrt{m}$

The comparisons between observation and theory in this latter case are shown in Figure B.8.5 for an older data base [9] where a variety of loading conditions have been applied and in Figure B.8.6 [8] for a constant load data set from one laboratory [21-23] that has been screened for data quality. In these cases it is seen that, in general, the "low sulfur" line bounds the data sets, except at high stress intensity factors (a point that is addressed later).

It should be emphasized that the "low sulfur" propagation rates defined by Eqn. 5 are limiting values and the reason for this is that, in addition to maintaining a given dissolved sulfur activity at the crack tip, it is also necessary to maintain the crack tip strain rate. As discussed elsewhere [11, 12, 25-27], the formulation of the crack tip strain rate in terms of engineering parameters (stress intensity, yield stress, etc) has been the source of much international debate, which is still not finally resolved. However certain over-riding concepts are understood and accepted, and it is expected that, under constant load or displacement conditions, the crack tip strain rate will decrease according to a logarithmic creep relation of the general form;

$$(d\varepsilon/dt)_{ct} = B.(C\sigma^{m}).\ t^{-1} \tag{6}$$

where σ is the tensile stress

Thus, there are two phenomena that indicate that the stress corrosion cracks may arrest under certain system conditions; the first is due to the lack of maintenance of a critical dissolved sulfur content at the crack tip, referred to earlier, and the second is the lack of

maintenance of the crack tip strain rate under constant load. In fact [27-29], crack arrest is frequently observed (Figure B.8.7) [27] and, as analyzed by Laepple [29], the crack propagation rate decelerates by approximately the predicted t^{-1} relationship in high purity BWR environments

Taking into account that there is an observed and understood tendency for crack arrest under closely controlled water chemistry purity (with no significant transients) and constant load conditions, the engineering judgment [30-33] is that, for disposition purposes, the average crack propagation under full power operations is given by;

$$V \leq 2 \times 10^{-8} \quad mm.s^{-1} \qquad (7)$$

up to a stress intensity factor of 55 MPa$\sqrt{m}$. Above this K_1 level, but also below it (Figure B.8.8) in the case of either water chemistry transients or slight load variations, the low sulfur line of Eqn. 5 is considered more appropriate. It is also relevant to point out that the limiting nature of Eqn. 7 also applies (under the stated stressing and environmental purity conditions) to irradiated material and environmental conditions [23].

It should be emphasized that, although crack arrest is both predicted and observed, this may be counteracted by other material/environment/stressing factors and, thereby, may challenge the appropriateness of the disposition relations in Eqn. 5 and 7 when the strict water chemistry and loading caveats associated with these equations are violated [32]. Such factors may be categorized as those that increase the effective crack tip strain rate and/or markedly increase the crack tip anionic impurity concentration.

Examples of the effect of "inadvertent" increases in effective crack tip strain rate leading to increases in the crack propagation rate values in excess of those calculated by Eqn. 5 and 7 include;

- *Enhanced crack tip plasticity due to a loss of plastic constraint.* This concern is illustrated in Figures B.8.6 and 8 by the increase in crack propagation at stress intensity values beyond that where plane strain constraint to the crack tip plasticity is largely overcome. For the usual 25mmT fracture mechanics laboratory specimens this limit is defined as K values > 55 MPa$\sqrt{m}$. [22,23,24,28]. In large section pressure vessel components it is unlikely that this plane strain related criterion would be exceeded, but it may be a factor to be considered in thin section components.

- *Yield stress and dynamic strain aging.* Major increases in yield strength or hardness and/or in the degree of dynamic strain aging may increase the crack propagation rate of low alloy steels. The former effect has long been noted in the field of stress corrosion. As indicated in Figure B.8.9, the hardness effect on cracking susceptibility under constant load in oxygenated water is relatively minor over the hardness range associated with LWR pressure vessel steels, but a significant increase in susceptibility is observed should the heat treatment be such as to produce a (hard) martensitic microstructure [34]. On the other hand the effect of discontinuous yielding at a crack tip, which effectively increases the crack tip strain rate, and thereby the stress corrosion susceptibility, has been demonstrated in a variety of other cracking systems. The possibility of dynamic strain aging (DSA) having such an accelerating effect on the cracking of low alloy steels in LWR systems has been demonstrated by a number of investigators [34-39]. This opens

39]. This opens up the question of the definition of the allowable compositional limits for the low alloy steel, (mainly aluminum and nitrogen), and the resultant temperature ranges where the increase in cracking susceptibility is most marked. This latter aspect is of particular importance with respect to evaluating the susceptibility of, for example, feedwater piping which may operate in the temperature range 220-250^{0}C rather than at 288^{0}C where the majority of investigations have been focused. The cracking susceptibility can maximize in this lower temperature region under cyclic, monotonically increasing strain as well as static loading conditions. Historically this peak in the susceptibility has been attributed to a balance between the expected thermal activation of the corrosion processes fundamental to the crack propagation mechanism, and the changes in corrosion potential with temperature, especially at dissolved oxygen contents in the water less than 400ppb. This added contribution due to DSA is not yet fully evaluated

- *Transient or "ripple loading"* It has long been recognized that small repeated transients in loading (e.g. "ripple loading") can accelerate crack propagation due to the Bauschinger effect that leads to enhanced plasticity at the crack tip. This is illustrated in Figure B.8.10 for laboratory tests on low alloy steels in high temperature water involving high R (ratio of minimum stress intensity to maximum stress intensity) loading [34]

As emphasized earlier, the crack tip chemistry is of vital importance in defining the cracking susceptibility, and this impacts on the required degree of water purity control during steady state operation, and the control of the magnitude and duration of water chemistry transients. Of particular importance is the extent of chloride transients since, as illustrated in Figure B.8.11, chloride transients, in marked comparison with sulfate transients, may give extremely high sustainable crack growth rates approaching the theoretical maximum values defined by Eqn. 4; it should be noted that although the chloride transient (to 49 ppb) illustrated in Figure B.8.11 would be excessive for current BWR operating conditions and would have triggered an orderly plant shut down action, lower level transients (to10 ppb) also lead to significantly increased crack propagation rates [32].

Service History

In the 1970's there were numerous occurrences of *intergranular* stress corrosion cracking of low alloy NiCrMoV steels in steam turbine wheels (or discs) and, to a lesser extent turbine rotors. The specific cracking locations were primarily regions of high stress (due to wheel/disc shrink-on and centrifugal stresses) and creviced regions such as keyways or blade attachment where stress localization and contaminant concentration was possible. Initially these cracking incidents were primarily in fossil fired plant in low pressure turbine stages where steam condensation was possible and high alkalinity concentration could be attained due to the boiler water chemistries employed. However, since the mid to late 1970s cracking has been noted in lower temperature PWR and BWR driven turbines. These incidents have been widely reported and discussed [40-43]. It is significant, however, that many of the mechanisms-based concepts discussed earlier in this background report are of relevance. For instance, these concepts explain the narrow potential range for cracking associated with caustic cracking and the aggravating role vis à vis cracking susceptibility of contaminants such as chloride, sulfide (from lubricant), the presence of dissolved oxygen or other oxidants (e.g. Cu^{2+}), increased surface hardness due to abusive reaming of keyways and, finally, high yield strength associated with the bainitic or martensitic structures. Thus these earlier steam turbine experiences act as an historical guide to understanding service failures in the LWR systems of interest in this topical report that occurred in the late 1970s and early 1980s.

The accumulated operating experience and performance of the ductile carbon and low alloy steels in the majority of LWR systems has been very good worldwide and this is likely to continue. The reason for this optimistic statement is that the primary system in PWRs operates at low corrosion potentials because of the hydrogen overpressure, and the same observation applies to the vast majority of BWRs (in the US) that are currently operating under hydrogen water chemistry and/or noble metal addition (e.g., "NobleChem™") conditions; these factors ensure that there is a considerable margin in corrosion potential (see Figure B.8.4) before transgranular cracking would be expected.

There is cause for concern, however, in the PWR secondary systems for although they also operate at low corrosion potential (which is very strictly applied because of concerns that a more oxidizing potential will aggravate corrosion problems with Alloy 600 steam generator tube bundles), there is a higher risk of oxidizing corrosion potentials in the event of persistent leaks at interfaces with the environment, particularly in the condenser. There are also concerns for BWRs not consistently on hydrogen water chemistry, since cracking may be possible under more oxidizing conditions, especially if there are other aggravating factors. Indeed there have been two relatively major classes of cracking incidents of unclad carbon or low alloy steel components in operating LWRs that illustrate these concerns; cracking of carbon steel BWR feedwater piping due to strain-induced cracking, and cracking of PWR steam generator girth welds due primarily to water chemistry transients. These are discussed below in order to lay the basis for the next section that evaluates the potential erosion of margins due to evolving fabrication (or repair) and operational practices.

Strain-Induced Cracking of Steam, Feedwater and Condensate Piping

The cracking of steam, feedwater and condensate piping systems due to strain-induced stress corrosion has been extensively analyzed [1, 44-46] for German BWRs where these components have been fabricated with relatively fine-grained, higher-strength

steels (WB 35, WB36) that allow the use of thinner walled piping without stress relief treatment of the welds. The features that aggravated the cracking susceptibility in these incidents were;

- *Dynamic straining* associated with, for instance, reactor start-up or thermal stratification during low feedwater flow or hot standby conditions. Such operations lead to a wide range of applied strain rates [47] that may be as high as 10^{-4} s^{-1}, and would be expected to increase the crack propagation rate (see Figure B.8.2).
- *High local stress* at or above the high temperature yield stress, thereby giving a lack of plastic constraint at the incipient crack tip, and consequently an anomalous increase in crack propagation rate (see Figures B.8.6 and 8) due to the effective increase in crack tip strain rate. Such high local stresses were attributed in the failure analyses to weld defects (e.g. misalignment of weld edges, presence of root notches, etc), piping fit-up stresses and, in some cases inadequate pipe support at elbows. The combination of this high stress adjacent to the weld and the high applied strain rate led to a distribution of multiple cracks around the circumference of the pipe that was no longer confined by the asymmetric azimuthal distribution of weld residual stresses. These cracks propagated on separate planes and did not interlink, thereby potentially alleviating concerns about "leak before break" safety analyses that would be raised for a fully circumferential crack propagating evenly through the pipe wall.
- *Oxidizing* conditions, in conjunction with intermediate temperatures and potential anionic impurities. The affected piping generally operates in the temperature region 220^{0}C -250^{0}C where, as discussed earlier, the cracking susceptibility is at a maximum. Moreover, cracking was often observed in stagnant steam lines where. the dissolved oxygen concentration may be in excess of 100ppb, that is well in excess of the 30ppb quoted to be the "threshold" value above which strain-induced cracking is to be expected in these steels at 250^{0}C [48]; note that, as with the majority of EAC phenomena, the quotation of a firm "threshold" parameter (stress/strain rate, corrosion potential, anionic activity, temperature, etc.) is open to discussion, since the value defined will depend on the other relevant corrosion system parameters. This conjunction of environmental factors was further aggravated by the fact that during reactor shut-down stagnant water was sometimes left exposed to air in horizontal portions of piping; pitting and general corrosion occurred under these low temperature conditions, and these pits were observed to act as crack initiators during subsequent power operation conditions.

Stress Corrosion Cracking of Steam Generator Girth Welds

Very similar aggravating factors have been observed in transgranular cracking incidents in Model 44 and 51 designs of Westinghouse steam generators, starting with an isolated occurrence in Europe which was followed in 1982 with a well analyzed cracking incident at the Indian Point-3 PWR after approximately three effective full–power years. This cracking occurred at the upper shell to cone girth weld and was extensive with over a hundred circumferential cracks propagating to a maximum of 25mm. The cracking was attributed primarily to stress corrosion cracking with a component due to fatigue [49]. Similar incidents were subsequently observed at other US and European PWRs plants [50].

As with the case with the strain–induced cracking cases discussed above for the higher strength steels in German BWRs, the cracking in the PWR steam generator manufactured with lower strength SA 302 grade B weldments and SA 533 grade B plate steels, was aggravated by the fact that the weld was subjected to significant dynamic thermal stresses, in this case due to the fact that the incoming feedwater at 204-227^{0}C was impacting on the hotter steam generator shell before mixing with the steam generator recirculating water. Moreover in the affected plants this particular weld was the final closure weld, with a localized stress relief being applied; subsequent hardness measurements indicated that this stress relief had not been fully effective. Finally, with respect to the stress/strain rate conditions, there had been extensive weld repairs applied at Indian Point-3, an operation which has been widely associated with premature cracking in, for instance, nickel-base alloys in PWR primary components due to the attendant weld residual stresses.

Start-up operations in many of the cracking cases for this component involved the introduction of auxiliary feedwater from the condensate storage tank (CST) into the steam generator; unfortunately this water was aerated, since a nitrogen blanket was not applied to the CST. This deleterious oxidizing condition (Figure B.8.4) was exacerbated by the presence of Cu^{2+} associated with corrosion of the brass condenser tubes. Such oxidizing conditions promoted pitting, which, in turn acted as initiation sites for the stress corrosion cracks and poor chemistry control may also have increased the crack propagation rate.

Thus the unusual circumstances behind the cracking in these incidents were the conjoint presence of oxidizing secondary water conditions, high residual stress with a component of dynamic straining and a strong indication of high hardness due to inadequate stress relief.

Stress Corrosion Cracking in Tertiary Systems

Certain tertiary systems, which are fabricated of carbon steel such as the component cooling water system, have sustained SCC in the range of 90-150°F within times in the range of 5-10 years. Such SCC has perforated the walls especially at the higher range of temperature. These systems sustain such SCC in normal aerated chemistry with various inhibitive additives, within their nominal concentrations, such as molybdate and nitrite. Such SCC occurs where residual stresses are high due to fabrication, i.e. elbows, or at welds.

Observations of SCC in carbon steel in oxygenated water in this low range of temperature have been observed at least in six plants. However, these systems are not extensively inspected. Also, there are possibly ten different water chemistry treatment programs among the world utilities. There may be some interaction with MIC in some cases, but SCC can occur without the MIC and MIC does not always occur.

Other Cases

There have been other reported incidences of environmentally-assisted-cracking of carbon and low alloy steel in, especially, BWRs. The most significant of these have been cracks at nozzles associated with mixing of lower temperature water with hot water in a vessel, i.e., thermal fatigue cracks in BWR reactor vessel feedwater nozzles and control rod drive return line nozzles [51-55]. Although a component of SIC or stress corrosion cracking might be appropriate, it is apparent that the dominating degradation mechanism in these cases was corrosion fatigue, and discussion of these incidents is given in the fatigue background report.

Other potential cracking incidents have been reported but have been either isolated in occurrence or inadequately analyzed to allow a positive attribution to stress corrosion cracking. For instance, a through-wall crack developed in the low alloy steel wall of an early BWR (Garigliano) secondary steam generator channel head. The crack appeared to have grown due to SCC and was attributed to the presence of cracks in the Alloy 400 type cladding (Alloy 190 weld metal) that acted as initiating sites for the SCC in the base material, combined with high residual stresses due to an ineffective post weld heat treatment and, possibly, to an unusually high dissolved oxygen content in this unique BWR design.

In addition, a few flaw indications have been detected in vessel base materials by UT performed for baseline or in-service inspections, e.g., due to laminations or inclusions in the steel plates or forgings. The base material flaws have rarely if ever required repair. There appear to be no reported cases of service-induced growth of flaws present in the base plates or forgings. Finally, significant numbers of cracks have developed in the cladding of BWR reactor vessel heads. In some cases, the cracks have penetrated short distances into the low alloy steel base material. This cracking has required significant inspection and analysis to demonstrate the continued safe condition of the affected parts. In a few cases it has been concluded that the cladding cracks may have penetrated into the base material as the result of service, but it appears more likely that such ***penetration occurred during fabrication.***

Concerns Associated with Lack of Predictive Knowledge in Conjunction with Changing Operational Practices

There is no question that our capability to predict the changes in stress corrosion or strain-induced cracking of carbon and low alloy steels in LWRs due to the effects of materials, environment and stressing modes has significantly improved over the last 20 years. Prior to that time we would not have been able to quantitatively rationalize the cracking response of safety-related components and thereby define appropriate remedial actions beyond qualitative judgments to "reduce stress," improve chemistry control," etc. Consequently we understand in some quantitative detail the reasons why it is relatively hard to initiate and propagate stress corrosion cracks in carbon and low alloy steels in LWRs operating under good water chemistry control. We also understand many of the "upset" operating criteria necessary to give cracking, and these are generally met for the few instances where cracking in the plant has been observed.

However the bar is rising as reactors (in the US) apply for license renewal, power uprate, extended fuel cycles (and therefore increased time periods between inspection) and, possibly, limited load following. All of these changes potentially increase the danger of undetected stress corrosion degradation. Items of concern that need research attention in order to reduce that risk for stress corrosion (and strain-induced cracking) of carbon and low alloy steels include:

- A quantification of the sequential actions of pit formation, microcrack initiation and coalescence, followed by "short" and then "long" crack propagation. This sequence is well recognized in carbon and low alloy steels and has been quantified for gas pipelines. Such quantification has not been conducted for the nuclear systems. It is known that cracks may accelerate or arrest during this sequence; the quantification of this is inherent to the prediction of cracking of unclad ferritic piping

- The propagation rates are, in general, reasonably well understood; There are, however, some system parameters that can affect these rates, but which are insufficiently characterized at this time. Until this is done, the industry is open to unforeseen incidents. Prime examples include;

    - Ripple loading. As indicated in Figure B.8.10, ripple loading can significantly increase the crack propagation rate above the current disposition value, but we do not know the full extent (in terms of amplitude and periodicity) of these effects.

    - Dynamic strain aging. This is also a recognized effect, but insufficiently characterized. This has a direct impact on the definition of the maximum temperature for cracking degradation and on the compositional specifications for the steel. This latter aspect is of particular importance since steel manufacturers globally are modifying steel compositions (and in particular Al and N contents) in order to improve toughness together with higher yield stress. It imperative that such mechanical property driven changes also account for potential changes to the EAC resistance.

    - Heat affected zone (HAZ) anomalies. IGSCC in the weld HAZ is well recognized in austenitic alloys for a variety of material and local

stress/strain reasons. There is not a similar understanding of the potential increases in crack propagation rate in the HAZ of carbon and low-alloy steels.

- IGSCC of Carbon and Low Alloy Steels. IGSCC of higher strength bainitic steels used in steam turbines is a recognized phenomenon and has been related to the presence of grain boundary interstitials, which may also give rise to temper embrittlement. IGSCC in carbon and low alloy steels in the LWR systems has not, however, been widely observed, leaving the possibility that there may be unrecognized and potentially kinetically faster degradation modes under very specific operating and material conditions. There has been a recent isolated incidence of such cracking in a CANDU feeder elbow [56] that was associated with higher than normal hardness and residual stress associated with cold bending; flow assisted corrosion was also observed at the (assumed) crack initiation site. Moreover laboratory information [57] indicates that IGSCC is possible in higher hardness HAZs at temperatures < 265°C. It is necessary, therefore, to evaluate this degradation mode with respect to the relevant system variables, with some attention to potential synergisms with flow assisted corrosion and the associated hydrogen production.

References for B.8

[1] J. Hickling, D. Blind, "Strain-induced corrosion cracking of low-alloy steels in LWR systems – Case histories and identification of conditions leading to susceptibility," Nuclear Engineering and Design, 91, pp. 305-330, (1986).

[2] T.R.Beck Corrosion, 30, 408,1974

[3] T.P Hoar "Theory of Stress Corrosion Cracking" Ericiera, Portugal, March 1971, p106, Pub. NATO, Brussels, Ed. J.C.Scully

[4] R.N.Parkins "Stress Corrosion Cracking" in "Environment – Induced Cracking of Metals," Kohler Oct 2-7 1988 pp 1-19, Ed R.P.Gangloff & M.B.Ives. Pub NACE

[5] F.P.Ford in "BWR Environmental Cracking Margins for Carbon Steel Piping" General Electric Report NEDC24625, January 1979

[6] F.P. Ford, "Stress-Corrosion Cracking," chapter in "Corrosion Processes" (Ed. RN Parkins), (Pub. Applied Science Publishers, 1982). ISBN 0-85334-147-8.

[7] F.P. Ford, "Status of Research on Environmentally-Assisted Cracking in LWR Pressure Vessel Steels". Proc. of ASME/PVP Conference, San Diego, CA, June 28-July 2, 1987 (Ed. R. Rungta), ASME PVP119, pp. 43-62.

[8] J. Hickling: "Evaluation of Acceptance Criteria for Data on Environmentally Assisted Cracking in Light Water Reactors" SKI Report 94:14 from September 1994

[9] F.P. Ford, "Environmentally Assisted Cracking of Low Alloy Steels" EPRI/report NP7473L, January 1992, EPRI Contract C102-1.

[10] P.M. Scott, "A Review of Environmental Effects on Pressure Vessel Integrity," Proc. of Third International Symposium on Environmental Degradation of Materials in Nuclear Power Systems/Water Reactors, Traverse City (August 1987).

[11] F.P. Ford, et al., "Corrosion-Assisted Cracking of Stainless and Low-Alloy Steels in LWR Environments" EPRI Contract RP2006-6, Report NP5064M, (February 1987).

[12] F.P. Ford, Trans ASME J. of Pressure Vessel Tech. 110, 2, 113-128, (1989).

[13] F.P. Ford, et al., "Stress Corrosion Cracking of Low Alloy Steels in High Temperature Water "Proceedings of 5th International Environmental Degradation of Materials in Nuclear Power Systems, Monterey, August 1991, p. 561-569.

[14] P. Combrade "Prediction of Environmental Crack Growth in Nuclear Power Plant Components" . Final Report of EPRI Contact RP2006-1 and RP2006-8.

[15] L.Young, P.L.Andresen, "Crack Tip Microsampling and Growth Rate Measurements in a 0.01%S Low Alloy Steel," Proceedings of 7th International Environmental Degradation of Materials in Nuclear Power Systems, Breckenridge, August 1995, p.1193-1204.

[16] R.C. Cowan, et.al. "The ICCGR Interlaboratory Round Robin on Slow Strain Rate SCC of PWR Forging," From Proc. of Second International Atomic Energy Agency Specialists Meeting on Subcritical Crack Growth, Sendai Japan, NUREG CP-0067 (May 15-17, 1985) pp. 181-197.

[17] K. Kussmaul, et. al., Int. J. Pressure Vessels and Piping 25, pp. 111-138 (1986).

[18] M.O. Speidel, R. Magdowski, Intl. J. Pressure Vessels & Piping 34, 119-142, (1988).

[19] E. Tenckhoff, et al., Nuclear Eng.& Design 119, 371-378, 1990.

[20] K. Matocha, et al., "Environmentally-Assisted Cracking of Steam Generator Pressure Vessel Steel in High Temperature Water," Proc. of Third International Atomic Energy Agency Specialists Meeting on Subcritical Crack Growth, Moscow, USSR, (May 1990).

[21] K. Kussmaul, B. Iskluth, "Environmentally assisted crack growth in a low alloy boiler steel in high temperature water containing oxygen" Nucl. Eng. & Design, 119, (1990), 415-430

[22] K. Kussmaul, D. Blind, V. Läpple, "New observations on the crack growth of low alloy nuclear grade ferritic steels under constant active load in oxygenated high-temperature water" Nuclear Eng. and Design, 168 (1997) 53-75.

[23] G. Bruemmer, et al., "Investigation on Environmentally Assisted Cracking Behavior of a Ferritic Reactor Pressure Vessel Steel Under the Simultaneous Influence of Simulated BWR Coolant and Irradiation" Proceedings of 11th Environmental Degradation Conference, Stevenson, August, 2003

[24] V. Läpple, D. Blind, P. Deimel: "Stand der Forschung zum korrosionsgestützte Rißwachstum niedriglegierter ferritischer Stähle in sauerstoffhaltigem Hochtemperaturwasser" VGB-Konferenz "Chemie im Kraftwerk 1996," October, 1996.

[25] R.N. Parkins, G.P. Marsh, J.T. Evans: "Strain Rate Effects in Environment Sensitive Fracture," Proceedings of EPRI Conference on "Predictive Methods for Assessing Corrosion Damage to BWR Piping and PWR Steam Generators," Mt. Fuji, Japan, May/June 1978. Eds. H. Okada and R. Staehle. Pub. NACE (1982).

[26] T Shoji "Progress in Mechanistic Understanding of BWR SCC and Implication to predictions of SCC Growth Behavior in Plants," .Proceedings of Eleventh International Conference on Environmental Degradation in Nuclear Power Systems – Water Reactors, Skamania Lodge August 5-9, 2003. Eds. G. Was, L. Nelson, Published by American Nuclear Society.

[27] J. Heldt, H-P Seifert "The Stress Corrosion Cracking of Reactor Pressure Vessel Steel under BWR Conditions" Proceedings of 9th Environmental Degradation of Materials in Nuclear Power Systems Conference. Newport Beach 1999 pp 901-910

[28] D. Weinstein, et al, "Stress Corrosion Cracking in low alloy steels, Interim Technical Report" GE Nuclear Energy Report on EPRI Contract. No. RP C102-4, dated February 1994

[29] V. Laepple: "Einfluß von Probengeometrie und Belastungsart auf das Bedingungen. korrosionsgestützte Rißwachstum niedriglegierter ferritischer Stähle unter SWR-Zusatzauftrag: Auswertung des EPRI-Forschungsberichtes RPC 102-4 und Vergleich mit Korrosionsergebnissen der MPA Stuttgart" MPA/VGB Forschungsvorhaben 3.1.2.5; MPA Auftrags Nr 944 703 700 February 1997.

[30] R.Pathania et al "Stress Corrosion Cracking in Low Alloy Steels," EPRI Report RPC 102-4, EPRI Palo Alto CA USA February, 1994

[31] "BWR Vessel and Internals Project; Evaluation of Stress Corrosion Cracking in Low Alloy Steel Vessel Materials in the BWR Environment (BWRVIP-60)" March 1999. Submission from EPRI - BWRVIP to USNRC.

[32] F.P.Ford, et al., "Stress Corrosion of Low Alloy Steels under BWR Conditions; Assessment of Crack Growth Rate Algorithms," Proceedings of 9th Environmental Degradation of Materials in Nuclear Power Systems Conference, Newport Beach 1999, pp.855-869.

[33] J.Hickling, H-P. Seifert, S Ritter "Research and Service Experience with Environmentally Assisted Cracking of Low Alloy Steel," Power Plant Chemistry 7(1) pp.4-15, 2005.

[34] H.P.Seifert, S. Ritter "New Observations of the SCC Crack Growth Behaviors of Low-Alloy RPV Steels under BWR/NWC Conditions," Proceedings of 11th Environmental Degradation Conference. Stevenson August 2003, pp 341-350

[35] H.Hanninen et al, "Effects of Dynamic Strain Aging on Environment-Assisted Cracking of Low Alloy Pressure Vessel and Piping Steels" Proceedings of10th Environmental Degradation of Materials in Nuclear Power Systems Conference. Lake Tahoe,August 2001, pp 341-350

[36] H.D.Solomon, R.DeLair , E.Tolksdorf , "LCF Crack Initiation in WB 36 in High Temperature Water," Proceedings of 9th Environmental Degradation of Materials in Nuclear Power Systems Conference. Newport Beach 1999, pp. 865-874

[37] J.Hickling, "Strain Induced Cracking of Low Alloy Steels under BWR Conditions; are there still open issues," Proceedings of 10th Environmental Degradation of Materials in Nuclear Power Systems Conference. Lake Tahoe, August 2001.

[38] J.D. Atkinson, J.Yi "The Role of Dynamic Strain Aging in the Environment Assisted Cracking Observed in Pressure Vessel Steels" Fatigue, Fracture Eng. Mater. Struct. Vol 20,pp1-12,1997

[39] H.D.Solomon, R.E.DeLair, "The Influence of Dynamic Strain Aging on the Low Cycle Fatigue Behavior of Low Alloy and Carbon Steels in High Temperature Water," Proceedings of 10th Environmental Degradation of Materials in Nuclear Power Systems Conference. Lake Tahoe, August 2001.

[40] Hodge J.M., Mogford I.L. UK Experience of Stress Corrosion Cracking in Steam Turbine Discs). Proceedings of Inst. Mech Eng. Vol.193, No.11, 93 1979.

[41] Lyle F.F., Burghard H.C. Materials Perf. Vol.21, 11, pp35-44, Nov. 1982

[42] M.O.Speidel, "Stress Corrosion Cracking of Steam Turbine Steels" Proceedings of 2nd Environmental Degradation of Materials in Nuclear Power Systems Conference.Monterey, September, 1985 pp 267-275.

[43] F.F.Lyle, A.McMinn , G.R.Leverant "Low Pressure Steam Turbine Disc Cracking – an Update" Proceedings of Inst. Mech Eng. Vol.199, pp 59-67, 1985.

[44] H.P.Seifert, S Ritter, J. Hickling " Environmentally-Assisted Cracking of Low Alloy RPV and Piping Steels under LWR Conditions," Proceedings of 11th Environmental Degradation of Materials in Nuclear Power Systems Conference. Stevenson August 2003, pp 73-89.

[45] E.Lenz, N.Weiling Nucl.Eng. Design Vol.9 pp331-344, 1986

[46] H.P Seifert, S. Ritter, J. Heldt " Strain-Induced Corrosion Cracking of Low Alloy RPV Steels under BWR Conditions," "Proceedings of 10th Environmental Degradation of Materials in Nuclear Power Systems Conference. Lake Tahoe, August 2001.

[47] F.P.Ford, S.Ranganath, D.Weinstein "Environmentally-Assisted Cracking Fatigue Crack Initiation in Low Alloy Steels – A Review of the Literture and the ASME Code Requirements" EPRI TR-102765, EPRI Palo Alto CA USA 1993.

[48] T.Aria et al, Paper 140 NACE Corrosion Conference 1998.

[49] W.J.Bamford, G.V.Rao, J.L.Houtman "Investigation of Service –Induced Degradation of Steam Generator Shell Materials" Proceedings of 5th Environmental

Degradation of Materials in Nuclear Power Systems Conference.Monterey, August,1992.

[50] NRC Information Notice No. 90-04, "Cracking of the upper shell to transition cone girth welds in steam generators," (1990).

[51] R. Snaider, BWR Feedwater Nozzle and Control Rod Drive Return Line Nozzle Cracking: Resolution of Generic Technical Activity A-10 (Technical Report), NUREG-0619-REV-1, Nov. 1980.

[52] B. M. Gordon, G. M. Gordon, "Corrosion in Boiling Water Reactors," Metals Handbook, Volume 13, Corrosion, p927-937, ASM International, 1987.

[53] B.M. Gordon, D.E. Delwiche, G.M. Gordon, "Service Experience of BWR Pressure Vessels," Performance and Evaluation of Light Water Reactor Pressure Vessels, PVP-Vol. 119, p9-17, ASME, 1987.

[54] N.G. Cofie, et al., Evaluation of Stress Corrosion Crack Growth in Low Alloy Steel Vessel Materials in the BWR Environment (BWRVIP-60), EPRI TR-108709, March 1999.

[55] R. Snaider, BWR Feedwater Nozzle and Control Rod Drive Return Line Nozzle Cracking: Resolution of Generic Technical Activity A-10 (Technical Report), NUREG-0619-REV-1, Nov. 1980.

[56] A. Celovsky et al.,"S-08; Investigation and Repair of a Cracked Feeder at Point Lepreau GS" CANDU Maintenance Conference., 2000

[57] Nakayama G., Akashi M "Effects of Test Temperature and Hardness of Material on the Intergranular Stress Corrosion Cracking Behavior of Carbon Steel in a Simulated BWR Environment". Proceedings of 8th Environmental Degradation of Materials in Nuclear Power Systems Conference, Amelia Island, August 1997, pp947-952.

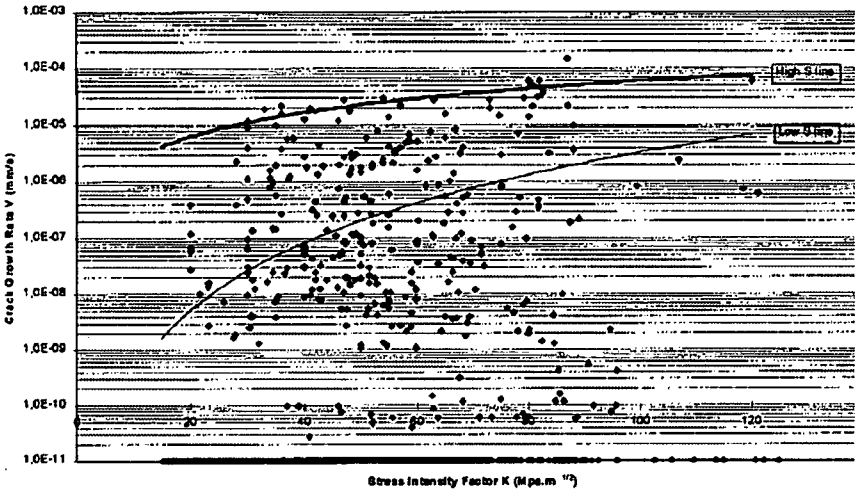

Fig. B.8.1 Crack propagation rate vs. stress intensity factor data for low alloy steels in "BWR" water at 288^{0}C [8]. Note that there must be a sound technical basis for the choice of the indicated disposition relationships.

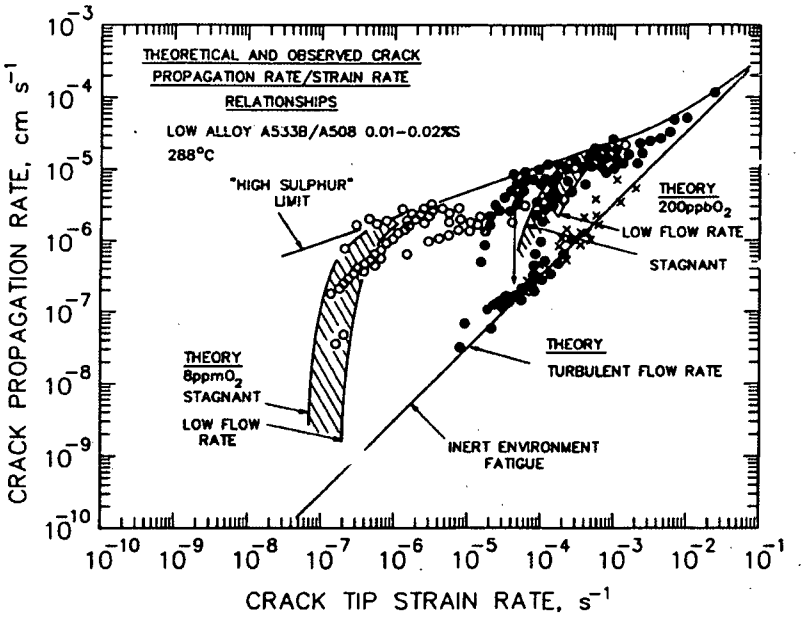

Fig. B.8.2 Observed and theoretical crack propagation rate / crack tip strain rate relations for low alloy steel in 288°C water at various corrosion potentials [9,12]. *(Used by permission of EPRI)* The strain rate values are pertinent to tests conducted under corrosion fatigue (at the higher end), slowly increasing applied strain, and constant load creep (at the lower end).

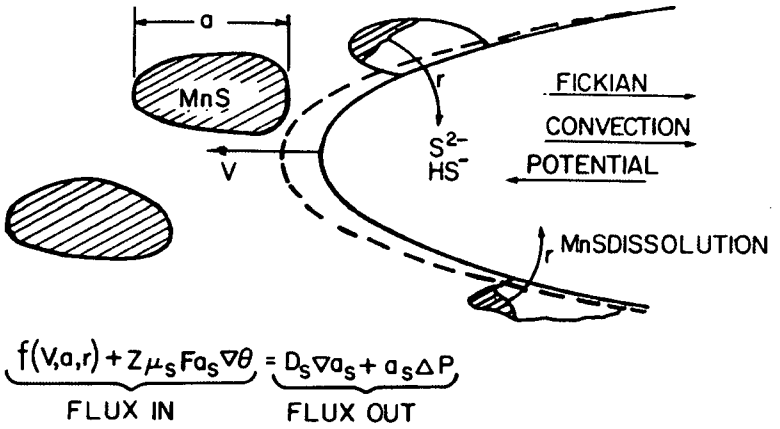

Fig. B.8.3 Schematic of crack tip illustrating the relationship between the MnS precipitate morphology and the advancing crack tip, and the various mass transport phenomena that will control the anionic activity at the crack tip.

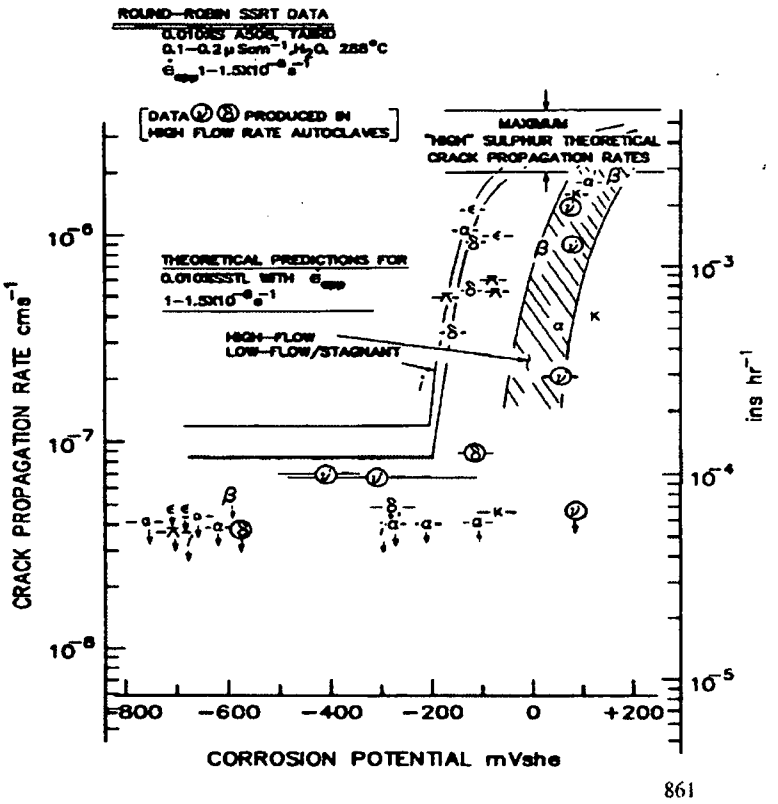

Fig. B.8.4 Observed (16) and theoretical (9) dependency of the average stress corrosion crack propagation rate on corrosion potential for 0.010% sulfur

A508 steel strained at 1-1.5 x 10 $^{-6}$ s.$^{-1}$ in 288°C water with conductivity of 0.02μS. cm $^{-1}$ *(Used by permission of EPRI)*

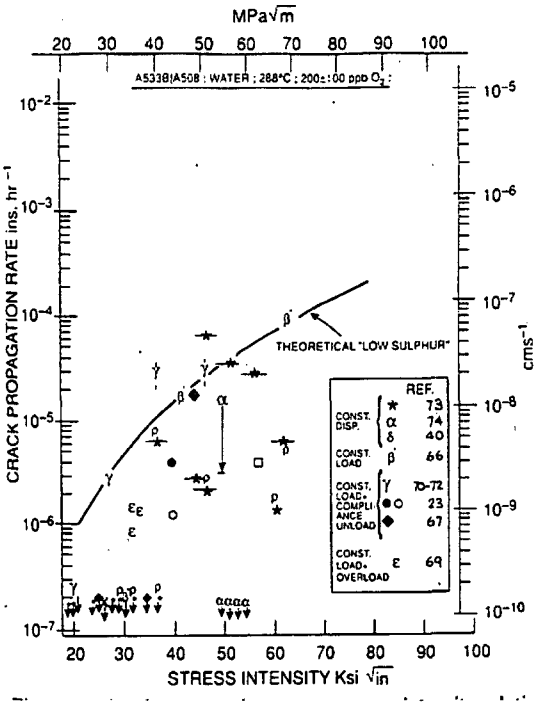

Fig. B.8.5 Theoretical "low–sulfur" crack propagation rate vs. stress intensity relationship (Eqn. 5) compared with selected laboratory data obtained in 288°C water containing 200 ppb oxygen, and stressed under constant load, constant displacement or constant load with periodic cycling conditions. [9] *(Used by permission of EPRI)*

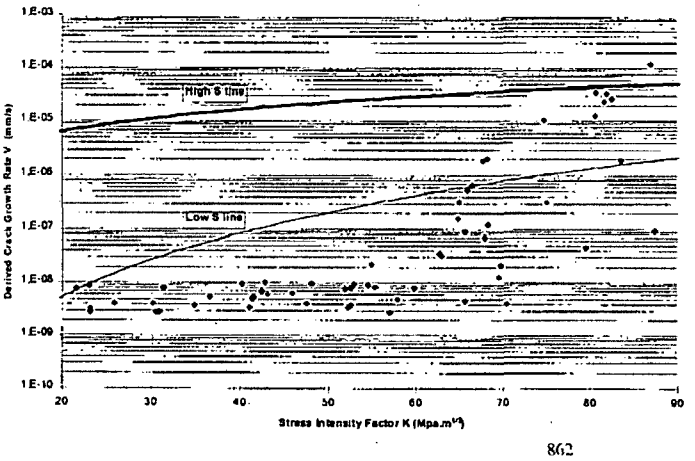

862

Fig. B.8.6 Observed (21-24) crack propagation rates, screened for quality (8), obtained under constant load for low alloy steels in 240°C water with 0.4 or 8.0 ppm oxygen. These data are compared with the theoretical relationship in Eqn. 5.

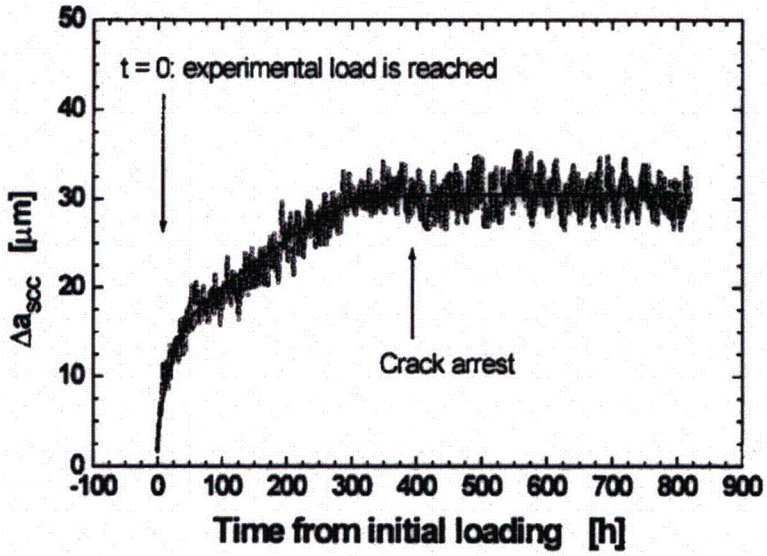

Fig. B.8.7 Crack length as a function of time for a low alloy steel specimen under constant load in BWR coolant. [27] *(Reprinted with permission from TMS)*

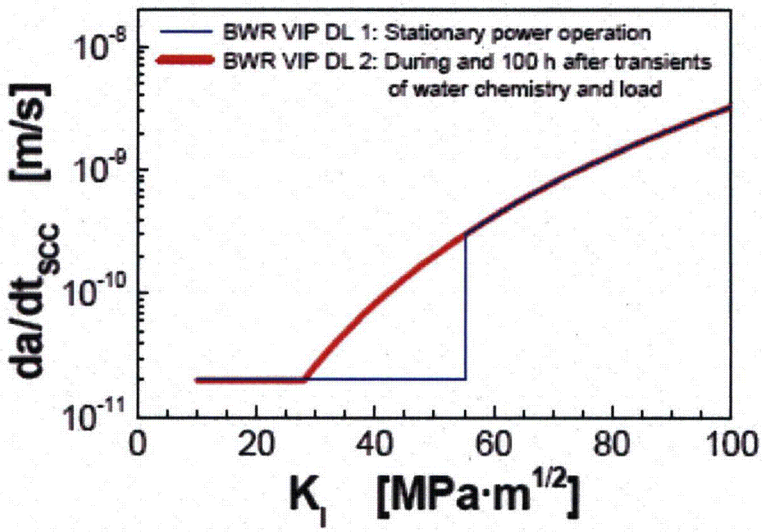

Fig. B.8.8 Propagation rate vs. stress intensity relationships for low alloy steels in BWR environments proposed by industry for disposition of cracks under stationary power operation (Eqn. 7), and during the 100 hours after limited water chemistry and load transients. (Eqn. 5). Also shown are relevant data obtained under unirradiated and irradiated (marked "IR") conditions. [23] *(© 2003 by The American Nuclear Society, La Grange Park, Illinois)*

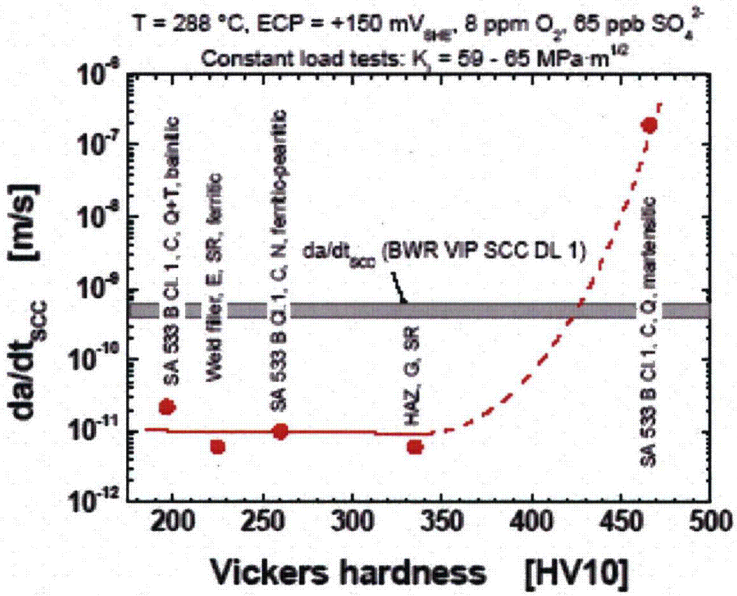

Fig. B.8.9 Effect of hardness on the crack propagation rate for various low alloy steel weldments, plate, etc. in 8 ppm oxygenated water at 288°C in comparison with the disposition propagation rate defined by Eqn. 5. [34] *(© 2003 by The American Nuclear Society, La Grange Park, Illinois)*

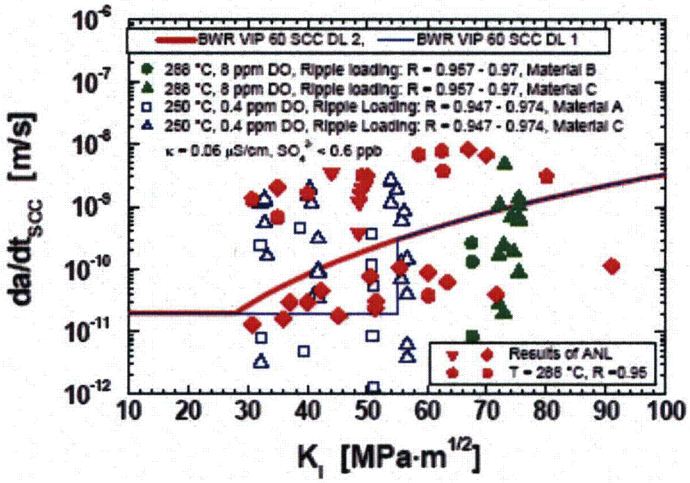

Fig. B.8.10 Effect of ripple loading (R>0.95) on the crack propagation rates for various low alloy steels in high purity, oxygenated water, indicating the possibility of exceeding the disposition propagation rates in Eqn. s 5 and 7 depending on the specifics of material condition. [34] *(© 2003 by The American Nuclear Society, La Grange Park, Illinois)*

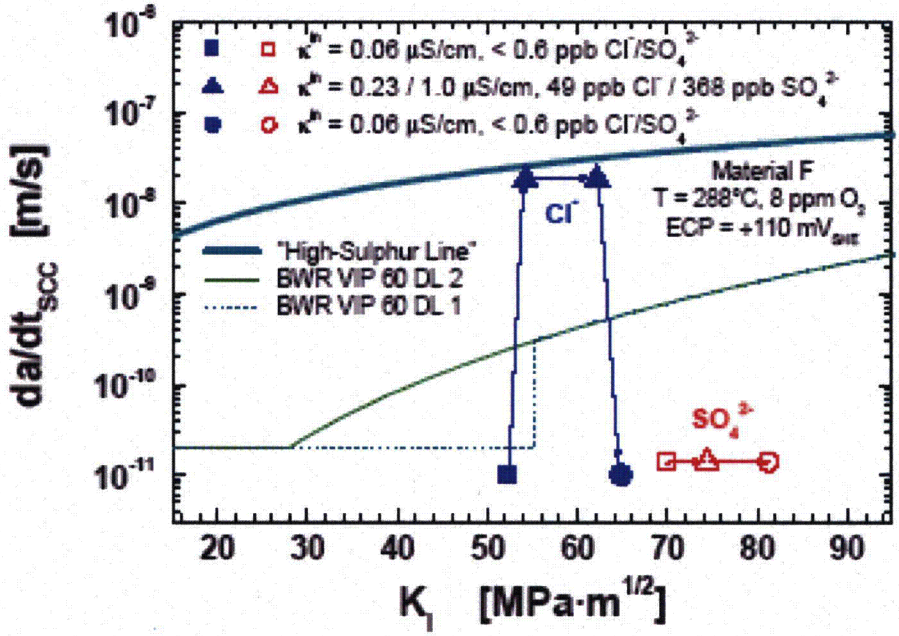

Fig. B.8.11 Effect of chloride and sulphate on the crack propagation rate of a low alloy steel in 8ppm oxygenated water at 288^{0}C. [34] *(© 2003 by The American Nuclear Society, La Grange Park, Illinois)*

B.9 "Environmental Degradation of High Strength Materials," by Peter M. Scott

Introduction

Many high strength materials are used in PWRs and BWRs for bolts, studs and springs. Typical uses of high strength, martensitic, low alloy steels are for the closure studs and nuts of pressure vessels and manway cover plates, pump casings and support assemblies, valve bonnets and packing glands. They are also used for bolts and tie rods in PWR secondary water in steam generators. High strength stainless steels and nickel base alloys are deployed in many components in the primary coolant circuits of both PWRs and BWRs. Examples include valve stems, internal bolting and springs in main coolant pumps and valves, control rod drive assemblies, core internals, fuel hold down springs, etc.

Failures of internal bolts and springs can give rise to loose parts and loss of essential function of the component concerned. External bolts and studs are clearly critical to maintaining the integrity of the principal pressure boundary. From the very beginning of exploitation of PWRs and BWRs for power production, small but significant numbers of failures of high strength materials have occurred in service. They have usually been attributed to stress corrosion cracking (SCC) or hydrogen embrittlement (HE). A few have also been attributed to corrosion fatigue and in the specific case of low alloy steels used for external bolting in the primary circuit, also to boric acid corrosion by primary water leaks and steam cutting. Recurring themes in the case of high strength low alloy and stainless steels have been the initial unsuitability of the heat treatment and hardness of the as-installed component, or in some cases after thermal aging leading to unacceptable hardness, and the presence of inappropriate lubricants to facilitate assembly. For the nickel base alloys, attention has also been focused on the suitability of the initial heat treatment to obtain the desired mechanical properties but here the in-service problems encountered have been more analogous to those of nickel base alloys in general, particularly in PWR primary water service.

Nickel base alloys

Alloys X750 and 718 are nickel base alloys that are age hardened to precipitate the strengthening phases γ' and/or γ''. Their chemical compositions are given in Table B.9.1. Bolts in alloy X750 can have yield strengths of 115-140 ksi (790-965 MPa) while Alloy 718 can be hardened to higher strengths, for example 170-180 ksi (1170-1240 MPa) for bolts and even over 200 ksi (1380 MPa) for springs dependent on the level of cold work applied before age hardening.[1] Many more components fabricated from alloy X750 have experienced intergranular stress corrosion cracking (IGSCC) in service in both PWRs and BWRs while only a very limited number of similar failures of alloy 718 have been observed in PWR service.[1,2]

Improvements have been made to alloy X750 for PWR primary water service by increasing the solution annealing temperature to 1950-2100°F (1060-1150°C) and with it the resultant grain size, and by the adoption of a single step aging heat treatment at 1300°F (704°C) for 20 hours. Although the main goal of the aging heat treatment is to precipitate the strengthening phase γ', $Ni_3(Ti, Al)$, an added advantage of these particular heat treatment conditions for PWR primary water service is a fine, dense $M_{23}C_6$ carbide

distribution at grain boundaries.[3] In addition, great attention is now paid to keeping the design stresses, including those at stress concentrations, at least below the proportional limit. Surface condition of components is also known to influence the risk of IGSCC, in particular cold work and residual stress. Moreover, the atmosphere used during the aging heat treatment alloy of X750 was found to have a profound influence on initiation times for IGSCC in PWR primary water.[3] This was due to oxidation of surface layers that had to be removed by machining after heat treatment in order to ensure optimum performance in service. The combination of all these improvements has seemingly stopped the previously generic failures of alloy X750 control rod drive split pins, for example, with operating periods presently exceeding 100,000hours without failure.

Alloy 718 is a normally highly reliable high strength alloy for use in PWR primary water although a few failures in PWR service are known.[1,2] Some studies in the literature have implicated the formation during thermal aging of δ phase, the thermodynamically most stable form of the strengthening phases γ," as having an aggravating influence on subsequent IGSCC susceptibility.[4] Others have not observed a major effect of δ phase on product performance.[2] Indeed, δ phase is a necessary feature to avoid excessive grain growth during solution treatment prior to aging.[2] By contrast, intergranular oxidation of the surface during product rolling and heat treatment can have a severe adverse influence on IGSCC initiation in PWR primary water. For optimum IGSCC resistance in plant, it is essential to remove the layer affected by the furnace atmosphere, as observed previously for alloy X750.

Stainless steels

The most commonly used high strength bolting material in PWR primary circuits is cold worked Type 316 stainless steels with strength levels, depending on component diameter, up to 100 ksi (700 MPa), which requires typically 10 to 20% cold work. The NRC position is that strain-hardened austenitic steels shall not exceed 90 ksi (630MPa). Even cold worked Type 304 (not L grade) may be used in PWR primary water although the practical extent of its use is not for the moment clear. With the exception of heavily neutron irradiated core baffle bolts there have been no known failures in service.

Where higher strength levels are required for components such as bolts, springs and valve stems, materials such as A286 precipitation hardened austenitic stainless steel, A410 and similar martensitic stainless steels and 17-4PH precipitation hardened martensitic stainless steel are used (Table B.9.1). Over the years, small numbers of such components have cracked in service usually attributed to stress corrosion or hydrogen embrittlement.

A286, an austenitic, precipitation hardened, stainless steel is strengthened by γ', $Ni_3(Ti,Al)$, formed during aging at 1330°F (720°C). Its use is favored where the expansion coefficient relative to other austenitic stainless steels is an important design factor. Unfortunately, it is susceptible to IGSCC in PWR primary water when loaded at or above the room temperature yield stress, typically 100 ksi (700 MPa).[5-10] Cold work prior to aging in combination with the lower of two commonly used solution annealing temperatures of 900 and 980°C has a particularly adverse effect on IGSCC resistance.[8] Hot heading of bolts, which can create a heat-affected zone between the head and shank, is another known adverse factor. Nevertheless, even if these metallurgical factors are optimized, immunity from cracking cannot be assured unless the stresses are

maintained below the room temperature yield stress, which necessitates strictly controlled bolt-loading procedures. There is also strong circumstantial evidence that superimposed fatigue stresses can lower the mean threshold stress for IGSCC even further. Finally, the role of impurities, including oxygen introduced during plant shut down and possibly consumed only slowly in confined crevices, in helping crack initiation is clear from all the evidence available. Once initiated, cracks grow relatively easily even in well-controlled PWR primary water.[7]

Components such as valve stems, bolts and tie rods requiring rather high strength combined with good corrosion resistance in PWR primary circuit water have been typically fabricated from martensitic stainless steels, particularly Type 410 and 17-4 PH. A significant number of failures of martensitic stainless steels such as Type 410, for example, have occurred.[11] In most cases, the affected components have usually entered service in an overly hard condition due to tempering at too low a temperature but no in-service aging seems to have been involved in these cases, the materials proving susceptible to stress corrosion cracking / hydrogen embrittlement in PWR primary water in the as-fabricated condition. A high tempering temperature above 1100°F (600°C) is preferred to avoid hydrogen embrittlement susceptibility. An additional problem has been caused by pitting/crevice corrosion of Type 410 and similar martensitic stainless steels in contact with graphite containing materials in the packing glands of valves, sometimes leading to valve stem seizure. The preferred replacement material has often been 17-4 PH with its higher chromium and molybdenum content conferring better resistance to crevice corrosion.

A significant number of service failures of 17-4 PH precipitation hardening stainless steel have also occurred in PWR primary water.[11-14] Initially, intergranular cracking by stress corrosion/hydrogen embrittlement was associated with the lowest temperature aging heat treatment at 900°F (480°C) designated H900. This gives a minimum Vickers hardness value of 435HV well in excess of the limit of 350HV commonly observed to limit the risk of hydrogen embrittlement. The H1100 (593°C) aging heat treatment was subsequently widely adopted and normally yields a hardness value below 350HV. Nevertheless, a small number of failures, due either to brittle fracture or stress corrosion / hydrogen embrittlement, have continued to occur. The origin of these failures appears to be thermal aging in service.

Two main thermal aging mechanisms of martensitic stainless steels are recognized. The first "reversible temper embrittlement" is related to the diffusion of phosphorus (and arsenic, antimony and tin) to grain boundaries at aging temperatures generally above 750°F (400°C) and can occur in both Type 410 and 17-4 PH stainless steels. The grain boundaries are consequently embrittled and are particularly susceptible to intergranular hydrogen embrittlement but no general increase in hardness is observed. It can be reversed by heat treating around 1100°F (600°C) and avoided by reducing the phosphorus content and by small (1%) alloying additions of molybdenum.

The second thermal aging embrittlement mechanism is relevant only to precipitation hardened stainless steels such as of 17-4 PH. It arises from an intra-granular decomposition of the martensitic matrix into two phases, α which is rich in iron, and α' which is chromium rich. Further hardening arises from additional precipitation of the copper rich ε phase. A generalized increase in hardness is observed with corresponding increases in strength and ductile / brittle transition temperature and loss of fracture toughness. This hardening cannot be reversed without re-solution annealing. French

studies have shown that this aging mechanism can occur in 17-4 PH steels on time scales relevant to the design lives of PWRs at temperatures exceeding 485°F (250°C) and quantitative models for component assessment have been developed.[12,13] Mechanical fractures occur by cleavage although those involving corrosion can also be intergranular. Both types of failure have been associated with hardness values after in-service aging significantly exceeding 350HV. Corrosion related failures have also been aggravated by impurities coming from valve packing gland materials.

Low alloy martensitic steels

High strength martensitic and maraging steels are used in many external fastener applications in nuclear power reactors and a significant number of failures of this class of component have occurred.[15] Most have been described as corrosion related failures. The problems encountered with external bolting have affected both support bolting and pressure boundary fasteners. Support bolting, in particular, can be affected by severe localized corrosion at interfaces with concrete where water may accumulate and protective plating or a polymeric coating system is often necessary.

Cracking of low alloy (AISI 4340 and 4140) and maraging steel support bolting has been attributed mainly to hydrogen embrittlement. Steels with ultra high yield strengths greater than 150 ksi (1035 MPa) have failed due to a combination of too high applied stresses and humid or wet environments collecting around the bases of components. Steels with lower yield strengths have also failed due to poor heat treatment or material variability. Consequent on these failures, a review of environmental cracking properties of high strength steels exposed to water or salt water at low temperatures was carried out and regulatory guidelines based on this information were published in the USA.[16] Acceptability of high strength bolting was based on a lower bound approach to KISCC as a function of yield strength. This fracture mechanics based approach may have some attractions for defining a quality assurance procedure and for defect assessment. However, hydrogen cracks can start from surfaces, usually in crevices or from pits. Consequently, it is advisable also to have an upper hound strength limit (such as 150 ksi given in the EPRI Materials Handbook as the upper limit below which no service failures have been observed) to avoid this type of cracking.

The second category of bolt failures is concerned with the integrity of the primary pressure boundary at locations such as the flanges of manway covers, pump casings and valves. Most of these incidents have been caused by boric acid corrosion or steam cutting (erosion-corrosion) due to PWR primary water seal leaks. A small number of failures among this category of bolts have, however, been associated with stress corrosion cracking/hydrogen embrittlement rather than wastage.[16] The ferritic bolting steels involved were not out of specification but had been in contact with molybdenum disulfide lubricants. It has been postulated that the lubricant dissociated on contact with hot water to yield hydrogen sulfide, which is a severe hydrogen embrittling agent for ferritic steels. Consequently sulfide containing lubricants are no longer permitted. More generally, the main remedy for this category of high strength bolting failures is to avoid leaks at flanges seals by improved gasket design.

References for B.9

[1] A.R. McIlree, "Degradation of High Strength Austenitic Alloys X-750, 718 and A286 in Nuclear Power Systems," Proceedings of 1st Int. Symposium on Environmental Degradation of Materials in Nuclear Power Systems - Water Reactors, pp. 838-849, Myrtle Beach, NACE 1984.

[2] P.M. Scott, "Stress Corrosion Cracking in Pressurized Water Reactors - Interpretation, Modeling and Remedies," *Corrosion, 56,* 8, pp. 771-782, 2000.

[3] M. Foucault, C. Benhamou, "Influence of Surface Condition on the Susceptibility of Alloy X-750 to Crack Initiation in PWR Primary Water," Proceedings of 6th International Symposium on Environmental Degradation of Materials in Nuclear Power Systems – Water Reactors, pp. 791-797, San Diego, CA, The Metallurgical Society 1993.

[4] M.T. Miglin, et al., "Stress Corrosion Cracking of Chemistry and Heat Treat variants of Alloy 718, Part 1: Stress Corrosion Test Results," Proceedings of 6th International Symposium on Environmental Degradation of Materials in Nuclear Power Systems – Water Reactors, pp. 815-818, San Diego, CA, The Metallurgical Society 1993.

[5] G.O. Haynor, et al., "Babcock & Wilcox Experience with Alloy A-286 Reactor Pressure Vessel Internal Bolting," Proceedings of Fontevraud I, SFEN, pp. 93-101, 1985.

[6] P.J. Plante, J.P. Mieding, "Degradation of Reactor Coolant Pump Impellor-to-shaft Bolting in a PWR," Proceedings of 4th International Symposium on Environmental Degradation of Materials in Nuclear Reactor Systems- Water Reactors, Jekyll Island, Georgia, pp. 11-45 to 11-55, NACE, 1990.

[7] US NRC Information Notice, "Stress Corrosion Cracking of Reactor Coolant Pump Bolts" 90 – 68 (1990) and supplement 1 (1994).

[8] R.S. Piascik, et al., "Stress Corrosion Cracking of Alloy A-286 Bolt Material in Simulated PWR Reactor Environment," Proceedings of the Second International Symposium on Environmental Degradation of Materials in Nuclear Reactor Systems- Water Reactors, pp. 18-25, Monterey CA, American Nuclear Society 1986.

[9] I. Wilson, T. Mager, "Stress Corrosion of Age Hardenable NiFeCr Alloys," *Corrosion, 42,* 6, pp. 352-360, 1986.

[10] J.B. Hall, S. Fyfitch, K.E. Moore, "Laboratory and Operating Experience with Alloy A286 and Alloy X750 RV Internals Bolting Stress Corrosion Cracking," Proceedings of 11th International Conference on Environmental Degradation of Materials in Nuclear Power Systems – Water Reactors, pp. 208-215, Stevenson, Washington, American Nuclear Society 2003.

[11] US NRC Information Notice 85-59, "Valve Stem Corrosion Failures," 1985.

[12] J.M. Boursier, et al, "Vieillissement en service des aciers inoxydables," Proceedings of Fontevraud IV, SFEN, pp. 1123-1134, 1998.

[13] B. Yrieix, M. Guttmann, "Aging Between 300 and 450°C of Wrought Martensitic 13-17 wt% Cr Stainless Steels," *Materials Science and Technology, 9,* 2, pp. 125-134,1993.

[14] H. Xu, S. Fyfitch, "Aging Embrittlement Modeling of Type 17-4PH at LWR Temperature," Proceedings of the 10th International Conference on Environmental Degradation of Materials in Nuclear Power Systems – Water Reactors, Lake Tahoe, CA, NACE International 2001, August 3 to 9, 2001.

[15] C.J. Czajkowski, "Corrosion and Stress Corrosion Cracking of Bolting Materials in Light Water Reactors," Proceedings of 1st Int. Symposium on Environmental

Degradation of Materials in Nuclear Power Systems - Water Reactors, pp. 192-208, Myrtle Beach, NACE 1984.

[16] A. Goldberg, M.C. Juhas, "Lower Bound KIscc Values of Bolting Materials – A Literature Study," NUREG/CR 2467, 1982.

Table B.9.1 Composition of Some Common High Strength Nickel Base Alloys and Stainless Steels

Element	Alloy X750	Alloy 718	A-286	17-4PH
Nickel	>70.0	50-55	24-27	3.0-5.0
Chromium	14-17	17-21	12-15	15-17.5
Iron	5-9	Bal.	Bal.	Bal.
Titanium	2.25-2.75	0.65-1.15	1.55-2.0	
Aluminum	0.4-1.0	0.2-0.8	≤0.35	
Niobium plus Tantalum	0.7-1.2	4.75-5.50		0.15-0.45
Molybdenum		2.8-3.3	1.00-1.50	
Carbon	≤0.08	≤0.08	≤0.08	≤0.07
Manganese	≤1.0	≤0.35	≤2.0	≤1.0
Sulfur	≤0.010	≤0.010	≤0.030	≤0.030
Phosphorus			≤0.040	≤0.040
Silicon	≤0.5	≤0.35	≤1.0	
Copper	≤0.5	≤0.30		3.0-5.0
Vanadium			0.10-0.50	

B. 10 "BWR Water Chemistry: Effects on Materials Degradation and Industry Guidelines,"

by Robin L. Jones, Peter L. Andresen, and Christopher Wood

This background paper is comprised of an introductory section (Section A) that focuses specifically on the evolution of BWR water chemistry over time, and more specifically its effects on materials degradation. It is followed by a broader summary (Section B) based primarily on BWR Water Chemistry Guidelines that addresses such topics as chemistry effects on radiation build-up, fuel cladding corrosion, chemistry monitoring, and action level treatment of chemistry transients.

A. Effects on Materials Degradation

Introduction

Boiling water reactor (BWR) water chemistry is necessarily of high purity because boiling occurs on the fuel rods and the resulting steam directly drives the turbine; if high purity were not maintained then high concentrations of aggressive species would be formed on the heat transfer surface where boiling occurs. By contrast, pressurized water reactors (PWRs) have a primary system comprised of liquid water containing B, Li and H_2 that is pumped through tubing in several steam generators (the secondary system).

To understand the basics of BWR water chemistry, the water flow path must be clear, Figures B.10.1 and B.10.2). After the turbine, steam is condensed and demineralized, then returned as feed water. Feed water is heated to about 200°C, then it enters the pressure vessel, and its flow is distributed via feed water spargers, which are distributed near the inside diameter of the pressure vessel at an elevation somewhat above the top of the core (Figure B.10.1). Water is circulated through the core via jet pumps, with the average water molecule circulating about 7-10 times before becoming steam. A large pipe (the core shroud) separates the up-flow (in the core) from the down flow (in the annulus). In jet pump plants (all current US plants), the drive water is drawn from the annulus at an elevation below the bottom of the core, and flows through the recirculation piping and pumps, then flows back into the pressure vessel. In jet pumps, about one-third of the flow is drive water and two-thirds is drawn into the jet pump by the water jet. Thus, two-thirds of the water moves rapidly through most of the annulus region, and is exposed only briefly to the gamma field emanating from the core; the relevance of this factor is discussed later.

The bottom of the jet pumps seals into a ledge that blocks off the annulus region. The water flows into the bottom plenum (the bottom hemisphere of the reactor pressure vessel), then back up through the core. Advanced BWRs and some overseas designs use internal pumps and therefore have no recirculation piping.

BWR fuel rods (Figure B.10.3) are enclosed in "channels" or zirconium alloy wrappers around the fuel bundle (BWR fuel is comprised of an array of roughly 9 x 9 fuel rods = 81 total – the designs have evolved over time). About 90% of the water flows through the fuel channel, and 10% flows in the "bypass" regions between fuel bundles or around the periphery of the core along the inside of the shroud. The core inlet temperature is about 274°C, and about one-third of the way up the fuel the water temperature reaches 288°C and begins to boil. The volume fraction of steam ("steam quality") rises with elevation in the core. At the top of the core there is a dome or upper plenum at the top of which are steam separators, then steam dryers. The separators produce a rotating vortex flow, and the liquid water is centrifugally forced to the outside, where it is

is routed outside the separator and falls on the top of the dome, then into the annulus. This 288 °C water is cooled by the ≈200°C feed water to 274°C. Thus, most structural materials (the vessel, the external piping, the outside of the shroud, the bottom plenum and the core support plate, etc.) are exposed to 274°C water.

The steam continues upward through the separators and steam dryer to the top dome of the reactor pressure vessel and out the main steam nozzle and piping to the turbine. The liquid content of the saturated steam is typically ≈ 0.1%. Thus, the upper half of the vessel internals is exposed to 288°C saturated steam, and all steam path surfaces are expected to have a water film.

While the condensate from the turbine is fully demineralized before returning to the reactor pressure vessel as feed water, the reactor water must also be cleaned up, because otherwise nonvolatile impurities would concentrate because of boiling. The reactor water clean up system typically runs at 0.5 to 1% of the feed water flow rate, cooling the water before running it through demineralizers.

As water flows through the core and is exposed to ionizing radiation (esp. neutrons, which are slowed by their collisions with water (esp. H) and eventually reach "thermal" energies, at which point they are most effective in producing fission reactions), a wide variety of radiolysis products are produced. For simplicity, the primary species can be considered to be H_2 and H_2O_2. H_2 partitions to the steam phase, so the recirculated water is always oxidant rich. H_2O_2 decomposes to H_2O and O_2, and the relative proportions of O_2 and H_2O_2 changes with time and distance away from the core. Expressed as O_2, typical recirculation water has ≈ 200 ppb O_2 and ≈10 ppb H_2. It is helpful to note that O is 16 times heavier than H, but there are two H atoms in H_2O, so a stoichiometric balance is 2:1 H:O by atom ratio, but 1:8 H:O by weight. Thus, 10 ppb H_2 and 80 ppb O_2 represents a stoichiometric mixture.

In the core, some ^{16}O is transmuted to ^{16}N, which has a half-life of 7.13 seconds. In "normal water chemistry," the stable form of N is NO_3^-, which remains soluble. However, when sufficiently high H_2 is injected into BWRs, the stable form becomes NO_X (and eventually NH_3), which are volatile. Thus, rather than remaining in the recirculated reactor water as it decays, ^{16}N becomes volatile and can cause a large increase (up to (10X) in the turbine radiation level.

Apart from very slight consumption of H2O2 and O2 (e.g., by corrosion reactions) and some recombination of oxidants and H2, all of the radiolysis products eventually go up with the steam as H2 and O2. They are catalytically recombined in the off-gas system after the turbine and condenser.

SCC Mitigation by Water Purity Control

Control of water purity is particularly important in BWRs because the higher corrosion potential traditionally present creates a potential gradient in crevices and cracks which concentrates anionic impurities like Cl– and SO4= [1-7]. Until the late 1980s, many BWRs operated at solution conductivities between 0.3 and 0.8 (S/cm, which corresponds to 30 – 90 ppb of (usually acidic) impurities (these were often Cl– and SO4=, which are particularly damaging and were responsible for extensive cracking). Several plants had severe intrusions of impurities from seawater or release of resins into the reactor water, and experienced severe and immediate SCC. By the early 1990s (Figure B.10.4) the fleet average conductivity had decreased to (0.13 (S/cm, and it is cur-

rently (0.11 (S/cm, with much of the residual conductivity (theoretical purity water is 0.055 (S/cm) related to chromate (Cr in the oxide films of structural materials becomes soluble at high potential) and Zn ion (which is introduced into the feed water of most BWRs to control radiation build-up and provide some SCC initiation benefit). SiO2 is almost always present at higher levels (e.g., 100-500 ppb), but it ionizes only very slightly in 288(C water. It should be emphasized that chloride and sulfate have the largest effect on stress corrosion cracking; some ions, like chromate, nitrate and silicate anions have little effect on SCC unless their concentrations exceed 25 ppb, 100 ppb or 1000 ppb respectively [5-7].

A conductivity of 0.10 μS/cm represents only about 6 ppb Cl^- as HCl (1.7×10^{-7} N), and there is a limited value in striving for theoretical purity water because OH^- is present at 2.3×10^{-6} N in pure water; both logic and modern data support the idea that, when the "foreign" anions concentration is well below a tenth of the OH^- concentration, their role in carrying ionic current and thereby changing crack chemistry diminishes. However, SCC growth rates in autoclave outlet water of <0.065 μS/cm remain reasonably high at high potential, and crevice chemistry measurements show that a shift from acidic to alkaline crack/crevice chemistry occurs in pure water [3-6]. Thus, water purity alone cannot be used to reduce SCC to acceptable levels in BWRs.

SCC Mitigation by Hydrogen Water Chemistry

The presence of oxidants like H_2O_2 and O_2 in the water cause an increase in the corrosion potential of metals (Figure B.10.5). This in turn produces an aggressive crack chemistry that accelerates SCC growth rates (Figure B.10.6). The most effective way to mitigate SCC in BWRs is to modify the water chemistry by reducing the corrosion potential. Hydrogen Water Chemistry (HWC) does this by injecting H_2 into the feed water. H_2 levels above ≈500 ppb effectively suppresses radiolysis (PWRs use ≈3 ppm H_2), but such high levels are not economically achievable in BWRs because most of the H_2 is lost to the steam during each pass through the core (thus, the feed water would need to have 7-10 times more H_2, or ≈4 ppm).

However, the addition of some H_2 to the feed water is effective in reducing the oxidant levels and therefore the corrosion potential (Figure B.10.7) enough to effectively suppress stress corrosion cracking when the corrosion potential reaches a "protection potential" of -230 mV_{she} [8-9]. This decrease in corrosion potential occurs not by suppressing radiolysis but by gamma-radiation enhanced recombination in the annulus (or downcomer). The gamma level in the downcomer varies with reactor design, and some wide annulus plants have insufficient gamma radiation at the outside of the annulus (i.e., at the inside of the reactor pressure vessel) to produce very effective recombination – thus, the effectiveness of a given H_2 injection rate varies from plant-to-plant. In the best plants, HWC drops the oxidant levels from ≈200 ppb to < 1-2 ppb at the bottom of the annulus, which feeds the recirculation piping. However, since two-thirds of the jet pump flow is drawn from an area closer to the top of the annulus, the water that flows into the bottom plenum has a higher oxidant concentration. Thus, in "standard HWC" plants (where ≈300-500 ppb H_2 is injected into the feed water, which is diluted by 7-10X in the reactor water), the good plants achieve low corrosion potentials (e.g., < –300 mV_{she}) in the recirculation piping, along some of the outside of the shroud, and on the top surface of the ledge, but are not as effective in the bottom plenum where there are many structural welds and pressure vessel penetrations for the control rods and instrumentation tubes. (Figure B.10.8). No "standard HWC" plant is able to significantly lower the corrosion potential in-core.

Attempts to improve the coverage of HWC considered the obvious option of increasing the H_2 to higher levels. "Moderate HWC" plants inject about 5-10 times more H_2, e.g., ≈2 ppm H_2 in the

feed water. In many plants, this produces an adequately low corrosion potential in the bottom plenum and perhaps along the inside of the shroud (there are uncertainties in the measurements and models that make this less than certain). At such high H_2 levels, all plants see a large increase in "turbine shine" (^{16}N in the steam).

Note that once boiling occurs (essentially no boiling occurs in the bypass water outside of the fuel bundles), the H_2 level in the water drops significantly. Thus, components exposed to this water remain at high corrosion potential and remain unprotected from stress corrosion cracking (Figure B.10.8). Such components can include the top guide, the dome (upper plenum), the steam separators, the core spray piping and spargers, the feed water piping and spargers, and perhaps some area at the upper part of the core shroud. While there are a large number of feed water spargers distributed around the periphery of the core, there is also some concern for how quickly the H_2-rich feed water becomes thoroughly mixed with the core "over-flow" (recirculated) water, and therefore at which point down the outside the shroud a low corrosion potential is achieved. On the basis of an exhaustive qualification process for hydrogen water chemistry in the laboratory and in test reactors, all US BWRs now employ this technique for mitigating stress corrosion cracking in the components outlined in Figure B.10.8. However, a cautionary note is appropriate in that reduced corrosion potentials have been confirmed in a few locations in a limited number of operational BWRs. There is no direct confirmation of the benefit of HWC on SCC of BWR components due to the limited number of repeat inspections.

SCC Mitigation by NobleChem™

Rather than achieving a reduction in oxidant concentration in all of the reactor water, a novel technique (NobleChem™) was developed by GE in which all wetted surfaces could be made catalytic [10-13]. Metals such as Pt, Pd, Rh, Ru, Os and Ir are electro-catalytic; i.e., reactions (esp. H_2 and O_2 or H_2O_2 reactions) are dramatically accelerated. While these Pt-group metals can be added to alloys and used in thermal spray powders, the most efficient way to create catalytic surfaces is to introduce low concentrations of Pt salts (e.g., $Na_2Pt(OH)_6$) into BWR water, which results in Pt depositing on the surfaces of all wetted parts. Pt concentrations below 1% of a monolayer are adequate, and NobleChem™ application is performed at shutdown at ≈135°C. An "OnLine NobleChem™" is being developed that introduces Pt during full-power operation.

The development of electrocatalytic processes for improving the efficiency of the oxygen/ hydrogen recombination process and thereby extending the region of protection to the reactor core region (Figure B.10.9) has, like the hydrogen water chemistry process described earlier, been subject to years of qualification in the laboratory and test reactors. Currently the majority of US BWRs use, or are about to use, the NobleChem™ process (Figure B.10.10), in large part due to the fact that under the Noblechem process protection of the core internals from stress corrosion cracking can be achieved at lower feedwater hydrogen concentrations that do not give rise to accelerated ^{16}N offgas rates and increases in the main steam line radiation (Figure B.10.11). As with the hydrogen water chemistry, the benefit of NobleChem™ has only been confirmed in terms of reduced corrosion potentials in a few locations in a limited number of BWRs. There is no direct confirmation of the benefit of NobleChem™ on SCC of BWR components due to the limited number of repeat inspections. There are also some precautionary notes with respect to plant verification and inherent limitations to the effectiveness of NobleChem™. For instance:

- To achieve low corrosion potential at all locations of interest, H_2 must be in stoichiometric excess. Considering only O_2 (not H_2O_2), there must be two moles of H_2 per mole of

O_2, which translates to a ppb level of H_2 at least one-eighth of O_2. This is easily achieved at fairly low levels of H_2 injection to the feed water at all locations until boiling occurs. Thus, areas above the fuel channel (upper plenum, steam separators, core spray lines, etc.) are not protected. Additionally, there may be areas in the upper regions of the annulus where the (H_2-rich) feed water does not adequately mix with the core water, and stoichiometric excess H_2 might not exist in some local regions.

- Low corrosion potential does not translate to immunity to SCC. Indeed, higher yield strength materials (such as alloy 182/82 weld metal, irradiated stainless steel, cold worked stainless steel or alloy 600 – including regions of the weld heat affected zone – etc.) benefit less than, e.g., sensitized stainless steel, because cold work causes higher growth rates at both low and high corrosion potential (Figure B.10.6).

- If cracks grow extensive in between NobleChem™ applications, O_2 can get to areas of the crack flank that are not catalytic, so no catalytic benefit is observed [13]. This is a well-understood limitation, and where it has occurred in the operational reactors, it has been associated with a digression from operational procedure and the inadequate control of the hydrogen feed rate. OnLine NobleChem™ is under development and being demonstrated in plants to help resolve this concern.

Effects of Corrosion Potential on Corrosion Fatigue Initiation and Growth

The discussions above have mainly been associated with mitigating stress corrosion and irradiation assisted cracking of stainless steels and stress corrosion of nickel base alloys. In addition to these examples, there is a strong benefit of HWC and NobleChem™ on stress corrosion and corrosion fatigue crack initiation and growth in carbon and low alloy steels. Cracking in these systems is attributed primarily to the role of MnS inclusions, which readily (but not very rapidly) dissolve in high temperature water and affect crack growth by changing the crack tip chemistry. For many years it was assumed that stainless steels would behave in a similar fashion, and indeed they do from the perspective of crack growth, where the lowered corrosion potential makes the crack chemistry less aggressive. However, corrosion fatigue crack initiation is accelerated at low corrosion potentials, and this may result from the (≈5 times) higher general corrosion rate on stainless steels exposed to deaerated (or hydrogenated) high temperature water.

Other Chemistry Related Mitigation Approaches for Stress Corrosion Cracking

Zn Injection [9, 14-16] and *Insulated Protective Coatings* [17-19] are other methods that can mitigate SCC in BWRs. *Zn injection*, originally undertaken to reduce ^{60}Co absorption into the oxide on BWR piping and thereby increasing the maintenance dosage rates, also improves SCC initiation. It appears to be less effective on crack propagation, especially at high corrosion potential (where cation transport in cracks is resisted by the potential gradient). However, even at low corrosion potential, providing an adequate and continuing supply of Zn to the tip of a long, growing crack may be difficult.

Insulated protective coatings (ICP) depend on forming a dense or slightly porous layer on the surface that has very low electrical conductivity. The most attractive coating is ZrO_2, which can be deposited by various coating techniques, or formed in situ after creating a metallic Zr layer

on the surface, e.g., by wire arc or thermal spray techniques. IPC does not rely on H_2 injection or even the presence of H_2, but it is very unlikely that any technique can be developed to form effective, durable coatings in-situ as is done by NobleChem™.

References for B.10 Section A

[1] F.P. Ford, P.L. Andresen, "Corrosion in Nuclear Systems: Environmentally Assisted Cracking in Light Water Reactors," in "Corrosion Mechanisms," Ed. P. Marcus and J. Ouder, Marcel Dekker, p.501-546, 1994.

[2] F.P. Ford, et al., "Corrosion-Assisted Cracking of Stainless Steel and Low-Alloy Steels in LWR Environments," NP5064S, Electric Power Research Institute, February 1987.

[3] P.L. Andresen, L.M. Young, "Characterization of the Roles of Electrochemistry, Convection and Crack Chemistry in Stress Corrosion Cracking," Proc. Seventh International Symposium on Environmental Degradation of Materials in Nuclear Power Systems - Water Reactors, NACE, p.579-596, 1995.

[4] P.L. Andresen, "SCC Growth Rate Behavior in BWR Water of Increasing Purity," Proc. Eighth Int. Symp. on Environmental Degradation of Materials in Nuclear Power Systems - Water Reactors, p.675, AIME, 1998.

[5] P.L. Andresen, "Effects of Specific Anionic Impurities on Environmental Cracking of Austenitic Materials in 288C Water," Proc. Fifth International Symposium on Environmental Degradation of Materials in Nuclear Power Systems - Water Reactors, p.209-218, Monterey, August 1991, American Nuclear Society, 1992.

[6] P.L. Andresen, "Specific Anion and Corrosion Potential Effects on Environmentally Assisted Cracking in 288C Water," GE CRD Report 93CRD215, December 1993.

[7] P.L. Andresen, "The Effects of Nitrate on the Stress Corrosion Cracking of Sensitized Stainless Steel in High Temperature Water," Proc. Seventh International Symposium on Environmental Degradation of Materials in Nuclear Power Systems - Water Reactors, NACE, p.609-620, 1995.

[8] B.M. Gordon, et al., "Mitigation of Stress Corrosion Cracking through Suppression of Radiolytic Oxygen," Proc. 1st Int. Symp. on Environmental Degradation of Materials in Nuclear Power System-Water Reactors, NACE, p. 893, 1983.

[9] R.L. Cowan, E. Kiss, "Optimizing BWR Water Chemistry," Proc. 6th. Int. Conf. on Environmental Degradation of Materials in Nuclear Power System-Water Reactors, TMS, p. 889, 1993.

[10] Y.J. Kim, et al., "Applications of Noble Metals in Coatings and Alloys for Light Water Reactors," *Journal of Metals, 44*, No. 2, p. 14-18, April 1992.

[11] S. Hettiarachchi, et al., "The Concept of Noble Metal Addition Technology for IGSCC Mitigation of Nuclear Materials," Proc. Seventh Int. Symp. on Environmental Degradation of Materials in Nuclear Power Systems - Water Reactors, NACE, p.735-746, 1995.

[12] P.L. Andresen, "Application of Noble Metal Technology for Mitigation of Stress Corrosion Cracking in BWRs," Proc. Seventh International Symposium on Environmental Degradation of Materials in Nuclear Power Systems - Water Reactors, NACE, p.563-578, 1995.

[13] P.L. Andresen, T.P. Diaz, S. Hettiarachchi, "Resolving Electrocatalytic SCC Mitigation Issues in High Temperature Water," Paper #04668, Corrosion/04, NACE, 2004.

[14] P.L. Andresen, T.P. Diaz, "Effects of Zinc Additions on the Crack Growth Rate of Sensitized Stainless Steel and Alloys 600 and 182 in 288C Water," Bournemouth Conference, BNES, England, October 1993.

[15] P.L. Andresen, T.M. Angeliu, "Effects of Zinc Additions on the Stress Corrosion Crack Growth Rate of Sensitized Stainless Steel, Alloy 600, and Alloy 182 Weld Metal in 288C Water," Corrosion/95, Paper #95409, T-2A Symposium, NACE, 1995.

[16] W.J. Marble, R.L. Cowan, .J. Wood, "Control of Cobalt-60 Deposition," Water Chemistry of Nuclear Reactor System 4, BNES, October 1986.

[17] P.L. Andresen, Y.J. Kim, "Insulated Protective Coating for Mitigation of SCC in Metal Components in High Temperature Water," U.S. Patent No. 5,463,281, November 7, 1995.

[18] Y.J. Kim, P.L. Andresen, "Application of Insulated Protective Coatings for Reduction of Corrosion Potential of Type 304 Stainless Steel in High Temperature Water," Corrosion 54, p.1012-1017, 1998.

[19] Y.J. Kim, et al., "Corrosion Behavior of YSZ Coatings in High Temperature Water," GE CRD Technical Report 2000CRD090, July 2000.

[20] Y.J. Kim, et al., "Application of Zircaloy-2 Coating for Reducing the 304 SS ECP in High Temperature Water," GE CRD Technical Report 2001CRD006, January 2001.

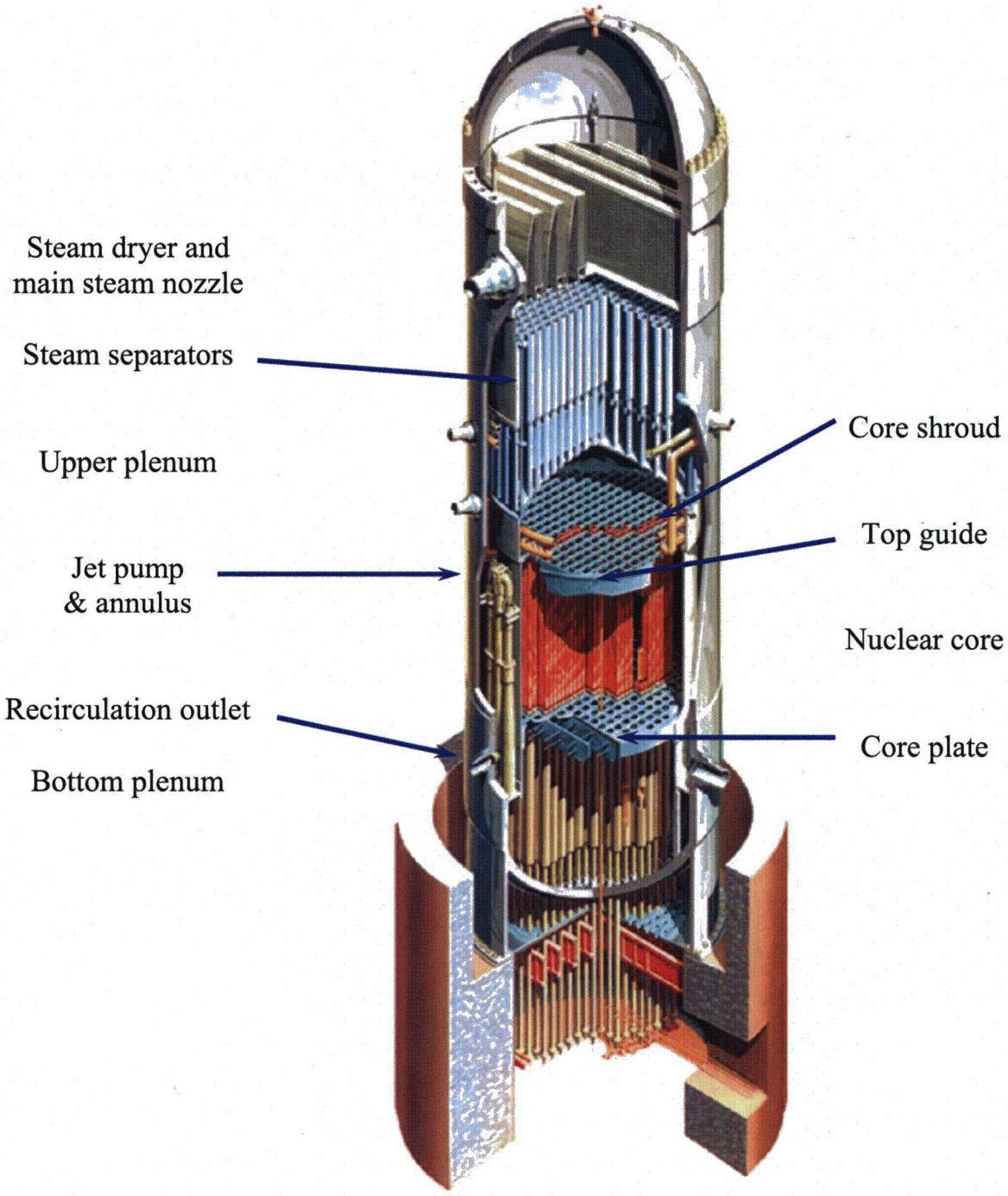

Figure B.10.1. Schematic of a BWR/6

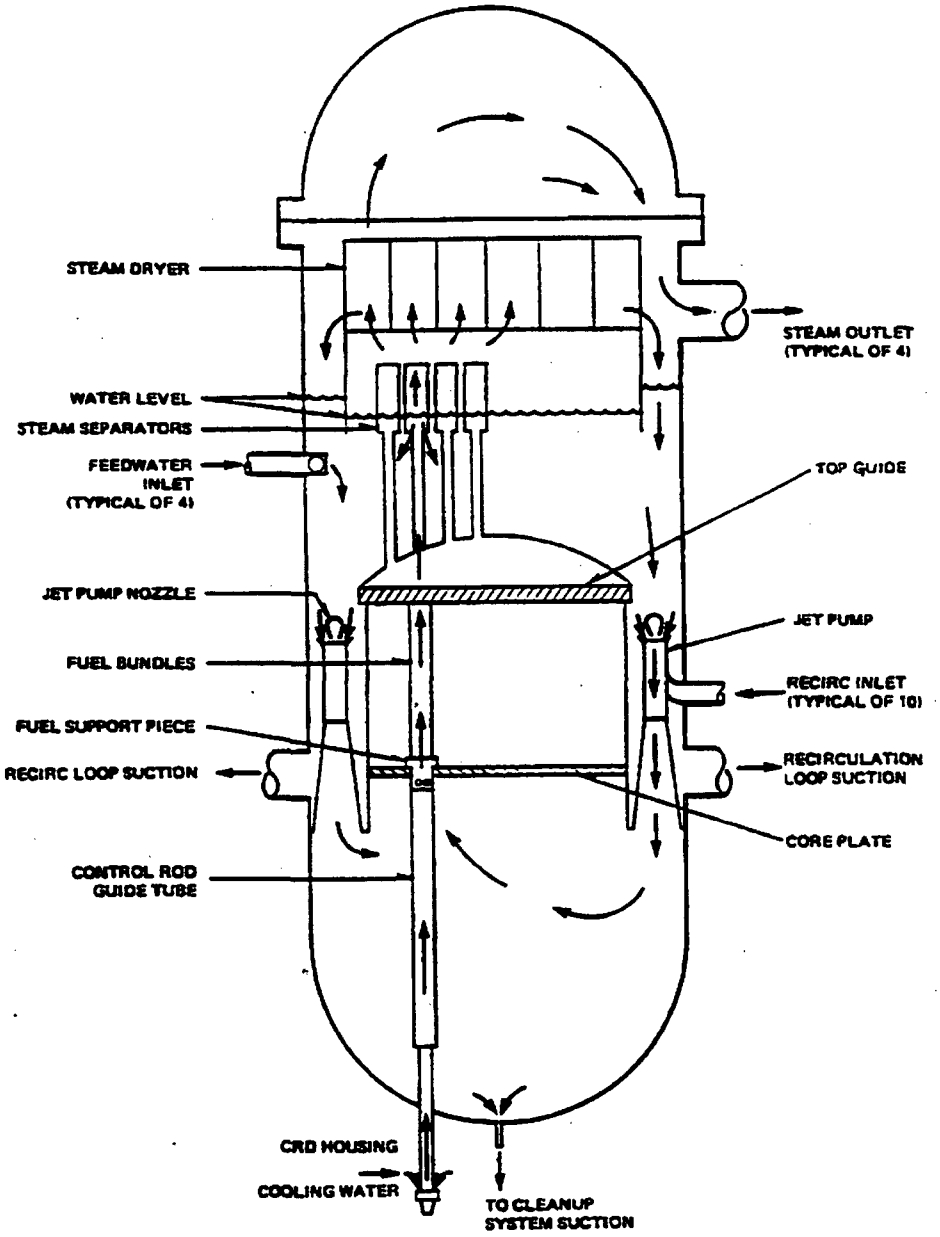

Figure B.10.2. Schematic of coolant flow path within BWR pressure vessel.

Figure B.10.3. Schematic of a BWR-6 fuel assembly, illustrating the relationship between the fuel channels and rods, and the different coolant flow paths inside and outside the fuel channels.

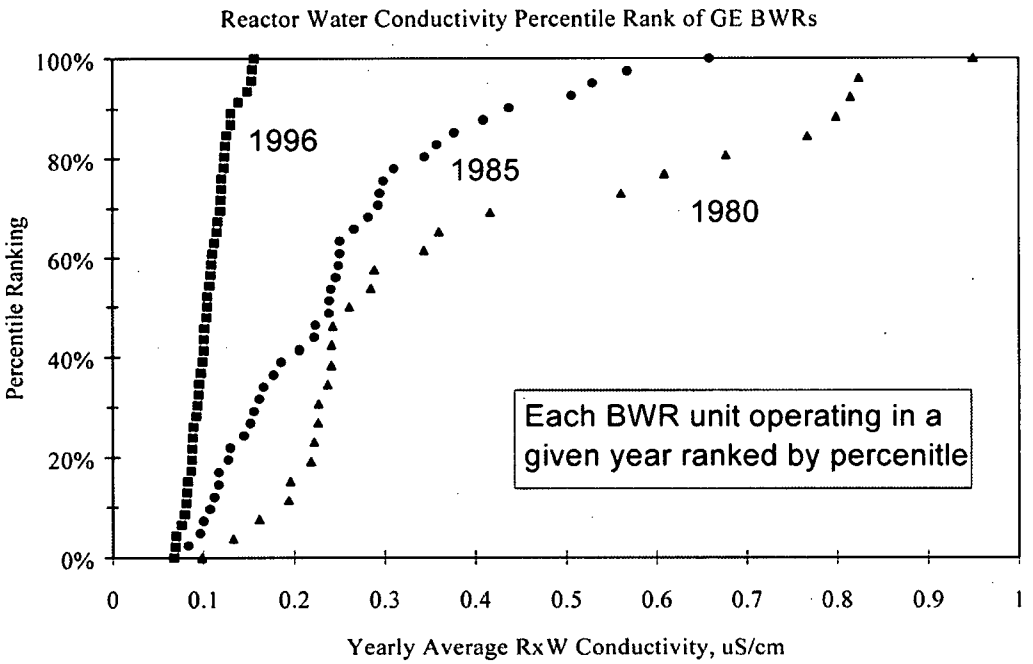

Figure B.10.4. Distribution in reactor coolant purity in the US BWR fleet at specific time periods.

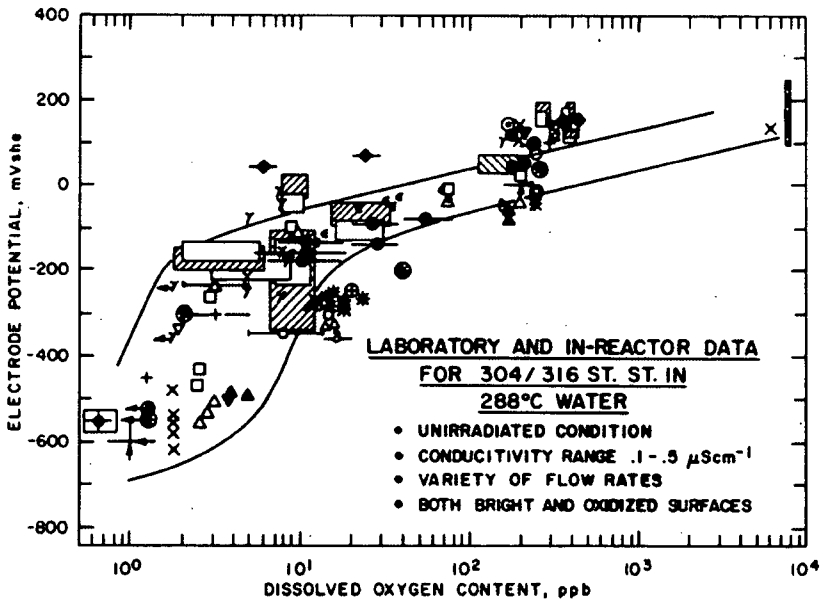

Figure B.10.5. Relationship between corrosion potential of 304 SS and dissolved oxygen content as a function of water temperature [2].

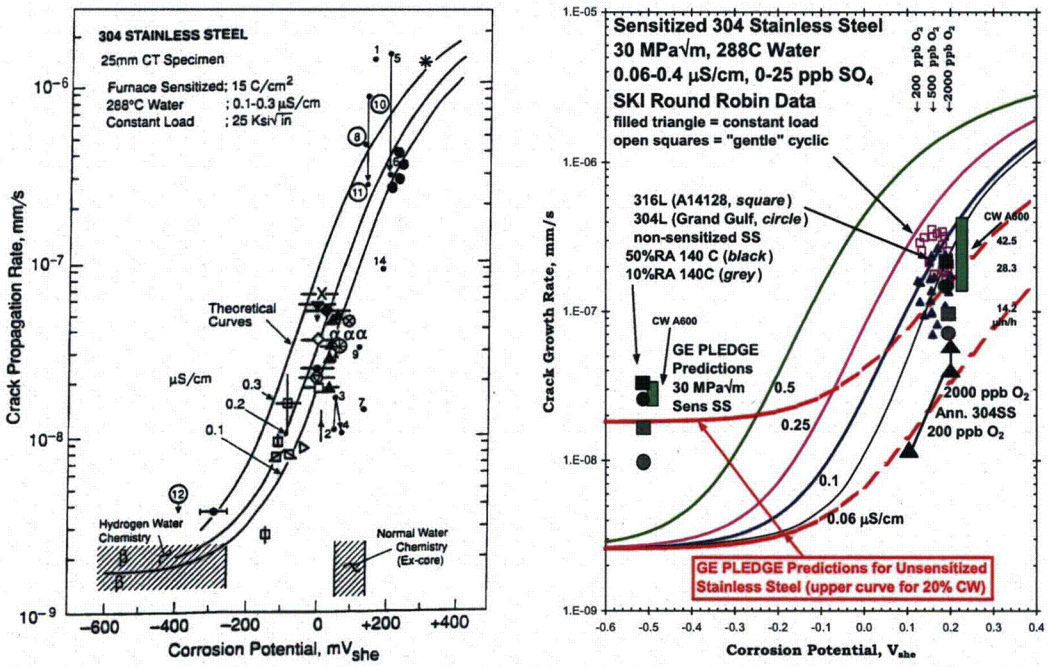

Figure B.10.6. SCC growth rate vs. corrosion potential for stainless steels tested in 288 °C high purity water containing 2000 ppb O_2 and 95 – 3000 ppb H_2.

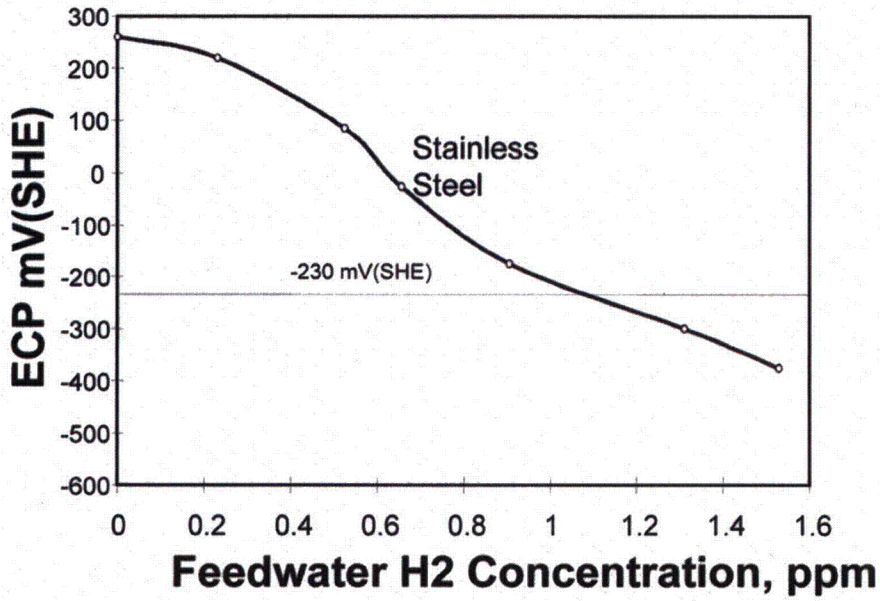

Figure B.10.7. Relation between corrosion potential and injected feedwater hydrogen content observed in feedwater line at a specific BWR.

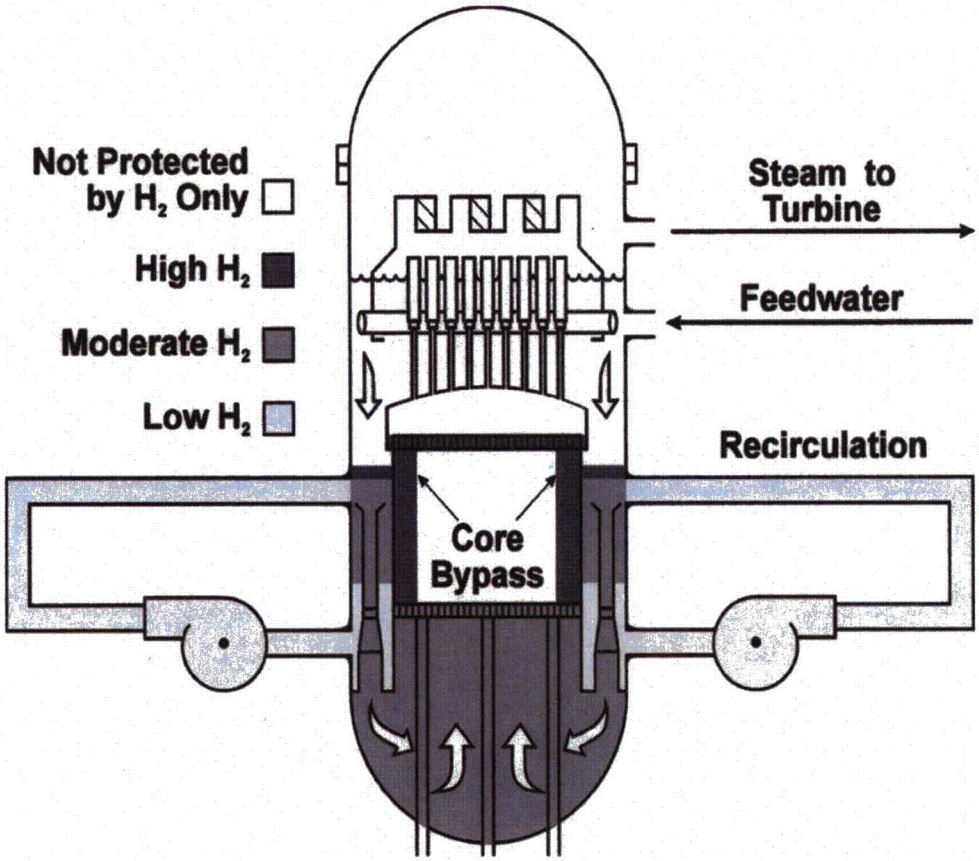

Figure B.10.8. Regions of the pressure vessel internals and recirculation piping protected by hydrogen water chemistry.

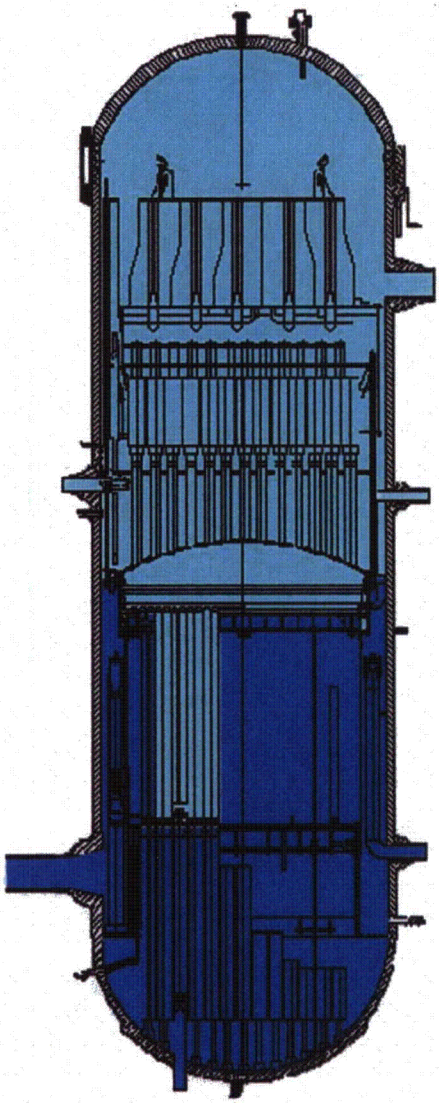

Figure B.10.9. Regions of the reactor core internals, colored dark blue, that are protected by NobleChem™ from stress corrosion cracking and irradiation assisted SCC.

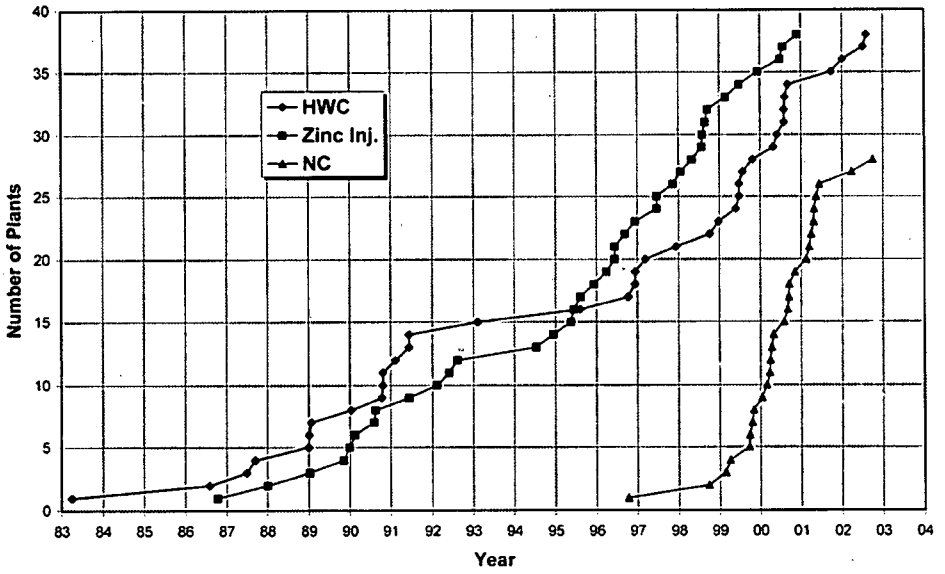

Figure B.10.10. Number of BWR plants transitioning to hydrogen water chemistry and NobleChem™ processes as a function of year.

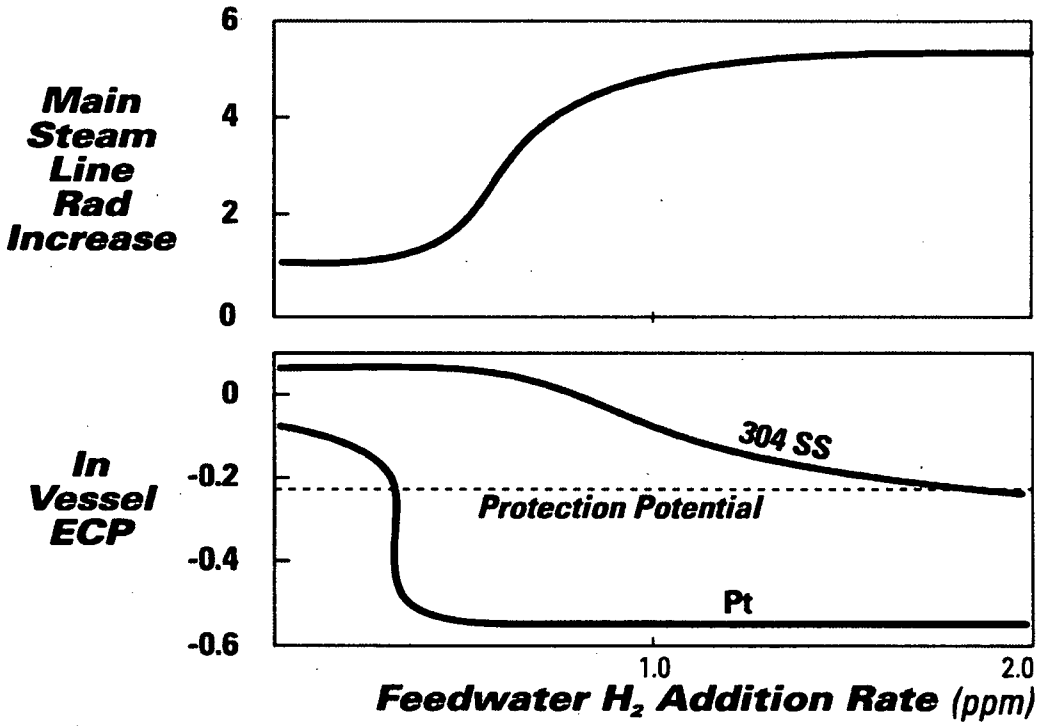

Figure B.10.11. Changes in corrosion potential and main steam line radiation increase as a function of feedwater hydrogen addition rate and the application of NobleChem™.

B. BWR Water Chemistry Guidelines

Introduction

The 2004 revision of the BWR Water Chemistry Guidelines continues to focus on intergranular stress corrosion cracking (IGSCC), which can limit the service life of susceptible materials and components in BWR water environments. In addition, the guidelines place increased emphasis on fuel performance concerns, in view of the increasing incidence of fuel failures since the last revision in 2000. Many plants have adopted noble metal chemical application (NMCA) in the past four years, and this document addresses the resultant issues with IGSCC mitigation, fuel performance and radiation fields.

This document provides proactive water chemistry recommendations for BWRs during all modes of operation. It summarizes the technical bases for all water chemistry alternatives and provides guidance on the development of plant-specific chemistry programs. The guidelines recommend tightening some limits, relaxing others, and implementing more cost-effective monitoring, which will improve protection against materials and fuel problems and also reduce the risks of loss of output from chemistry transients.

Background

The first edition of these guidelines focused on impurity control to reduce stress corrosion cracking and fuel degradation. Consideration of hydrogen water chemistry to reduce electrochemical potential was added subsequently, and noble metal chemical addition was considered in the latest revision, including the effects on radiation buildup. With fuel heat rates increasing, and examples of corrosion induced fuel failures in recent years, fuel/water chemistry interactions are now a central theme in the latest edition.

The BWR Water Chemistry Guidelines Committee and the Mitigation Committee of the BWR Vessel and Internals Program (BWRVIP) issued this document to provide proactive water chemistry guidance for mitigating IGSCC, maintaining fuel integrity, and controlling radiation fields. The BWR Fuels Focus Group of the Fuel Reliability Program has been closely involved in the development of this document to address the increased industry concern about fuel performance issues. It updates the *BWR Water Chemistry Guidelines - 2000,* providing an enhanced methodology for establishing site-specific BWR water chemistry control programs.

A committee of industry experts collaborated to review the available field and laboratory data on BWR water chemistry controls and their impact on plant operation, corrosion mechanisms, fuel performance and radiation fields. The committee included utility specialists, Nuclear Steam Supply System (NSSS) vendors and fuel vendor representatives, Institute of Nuclear Power Operation (INPO) representatives, consultants, and EPRI staff. The committee identified a range of water chemistry regimes from which utility personnel can select their site-specific program.

Key Points and Technical Issues

The content of this document is summarized below, with major changes from the 2000 revision noted:

Management Issues: Section 1. A recent policy of the U.S. nuclear industry commits each nuclear utility to adopting the responsibilities and processes on the management of materials aging issues described in "*NEI 03-08: Guideline for the Management of Materials Issues.*" Section 1 of the BWR Water Chemistry Guidelines specifies which portions of the document are "*Mandatory,*" "*Needed,*" or "*Good Practices,*" using the classification described in NEI 03-08.

Intergranular Stress Corrosion Cracking: Section 2 discusses the technical basis for water chemistry control of IGSCC. This Section has been updated with the latest information on the effects of impurities such as sulfate and chloride on crack growth rate and covers a wider range of electrochemical potential (ECP). The strong effect of copper ions on the effectiveness of hydrogen water chemistry (HWC) is detailed. The overall goal of demonstrating the effectiveness of mitigating IGSCC of piping and reactor internals using HWC and NMCA is discussed in detail, including the *Guidelines'* relationship to inspection relief programs contained in BWRVIP-62 and BWRVIP-75.

Some of the previous IGSCC concerns in BWRs have largely been resolved by replacing the impacted materials with more IGSCC-resistant materials or by performing simple repairs. However, there is a limit to what can be achieved by replacement and repair. For example, repair/replacement of internals below the core is expensive and could lead to premature shutdown and decommissioning in the worst cases. An aggressive mitigation strategy will reduce the probability of escalating repair costs.

For many BWRs, the best-available initial strategy is likely to be to adopt HWC-M (1.0-2.0 ppm hydrogen in feedwater) to protect components in the lower core region as soon as possible. This provides mitigation to plant components thought to be the most difficult to repair. Plant data should be used to optimize the hydrogen feed rates. For other BWRs, HWC-M may not be economically feasible and the implementation of NMCA will provide the IGSCC mitigation solution.

All utilities not currently using HWC-M or NMCA are recommended to conduct an updated economic analysis. If the analysis indicates that HWC-M or NMCA is cost-beneficial, it is recommended that they implement HWC-M or NMCA to protect components in the lower core and lower plenum region. However, additional fuel technical issues need to be assessed with NMCA implementation. NMCA has several benefits compared to HWC-M such as reduced hydrogen injection rate, operation with NWC dose rates, decreased personnel exposure during operation, elimination of increased localized shielding requirements and increased mitigation of components in the upper shroud annulus. On the other hand, HWC-M offers several benefits compared to NMCA such as no outage time for the "classical" NMCA application, no "crack flanking" concerns and no potential fuel crudding and corrosion issues.

Radiation Field Effects: Section 3. The discussion of the effects of NMCA and zinc injection on radiation fields has been updated with the most recent plant data. The discussion on control of feedwater iron has been strengthened, with the recognition that iron increases fuel crud formation and decreases the efficiency of zinc. The "desired range" recommendations for feedwater iron have been specified as 0.1 – 1.5 ppb for HWC and NMCA plants, and 0.5 – 1.5 ppb for normal water chemistry plants.

The technologies available to mitigate IGSCC via BWR water chemistry control can significantly affect both operating and shutdown dose rates. The injection of hydrogen into the feedwater at levels required for mitigation increases the main steam line radiation level by a factor of 5X and requires either increased shielding or changed operation modes or both. In addition, operation with feedwater hydrogen injection results in increased shutdown dose rates due to increased ^{60}Co uptake into the oxides formed under reducing conditions. Mitigation of the increased shutdown dose rates can be accomplished with feedwater zinc injection.

The NMCA method uses low feedwater hydrogen addition rates and operating dose rates are increased by only 10% or less. To mitigate the increased shutdown dose rates due to increased uptake of ^{60}Co into corrosion films, the reactor water ratio of soluble ^{60}Co to soluble Zn must be kept below 2.0×10^{-5} µCi/ml/ppb. Due to the nature of the restructuring of the corrosion films during initial operation during the first post NMCA cycle the resulting shutdown dose rates can be kept very low if this ratio is established early in the first post-NMCA cycle. For this reason, some plants may need to increase feedwater zinc concentrations. Increased zinc may also be desirable for a period following a chemical decontamination. However, because of fuel performance concerns, it is best to limit the average feedwater zinc concentration value (below 0.6 ppb for HWC and 0.4 ppb for NMCA plants) while establishing and maintaining this ratio. Feedwater iron input is also an important parameter to control shutdown radiation dose rates. A long-term goal of less than 1 ppb input is recommended with a minimum value of either 0.1 ppb or 0.5 ppb. Establishing this goal will make establishing the $^{60}Co(s)$/ Zn(s) ratio much easier when limiting feedwater zinc levels as suggested above.

Flow Accelerated Corrosion (FAC): Section 4. Flow-accelerated corrosion (also called flow-assisted corrosion and, misleadingly, erosion/corrosion) causes wall thinning of carbon steel piping, vessels, and components. The wall thinning is caused by an increased rate of dissolution of the normally protective oxide layer, (e.g., magnetite), that forms on the surface of carbon and low alloy steel when exposed to high velocity water or wet steam. The oxide layer reforms and the process continues. The problem is widespread in all types of conventional and nuclear power plants. Wall thinning rates as high as ~120 mpy (3 mm/year) have been observed. If the thinning is not detected in time, the reduced wall cannot withstand the internal pressure and other applied loads. The result can be either a leak or complete rupture.

The rate of wall loss (wear rate) of a given component is affected by the alloy composition, the pH at operating conditions, the liquid phase dissolved oxygen concentration, fluid bulk velocity, component geometry and upstream influences, fluid temperature and steam quality.

The effect of NMCA on the corrosion behavior of carbon steel in 550°F (288 °C) water containing various amounts of oxygen and hydrogen was examined and the data confirm that there is no adverse effect of NMCA on FAC. At low oxygen concentrations and a reducing environment, noble metal treatment of carbon steel surfaces raised the corrosion potential to values closer to the hydrogen/water reversible potential, suggesting that FAC of wetted carbon steel components will be reduced under these conditions.

Overall, due to the catalytic nature of noble metals, plants that undergo NMCA are able to inject lower amounts of hydrogen while still achieving SCC mitigation of the reactor vessel and internals (wetted regions). Plants with low HWC have higher reactor water oxygen contents when compared to moderate HWC plants. Typical reactor water oxygen levels with low HWC/NMCA plants have often been in the region of 30 to 80 ppb whereas under moderate HWC conditions, the reactor water oxygen is often less than 2 ppb. Consequently, there is less suppression of

radiolysis and a higher oxygen concentration in steam. In those regions of the steam cycle where moderate HWC causes an increase in FAC, there will be less of an increase with NMCA-HWC

Control of Chemistry for Fuel Integrity Concerns. Section 5 discusses water chemistry impacts on fuel integrity, and now includes a discussion of corrosion-related fuel failures. The need for control of feedwater zinc, iron and copper is discussed. Based on fuel integrity issues, quarterly average maxima for feedwater zinc of 0.6 ppb for HWC plants and 0.4 ppb for NMCA plants are recommended. A feedwater copper limit of <0.1 ppb is highly desirable for all plants. Given the industry trend of increasing fuel duty and the possibility of further chemistry modifications for plant system material protection, reducing the feedwater iron to <1.0 ppb should be considered at all plants.

Largely through improvement of cladding nodular corrosion resistance and vigilant utility efforts in maintaining good water purity, no industry-wide events relating to cladding corrosion fuel failure, with the exception of an isolated case, was reported throughout the decade of 1990-2000. However, the industry has experienced rapid changes in fuel designs and the water chemistry environment over the past decade. Higher efficiency fuel designs and operational procedures have been introduced to meet the needs for higher discharge burn-up, longer cycle lengths, and improved cycle economics. Increasing fuel duty can increase rates of deposition of crud and hideout of harmful chemical species if present. Water chemistry conditions that were acceptable in the 1990s may no longer provide adequate margin for maintaining fuel reliability. Thus, the rapid changes in fuel and chemistry have created highly challenging conditions for the industry to maintain the high fuel integrity achieved during the 1990s.

This Section reviews fuel cladding corrosion observations and assess the potential role of water chemistry and possible mitigation measures. The current state of knowledge of the effects of chemistry additives, hydrogen, zinc, NMCA, and impurities, such as Fe, Cu, electro-hydraulic control (EHC) fluid, etc., on fuel crud deposition and Zircaloy cladding corrosion is critically reviewed based on fuel surveillance results, fuel operation experiences, and simulation tests. Finally, recommendations on water chemistry conditions are provided with the aim of mitigating the future occurrence of fuel failures due to accelerated cladding corrosion.

Minimizing tenacious crud formation and preventing intrusion of potentially harmful chemical impurities are two key chemistry considerations to improve fuel operational margin and prevent fuel cladding corrosion-related issues. Each plant must optimize their reactor chemistry programs to maximize fuel performance and minimize the risks to reactor integrity and personnel dose.

BWR Water Chemistry Control: Section 6. Recognizing the increasing urgency of corrective actions with increasing impurity concentrations, the following rationale was used for establishing water chemistry control parameters, recommended operating limits, and recommended monitoring frequencies:

- Ingress of impurities into the RCS should be kept to a practical and achievable minimum.

- The oxidizing power of the reactor water should be maintained below a value at which both laboratory and specific reactor experience demonstrate that sensitized austenitic stainless steels and nickel-based alloys do not exhibit significant rates of IGSCC.

- Action levels should be based on quantitative information about the effects of the chemistry variables on the corrosion behavior of RCS materials, fuel performance and radiation field buildup. In the absence of quantitative data, achievable action level values should be specified.

- Action Levels and responses to exceeding Action Levels can vary with the approach to chemistry control, i.e., normal water chemistry (NWC), hydrogen water chemistry (HWC), or HWC following noble metal chemical application (NMCA).

- Recommended control, diagnostic and confirmatory parameters should be reliably measurable at the levels specified using currently available equipment and procedures.

- Monitoring frequencies should be established with the recognition that utility resources should be devoted to high-priority work.

This section comprises the recommendations for water chemistry control and diagnostic parameters, for start up, operation and shutdown. These now include separate tables for hydrogen water chemistry, HWC/ NMCA and normal water chemistry. The Action Level tables now address the possibility that IGSCC may be reduced with continued operation if the Action Levels are exceeded.

Recommended Goals for Water Chemistry Optimization: Section 7. This is a new section containing recommended goals for water chemistry optimization. These are "good practice" recommendations for targets that plants may use in optimizing water chemistry that balances the conflicting requirements of materials, fuel and radiation control. Significant time and expense may be required to meet these targets; thus efforts to achieve these goals should be considered in the context of the overall strategic plan for the plant.

Data Monitoring and Evaluation: Section 8. This Section discusses recommended chemistry surveillance. Recommendations from the 2000 revision of the *Guidelines* were reviewed. In support of the utilities' need to reduce O&M costs, recommended surveillance and monitoring frequencies were reduced when such could be done without significant adverse impact on plant chemistry.

Appendix A discusses the effects of impurity transients on crack growth rates. It has been considerably enhanced, including two tables of documented BWR transients that have occurred during operation and shutdown, possible water chemistry responses to transients plus examples of decision trees for evaluating actions to minimize the detrimental effects on IGSCC.

Appendix B covers auxiliary systems.

Appendix C is new. It addresses calculations that may be made to correct the measured conductivity for the presence of ionic species that are benign toward system integrity.

Appendix D is a new appendix covering ultrasonic fuel cleaning.

Appendix E updates the appendix on the BWRVIA model in the 2000 revision.

References for B.10 Section B

[1] BWR Water Chemistry Guidelines, 2004 Revision. EPRI Report 1008192

[2] R.L. Jones, "Mitigating Corrosion Problems in LWRs via Chemistry Changes," Power Plant Chemistry, November 2004, pp663-669

[3] R.L. Cowan, "Modern BWR Chemistry Operating Strategies," International Conference on Water Chemistry of Nuclear Reactor Systems, San Francisco, October 2004

B.11 "PWR Primary Water Chemistry Guidelines,"
by Robin L. Jones and Christopher Wood

Introduction

The fifth revision of the PWR Primary Water Chemistry Guidelines, published in 2003, describes an effective, state-of-the-art program from which a utility can develop an optimized program for their plant. The philosophy embodied in this document has generic applicability, but can be adapted to the particular conditions of the utility and the site. The detailed guidelines presented in Volume 1 on operating chemistry and in Volume 2 on startup and shutdown chemistry comprise a program that should serve as a model for the development of site-specific chemistry plans.

Ensuring continued integrity of RCS materials of construction and fuel cladding and maintaining the industry trend toward reduced radiation fields requires continued optimization of reactor coolant chemistry. Optimization of coolant chemistry to meet site-specific demands becomes increasingly important in light of material corrosion concerns in steam generator and reactor vessel penetrations, the movement toward extended fuel cycles, higher duty cores, increasingly stringent dose rate control, decreased refueling outage duration, and reduced operating costs. This document is the sixth in a series of industry guidelines on PWR primary water chemistry. Like each of the others in the series, it provides a template for development of a plant-specific water chemistry program.

Background

Historically, the guidelines focused on radiation field control while maintaining fuel and materials integrity. Thus a trend of gradual increase in recommended pH levels can be seen in successive revisions. With some plants increasing fuel duty, more attention is now been paid to water chemistry/fuel interactions, particularly crud deposition. Increasing pH is also beneficial in controlling crud buildup. The guidelines have always considered the small effects of chemistry on initiation of stress corrosion cracking of nickel-based alloys. Although chemistry effects are minor, one exception has been zinc injection, where a delay in crack initiation has been observed in laboratory tests. Recent crack growth data have also been considered, but again the influence of chemistry was found to be minor. The latest data shows a potential benefit from increasing hydrogen during operation, and this will be addressed in future editions, as will the possibility of mitigating low temperature crack propagation by adjusting shutdown procedures.

The *Guidelines* were prepared by a committee of experienced industry personnel through an effort sponsored by EPRI. Participation was obtained from chemistry, materials, steam generator, and fuels experts to ensure the Guidelines present chemistry parameters that are optimum for each set of operating and material conditions. Each EPRI-member utility operating a PWR participated in generation or review of these *Guidelines*. Therefore, this document serves as an industry consensus for PWR primary water chemistry control. In essence, it is a report from industry specialists to the utilities documenting an optimized water chemistry program.

Key Points and Technical Issues

The content of the 2003 revision is summarized below, with major changes from the previous revision noted:

Volume 1

Relative to Rev. 4 of these *Guidelines*, the major changes in Volume 1 of this document are as follows:

Management Responsibilities: Section 1. The U.S. nuclear industry established a framework for improving the reliability of steam generators, described in "*NEI 97-06: Steam Generator Program Guidelines*" Section 1 of the PWR Primary Water Chemistry Guidelines specifies which portions of Volume 1 *are* required in a "strategic water chemistry plan" to meet the intent of NEI 97-06. Volume 2 of these *Guidelines* addresses aspects of startup and shutdown chemistry practices which are not believed to impact SG tube integrity. Therefore, utilities need not meet the intent of Volume 2 to be in compliance with the NEI Initiative.

Technical Basis for Coolant Chemistry Control: Section 2 has been updated to include recent field experiences, laboratory test results and related investigations. Some of the key changes in Section 2 include:

- The quantitative discussion of the influence of water chemistry on primary water stress corrosion cracking (PWSCC) was updated to reflect recent data and a revised statistical evaluation of relevant test data. This evaluation indicates that use of the higher lithium levels required for constant elevated pH_T regimes (e.g., pH_T of 7.1 - 7.3 constant vs. earlier pH_T 6.9 constant or modified pH_T 6.9 regimes) results in little or no penalty in the characteristic time to PWSCC, and that any chemistry effect will be much smaller than the influence of material composition, stress or temperature. This conclusion is supported by plant experience where no significant effects of higher pH regimes have been observed at French, Swedish and U.S. plants that are experiencing PWSCC at low levels and have increased pH_T from 6.9 or 7.0 to 7.1 or higher. The discussion regarding the effects of hydrogen on PWSCC was revised to reflect recently published information that shows that the hydrogen concentration associated with the highest crack growth rate varies as a function of temperature.

- A brief discussion was added of recent test results regarding low temperature crack propagation (LTCP) in thick parts made from nickel-base alloys X-750, 82, 52, and 690, and how this cracking mode is affected by hydrogen levels in low temperature water.

- The discussion regarding the use of zinc in the field as an additive to mitigate PWSCC was updated. The discussion regarding use of zinc to reduce shutdown dose rates was updated to reflect the continuing encouraging results from both domestic and foreign plants. Even low levels of zinc added continuously are resulting in significant dose rate reductions in U.S. and German plants over multiple cycles. Approximately 20 PWRs are currently injecting zinc, mainly to control radiation fields, but plants using higher zinc concentrations are starting to see a reduction in PWSCC in steam generator tubing.

- An expanded discussion was included of the benefits of constant high pH regimes with regard to crud management, fuel deposits, and radiation dose rate. This discussion ap-

plies to all plants, but is especially relevant to plants with high duty cores where risks of fuel deposits and associated problems such as axial offset anomaly (AOA), or under-deposit clad corrosion failures are a concern.

- The review of the influence of the effects of primary water chemistry on corrosion of fuel cladding and on core performance was updated. The discussion emphasizes the importance of crud to corrosion of cladding, and discusses how increasing core duty increases the potential for crud deposition, cladding corrosion, and occurrence of axial offset anomaly (AOA). The review of fuel issues takes into account substantial industry experience with lithium concentrations up to 3.5 ppm, and use of lithium over 3.5 ppm for short periods of time. The review also reflects increased experience with use of zinc additions to the primary coolant, but indicates that use of zinc still demands successful completion of a field demonstration program for high duty cores. The review updates the evaluation of the effects of high silica on fuel performance, and indicates that increasing amounts of experience with silica levels of up to 3 ppm and even higher have been accumulated with no adverse effects.

Power Operation Chemistry Control Recommendations: Section 3 was revised to provide increased emphasis on the desirability of using a constant elevated pH_T (such as constant pH_T between 7.1 and 7.3) at all plants, but especially those with high duty cores, and to provide guidance with regard to making a transition to a constant elevated pH_T regime. Constant elevated pH_T has been shown to provide benefits in crud management, fuel deposits, AOA, and shutdown dose rates. The guidance also reflects the two potential concerns regarding high pH_T regimes that need to be considered: possible effects of higher lithium (e.g., over 3.5 ppm) on fuel cladding corrosion, and possible effects of higher lithium or pH on PWSCC. With regard to the effects of lithium on fuel, it was agreed to raise the level at which consideration of a fuel vendor review is indicated as being appropriate from 2.2 ppm to 3.5 ppm. Table 3-4, "Reactor Coolant System Power Operation Diagnostic Parameters (Reactor Critical)," was revised to add zinc as a diagnostic parameter. This reflects the Committee decision to recommend that all plants consider the use of zinc for its demonstrated dose reduction benefits.

Methodology for Plant-Specific Optimization: Section 4 was updated to reflect lessons learned from its use since it was first published in Revision 4. This mainly involved revising Table 4-1, "Chemistry Control Program Approaches," to reflect the latest assessments of the positive and negative impacts of various options.

Appendix A "Calculation of pH_T and Data Evaluation methodology," was modified to incorporate first order ionic strength corrections to 25°C values of pH and conductivity relevant to the spent fuel pool, and to include a discussion of thermodynamically predicted pressure and temperature effects on pH that are produced by the strong dependence of the ionization product of water on these variables.

Appendix B "Chemistry Control of Supporting Systems," was thoroughly reviewed and many corrections and improvements were incorporated. The changes made included additions to the descriptions of plant experiences, and some minor changes to the chemistry monitoring tables for the volume control tank, boric acid storage tanks, refueling water storage tank, and spent fuel cooling and cleanup system. Sulfate was added as a diagnostic parameter for the reactor water storage tank and for the spent fuel pool water.

Appendix C "Status of Enriched Boric Acid (EBA) Application," was updated to reflect industry experience of the past few years.

Appendix D "AOA and Ultrasonic Fuel Cleaning," that describes EPRI ultrasonic fuel cleaning technology and field experience demonstrating its promising role in ameliorating AOA and reducing dose rates was added.

Appendix E "Oxygen and Hydrogen Behavior in PWR Primary Circuits," was revised to incorporate a few minor improvements.

A new **Appendix F**, "Sampling Considerations for Monitoring RCS Corrosion Products," was added. It provides a description of typical PWR RCS letdown sampling systems and considerations, and includes descriptions of modern, high temperature, RCS hot leg particulate corrosion product sampling systems that can be used to provide improved monitoring of RCS particulates that are derived by re-entrainment of activated core deposits.

A new **Appendix G**, "Reactor Coolant Radionuclides," was added as an aid to chemistry staff and laboratory personnel for dealing with radionuclides and the potential significance of their trends during transient evolutions as well as trends from cycle to cycle.

A new **Appendix H**, "Definition of High Duty Core," was added to provide guidance with regard to the use and meaning of the high duty core index (HDCI) parameter, which is considered when evaluating effects of chemistry on fuel performance in cores with elevated local assembly steaming or core-wide subcooled nucleate boiling, as discussed in Section 2.4. The HDCI was defined and statistically tested against available cores that produced elevated steaming and/or AOA by the Robust Fuel Program specifically for this revision of the *Guidelines*.

Guidance in both Volume 1 and Volume 2 with respect to oxygen control in pressurizers was revised to reflect the interim guidance issued on August 31, 2001 by the Steam Generator Management Program. In addition, the guidance was expanded to cover control of oxygen during shutdowns, as well as during startups as addressed by the interim guidance.

Volume 2

This second volume of the PWR Primary Water Chemistry Guidelines focuses on startup and shutdown chemistry. As noted for the previous revision, the decision to cover startup and shutdown chemistry in a separate volume was made for two main reasons: (1) the increasingly large amount of information regarding shutdown and startup chemistry contained in the Guidelines warrants a separate volume, and (2) locating the startup and shutdown information in a separate volume separates it from the NEI Steam Generator Initiative requirements of Volume 1. This Volume 2 contains no specific requirements (with limited exceptions identified in Tables 4-2 and 4-3) which must be met by utilities to be in compliance with the NEI 97-06 Initiative. The combined shutdown and startup chemistry coverage in this Volume 2 was updated from that in Revision 4 of the Guidelines to reflect new information and experience gained since issuance of that revision. Volume 2 continues to provide: (1) technical discussions regarding plant experiences with different types of shutdown and startup chemistries; and (2) tables of demonstrated options, together with their perceived benefits and possible negative impacts, for refueling and mid-cycle outages. Section 2 is modified to include the substantially new information since Revision 4 on the nature of fuel deposits and their role in activity transport for plants operating high duty cores. Sections 3 and 4 contain industry guidance for shutdown and startup, respectively, together with accompanying discussion and technical support.

Relative to Revision 4 (March 1999) of these Guidelines, the major changes made to Volume 2 are as follows:

1. Descriptions of the morphology and properties of the newly discovered fuel crud constituents bonaccordite and zirconium oxide were added to Section 2, as well as a discussion of how their largely insoluble nature affects shutdown chemistry strategies.

2. Discussions were added and expanded of methods for monitoring and controlling hydrogen and oxygen concentrations in the pressurizer during shutdowns and startups.

3. Discussion was expanded regarding the use of acid reducing conditions during mid-cycle outages in a manner that might reduce AOA in high duty cores.

4. Plant experience was described that shows strong benefits from using the maximum practical RCS cleanup flow during shutdowns. This experience indicates that modifying system designs to increase the maximum cleanup flow rate can be beneficial.

5. Discussion was expanded of the need and methods to maintain oxidizing conditions in the reactor water through flood-up in order to minimize activity release during that operation.

6. Oxygen control strategies (including hydrogen degassing on shutdown and oxygen removal on startup) appropriate to plants that maintain a two-phase pressurizer are offered that are consistent with material integrity goals for pressurizer materials.

7. A variety of experiences were described regarding use or non-use of reactor coolant pumps during shutdown, including when adding hydrogen peroxide.

8. A discussion was added regarding the benefits of using higher cross-linked resins.

9. Many changes were made to the startup and shutdown tables in Sections 3 and 4. These tables present the various options that are available, and their possible benefits and negative impacts. The changes reflect the experience gained since the last revision, including the topics noted above, and also reflect concerns that the industry must develop methods appropriate to PWR materials, temperature and stress intensities to assess the possibility of low temperature crack propagation (LTCP) in nickel-base alloys.

10. A new Appendix was added that details an example of the decision logic that chemists may find useful when deciding what options are consistent with cycle chemistry goals when faced with unplanned mid-cycle outages whose duration may not be known precisely at the point in time of shutting down the reactor.

References for B.11

[1] "PWR Primary Water Chemistry Guidelines," Revision 5, EPRI Report 1002884, Electric Power Research Institute, 2003.

[2] R.L. Jones, "Mitigating Corrosion Problems in LWRs via Chemistry Changes," Power Plant Chemistry, pp 663-669, November 2004.

[3] K. Fruzzetti, "A Review of EPRI PWR Water Chemistry Guidelines," International Conference on Water Chemistry of Nuclear Reactor Systems, San Francisco, October 2004.

B.12 "PWR Secondary Water Chemistry Guidelines,"
by Robin L. Jones and Christopher Wood

Introduction

The sixth revision of the PWR Secondary Water Chemistry Guidelines, published in 2004, describes an effective, state-of-the-art program from which a utility can develop an optimized program for their plant. Previous revisions of these Guidelines have identified a detailed water chemistry program that was deemed to be consistent with the then current understanding of research and field information. Each revision, however, has recognized the impact of these *Guidelines* on plant operation and has noted that utilities should optimize their program based on a plant-specific evaluation prior to implementation. To assist in such plant-specific evaluations, Revisions 4 and 5, issued in 1996 and 2000, respectively, provided an increased depth of detail regarding the corrosion mechanisms affecting steam generators and the balance of plant, and provided additional guidance on how to integrate these and other concerns into the plant-specific optimization process. Revision 6 retains the format of Revisions 4 and 5, and adds to the detailed information contained in these revisions.

Background

The main thrust of the secondary guidelines has always focused on controlling intergranular stress corrosion cracking of steam generator tubing. Successive revisions have tightened impurity limits, and have added recommendations to control sludge build-up using amines and crevice corrosion through molar ratio control. Future additions will probably consider the use of polyacrylic dispersants to minimize sludge deposition.

A committee of industry experts—including utility specialists, nuclear steam supply system vendor representatives, Institute of Nuclear Power Operations representatives, consultants, and EPRI staff—collaborated in reviewing the available data on secondary water chemistry and secondary cycle corrosion. From these data, the committee generated water chemistry guidelines that should be adopted at all PWR nuclear plants. Recognizing that each nuclear plant owner has a unique set of design, operating, and corporate concerns, the guidelines committee developed a methodology for plant-specific optimization.

This sixth revision of the *PWR Secondary Water Chemistry Guidelines*, endorsed by the utility executives of the EPRI Steam Generator Management Project, represents another step in maintaining proactive chemistry programs to limit or control steam generator degradation, with consideration given to corporate resources and plant-specific design/operating concerns.

Key Points and Technical Issues

Revision 6 of the *PWR Secondary Water Chemistry Guidelines*—which provides recommendations for PWR secondary systems of all manufacture and design—includes the following chapters:

Chapter 1 identifies Management Responsibilities. It also describes which elements of the *Guidelines* are mandatory and "shall" requirements under NEI 03-08, Guideline for the Management of Materials Issues, (consistent with NEI 97-06) and which are recommendations. The only mandatory requirement is to have a Strategic Water Chemistry Plan. "Shall" requirements include the Action Level 1, 2 and 3 control parameters and responses and the hold parameters in the control tables of Chapters 5 and 6, including both values and monitoring

frequencies for these parameters. The balance of the guidance elements provided in the *Guidelines* are recommendations.

Chapter 2 presents a compilation of corrosion data for steam generator tubing and, to a lesser extent, balance-of-plant materials. It is not intended to relate operational bulk water chemistry to the corrosion phenomena, which is covered in Chapter 3. The corrosion data presented in Chapter 2 serve as the technical bases for each of the specific parameters and programs detailed in the balance of the document. Chapter 2 was revised to reflect recent research results regarding specific impurity effects on IGA/SCC, the effects of hydrazine on flow accelerated corrosion, and regarding the effects of amines on secondary side deposition processes.

Chapter 3 discusses the role of the concentration processes in the various locations of the steam generator and the chemistry "tools" available for modifying the resulting chemistry within these concentrating regions. It briefly identifies the supporting aspects of and the considerations for adopting these chemistry regimes. It refers the reader to more detailed documents for application of the chemistry strategies. The treatment of deposit control practices was significantly modified in Chapter 3 to reflect current practices and currently available methods. Chapter 3 also contains an expanded discussion on thermal performance issues, and new sections on the loss of hydrazine scenario and startup oxidant control.

Chapter 4 presents a detailed methodology for performing the plant-specific optimization that can be used to develop a modified chemistry program that satisfies site-specific concerns. Chapter 4 also presents example startup and operating chemistry parameters and limits that can be used as a starting point for site-specific evaluations. The main discussion of integrated exposure was relocated from Appendix A to Chapters 4 and 7, and the discussion was revised to reflect its removal as a diagnostic parameter from Chapters 5 and 6. Chapter 4 was also revised to include a list of items that should be covered in strategic water chemistry plans.

Chapters 5 and 6 present water chemistry programs for recirculating steam generators (RSGs) and once-through steam generators (OTSGs), respectively. These are the chapters most frequently referred to by chemistry personnel. The tables contained within these chapters provide boundaries of the envelope within which plant-specific optimization should occur.

Chapter 5 was revised to incorporate additional guidance regarding control of wet layup during short outages. The condition to which plants should go to as part of an Action Level 3 response was changed to "<5% power" from "hot or cold shutdown." The control tables for RSGs in Chapter 5 were thoroughly reviewed and edited. Some of the more significant changes to the tables were:

- Inclusion of Action Level 2 and 3 actions for loss of hydrazine.
- Addition of a requirement that plants reduce power to below 5% power if sodium, chloride or sulfate exceed 250 ppb, or if they exceed 50 ppb for more than 100 hours, while between 5% and 30% power.
- Reduction in the blowdown impurity level for sodium at the 30% power hold from 20 to 10 ppb, and addition of an explicit recommendation that plants achieve sodium, chloride and sulfate blowdown concentrations below their respective Action Level 1 concentrations prior to exceeding 30% power.

- Additional guidance was added such that plants are no longer required to go to Action Level 3 as long as the impurity concentrations remain below Action Level 2 values.

- Deletion of integrated exposure as a diagnostic parameter, and inclusion of lead and integrated corrosion product transport as diagnostic parameters.

- Addition of a footnote to allow reduced frequency for sampling for copper for plants that are copper free or have confirmed low levels of copper transport (<20 ppt).

Chapter 6 was revised to incorporate additional guidance regarding control of wet layup during short outages. The Action Level 3 response was modified to indicate that there may be some circumstances under which plant shutdown may not be necessary, and to provide an initial two-hour period with impurities over the Action Level 3 limit (but less than 20 ppb) before shutdown is required. Some of the main changes to the OTSG control tables in Chapter 6 were:

- Inclusion of Action Level 2 and 3 actions for loss of hydrazine.

- Deletion of integrated exposure as a diagnostic parameter, and inclusion of integrated corrosion product transport as diagnostic parameters.

- Addition of guidance indicating that monitoring moisture separator drain concentrations of sodium and chloride is the preferred method to monitor these species, as opposed to monitoring them directly in the feedwater.

- Addition of a footnote to allow reduced frequency for sampling for copper for plants that are copper free or have confirmed low levels of copper transport (<20 ppt).

- Addition of a clarifying note indicating that silica limits are provided to protect the turbines and not the steam generators, and therefore do not fall under the purview of NEI 97-06.

Chapter 7 provides information on data collection, evaluation, and management. This chapter covers use of *EPRI chemWORKS*™ modules for evaluating plant data and predicting high-temperature chemistry environments throughout the cycle. Chapter 7 was revised to delete tables detailing sampling data requirements, to add more guidance regarding hideout returns, species to analyze in deposits, and integrated exposure evaluations, and to add a new section regarding effectiveness assessments. A discussion of lead sampling and additional recommendations on corrosion product transport sampling was also added.

Appendix A provides detailed guidance with regard to use of the integrated exposure concept, for example ppb*days. This appendix was created to demonstrate how some plants use integrated exposure in practice. Three plant documents (or summaries of plant documents) are presented, which describe different methodologies for use of integrated exposure.

Appendix B provides a review of PWR steam chemistry considerations. Steam chemistry is controlled in power plants to prevent or control deposition of impurities on turbine blades, to minimize erosion of turbine blades and to control general and localized corrosion of turbine blades and discs, cross over piping and extraction lines. In well-operated nuclear plants, the major consideration for steam chemistry control is the environmentally assisted cracking of

turbine blade/disc attachments and FAC of piping in two-phase regions of the BOP. The latter consideration is addressed through pH control by organic amines and/or ammonia based AVT. This revision of the *Guidelines* continues the approach of helping utilities maintain a proactive chemistry program to limit or control steam generator degradation while taking into consideration limits on corporate resources and plant-specific design/operating concerns.

It is recognized that a specific program applicable to all plants cannot be defined due to differences in design, experience, management structure, and operating philosophy. However, the goal is to maximize the availability and operating life of major components such as the steam generator and the turbine. To meet this goal, an effective corporate policy and water chemistry control program are essential and should be based upon the following:

- A recognition of the long-term benefits of, and need for, avoiding or minimizing corrosion degradation of major components.
- Clear and unequivocal management support for operating procedures designed to avoid this degradation.
- Adequate resources of staff, equipment, funds, and organization to implement an effective chemistry control policy.
- An evaluation of the basis for each chemistry parameter, action level and specification, as well as those of similar guidelines.
- Management agreement at all levels, prior to implementing the program, on the actions to be taken in response to off-normal water chemistry and the methods for resolution of conflicts, and unusual conditions not covered by the guidelines.
- Continuing review of plant and industry experience and research and revisions to the program, as appropriate.
- A recognition that alternate water chemistry regimes, if used, should not be a substitute for continued vigilance in adherence to the guidelines.

References for B.12

[1] "PWR Secondary Water Chemistry Guidelines," Revision 6, EPRI Report 1008224 Electric Power Research Institute, 2004.

[2] R.L. Jones, "Mitigating Corrosion Problems in LWRs via Chemistry Changes," Power Plant Chemistry, pp663-669, November 2004.

[3] K. Fruzzetti, "A Review of EPRI PWR Water Chemistry Guidelines," International Conference on Water Chemistry of Nuclear Reactor Systems, San Francisco, October 2004.

B.13 "Degradation of Fracture Resistance: Low Temperature Crack Propagation (LTCP) in Nickel-Base Alloys,"

by Robin L. Jones and Anne Demma

This topical paper provides a summary of the information currently available on a form of fracture resistance degradation called Low Temperature Crack Propagation (LTCP). LTCP is a form of hydrogen embrittlement which has not yet been identified in commercial nuclear reactors but which causes severe degradation of the fracture resistance of certain nickel-base alloys in laboratory tests performed under specific test conditions. In this paper, the term "LTCP fracture toughness" will be used instead of "fracture toughness (J_{IC})", and "LTCP tearing modulus" instead of "tearing modulus (T)", to describe this phenomenon when using J-R type of tests. The tearing modulus is a measure of the tearing resistance after J_{IC} is exceeded.

The laboratory test results indicate that the LTCP fracture toughness of alloys 600 and 690 in low-temperature water is lower than the fracture toughness (test in air), but that the difference is relatively small[1]. Therefore LTCP is not considered to be an important degradation mechanism for alloys 600 and 690. However, alloys X-750, 182/82, and 152/52 (in order of decreasing susceptibility) all suffer substantial degradation of LTCP fracture toughness in laboratory tests in hydrogenated water when the following conditions are met:

- The test temperature is less than 150°C;
- The dissolved hydrogen concentration in the environment is between 150 and 0 cm^3 H_2/Kg H_20;
- Properly-oriented sharp cracks (e.g., fatigue cracks) are present that are open to the hydrogenated environment;
- The sustained stress intensity factor is higher than the equivalent critical stress intensity factor for LTCP determined from fracture testing, and;
- The stress intensity ramp rate (loading rate) is slow.

Mills et al.[1,2,3,4,5,6,7,8], Lenartova[9], and Symons[10] have performed studies on Ni-base alloys in low-temperature environments. A recent (2004) report by Brown and Mills[5] provides a thorough summary of some of these studies for alloys 82H, 52, and 690. A comparison of load-displacement curves for as-welded alloy 82H specimens is shown in Figure B.13.1[5]. For non-precharged specimens (Figure B.13.1(a)), the material response changes from ductile in 338°C hydrogenated water (similar to air) to brittle (intergranular) in 54°C hydrogenated water. The degree of embrittlement and the intergranular nature of cracking observed in 54°C water can be reproduced in specimens pre-charged in high-pressure hydrogen and then tested in air (Figure B.13.1(b)). This implies that the degradation is due to hydrogen-induced intergranular cracking. The presence of hydrogen at the crack tip, regardless of its source, reduces fracture resistance mostly by reducing grain boundary cohesion and promoting planar slip[7]. The combination of hydrogen-precharging and testing in hydrogenated water (54°C water with 150 cm^3 H_2/Kg H_20) results in additional degradation of LTCP fracture toughness (Figure B.13.1(b)). Presumably, hydrogen from the water further increases the hydrogen concentration ahead of the crack and reduces the loss of pre-charged hydrogen from the crack tip region[7]. The type of intergranular

cracking associated with LTCP in the case of 82H welds is believed to be caused by hydrogen trapping by fine niobium and titanium-rich carbonitrides at grain boundaries[6].

In 54°C water with 150 cm^3 H_2/Kg H_20 at an average pH of 10.2, the LTCP fracture toughness was an order of magnitude lower than the elastic-plastic fracture toughness, J_{IC}, (test in air) for alloys 82H, and 52, and 5 times lower for alloy 690[8]. The LTCP tearing modulus (test in environment) was two orders of magnitude lower than the tearing modulus (test in air) for alloys 82H, and 52[8]. However, the tensile properties of the alloys were unaffected by the environment, except for the total elongation of the weld materials[8]. For all alloys considered, LTCP fracture toughness and LTCP tearing modulus generally increase with increasing water temperature and decreasing hydrogen concentration – these effects are illustrated for alloy 52 in Figure B.13.2. The LTCP fracture toughness is also recovered at high rates of stress intensity factor increase (loading rates), presumably because there is insufficient time to embrittle grain boundaries ahead of the crack.

LTCP does not initiate at as-machined notches, but has been shown to initiate at sharp natural weld defects[5]. Testing showed that weld root defects and fatigue pre-cracks exhibit similar LTCP responses[5]. Mills et al. were not able to conclude (from the results of cooldown testing of alloy 82H under constant displacement[5]) whether or not residual stress contributes to LTCP. Given these results, residual stress cannot be eliminated as a contributor to LTCP, to date.

An EPRI study confirmed the Mills et al. test results for alloy 82H[11]. In rising-load tests at a temperature of 54°C in pH 10 water with 150 cm^3 H_2/Kg H_20, the LTCP fracture toughness of alloy 82H was an order of magnitude lower than the fracture toughness. Alloy 182 was also investigated in this study and its LTCP fracture toughness was also an order of magnitude lower than the fracture toughness under similar test conditions. Reducing the concentration of hydrogen to 100 cm^3 H_2/Kg H_20, and testing at pH 7 in simulated primary water, did not alter the magnitude of the difference between the LTCP fracture toughness and the fracture toughness in alloy 182. A current EPRI study is investigating the effects of chemical conditions closer to those typical during shutdown as well as the effects on LTCP in alloy 182 of using stress corrosion cracking (SCC) to produce the starter cracks instead of fatigue. The current test conditions are 30 or 10 cm^3 H_2/Kg H_20 water at 54°C, pH of 4.5, and an extension rate of 10^{-6} in. s^{-1}. The preliminary results for the tests with fatigue pre-cracks indicate that alloy 182 still exhibits a factor of 5 difference in 30 cm^3 H_2/Kg H_20 water between the LTCP fracture toughness and the fracture toughness and a factor of 4 difference in 10 cm^3 H_2/Kg H_20 water. Reducing the pH from 7 to 4.5 slightly increases the LTCP susceptibility (slight reduction in LTCP fracture toughness from pH 7 to 4.5). The data also indicate that LTCP fracture toughness is lower for a high temperature SCC starter crack than for a transgranular fatigue crack. Finally, the data indicate that as the dissolved hydrogen in the environment is decreased, part of the LTCP fracture toughness is recovered; but the LTCP fracture toughness in environment with no dissolved hydrogen is still lower than the fracture toughness.

Alloy X-750 is a precipitation-hardened high-strength nickel-base alloy used for bolts and springs in PWR service. Several studies related to LTCP have been performed on this alloy by Mills et al.[2] and by Symons[10]. X-750 is highly susceptible to LTCP below 150°C in pre-cracked specimens, especially in earlier heat treatments (AH and BH), with growth rates as high as 7 mm/min[2]. It appears that phosphorous and sulfur at grain boundaries act as hydrogen traps and increase the LTCP susceptibility[2]. The grain boundary carbides were shown to control the embrittlement of this alloy[10]. Some testing performed by Mills et al. in argon-sparged water[2], which corresponds to a non-hydrogenated water environment, shows that K_{Pmax} (stress intensity at maximum load) obtained during a rising load test is lower in non-hydrogenated water than in

air for X-750[2]. These observations suggest that the corrosion-generated hydrogen at the crack tip is sufficient to cause embrittlement for alloy X-750 in non-hydrogenated water.

The critical source of hydrogen for LTCP appears to be the environmental hydrogen, as the hydrogen has to diffuse only for a very short distance to get to the highly strained region ahead of the crack tip (Figure B.13.3) and therefore the hydrogen concentrations required to embrittle the crack tip in a water environment are very low (probably on the order of a few ppm)[5,10]. By contrast, in precharged specimens tested in air, hydrogen levels at the crack tip approach zero. The critical cracking location moves inboard toward the peak hydrostatic stress location where strains are much lower (Figure B.13.3); hence, higher local hydrogen concentrations are needed to embrittle grain boundaries. The hydrogen previously diffused in the metal from operation can be an additional hydrogen source for LTCP; but it is not identified as sufficient on its own, as the hydrogen concentrations in the bulk of the metal resulting from operation are low compared to the concentration required to embrittle hydrogen-precharged specimens.

EPRI has begun an assessment of whether or not the conditions necessary for the occurrence of LTCP exist in PWRs[12]. The necessary conditions for LTCP are material susceptibility, low temperature, hydrogen concentration, sharp cracks, sustained stress/strain level, and low strain rate. The hydrogen and temperature conditions that cause LTCP can be present in some PWRs depending on plant and shutdown practices[13,14], but do not appear to be present in PWR startups[15]. The sharp cracks that cause LTCP to initiate can potentially be present in the form of SCC cracks[16,17] or lack-of-fusion defects in alloys 82/182[18] and particularly in alloys 52/152, which exhibit weldability problems[19]. Some stress analyses for components like reactors vessel nozzles have been performed for critical PWR shutdown conditions. Preliminary results suggest that actual stress intensity factors in PWR components are lower than the equivalent critical stress intensity factor for LTCP for detectable crack sizes, but high enough to raise some concern. The current stress analysis for an RPV outlet nozzle butt weld with an ID weld repair showed that stress intensity factors were lower than the equivalent critical stress intensity factor determined from fracture testing for a circumferential flow. For an axial flaw equal to or under 0.5 inch deep, the current stress analysis also showed that stress intensity factors were lower than the equivalent critical stress intensity factor. Additional analyses are necessary, including some repaired components cases and using stress redistribution with crack growth for the stress intensity factors calculation. Finally, the strain rates during shutdown appear to be low enough that there is sufficient time for hydrogen to embrittle the region ahead of the crack.

Additional work is required to determine unequivocally whether or not LTCP of nickel-alloy components can occur under PWR primary system service conditions. Nevertheless, several interim conclusions can be reached at this point:

- First, because LTCP is only significant at temperatures below 150°C, it is not an issue either during normal power operation or during those stages of plant cool-down and start-up when the temperature of the primary coolant is above 150°C.

- Second, LTCP is unlikely to occur during either the stages of plant shut-down when the system is depressurized and hydrogen peroxide has been added or those stages of plant start-up when the temperature is below 150°C, because the primary coolant is not hydrogenated during these periods and the calculated hydrogen concentrations resulting from previously diffused hydrogen in the material are low compared to the concentration required to embrittle hydrogen-precharged specimens.

- Third, although most of the conditions required for LTCP are (or, potentially, could be) satisfied during the stages of cool-down when the coolant is hydrogenated and the temperature is below 150°C, additional stress analyses are required to determine whether or not the mechanical requirements (K levels) for LTCP identified in the laboratory tests are likely to be met in any nickel-alloy components, as well as additional testing to investigate the effects of loading, as most of the tests performed on LTCP to date are rising load tests.

Finally, additional laboratory tests and plant impact assessments should be considered to determine whether stopping hydrogenation of the primary coolant at an earlier stage of plant cool-down would be an effective and acceptable countermeasure to LTCP.

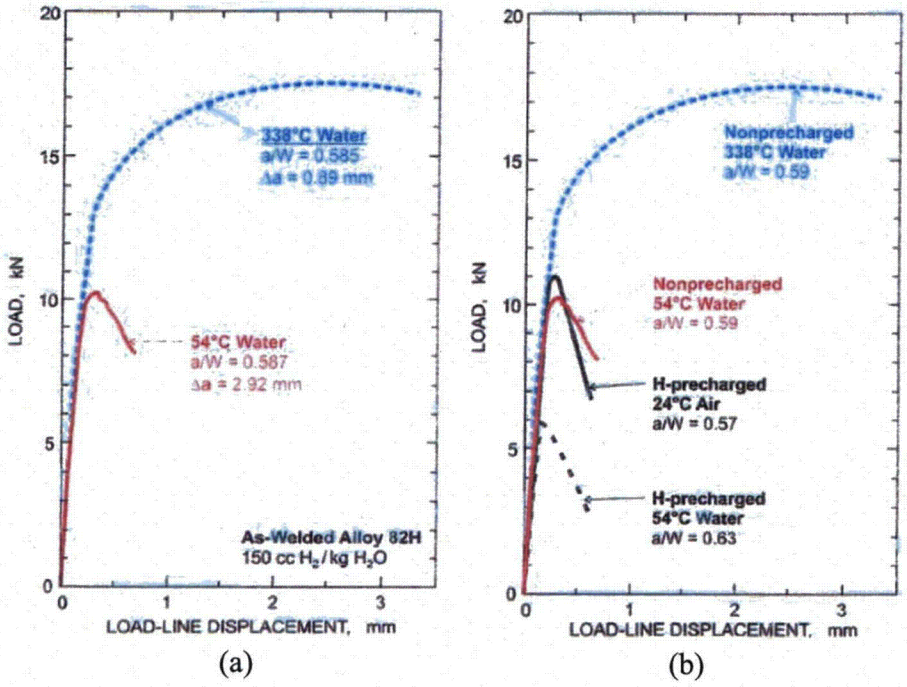

Figure B.13.1 Load-displacement curves for as-welded 82H[5]

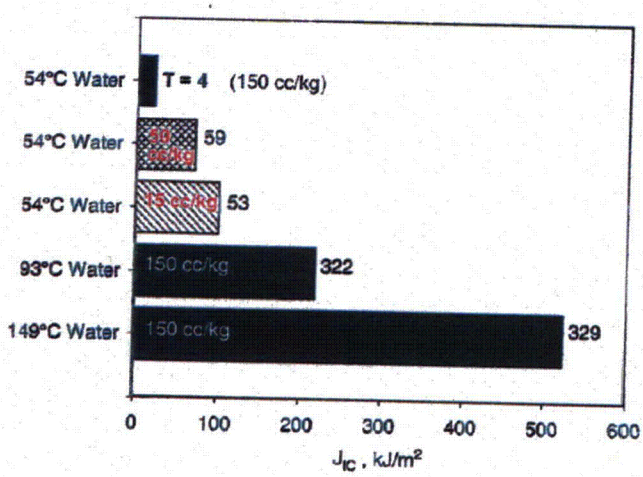

Figure B.13.2 LTCP fracture resistance (in water) of alloy 52 welds (values of LTCP tearing resistance are provided beyond each bar)[1,5]

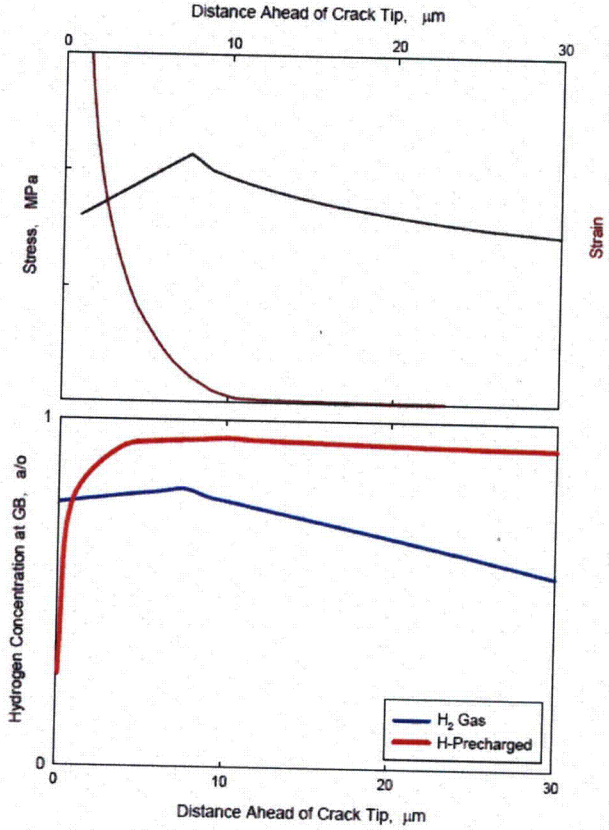

Figure B.13.3 Stress, strain and hydrogen concentration at grain boundaries for either specimens in environmental hydrogen (H_2 gas) or hydrogen precharged specimens (H-precharged), as a function of distance ahead of the crack tip[5]

References for B.13

[1] W.J. Mills, C.M. Brown, "Fracture Behavior of Nickel-Based Alloys in Water," Ninth International Conference on Environmental Degradation of Materials in Nuclear Power Systems - Water Reactors, pp. 167-174, TMS, 1999.

[2] W.J. Mills, M.R. Lebo, J.J. Kearns, "Hydrogen Embrittlement, Grain Boundary Segregation, and Stress Corrosion Cracking of Alloy X-750 in Low- and High-Temperature Water," *Metallurgical and Materials Transactions A, 30A*, pp. 1579-1596, 1999.

[3] C.M. Brown, W.J. Mills, "Fracture Toughness of Alloy 690 and EN52 Welds in Air and Water," *Metallurgical and Materials Transactions A, 33A*, pp. 1725-1735, 2002.

[4] W.J. Mills, C.M. Brown, "Fracture Toughness of Alloy 600 and an EN82H Weld in Air and Water," *Metallurgical and Materials Transactions A, 32A*, pp. 1161-1174 2001.

[5] W.J. Mills, C.M. Brown, "Low Temperature Crack Propagation Behavior of Alloy 82H Welds, Alloy 52 Welds and Alloy 690," Report B-T-3549, 2004.

[6] W. J. Mills, C. M. Brown, M. G. Burke, "Effects of Microstructure on Low Temperature Cracking Behavior of EN82H Welds," Tenth International Conference on Environmental Degradation of Materials in Nuclear Power Systems - Waters Reactors, NACE, 1999.

[7] W.J. Mills, C.M. Brown, "Fracture Toughness of Alloy 600 and EN82H Weld in Air and Water," Report B-T-3264, 1999.

[8] C.M. Brown, W.J. Mills, "Effect of Water on Mechanical Properties and Stress Corrosion Behavior of Alloy 600, Alloy 690, EN82H Welds, and EN52 Welds," *Corrosion, 55*, No. 2, pp.173-186, 1999.

[9] I. Lenartova, « Fragilisation par l'Hydrogène et Corrosion Sous Contrainte d'Alliages de Nickel et d'un Acier Inoxidable Utilisés dans les Generateurs de Vapeur: Influence de la Composition Chimique et de la Microstructure, » (English translation: Hydrogen Embrittlement of Nickel Base Alloys and a Stainless Steel Used in Steam Generators: Influence of Chemical Composition and Microstructure), PhD Thesis, Ecole Centrale de Paris, 1996.

[10] D.M. Symons, "A Comparison of Internal Hydrogen Embrittlement and Hydrogen Environment Embrittlement of X-750," *Engineering Fracture Mechanics, 68*, pp. 751-771, 2001.

[11] Materials Reliability Program: Low-Temperature Cracking of Nickel-Based Alloys and Weld Metals (MRP-108), Electric Power Research Institute, and U.S. Department of Energy, 2004.

[12] A.G. Demma, A.R. McIlree, "Low Temperature Crack Propagation," EPRI White Paper, Electric Power Research Institute, November 2004.

[13] "PWR Shutdown Chemistry Practices," EPRI TR-109569, 1998.

[14] Proceedings of the June 2004 EPRI PWR Primary Shutdown Workshop, Electric Power Research Institute, 2004.

[15] Analysis Report on 1999-2001 Field Experience with Elevated, Constant pH, Electric Power Research Institute, 2001.

[16] Materials Reliability Program: Reactor Vessel Closure head Penetration Safety Assessment for U.S. PWR Plants (MRP-110), Electric Power Research Institute, 2004.

[17] Materials Reliability Program: Welding Residual and Operating Stresses in PWR Plant Alloy 182 Butt Welds (MRP-106), Electric Power Research Institute, 2003.

[18] Materials Reliability Program: Evaluation of the Effect of Weld Repairs on Dissimilar Metal Butt Welds (MRP-114), Electric Power Research Institute, 2004.

[19] Materials Reliability Program: Resistance to Primary Water Stress Corrosion Cracking of Alloys 690, 52, and 152 in Pressurized Water Reactors (MRP-111), Electric Power Research Institute, 2004.

B. 14 "Fatigue,"
by Tetsuo Shoji and Karen Gott

Fatigue life evaluation (S-N approach)

High-cycle fatigue

The most 'classical' fatigue-related degradation mechanism is high-cycle (HC) fatigue. HC fatigue involves a high number of cycles at relatively low stress amplitude (typically below the material's yield strength but above the fatigue endurance limit of the material).[i] The crack initiation phase is dominant here, since crack growth is usually fairly rapid. High cycle fatigue may be:

Mechanical in nature, i.e. vibration or pressure pulsation, or due to flow-induced vibration (FIV). FIV can induce HC fatigue in otherwise normally passive components merely through interaction of flow adjacent to the component or within the system, establishing a cyclic stress response in the component. Power uprates are of some concern here, as an increase in flow may change the acoustical characteristics of the system and excite a HC mode where a resonant frequency is achieved.

Thermally induced due to mixing of cold and hot fluids, where local instabilities of mixing lead to low-amplitude thermal stresses at the component surface exposed to the fluid.

Due to combinations of thermal and high cycle mechanical loads, such as might occur on pump shafts in the thermal barrier region.

Low-cycle fatigue

Low cycle fatigue is due to relatively high stress range cycling where the number of cycles is less than about 10^4 to 10^5. To induce cracking at this number of cycles requires that the stress/strain range causes plastic strains that exceed the yield strength of the material. Cycling thus causes local plasticity leading to more rapid material fatigue degradation. In reactor coolant system components, the cumulative combined effects of reactor coolant system pressure and temperature changes are considered in the component design analysis. The stress or, more correctly, strain cycling that contributes to low cycle fatigue is generally due to the combined effects of pressure, piping moments and local thermal stresses that result during reactor operation. The latter are usually highest in connection with transients (such as plant start-up/shut-down or hot stand-by). Particular attention must be paid to the possibility of locally high component stresses (e.g. from notch effects at welds or from piping restraints), even though nominal system design criteria are met.

---

[i] One of the recent concerns for fatigue cracking is "Giga Cycle" fatigue, which may take place beyond the 10^6 cycles usually used to define fatigue endurance guidelines. There are several observations showing a change in the mechanism of crack initiation. In Giga Cycle fatigue, cracks initiate inside the material, not from a surface, as commonly observed in normal HC fatigue Also, there is almost no data on environmental effects for Giga Cycle fatigue, which may be related, for example, to the failure of socket welds.

The major difference between high and low cycle fatigue is that, for low cycle fatigue, it is the crack growth rate which dominates component life, since crack initiation can occur after relatively few loading cycles. Fatigue crack propagation is discussed separately in Section II.

Thermal fatigue

Thermal fatigue is due to the cyclic stresses that result from changing temperature conditions in a component or in the piping attached to the component. Thermal fatigue may involve a relatively low number of cycles at a higher strain (e.g., plant operational cycles or injection of cold water into a hot nozzle) or due to a high number of cycles at low stress amplitude (e.g. local leakage effects or cyclic stratification). Although such issues have been known (and intensively studied) for many years, fatigue damage sometimes still occurs (see Section 6) when unexpected thermal loading is encountered, e.g. due to thermal stratification arising from incomplete mixing of water streams at different temperatures, which has led to significant incidents (e.g. at feedwater nozzles).

Environmental fatigue

Environmental fatigue concerns the reduction in fatigue "life" in reactor water environments compared to "room temperature air" and is also known as corrosion fatigue. It involves two primary aspects: the effects of a reactor water environment on the overall fatigue life of reactor components (i.e. both crack initiation and crack growth), and the potential accelerated growth of an identified or assumed crack-like defect due to cyclic loading in high-temperature water environments. Important examples of the effects on overall life for carbon and low-alloy steels (C&LAS) and for stainless steels (SS) are to be found in the references.[1, 2] Another reference [3] contains extensive discussion of corrosion fatigue crack growth for C&LAS, while the workshop presentations in reference 4[4] give a good overview of what is known here for SS and nickel-base alloys.

With regard to the evaluation of fatigue for component aging management, consideration of the effects of a particular environment on the overall fatigue life is usually more relevant (see Section 5). Environmental acceleration of fatigue crack growth is also important, however, in dispositioning detected/postulated flaws in a component so as to permit continued operation.

It should be noted that confusion often arises through the (unrecognized) use of different definitions for fatigue crack initiation in terms of flaw size. In laboratory studies of low-cycle corrosion fatigue at constant strain amplitude, initiation is usually taken to correspond to a certain load drop (typically 25%) during testing. However this already corresponds to a relatively deep crack, and recent studies[5] confirm that incipient flaws form much earlier during cycling, although they may often not continue to grow. In the field, "initiation" is usually more arbitrarily defined as the crack length/depth that can reliably be detected during non-destructive component examination.

Fatigue crack initiation and crack growth rates are governed by a number of material, structural and environmental factors, such as stress (or, more fundamentally, strain) range, temperature, ECP (usually categorized only approximately as dissolved oxygen content), mean stress, loading frequency (although strain rate and wave form are more fundamental parameters), surface roughness and number of cycles. A factor that has often been left out of consideration to date is degree of coolant purity, which is surprising given the attention paid to this key environmental variable in studies of SCC field behavior. Some data is now available showing just how important this can be, at least for low-alloy steel in oxygenated BWR environments.[6]

In the field, cracks typically initiate at local geometric stress concentrations, such as welds, notches, other surface defects, and structural discontinuities. The presence of pits in the surface of many alloys is often presumed to decrease corrosion fatigue life, since they can act as stress concentrators and potential fatigue crack initiation sites. In fact, however, pitting may often reflect environmentally assisted enhancement of fatigue cracking more indirectly (by indicating the local presence of an aggressive medium at the metal surface[7]) rather than being a fundamental stage in the corrosion fatigue process.

The major factor that has not received adequate consideration in laboratory investigations of environmental fatigue is undoubtedly flow rate. For C&LAS, the high flow rates typical of reactor operation are known to be very beneficial in reducing corrosion fatigue effects (with regard to both the initiation and growth of cracks). For stainless steels, the picture is more complex and experimental work in this area is still ongoing.[8, 9, 10]

Fatigue crack propagation (da/dN vs. ΔK approach)

As has been described above, fatigue life evaluation is based mostly upon S-N curves, but several modes of fatigue crack propagation should also be taken into account in proactive materials aging management. Fatigue crack propagation can be caused by mechanical or thermal fatigue loading, and environmental fatigue effects may contribute to crack growth in both cases. The crack growth characteristics are interpreted in terms of da/dN vs. ΔK, taking account of the stress ratio R and the frequency of loading. Such curves are, of course, dependent upon both materials and the environment.

If environmental effects are present, the flow rate of the medium also affects the crack propagation rate and, in general, a higher flow rate results in a lower crack growth rate for pressure vessel steels in PWR environments. In the case of low alloy steels, local crack tip chemistry can be modified by dissolution of MnS inclusions, thus acidifying the crack tip environment and resulting in higher growth rates for high sulfur materials. Up to now, no systematic crack propagation testing in terms of flow rate effects has been done on austenitic alloys under PWR conditions.

Extensive research on fatigue crack propagation has been done for many years by members of the international cooperative group on cyclic crack growth (ICCGR, former name of the current ICG-EAC group). The outcome has been largely taken into account in ASME Section XI rules for flaw evaluation, although some aspects (e.g. with regard to rules for components exposed to NWC in BWR plants) are still a subject of debate. For PWR environments, in particular, da/dN vs. ΔK curves have been developed based upon a more mechanistic approach, i.e., time domain analysis.

One important issue, which was pointed out already in the 1970s, is the effect of ripple loading on crack growth rate, when the environmental effects associated with simultaneous stress corrosion cracking have to be considered. Such synergy of effects must be taken into account in the PMDA program. For example, low-alloy steels, which have a rather high resistance to SCC in LWR environments, showed crack growth at a stress ratio of 0.98 and high frequency, even in pure water at 85C.

Crack propagation caused by thermal stress is another important area. Many field incidences of cracking are associated with initiation from local thermal stresses due exposure to water streams of different temperatures. However, these thermal stresses cause mostly very shallow cracks, because the temperature changes due to such water mixing are surface phenomena. However,

such shallow cracks may start to propagate by other structural loads (including the effects of weld residual stress).

Significant reduction in the fatigue life of stainless steels has been observed in PWRs, but there is currently no mechanistic interpretation of these phenomena. Fatigue crack growth behavior in PWRs has been observed with mainly marginal enhancement, but it may be important to examine a possible impact on accelerated crack growth in PWR components due to this mechanism and studies are ongoing.

Synergistic effects of microstructural changes by aging at operating temperature and environmental effects can be a potential issue associated with license renewal. One example of such synergy involves dynamic strain aging and environmental fatigue crack propagation. Thermal aging of duplex SS, hydrogen entry into structural materials and irradiation can be other important microstructural changes with aging.

ASME Code rules on fatigue

Design against fatigue damage is based primarily on the fatigue curves in Section III, Appendix I (e.g., Figures I-9.1 and I-9.2) of the ASME Code. These curves indicate the number of stress cycles at a given amplitude of cyclic stress that is required to reach a so-called usage factor of 1.0. The fatigue curves are based on test data taken in air at room temperature, but reduced by a factor of 2 on stress range or 20 on cycles to failure (whichever is most conservative) to account for scatter of data, size effects, roughness, and non-laboratory environments. For carbon and low-alloy steel materials, the most adverse conditions of mean stress are used to correct the test data prior to applying these factors. The exact interpretation of the extent to which so-called "moderate service environments" were already taken into consideration when the ASME Code rules were drafted continues to be a major source of contention (see, e.g., reference 11[11]). Despite many years of development,[12,13] more appropriate treatment of reactor water effects by the application of a so-called environmental fatigue multiplier (F_{en} factor) has not (yet?) found favor in the US within the ASME Code, although it is being applied on a plant-specific basis in the context of license renewal applications.[14] Such approaches are already used in Japan, however,[15] and incorporate specific consideration of key factors such as strain rate, temperature, oxygen content and (for C&LAS) sulfur content of the material.

The ASME Code includes analytical approaches and criteria for determining usage factors for Class 1 components. For Class 1 code components, the cumulative usage factor must be shown to be less than 1.0 for the component life. However, a fatigue usage factor of unity does not imply actual crack initiation both because of the safety factors applied to the stress amplitude or number of allowed cycles for the Code fatigue curves and because of the often conservative nature of the design-basis loads that have been assumed. Fatigue monitoring of real components can be valuable to reveal margins in this context. The assumed load pairs present a particular challenge in evaluating environmental fatigue, where realistic strain rates are a key consideration.[16]

The crack growth that follows fatigue crack initiation can be predicted if the crack can be characterized and if the cyclic stress field is known. Procedures for performing crack growth analyses are contained in Section XI of the ASME Code. Again, the consideration given to environmental effects has sometimes been controversial and the present disposition lines do not necessarily reflect the current state of knowledge.[6] Significant progress has been made, however, for the specific case of LAS in PWR reactor water through the introduction of Code Case N-643,[17] which is currently undergoing further refinement. Work is ongoing to develop

analogous cases for SS in PWR environments and for all classes of material in BWR reactor coolant.

Service experience of fatigue

Mitigation of fatigue damage for existing components is accomplished by reducing the magnitude of the applied loads or thermal conditions or reducing the number of cycles of loading. For thermal transients, reduction in the rate of temperature change for extreme temperature cycles can be effective (although it should be noted that this can also increase any environmental component of damage, if present). However, the normal operating cycles are not generally the source of significant fatigue damage in nuclear plants. The observed fatigue cracking in service has mostly been due to high cycle fatigue as a result of conditions not anticipated at the time of original plant design. Some instances of (very) low-cycle fatigue cracking (with a significant environmental contribution) have also been reported, mainly in Germany.[7]

Major areas of plant where fatigue failures and leakage have occurred are as follows:

RCS Piping

A number of fatigue issues have been identified, as described below.

The major occurrence of leakage has been due to mechanical vibration-induced cracking of small attached lines (primarily socket welded instrument lines). Power uprate has contributed to a number of recent incidences.

Thermal fatigue has also caused cracking in normal flowing lines where relatively colder water is injected into flowing RCS lines.

Thermal fatigue has also occurred in a number of normally stagnant branch lines attached to flowing RCS lines. The source has been thermal stratification/cycling due to valve in-leakage in up-horizontal running safety injection line configurations and swirl-penetration thermal cycling in down-horizontal drain/excess letdown lines. This is being addressed by the MRP Fatigue ITG and new guidelines are to be issued in mid-2005.

Although no occurrences of leakage have been identified, an issue related to surge line stratification was identified in 1988. The issue was resolved by analysis; however, the computed usage factors were quite high. Environmental fatigue effects are potentially significant for these lines.

Other potentially susceptible locations include PWR charging nozzles and BWR RHR tees, where significant thermal transients can occur in some plants.

Reactor Pressure Vessels

The effects of fatigue are adequately managed by adherence to the plant design basis, where thermal transients were considered in the original plant designs. The notable exception was BWR feedwater nozzles and control rod drive nozzles, where the effects of cold water injection caused cracking early in the life of some plants. Mitigating actions and continued monitoring have been implemented and have proved to be effective.

Pressurizers

There have been no known fatigue failures in pressurizers. However, recent considerations of cold water insurge to pressurizers have been identified that may be a contributing factor to leakage that has been observed in pressurizer heater sleeve welds. The pressurizer spray nozzle is also affected by some significant thermal transients. Pressurizer surge nozzles can be affected by thermal stratification conditions in the surge line.

Steam generator shell, tubes, and internals

Steam generator feedwater nozzles have exhibited cracking as a result of thermal stratification and cycling, but high oxygen content of the feedwater for low-power conditions may have also increased environmental effects. Girth weld cracking of the steam generator shells and cracking at feedwater nozzle blend radii have also been observed, where both hot/cold water thermal fatigue and an environmental contribution were identified.

RPV internals components

The major issue identified has been that due to flow induced vibration of BWR steam dryers following power uprates. This has led to cracking of the vessel-attached support brackets at several plants.

Areas for further research

Although fatigue is not perceived to be an issue of safety consequence based on the studies reported in,[18] the combined effects of adverse loadings and environments may lead to more cracking in the future than has been observed in the past. In addition, the effects of power uprate have increased the occurrences of flow induced vibration failures and related damage to component supports. Thus, research in the following areas is recommended:

Develop a better understanding of the relationship between laboratory environmental testing and actual reactor water conditions. The conditions in laboratory testing are often significantly different than those observed in actual flowing reactor water (flow rate is a key variable deserving closer attention here)[ii].. In addition, material conditioning between the extremes of actual cyclic conditions may be beneficial in reducing environmental effects. Although this has been primarily identified as a License Renewal issue, the laboratory effects are real and indicate that the fatigue resistance in a water environment is not as good as was originally thought.

Understand better the extent to which laboratory test data (usually on small specimens) can really be transferred to complex component geometries.

[ii] Most of the experimental work on flow rate effects has been done in BWR environments, where effects of flow rate on fatigue life are very complicated. Sometimes higher flow rate seems to be beneficial and sometime harmful, depending upon materials, DO and corrosion potential. Flow rate affects the thickness of the surface boundary layer, supply rate of oxidants to the surface, removal of corrosion products from surfaces, flush out of cracks and, clearly, local water chemistry. Some experimental data obtained in the EFT program in Japan revealed such complicated effects of flow on fatigue life. More details in Japanese at http://www.jnes.go.jp/katsudou/seika/2003/pdf_kikaku/04kizai-0006.pdf

Investigate high cycle fatigue effects due to hot and cold water mixing. Several incidences of cracking in France have led to EdF embarking on major research programs in this area.

Improve methods for predicting and quantifying flow-induced vibration and acoustic loadings. A number of cases have been identified that have resulted in component wear and failure. Giga Cycle fatigue at very small amplitudes is one of the issues for further investigation here (including environmental effects).

Past attention to fatigue issues has related primarily to pressure-retaining components. Additional, more detailed, evaluations are probably needed to determine flow-induced fatigue effects and safety consequences for reactor internals (and possibly other support components).

Consider whether random loading spectra (which may be more typical of some plant components) are properly represented in the fatigue testing database.

Synergistic effects of various forms of material degradation, such as thermal aging, on fatigue need to be studied, with special emphasis on the effect of ripple loading together with time dependent (SCC) crack growth.

References for B.14

[1] "Effects of LWR Coolant Environments on Fatigue Design Curves of Carbon and Low-Alloy Steels," NUREG/CR-6583, Argonne National Laboratory, March 1998.

[2] "Effects of LWR Coolant Environments on Fatigue Design Curves of Austenitic Stainless Steels," NUREG/CR-5704, Argonne National Laboratory, April 1999.

[3] H.P. Seifert, S. Ritter, J. Hickling, "Environmentally-Assisted Cracking of Low-Alloy RPV and Piping Steels under LWR Conditions", *Proc. 11th Int. Conf. on Environ-mental Degradation of Materials in Nuclear Power Systems – Water Reactors*, 2003, CD-ROM, ANS/TMS/NACE, Stevenson, WA, August 10 – 14, 2003.

[4] Materials Reliability Program: Second International Conference on Fatigue of Reactor Components (MRP-84), Electric Power Research Institute, and Organisation for Economic Co-Operation and Growth (OECD/NEA/CSNI/R (2003) 2), and the U.S. NRC, 2003.

[5] H.D. Solomon, R.E. DeLair, E. Tolksdorf, Proc. 9th Int. Symp. on Env. Deg. of Materials in Nuclear Power Systems –Water Reactors, pp. 865 – 872, TMS, 2000.

[6] J. Hickling, H.P. Seifert, S. Ritter, "Research and Service Experience with Environmentally Assisted Cracking of Low Alloy Steel," PPChem 7(1) pp. 04-12, 2005.

[7] J. Hickling, "Strain-Induced Corrosion Cracking of Low-Alloy Steels under BWR Conditions: Are There Still Open Issues?," Proc. 10th Int. Conf. on Environmental Degradation of Materials in Nuclear Power Systems – Water Reactors, NACE, 2002.

[8] A. Hirano et al., "Effects of Water Flow Rate on Fatigue Life of Carbon Steel in Simulated LWR Environment Under Low Strain Rate Conditions," *Journal of Pressure Vessel Technology, 125*, pp. 52-58, 2003.

[9] A. Hirano et al., "Effects of Water Flow Rate on Fatigue Life of Carbon and Stainless Steels in Simulated LWR Environment," *Journal of Pressure Vessel Technology, 480,* pp. 109-119A, ASME, 2004.

[10] R. Kilian et al., "Environmental fatigue testing of stainless steel pipe bends in flowing, simulated primary water at 240°C," 3rd International EPRI Conference on Fatigue of Reactor Components, Seville, Spain, Oct. 2004 (proceedings to be published by MRP).

[11] W. Alan Van Der Sluys, "PVRC's Position on Environmental Effects on Fatigue Life in LWR Applications," Welding Research Council, Inc. Bulletin 487, December 2003.

[12] "An Environmental Factor Approach to Account for Reactor Water Effects in Light Water Reactor Pressure Vessel and Piping Fatigue Evaluations," EPRI TR-105759, Electric Power Research Institute, December 1995.

[13] H.S. Mehta, "An Update on the Consideration of Reactor Water Effects in Code Fatigue Initiation Evaluations for Pressure Vessels and Piping," *Journal of Pressure Vessel Technology, 410-2,* pp. 45-51, American Society of Mechanical Engineers, 2000.

[14] Materials Reliability Program Guidelines for Addressing Fatigue Environmental Effects in a License Renewal Application (MRP-47), Electric Power Research Institute, U.S. Department of Energy, 2001.

[15] "Guidelines for Environmental Fatigue Evaluation for LWR Component," Thermal and Nuclear Power Engineering Society (TENPES), June 2002 (Translated into English in November 2002).

[16] S. Ranganath, J. Hickling, "Development of a possible bounding corrosion fatigue crack growth relationship for low alloy steel pressure vessel materials in BWR environments", 3rd International EPRI Conference on Fatigue of Reactor Components, Seville, Spain, Oct. 2004 (proceedings to be published by MRP).

[17] ASME Code Case-643, "Fatigue Crack Growth Rate Curves for Ferritic Steels in PWR Water Environment," May 2000.

[18] "Fatigue Analysis of Components for 60-Year Plant Life," NUREG/CR-6674, Pacific Northwest National Laboratory, June 2000.

B.15 "Predicting Failures Which Have Not Yet Been Observed — Microprocess Sequence Approach (MPSA)," by Roger W. Staehle

1. Background

The purpose of this background paper is to describe a conceptual approach to predicting corrosion failures that have not yet been observed but could occur after long times, such as those associated with LWRs that are re-licensed. This approach is in the category of "*proactive*" prediction, where possibly future failures are intentionally sought out, and the credibility for producing failures is assessed. This approach also challenges conventional assumptions about the cause and nature of corrosion failures. In the past, failures have occurred first; and the nuclear materials community, then, has responded usually with excellent work aimed at explaining the observations. This is "*reactive*" research. We are concerned here, rather, with the mechanics of "*proactive*" prediction.

This discussion deals with predicting corrosion processes in LWRs, although the approaches described here would apply broadly to other industries. This discussion is also mainly concerned with stress corrosion cracking (SCC) and corrosion fatigue (CF), as they are connected; and, some aspects of flow-assisted corrosion (FAC) are included. These are the most likely modes of corrosion to produce failures. Other topics of damage include wear of steam generator tubes at anti-vibration bars (AVB), but these are not discussed here, although such modes are within the scope of this approach. As discussed in this paper, failure means the initiation of degradation, its progression, eventual propagation through the component wall, or any combinations of these.

An essential assumption of this discussion is that very long times until failure are not related to a monotonic progression of SCC processes. Rather, the long times are most likely associated with other factors that produce specific local conditions that "open the gate" for SCC or other relatively rapid processes as compared to general corrosion. These preliminary processes occur over a "precursor period." Schematically, such cases are shown in Figure B.15.1. Case I corresponds to SCC, starting upon initial exposure to an environmental condition that produces SCC, as described in Section 2.1; Case I corresponds to failure processes (e.g. to LPSCC) that initiate as soon as the surfaces are exposed to primary water at operating temperature. Case II corresponds to SCC that starts after necessary conditions for initiation are achieved in relatively short times (e.g. half to 20 years), for which there are already examples as described in Section 2.2.

The approach described here for predicting failures, which have not yet occurred, is the "Microprocess Sequence Approach" (MPSA). This approach utilizes sets of elements from the environments and materials where these elements can be identified, and quantified, and connected sequentially or in parallel, to provide a scenario leading to the initiation of failure. The overall procedure is described in Figure B.15.38.

What is actually being predicted here is not the course of the SCC itself but rather the time to arrive at the conditions for SCC to start, as shown for shorter cases in Case II and much longer times in Case III of Figure B.15.1. It is assumed here that existing correlations, (e.g. from Staehle and Gorman[1]) for the occurrence of SCC will be activated once the precursor period has produced the necessary conditions for SCC to initiate.

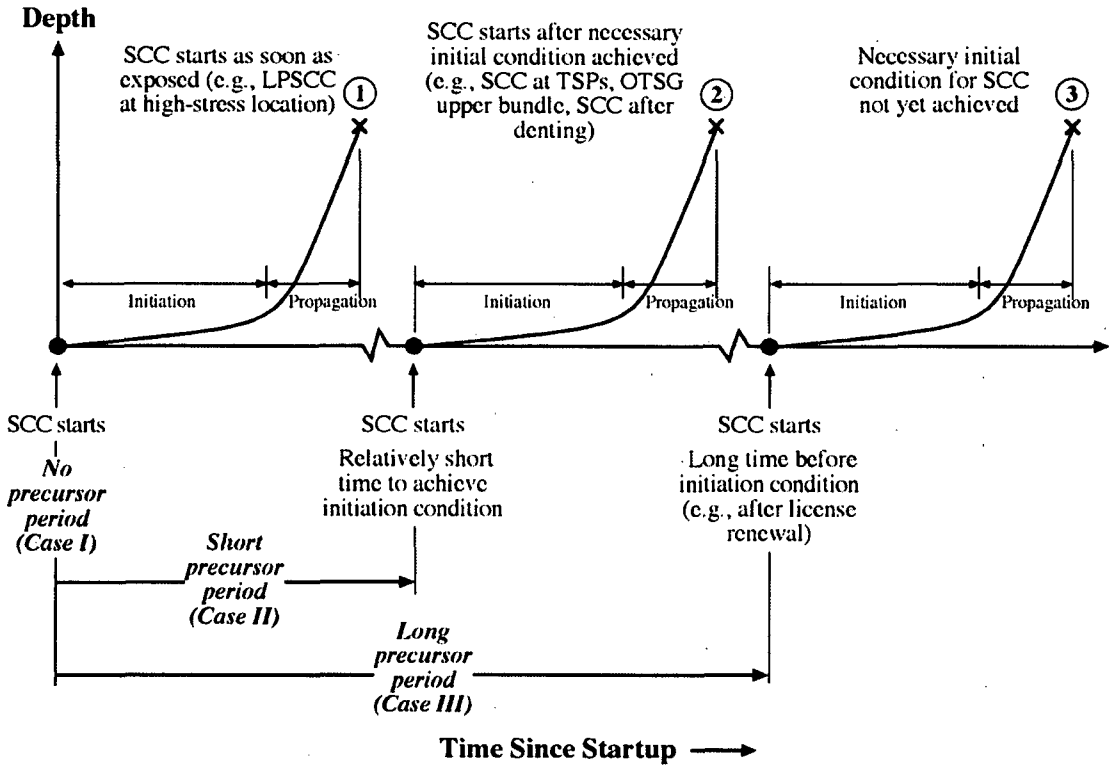

Fig. B.15.1 Schematic view of three cases for the time-dependence of SCC. Initiation and propagation times assumed to be the same. The three cases are differentiated by the length of the precursor periods.

Such longer times should be compared with the range of time over which re-licensing is expected to occur as shown in Figure B.15.2. Relative to the schedule for re-licensing, it appears that instances of SCC in the nuclear industry have occurred in essentially three stages as suggested in Figure B.15.3. In Stage I, failures occurred in the early use of stainless steel tubes and then in Alloy 600 tubes. These failures were extensive. In Stage II, the present stage, SCC is occurring in the laboratory for Alloy 690TT and in the non-decorated grain boundaries of stainless steel. This present discussion about prediction applies to Stage III, where a proactive approach could predict occurrences of future degradation based on the reasonableness of scenarios as described in Section 5.0 and Figure B.15.38. In this Stage III, a relatively long time is consumed by the precursor period in which conditions for the occurrence of SCC must first develop before SCC can start, as shown for Case III in Figure B.15.1.

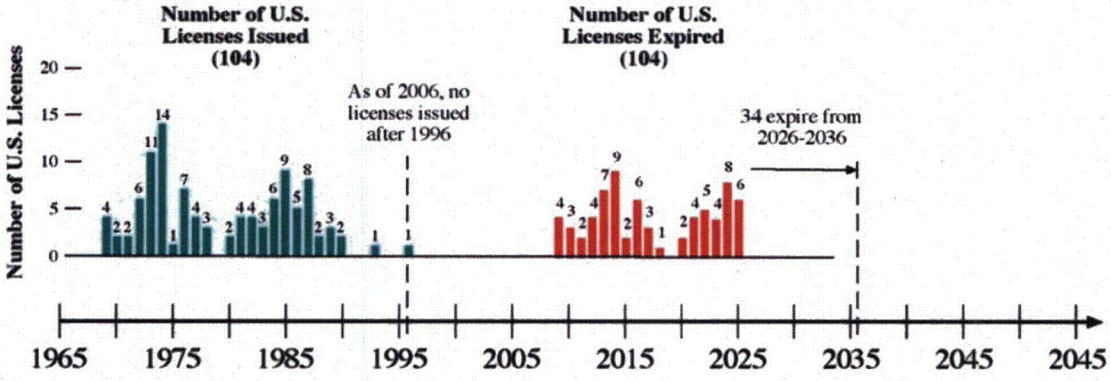

Figure B.15.2 Number of U.S. licenses issued and expired vs. time compared with a 20-year life extension after a presumed re-licensing.

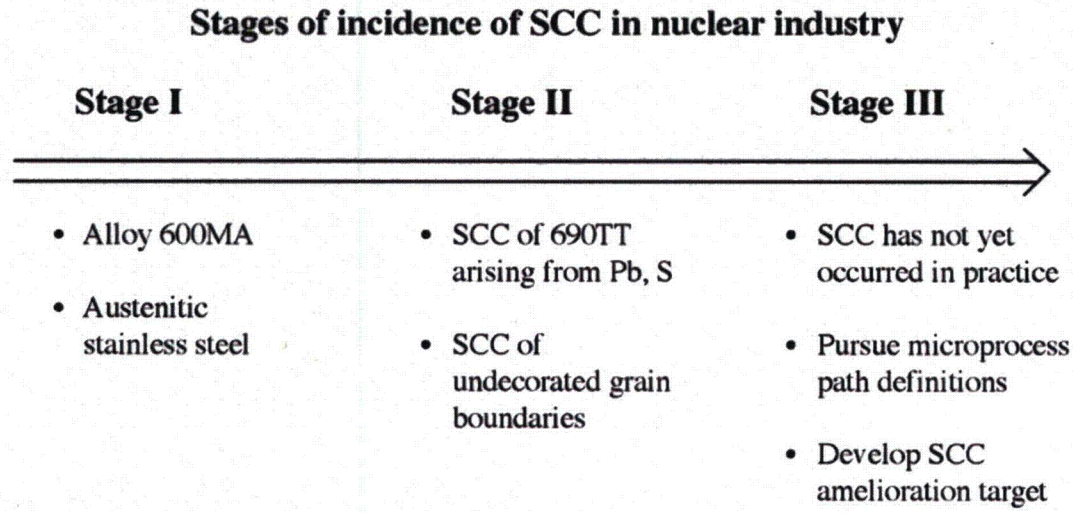

Fig. B.15.3 Schematic illustration of the stages of SCC occurrences over time in the LWR industry.

The theme of this paper is illustrated in Figure B.15.1 for Case III. Here, the conditions that are necessary for SCC to occur have not yet fully developed during the initial licensing period. The central question, then, is: what are the processes that could produce the necessary conditions that lead to SCC at this later time? Our assertion here is that predicting SCC/CF that has not yet occurred, i.e. *proactive* prediction, can be approached credibly by using information and understandings that are already available and linking them in sensible ways to predict the time required for completion of the precursor period, of Figure B.15.1 Case III, before the SCC can start. The challenge, then, is to identify this information and explore out understandings. Such an approach is described in Sections 3.0 and 4.0.

There are, presently, no serious predictive methods for SCC that are not based on extrapolating from already existing failures. Current methods include:

- Accelerated testing and carrying forward the data, usually the mean value, with experimentally determined dependencies such as the activation energy (e.g. Q=40kcal) or the stress exponent (e.g. n=4). This is more or less how performance is predicted at the present.

- Developing correlation equations and choosing limits for scatter (e.g. three sigma) for design, i.e. safety factors.

- Enclosing scattered data with an enveloping curve and assuming that the envelope gives a conservative value.

- Taking a Bayesian statistical approach where successive failures on a cumulative distribution give progressively more confidence to the shape factor and its extrapolation.

- Using probabilistic fracture mechanics where the probability of occurrence of critically sized defects and the probabilistic evaluation of the critical stress intensity provide the basis for the probability of future failures.[2,3,4,5,6]

- Applying a "fitness for service" approach where defects are assessed at some time during service, (e.g. an inspection period), and then assessing whether these defects can lead to potential failures.

- Using the Corrosion Based Design Approach (CBDA), as described by Staehle,[7] involving the ten segments of environmental definition, material definition, mode definition, superposition, failure definition, statistical definition, accelerated testing, prediction, monitoring and inspection, and feedback.

- Using the "Locations for Analysis" (LA_i) approach as described by Staehle,[7] where obvious locations containing multiple stressors of relatively intense values occur together.

- Using physically based statistics for predicting the "First Failure" as described by Staehle.[8,9] Here, each of the statistical parameters is modeled using existing data for the seven primary variables as shown in Figure B.15.4.[1,9,37] The final distribution then, includes the three, now physically dependent, statistical parameters with their respective dependencies.

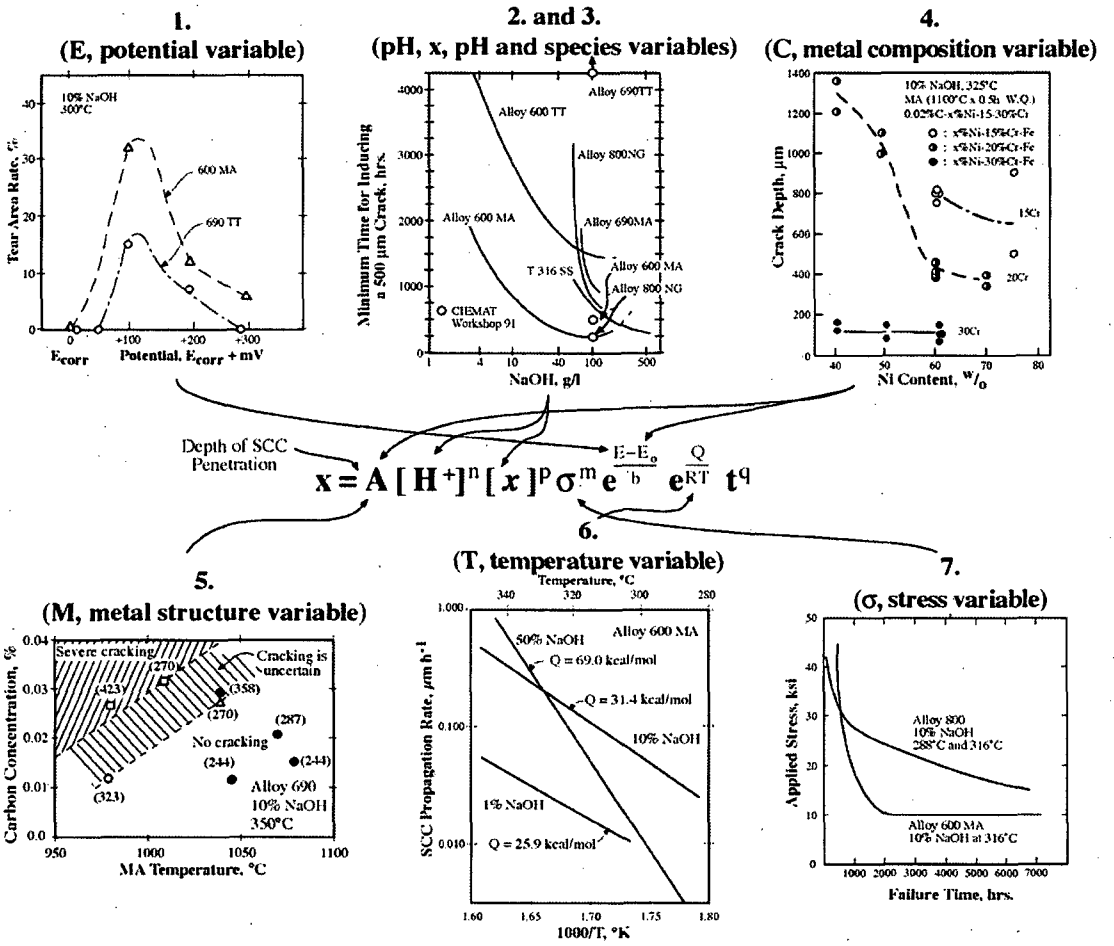

Figure B.15.4 Examples of dependencies on the seven primary variables for SCC as they apply to a correlation equation that might be used to model the statistical parameters for a statistical distribution. These examples are taken from data, which describe SCC in alkaline solutions. These data are discussed by Staehle and Gorman.[1] © NACE International 2003/2004.

A practical question here, is how can failures that have not yet occurred be found? The essence of the approach in this paper, the "Microprocess Sequence Approach (MPSA)" for predicting the precursor conditions that must coalesce before SCC occurs, as indicated in Figure B.15.1, consists of six steps as follows:

- The influences on materials can be divided into six domains and their respective microprocesses. The breakdown of the domains is somewhat arbitrary, but practical and convenient choices are: global environment, bulk environment, outside surface, protective surface layer, inside metal surface, and bulk metal. These domains, with examples of possible microprocesses, are identified in Figure B.15.5. These domains are discussed in Sections 3.0 and 4.0.

- Identify the modes of failure of interest, (e.g. SCC, CF, FAC), and develop information bases for their dependencies of occurrence, as described in Section 6.0. These define targets for scenarios, as described in Section 5.0, which involve practical aggregations of domains and their microprocesses.

- Identify the "microprocesses" of these domains that could affect the modes of failure. These microprocesses, as they apply for the six domains, are described in Section 4.0; and examples are shown in Figure B.15.5.

- Develop likely scenarios as suggested in Figure B.15.6 and Section 5.0, which connect microprocesses of the six domains, and which have a high likelihood for leading to failure. These scenarios would constitute the precursor period as identified in Figure B.15.1 for Cases II and III.

- Quantify possibly critical microprocesses in terms of their dependence on the variables that lead to critical conditions for SCC to occur at the end of the precursor period.

- Develop critical experiments to assess whether the proposed scenarios and their component microprocesses are credible.

Predicting SCC in LWRs in the past has been hindered by overly restrictive and often poorly informed assumptions on the microprocesses such as:

- SCC occurs only in the presence of "specific ions."

- SCC does not occur either in pure environments or in pure materials; i.e. SCC of Alloy 600 in pure deoxygenated water is not credible.

- Boiling $MgCl_2$ is a suitable environment to assess the dependence of SCC on alloy composition.

- Pure water cannot produce SCC of sensitized stainless steel.

- Water chemistry used for fossil boilers should be adequate for nuclear boilers.

- Tube support crevices will not accentuate any chemistry that could lead to SCC.

- There is not sufficient Pb in feed water to produce PbSCC even if it is concentrated.

- SCC due to Pb in Alloy 600MA is transgranular.

- Stainless steel without sensitization will not sustain SCC.

- The high purity of water in secondary OTSG water will not produce deposits on superheated upper bundle surfaces.

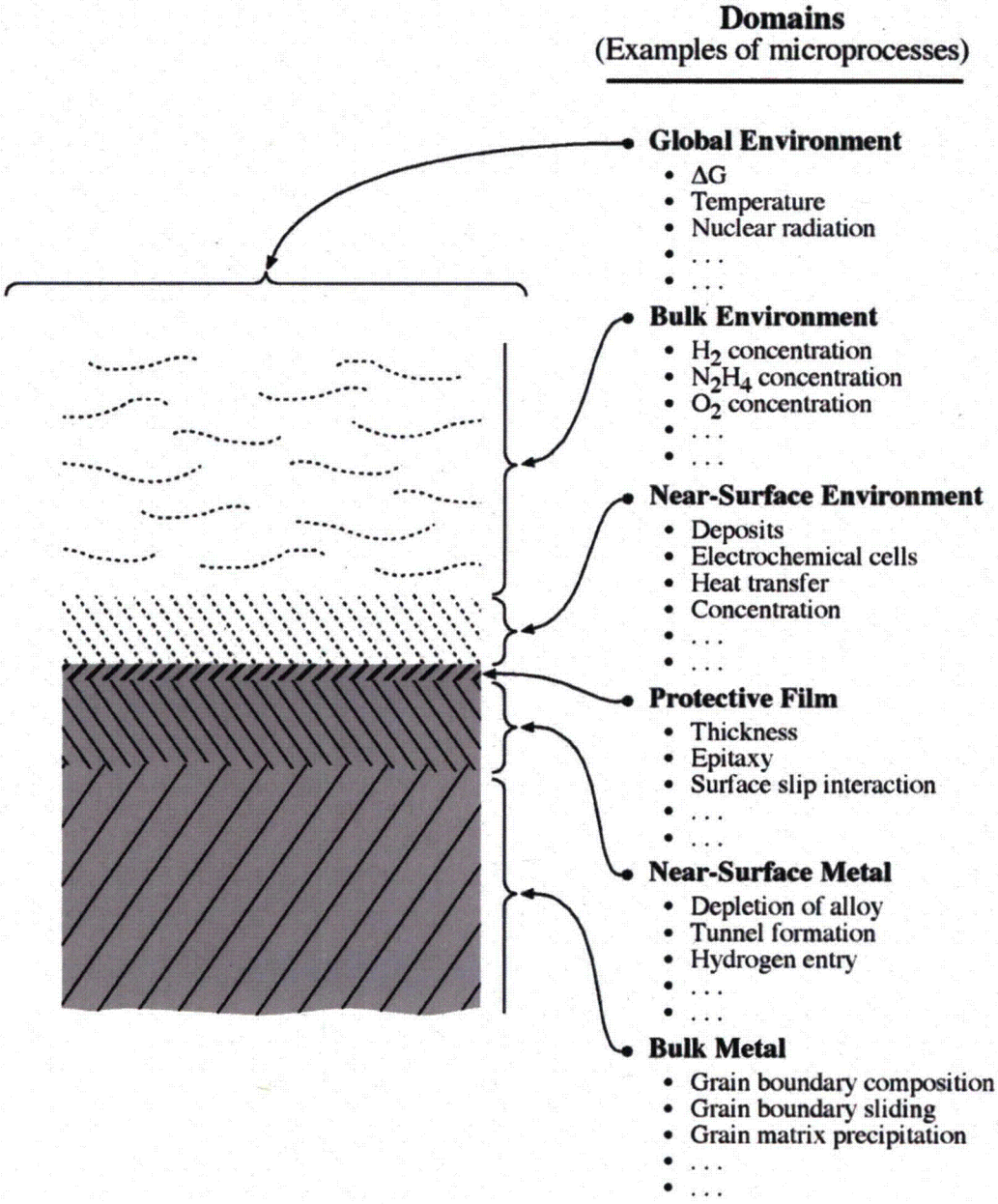

Figure B.15.5 Schematic view of six domains for quantifying microprocesses relating to the continuum from a global environment through to the bulk metal. Examples of microprocesses indicated.

There are more such assumptions. Similar assumptions may still hinder our capacity to predict the occurrence of degradation. In Section 2.0, examples of failures, which have occurred and are already known, and which follow this microprocess route are considered and provide examples of important aspects of the MPSA approach. Section 3.0 describes domains and their inherent microprocesses; Section 4.0 describes physical details of microprocesses and their implications; Section 5.0 describes how scenarios are developed and applied; Section 6.0 describes the failure target (e.g. start of SCC after the precursor produces necessary conditions)

for the development of scenarios; finally, in Section 7.0 some predictions for future and not yet observed damage are developed based on the procedures described in this report.

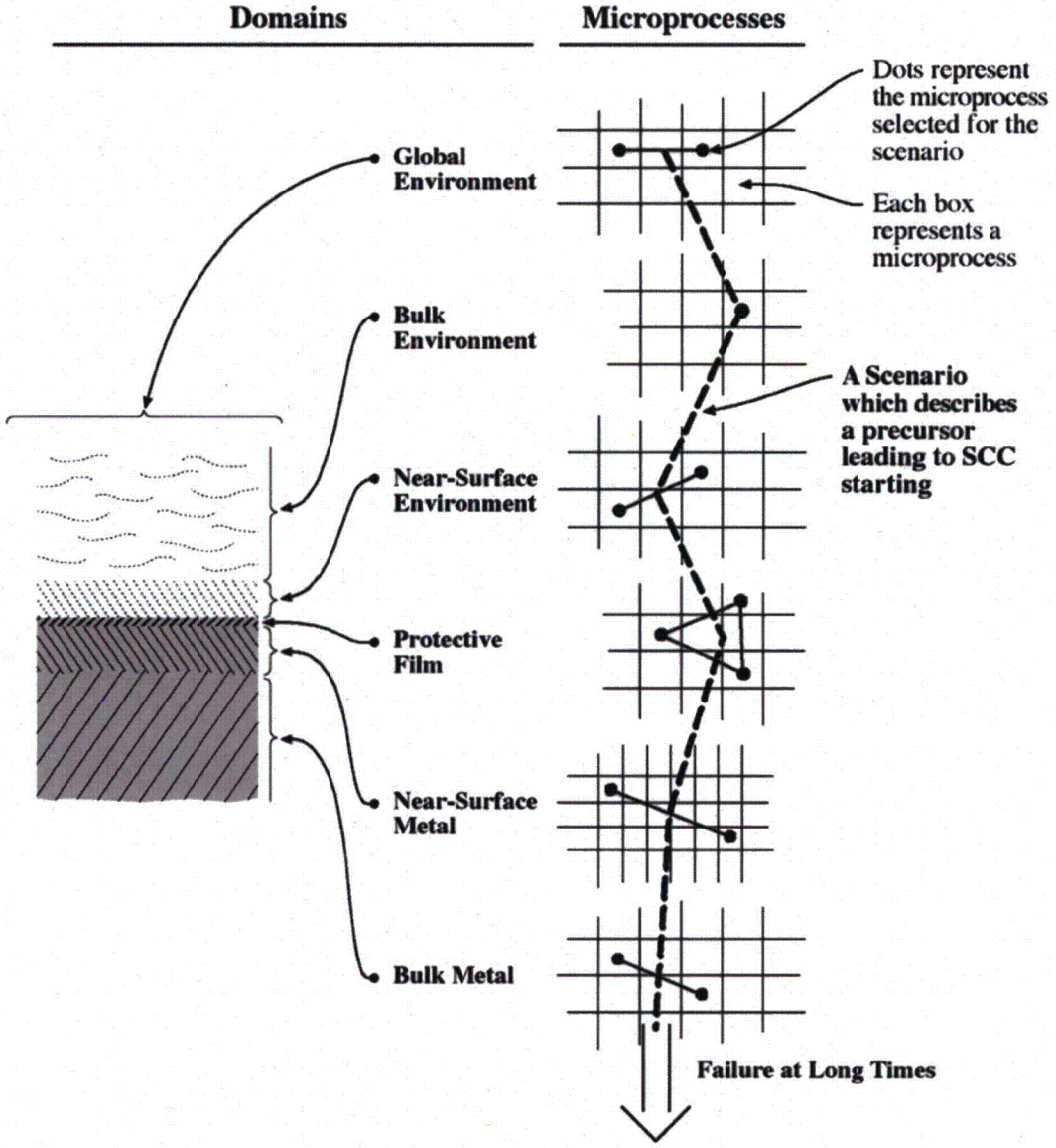

Figure B.15.6 Schematic view of a scenario that might be developed, which links microprocesses in successive domains as the scenario would apply to the precursor stage of Figure B.15.1.

2. Examples of Past Sequential Failures

The purpose of this section is to describe examples of failures that correspond to Cases I and II of Figure B.15.1. These failures provide insights to how failures with longer precursor times might evolve. Section 2.1 describes failures that begin when the plant starts and where the time-to-penetration is associated with the evolution of the SCC or FAC itself with no need to develop pre-conditions over time. This corresponds to Case I of Figure B.15.1. Section 2.2 corre-

sponds to Case II of Figure B.15.1 where a relatively short (e.g. half to 20 years) precursor period precedes the evolution of the SCC itself.

2.1 Failures without time-dependent pre-conditions, no precursors, Case I

SCC on the primary side, LPSCC--no precursor

On the primary side of steam generator tubes there are no crevices, and the chemistry is generally constant with time. The major stressors are residual stresses and temperature; thus, any SCC that occurs does not depend on accumulation processes in a precursor period. The highest residual stresses are initially present either at small diameter U-bends or at roll transitions at the top of the tubesheet; Figure B.15.7a[10] shows data for the temperature dependence of LPSCC in the small diameter U-bends of SGs. The earliest failures at the highest temperature, about 306°C, occurred after 20-30 months. Figure B.15.7b[11] shows a cumulative distribution function (cdf) in Weibull coordinates for the LPSCC in US and French plants. Here, the values of □ (characteristic space parameter in the Weibull distribution) are in the range of 10 to 41 EFPY and the values of □ (slope or "shape factor" in the Weibull distribution) are in the range of 1.36 to 4.93 (noting that these data were analyzed with a two parameter Weibull fit). Such data suggest that the first failures occur in the range of about 0.1 of the mean. The data of Figure B.15.7, taken together and recognizing the differences in temperature, indicate that early LPSCC can occur in about a year. Details of dependencies of LPSCC are described by Staehle and Gorman.[1]

Local cold work on the secondary side, Case I--no precursor

Figure B.15.8 describes a situation in which relatively deep scratches, which were present at the start of the operation, produced local cold work that initiated extensive SCC. Staehle and Gorman[1] have summarized numerous such instances. Such SCC has penetrated the full thickness of the tubes five years after the start of operation and was found on the surfaces of the cold leg of the secondary side. Hundreds of SCC events per inch occurred on some of the scratches. The fact that such SCC initiated and propagated on the free span of the cold side attests to the severity of the initial cold work.

Figure B.15.8 shows first in (a)[12] and then (b)[12] the location of the failures. Figure B.15.8c[12] shows details of the scratch in plan view, and Figure B.15.8d[12] shows the scratch in cross section with the SCC emanating. Figures B.15.8e[13] and B.15.8f[14,15] show the accelerative effects of cold work, which supports the conclusion that local cold work started the cracks nucleating early. The scratches here seem to be deeper than most ordinary scratches from processing.

sponds to Case II of Figure B.15.1 where a relatively short (e.g. half to 20 years) precursor period precedes the evolution of the SCC itself.

2.1 Failures without time-dependent pre-conditions, no precursors, Case I

SCC on the primary side, LPSCC--no precursor

On the primary side of steam generator tubes there are no crevices, and the chemistry is generally constant with time. The major stressors are residual stresses and temperature; thus, any SCC that occurs does not depend on accumulation processes in a precursor period. The highest residual stresses are initially present either at small diameter U-bends or at roll transitions at the top of the tubesheet; Figure B.15.7a[10] shows data for the temperature dependence of LPSCC in the small diameter U-bends of SGs. The earliest failures at the highest temperature, about 306°C, occurred after 20-30 months. Figure B.15.7b[11] shows a cumulative distribution function (cdf) in Weibull coordinates for the LPSCC in US and French plants. Here, the values of θ (characteristic space parameter in the Weibull distribution) are in the range of 10 to 41 EFPY and the values of β (slope or "shape factor" in the Weibull distribution) are in the range of 1.36 to 4.93 (noting that these data were analyzed with a two parameter Weibull fit). Such data suggest that the first failures occur in the range of about 0.1 of the mean. The data of Figure B.15.7, taken together and recognizing the differences in temperature, indicate that early LPSCC can occur in about a year. Details of dependencies of LPSCC are described by Staehle and Gorman.[1]

Local cold work on the secondary side, Case I--no precursor

Figure B.15.8 describes a situation in which relatively deep scratches, which were present at the start of the operation, produced local cold work that initiated extensive SCC. Staehle and Gorman[1] have summarized numerous such instances. Such SCC has penetrated the full thickness of the tubes five years after the start of operation and was found on the surfaces of the cold leg of the secondary side. Hundreds of SCC events per inch occurred on some of the scratches. The fact that such SCC initiated and propagated on the free span of the cold side attests to the severity of the initial cold work.

Figure B.15.8 shows first in (a)[12] and then (b) the location of the failures. Figure B.15.8c shows details of the scratch in plan view, and Figure B.15.8d[12] shows the scratch in cross section with the SCC emanating. Figures B.15.8e[13] and B.15.8f[14,15] show the accelerative effects of cold work, which supports the conclusion that local cold work started the cracks nucleating early. The scratches here seem to be deeper than most ordinary scratches from processing.

(a)

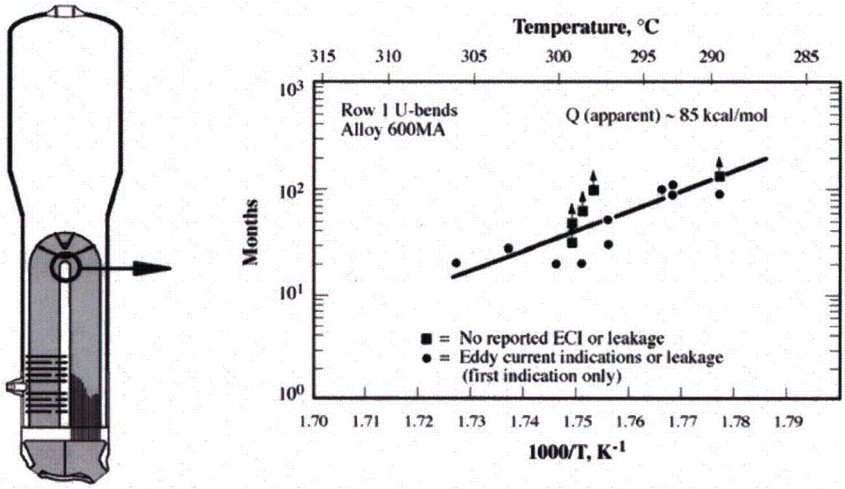

(b)

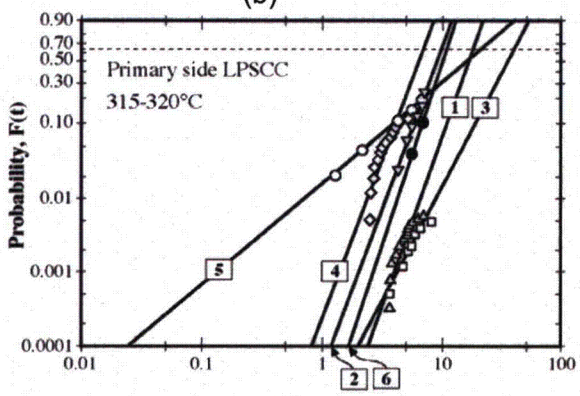

1. **French plants, LTMA tubing**
   θ = 18.7 EFPY
   β = 4.48
   r^2 = 0.82
2. **Part depth roll**
   θ = 10.0 EFPY
   β = 4.29
   r^2 = 0.95
3. **U.S.-made row 2 U-bends, French plants**
   θ = 41.1 EFPY
   β = 3.07
   r^2 = 0.95
4. **U.S.-made row 1 U-bends, French plants**
   θ = 7.13 EFPY
   β = 4.29
   r^2 = 0.77
5. **Roll transitions for kiss rolls**
   θ = 22.23 EFPY
   β = 1.36
   r^2 = 0.98
6. **Primary side denting**
   θ = 10.95 EFPY
   β = 4.93
   r^2 = 1.0

Figure B.15.7 (a) Time-to-failure for Row 1 U-bends of PWR steam generators on the primary side. From Begley et al. Courtesy of SFEN. (b) Probability vs. service time (EFPY) for the LPSCC occurring on the primary side of tubes from operating SGs in PWRs. Temperatures in the range of 315 to 320° C. From Staehle et al.[11] © NACE International 1994.

Figure B.15.8 also shows a scenario starting with M-1 ("M" identifies a "microprocess") through M-4, i.e. from the scratch through the cold work to the SCC, as accelerated by cold work and the SCC propagating as it moves beyond the cold work. However, here, this SCC certainly began at the start of life of the plant. The scratches accelerated the initiation. The

relatively long time for perforation, compared with Figure B.15.7, results from the lower cold leg temperatures.

Flow assisted corrosion (FAC) at Mihama—no precursor

Figure B.15.9 shows a failed pipe in a section from Mihama 3 at the orifice between the #4 low pressure heater and the deaerator operating at approximately 142°C. The pipe was 560mm in diameter and the wall was 10mm thick. The flow rate of water was 22m/s at a pressure of 0.93MPa and a pH of 8.6-9.3. The failure occurred after 185,700 hours of operation. The failure resulted from flow-assisted corrosion (FAC) at a location where there had been no inspections. The resulting failure killed five people and injured four others.

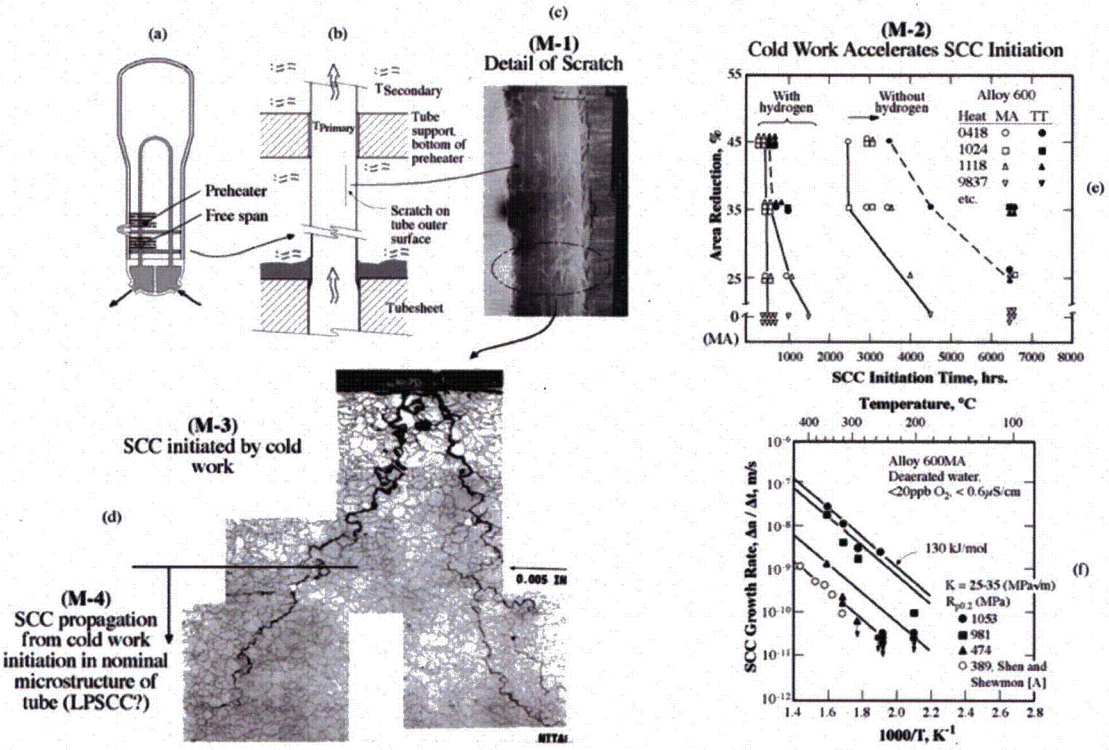

Figure B.15.8 SCC at free-span cold leg at McGuire-2 in an Alloy 600MA tube. (a) General location of scratch and SCC. (b) Schematic view of location of SCC. (c) Detail of scratch with SEM. (d) Cross section of SCC. Courtesy of R. Eaker. (e) Area reduction vs. SCC initiation time for Alloy 600 for several heats in environments with and without hydrogen. Used by permission of EPRI. (f) SCC growth rate vs. 1000/T for Alloy 600MA with various yield strengths achieved by cold work. From Speidel and Magdowski. Courtesy of EDF. Data from [A] Shen and Shewmon.

The pipe was a thin wall large diameter pipe with high velocity water flowing at 22m/s. The FAC involved in this accident most certainly started at the initial operation and did not involve any precursor period according to Case I of Figure B.15.1. Although the FAC proceeded at a relatively slow rate, no inspections were performed up to the time of failure.

Stress corrosion cracking in sensitized and non-sensitized stainless steels in BWR applications – no precursor

Figure B.15.10 shows three examples of data for SCC in stainless steels, which are used in BWR applications. These include sensitized Type 304, non-sensitized Type 304, and stabilized Types 321 and 347. Numerous instances of SCC in non-sensitized stainless steel have occurred.[16,17,18,19] In these cases, the local environment and condition of material do not change, although low temperature sensitization could aggravate the susceptibility to SCC.

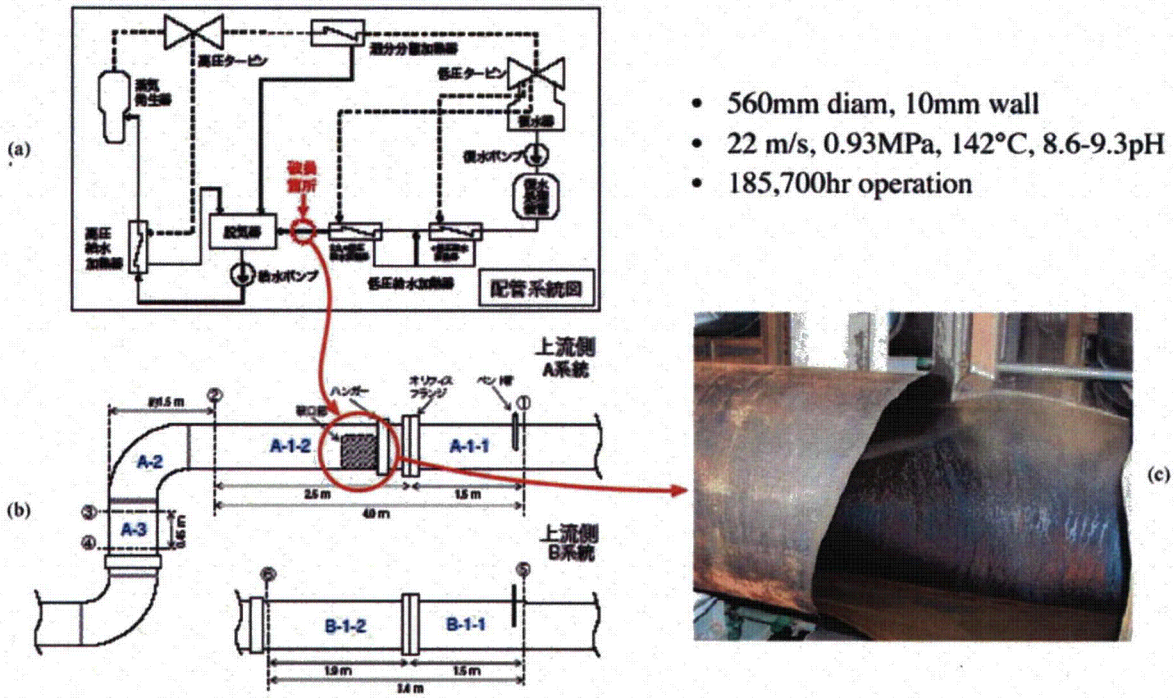

Figure B.15.9 (a) and (b) Locations of failure. (c) Failure of pipe.

Figure B.15.10a[20] shows the probability of cracking vs. time for SCC of 2-inch and 4-inch stainless steel piping that was sensitized at welds and exposed to BWR conditions. Here, the probabilistic nature of the ultimate failures is clear, although the initiation most likely started with the beginning of operation of the plants.

Figure B.15.10b, from work by Angeliu et al.,[21] compares sensitized and non-sensitized Type 304 stainless steel in BWR environments vs. the corrosion potential and shows that the crack growth rates of the non-sensitized materials is lower than for sensitized specimens (compare the large black triangles and large black squares with the smaller data points). The circles are both for cold worked material and indicate that cold work increases the rate of non-sensitized materials significantly in the same range of potentials. The half shaded circles refer to specimens cold worked at -55°C where mainly martensite is produced; the open circles refer to specimens cold worked at +140°C where only cold worked microstructure is produced. It is clear here that cold work accelerates the SCC of non-sensitized material regardless of the

resulting microstructure. It is also clear that SCC in sensitized material proceeds more rapidly than non-sensitized material.

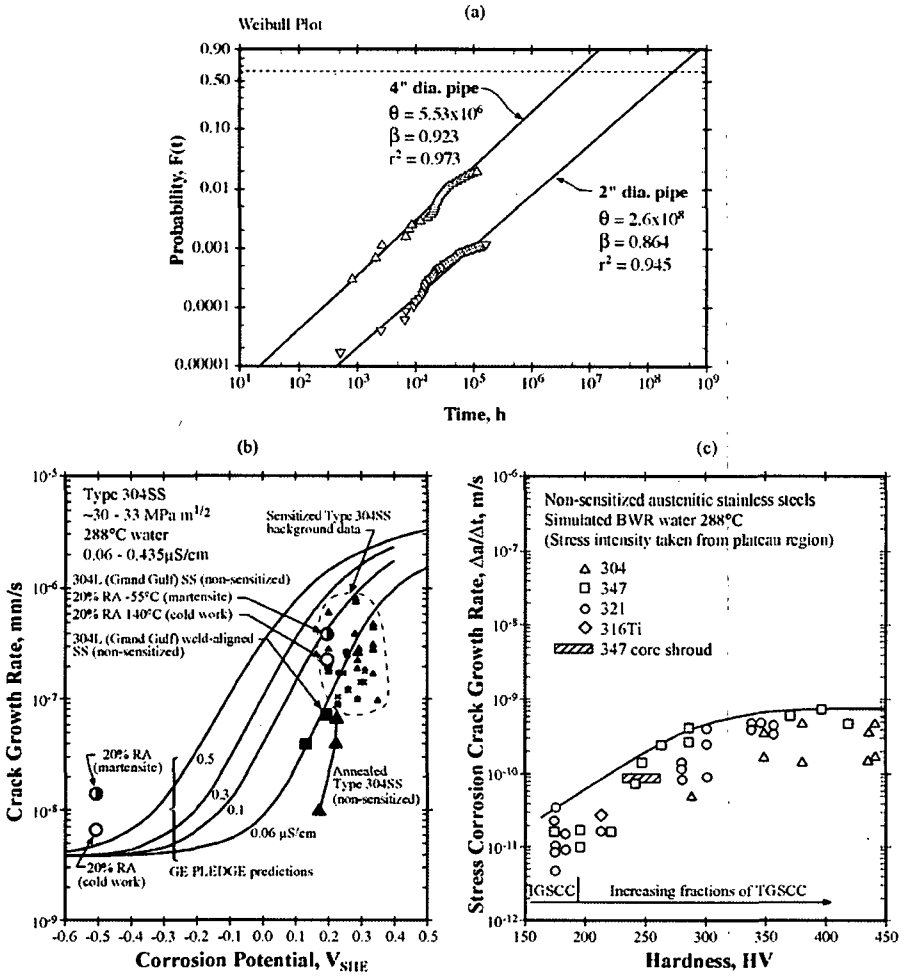

Fig. B.15.10 SCC of stainless steels exposed to normal BWR water chemistry. (a) Probability vs. time for the failure of Type 304 stainless steels in 2- and 4-inch diameter pipes in operating plants as shown in Weibull coordinates. Failures or indications have occurred at the smooth inside surfaces associated with welds. From Eason and Shusto. *Used by permission of EPRI* (b) Crack growth rate vs. corrosion potential for stainless steels in sensitized and non-sensitized Type 304 stainless steel. Smaller symbols indicate the SCC of sensitized stainless steel from background experiments. Larger symbols indicate more recent experiments. Large triangles are for non-sensitized and annealed Type 304. Squares are for weld heat affected specimens aligned with weld; low carbon and non-sensitized. Circles are for specimens with 20% reduction in area. The half shaded specimen was deformed at -55°C to produce mainly martensite. The open large circle is for cold work at 140°C to achieve only cold work. From Angeliu et al. (c) Crack growth rate vs. hardness for non-sensitized stainless steels. From Speidel and Magdowski.[22] *Reprinted with permission from TMS*

Figure B.15.10c, from work by Speidel and Magdowski,[22] compares Type 304 with stabilized stainless steels and with a core shroud as a function of hardness. Here, the trend in Figure B.15.10b is corroborated and extended.

2.2 Failures with significant but relatively short precursor times, Case II.

In this section, examples of failures are described where the SCC is preceded by a precursor step, as shown in Case II of Figure B.15.1. These examples suggest how such precursors might arise and proceed.

ODSCC at tubesheets and tube supports--precursor

Figure B.15.11 shows successive steps (M-X) leading to SCC on the outside diameter of SG tubes in heated crevices. The precursor steps involve at least the following:

a. Build-up of deposits in crevice (M-1).

b. Concentration of chemicals in heat transfer crevices (M-2).

c. Further concentration and chemical reactions inside the crevices (M-3).

Then, the resulting SCC, as shown at (M-4), can initiate. This precursor process is not lengthy, but the overall process is nonetheless a Case II process with a precursor preceding the initiation of SCC.

Denting associated with tubesheets and tube supports--precursor

Figure B.15.12 shows an integrated view of the denting processes as they may occur at tube supports or at the top of the tubesheet and as related to previous experimental work of Pickering et al.[23] and Pilling and Bedworth.[24] The precursor steps for denting are much like the ODSCC in Section 2.2-1. The precursor steps involve at least the following:

a. Build-up of deposit in crevice (M-1).

b. Concentration of chemicals in the heat transfer crevices (M-2).

c. Corrosion products expand, according to the predictions of Pilling and Bedworth, as the carbon steel of the tube supports corrodes. These corrosion products produce stresses (M-3), as measured by Pickering et al., in the tube wall and cause it to deform (M-4).

The straining of the tube, after the corrosion products expand, produces SCC from both inside and outside of the tubes (M-5). Such SCC has not been observed associated with denting at the top of the tubesheet, but such a result is possible. From the analysis of Staehle and Gorman, based on extensive work described in the literature, it appears that the growth of the oxide was particularly influenced by the presence of chloride and copper in the secondary environment. Thus, improving the integrity of the condensers and changing the condenser materials from copper-base alloys to titanium were the main avenues for mitigation.

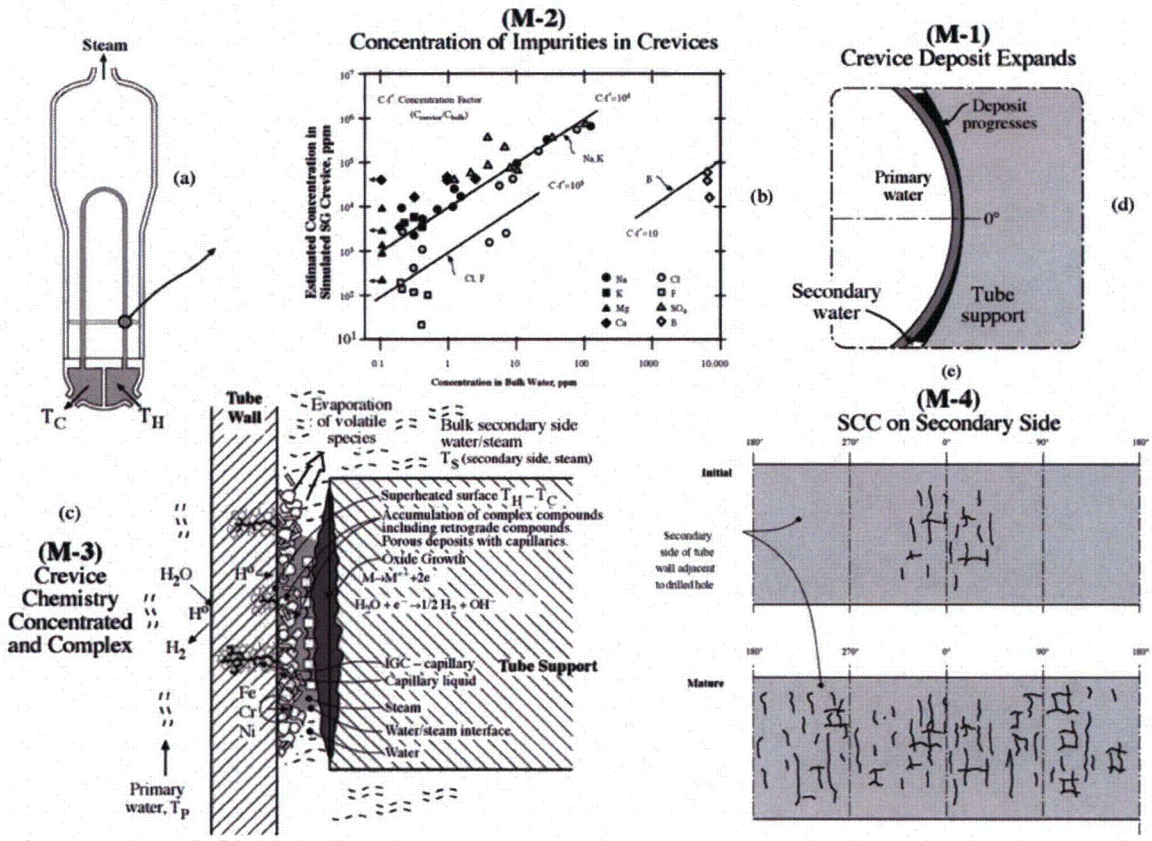

Figure B.15.11 Steps involved in the SCC on the OD of a tube associated with a drilled hole geometry of an Alloy 600-tubed steam generator.

SCC in OTSG upper bundle--precursor

SCC has occurred in the upper bundles of SGs where the steam is progressively superheated. While this SCC appears to be mostly focused at scratches, SCC and IGC occur outside these scratches to a lesser extent. The tube material is Alloy 600SR (stress relieved). Figure B.15.13a[25] shows the composition of various parts of the surface and SCC. It appears that the design of these OTSG units assumed that the water would be so pure that such accumulations of chemicals would not occur and would certainly not damage the tubes. The SCC was quite extensive in the superheated region. Figure B.15.13b[26] shows the tubes plugged vs. time. Significant tube plugging started after 12 years in 1986. The precursor step is comprised mainly of the accumulation of chemicals on the surfaces until a sufficient amount of chemicals is present. The precursor period appears to have been about 10-12 years.

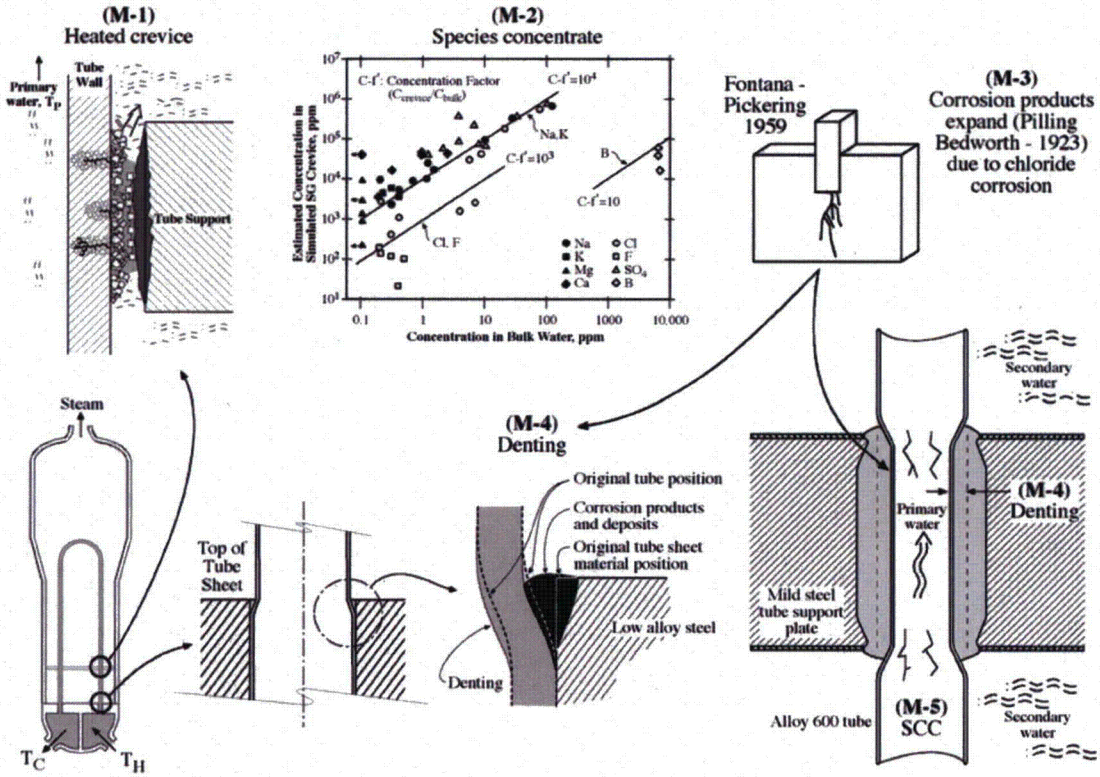

Figure B.15.12 Steps in the development of denting at both tube supports and at the top of the tubesheet. The straining is shown at the tube supports to have produced SCC starting from both inside and outside surfaces.[23,24]

Fuel failures in BWR plants--precursor

Fuel failures in BWR plants seem to be occurring as the heat flux increases with increasing demands for high outputs. The failure is not SCC, but rather a corrosion perforation. However, the precursor process is useful to analyze here. The precursor steps, as summarized in Figure B.15.14, are mainly:

a. High, and increasing, heat flux (M-1).

b. Impurities that participate in forming deposits with higher heat transfer resistance (M-1).

c. Increase in corrosion rate and formation of thicker oxide with higher heat transfer resistance (M-2).

d. Deposition of impurities and growth of oxide produces higher surface temperatures that accelerate perforation of cladding (M-3).

e. The cladding then perforates (M-4) as illustrated in Figure B.15.14d. This process occurs within a fuel cycle and is therefore a several year process.

Davis Besse--precursor

In the case of the Davis Besse failure, as shown in Figure B.15.15, LPSCC was part of the precursor, rather than the terminal part, and an extensive volume of corrosion ensued after an SCC-incited leak occurred in a control rod drive nozzle. The precursor elements were:

a. High residual stresses due to welding (M-1).

b. LPSCC in the Alloy 600MA nozzle (M-2).

c. Perforation of the Alloy 600MA permits borated water to exit and produce both a high velocity and corrosive solution (M-3).

The corrosion rate of the steel is about 2" per year and consumes a volume of steel that is the thickness of the head and about 6" in diameter. The precursor time, i.e. the time for the LPSCC to perforate the wall of the nozzle, was about 18 years, which is comparative to the rate for SG tubes when the differences in thicknesses are accounted for.

3. Structure of Domains and Microprocesses – Approach to Quantifying Precursors of Case III

3.1 Introduction

The purpose of this section is to describe the structure and application of "domains" and "microprocesses," as used in developing scenarios that are part of the precursor events that precede initiating SCC as shown in Figures B.15.1, B.15.5 and B.15.6. This discussion is the essence of the approach to quantifying precursors for Case III. Figures B.15.16 through B.15.21 describe each of the domains, which are identified in Figures B.15.5 and B.15.6, together with examples of relevant microprocesses.

Again, the purpose of this report is to propose an approach to predicting failure processes, mostly SCC, that have not yet been observed. In order to develop such a prediction, a rational intellectual structure and some assumptions are necessary. The intellectual structure is discussed in this section in terms of the domains and microprocesses. The principal assumptions and features of this intellectual structure are:

- Predicting failures, which have not yet occurred, is mostly related to long term changes in the domains and microprocesses, which are precursors, as described in Figure B.15.1 and Figure B.15.6, and which enable SCC to initiate and propagate at later times.

- Some new mode of SCC is not reasonably expected. It is more likely that the development of the precursors will permit some existing failure process to occur rather than some totally new one.

- The development of precursor conditions depends on the progression of microprocesses in various domains, as shown in Figure B.15.5, which may act conjointly or individually.

- The choices of specific domains and microprocesses must be based upon experience, and an awareness of the wide varieties of microprocesses that can be important.

- The idea of microprocesses focuses on specific processes that occur within the domains and have been shown to be critical processes in the nucleation, initiation, and growth of SCC. Further, these microprocesses are often capable of being quantified by known procedures of analysis.

- Finally, the domains and microprocesses can be linked to a scenario for the development of critical conditions for the initiation and propagation of SCC or a similarly aggressive process. Several scenarios could be envisioned as options for precursors. Section 7.0 provides suggestions for failure processes that might be predicted with the MPSA approach.

3.2 The "domains"

The "domains" in this discussion are shown in Figure B.15.5. These domains provide an intellectual framework for identifying explicitly the sequence of events and for organizing the microprocesses.

A sample scenario that might constitute a precursor to SCC could be the following:

a. Microprocess #1 (M-1): A line-contact crevice slowly accumulates deposit.

b. Microprocess #2 (M-2): The deposit gradually hardens.

c. Microprocess #3 (M-3): Even dilute species in the bulk water concentrate in the crevices.

d. Microprocess #4 (M-4): Metallurgical ripening over time increases slip coplanarity leading to sharper slip steps and greater local forces at internal barriers.

   These first four steps constitute a precursor as shown in Figure B.15.1, and may require many years.

e. SCC initiates when the environment in the crevice interacts with a metallurgical slip of greater coplanarity in the metal substrate.

Starting from the overall schematic view in Figure B.15.5, where the adjacent domains are identified and shown adjacent to a schematic cross-section of a metal in an aqueous solution, the respective domains are described in Figures B.15.16- B.15.21. These domains, as identified in the Figures, start from the global domain to the bulk metal according to the order in Figure B.15

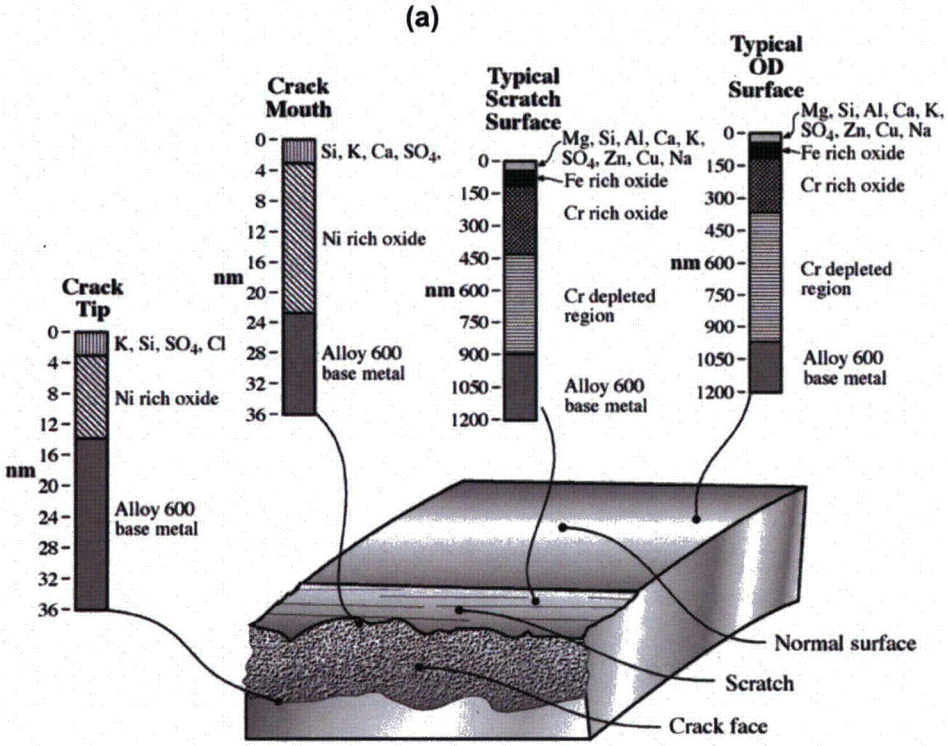

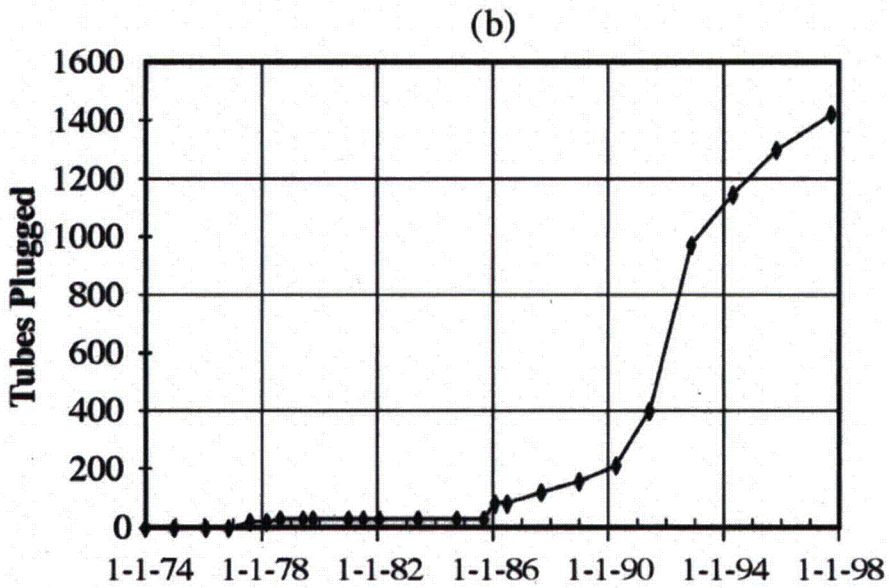

Figure B.15.13 (a) Compositions of surfaces of tubes at four locations in the upper bundle of Oconee Nuclear Station. Outside surfaces and inside SCC and IGC as determined by Auger spectroscopy. From Rochester.[25] Reprinted with permission from BNES. (b) Tubes plugged vs. time for Oconee-1B. From Rochester and Eaker.[26] Reprinted with permission from TMS.

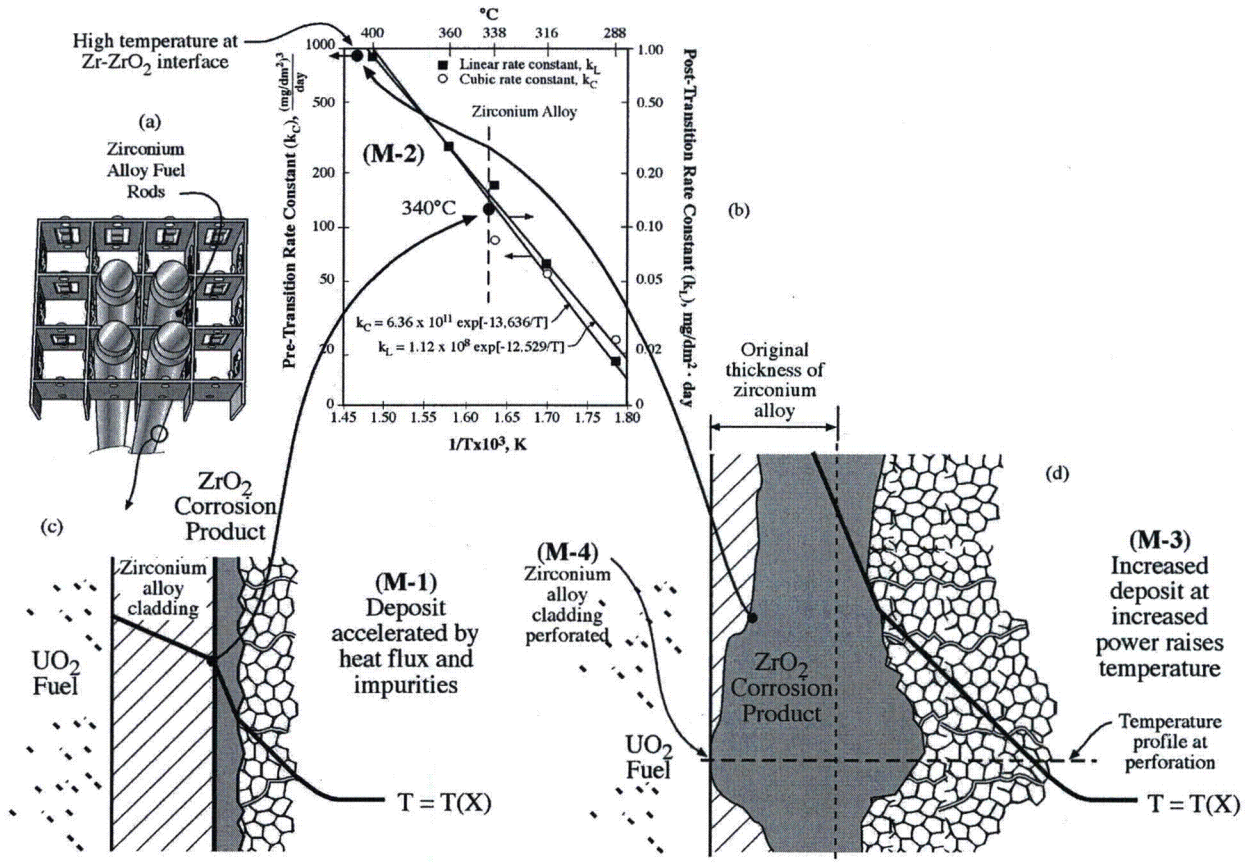

Figure B.15.14 Stepwise process for the perforation of fuel that results first from deposits, the formation of which is accelerated by high heat flux (M-1), then by accelerated corrosion (M-2), then by progressively higher surface temperatures (M-3), thereby increasing the corrosion rate, and ultimately failure (M-4).

Each of the domains consist of the "microprocesses" that are shown at the left, and some examples of nominal effects are identified at the right. These microprocesses are the elements, which contribute to the precursor, that would be quantified.

The "Global Domain" is shown in Figure B.15.16. The Global Domain is intended to include microprocesses that apply to all the domains, (e.g. temperature, neutron flux). The Global Domain also includes the free energy change, ΔG, as the environment reacts with the metal to produce reaction products.

The "Bulk Environment Domain" is shown in Figure B.15.17. The Bulk Environment Domain refers to the primary water, the secondary water, steam, tertiary water, ambient inside the containment or outside, and similar fluids to which components and materials are exposed.

The "Near-Surface Environment Domain" is shown in Figure B.15.18. The Near-Surface Environment Domain consists mainly of deposits, flow gradients, MIC pustules, and electrochemical cells. Such a domain has been a main part of the crevice deposits on the secondary side in heat transfer crevices or the accumulation of sludge at the top of the tubesheet in SGs.

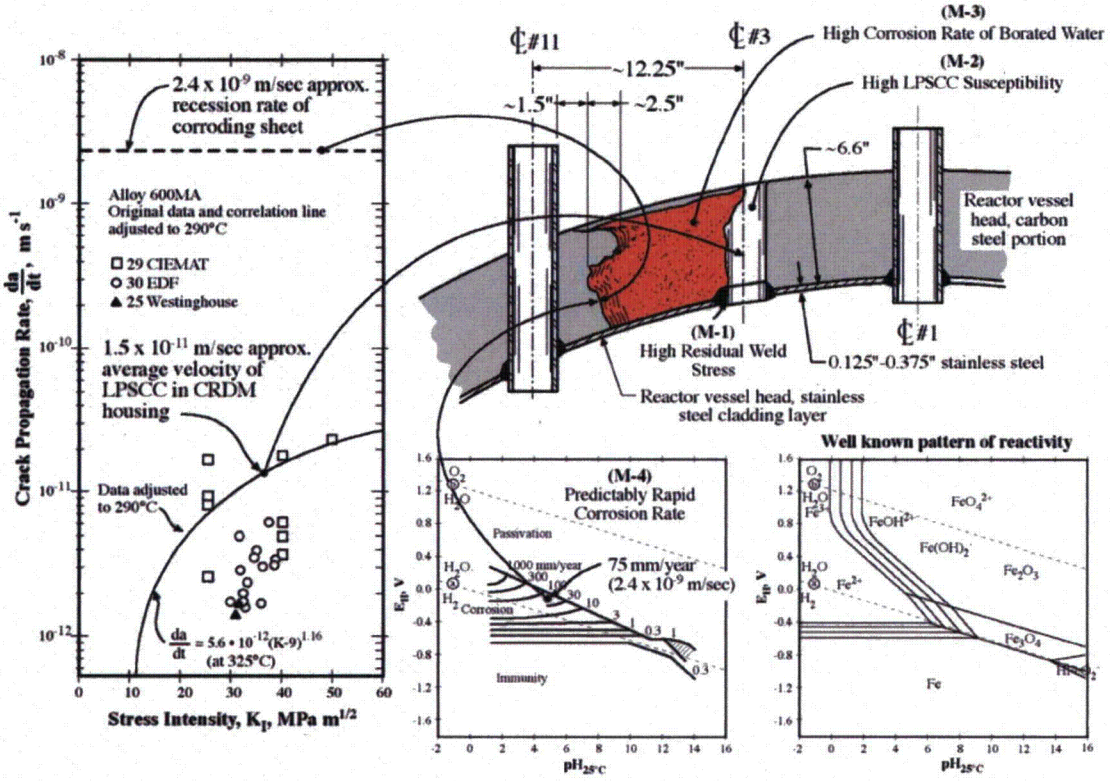

Figure B.15.15 Stepwise process leading to the failure at Davis-Besse. Here, LPSCC was part of the precursor, and rapid general corrosion was the propagation process. The LPSCC started with the high residual stresses from welding and the already well-known susceptibility of the Alloy 600MA.

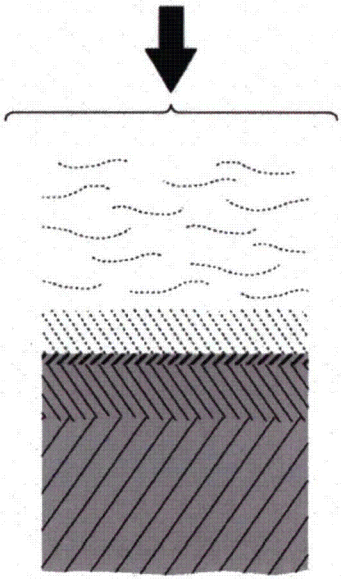

Global Domain

Microprocesses (Time Related)	Effects
1. Component in system	• Produce products that damage other components • Products from other components damage subject components
2. ΔG - Overall free energy change: environmental chemistry (pH, H_2O, O_2, H_2, N_2H_4) to material (Fe, Ni, Cr, Cu, Ti, . . .)	• Driving force for chemical reactions • Boundaries for SCC modes
3. Ambient temperature	• Reaction rates • Thermal stresses
4. Heat Flux	• Surface deposits • Surface temperatures
5. Cyclic stresses (Cyclic Frequency)	• Fatigue, corrosion fatigue
6. Crevices	• Accumulation of chemicals • Stress intensity
7. Irradiation	• Local differences • Voids • Radiolysis

Figure B.15.16 Microprocesses and their effects in the Global Domain.

The "Protective Film Domain," which is shown in Figure B.15.19, includes what is sometimes called the "passive film." However, there are other deposits that form as part of the protection, (e.g. carbonates), and are not part of the chemistry of the metal substrate. In the protective film, the electrochemical catalytic processes are affected as the defect structure of the protective film changes – such defect structures are changed by Pb, Cl^-, S^{2-} and others. Because this film is usually epitaxially attached to the surface, the protective film also affects both stresses in the substrate and the nucleation of dislocations at the surface. This film changes with time in its geometry and chemistry.

Bulk Environment Domain

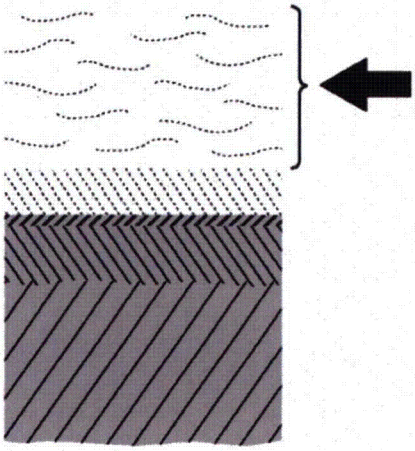

Microprocesses (Time Related)	Effects
1. Flow	• Transports chemical and suspended solids • Influence rates of surface reactions • Low flow / high flow deposits solids • FAC
2. Boiling	• Deposit solids
3. Transport to or from other components	• Cu^{2+}, HS^-
4. Chemical composition • O_2, H_2, N_2H_4 impurities (Pb, Cl^-, SO_4), pH inhibitors, suspended solids	• Electrochemical state • Corrosion reactions • Raise E with low H_2
5. Homogenous chemical reactions	• Reduce $SO_4^{=} \rightarrow HS^-$ with N_2H_4
6. Radiolysis and radiolytic synthesis	• $H_2O \rightarrow O_2 + H_2$ • $N_2 + H_2O \rightarrow HNO_3$ • $O_2 + N_2H_4 \rightarrow H_2O$
7. Multiple oxygen incidents	• Corrosion • SCC

Figure B.15.17 Microprocesses and their effects in the Bulk Environment Domain

The "Near-Surface Domain on the Metal Side," which is shown in Figure B.15.20, is the region in which near-surface processes occur such as slip dissolution, tunnel penetration, enrichment/depletion of species, solubilization of species that enter grain boundaries, and precipitation of vacancies.

Near-Surface Domain (Environment Side)

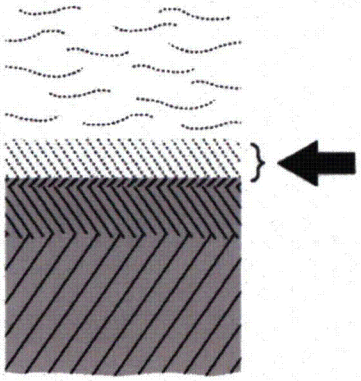

Microprocesses (Time Related)	Effects
1. Deposits	• Corrosion cells • Heat transfer resistance • Galvanic processes
2. Heat flux	• Concentrate chemicals • Raise surface temperatures
3. Sequestering, crevices	• Concentrate chemicals
4. FAC	• Remove material • Produce hydrogen • Inhibit initiation of SCC
5. MIC	• Act at temperatures below 100°C • Acidic and other corrosive environments

Figure B.15.18 Microprocesses and their effects in the Near-Surface Environment Domain

Protective Film Domain

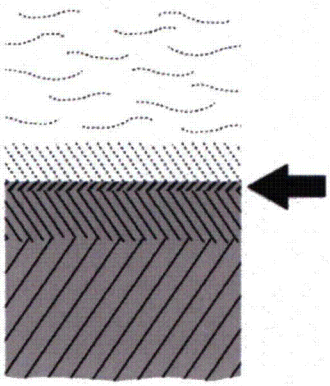

Microprocesses (Time Related)	Effects
1. Thickness	• Surface stress • Heat transfer
2. Composition (environment contribution, alloy contribution, defect structure, xtal/amorphous)	• Conductivity • Pit nucleation • SCC initiation
3.Stresses (average, metal interface)	• Film degradation
4. Kinetics (repassivation, dissolution, growth)	• Local penetration • Slip dissolution
5. Slip interactions	• Slip height • Step distribution • Dislocation nucleation

Figure B.15.19 Microprocesses and their effects in the Protective Film Domain

Near Surface Domain (Metal Side)

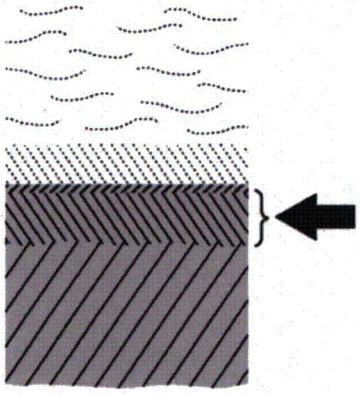

Microprocesses (Time Related)	Effects
1. Enrichment/depletion	• Brittle layer • Catalysis • Change chemistry into SCC mode • Galvanic • Voids
2. Hydrogen entry	• SCC
3. Surface slip	• SCC initiation
4. Grain boundary (composition, diffusion)	• IGC • G.B. diffusion
5. Irradiation-induced voids	• Stresses, distortion
6. Slip dissolution	• SCC initiation
7. Tunnels	• SCC initiation
8. General dissolution	• Surface recession
9. Pits, IG corrosion, electrochemical cells	• Penetration • CF initiation
10. SCC initiation	• Accelerate
11. FAC	• Recession • Remove SCC initiation • Hydrogen production
12. Abuse (dings, dents, machining, grinding)	• SCC initiation

Figure B.15.20 Microprocesses and their effects in the Near-Surface Metal Domain

The "Bulk Metal Domain," which is shown in Figure B.15.21, is, in a sense, the "semi-infinite region" of the metal, which, on a gross scale, is homogeneous but on a microscopic—and microprocess scale—is quite heterogeneous. These local heterogeneities provide paths or influences that affect the development and propagation of corrosion damage.

The six domains of Figures B.15.16 through B.15.21, as summarized in Figure B.15.5, are shown with associated small boxes in Figure B.15.6, each of which represents a microprocess. When a "scenario" is constructed as in Figure B.15.6, these boxes are connected, as they would be naturally. Such a scenario constitutes a precursor as shown in Figures B.15.1 and B.15.6 that identifies the relevant microprocesses, which need to be quantified and validated in order to

reach the conditions necessary for SCC to initiate. In this quantification, some kind of time dependence needs to be developed in order to predict when the resulting precursor can lead to the start of SCC.

Bulk Metal Domain

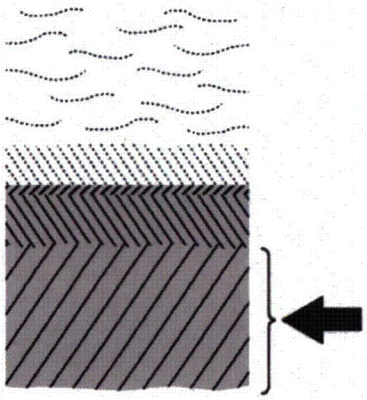

Microprocesses (Time Related)	Effects
1. G.B. composition, ppt	• Grain rotation • Grain shedding
2. G.B. composition, adsorb/desorb	• Preferential dissolution, diffusion
3. G.B. diffusion (O_2, N_2, C, ...)	• Embrittlement
4. G.B. movement, slip, rotation	• Break protective films
5. G.B. pile-up site for dislocation-induced stresses	• Promotes IGSCC, SCC
6. G.B. bubble formation (CH_4, NH_3)	• Promotes SCC
7. G. matrix - early precipitation	• Promotes slip coplanarity
8. G. matrix - transformation	• Promotes slip coplanarity
9. G. matrix - slip coplanarity	• Pile up stress
10. G. matrix - voids nucleation	• Stress

Figure B.15.21 Microprocesses and their effects in the Bulk Metal Domain

4. Examples and properties of microprocesses

The purpose of this section is to describe examples of microprocesses, which are part of the six domains. This description is not comprehensive but illustrative; there are probably 50-100 really significant microprocesses that might be identified.

As shown in Figures B.15.11- B.15.16, each domain contains a particular array of microprocesses, which are significant to the occurrence of corrosion damage. Many of these microprocesses are already known to participate in corrosion processes under various conditions of temperature, stress, environmental chemistry, and material chemistry.

The emphasis here is upon microprocesses that require some time to develop their roles in accelerating or intensifying future and aggressive corrosion; and during these early processes of development there is no support for SCC or other accelerated processes until certain necessary conditions conglomerate. Once some critical array of microprocesses develops, SCC can then initiate and propagate.

The "microprocesses" are the elements that are identified, quantified, and connected in scenarios to develop the characteristics of the precursor regimes as follows:

Identification

Identifying the microprocess in a domain, as in Figure B.15.6, is largely a matter of expert experience. Some of these microprocesses are well known and some maybe not. To identify further clues to microprocesses that are not obvious, it may be necessary to look into the physical and organic chemistry of homogenous materials and the surface chemistry of their interfaces in aqueous solutions. Other microprocesses might be identified from metal physics. "Identification" is a matter of making microprocesses explicit.

Quantification

Quantification of microprocesses provides bases for the dependencies that determine the duration of the precursor period. Such dependencies include considerations of growth rates, diffusion, rates of transformation, rates of accumulation, and rates of production. These can usually be approached with conventional knowledge of such processes as they respond to the temperatures and chemistries of LWRs. Developing the rates of microprocesses contributes to an overall model of a time-dependent precursor. From this model, the duration of the precursor can be calculated.

Connection into scenarios

Constructing a scenario, as in Figure B.15.6, involves essentially developing the features of the precursor. There may be several equally attractive scenarios. A scenario is shown schematically in Figure B.15.6, including selected microprocesses. Figure B.15.6 suggests that there may be several important microprocesses in some domains. A fully identified and connected scenario, as in Figure B.15.6, then, is a precursor to the occurrence of starting SCC or some similarly rapid process of penetration.

Note that FAC is probably not compatible with the development of these microprocesses since it starts from the beginning of operation, unless there is a change in velocity, pH, potential, inhibitors, or alloys that would activate the flow acceleration at some later time. However, FAC generally proceeds at a rate that is similar to the low end of SCC; and FAC might be initiated at a later time as a result of changes in chemistry (changes in oxygen or pH), temperature, and flow. This sequence is not so much a precursor as a later and influential change in operation.

4.1 Global Domain

A schematic view of the Global Domain is shown in Figure B.15.16. In Section 4.1 three examples of microprocesses are discussed, and a more extensive set is suggested in Figure B.15.16. Each of these examples is typical of important effects that could change the conditions for onset of SCC. Further, they are associated with the kinds of times that are involved with precursors that could lead to SCC at long times.

Mode diagrams, ΔG

One example of a microprocess here is the free energy difference between the environment and the material. This is usually identified by a diagram of potential vs. pH as shown in Figure B.15.22, and much of the necessary data are available in handbooks containing thermodynamic data. Here, the Ni-H_2O diagram is shown with some of the Fe equilibria. Superimposed on this diagram are the locations of the major submodes of SCC. This diagram represents the global domain where the lines in the diagram indicate equilibria for the metal and environment that react to produce chemical products. The application of this diagram and the incorporation of submodes of SCC have been described by Staehle and Gorman.[1] Such a global microprocess as the difference in free energy of metal and water, is important to virtually all of the scenarios.

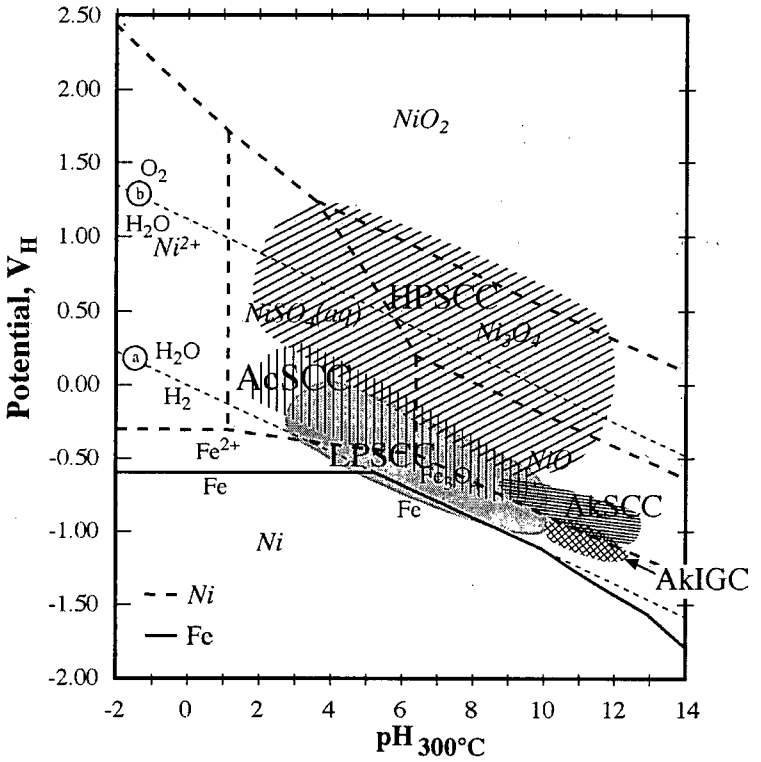

Figure B.15.22 Electrochemical potential vs. pH at 300°C for Ni in H_2O with important equilibria shown. Locations for AkSCC, LPSCC, AcSCC, and HPSCC of Alloy 600MA shown. From Staehle and Gorman.[1] © NACE International 2003/2004.

Neutron flux, void formation

Neutrons, as they react with Ni isotopes, produce helium atoms. These helium atoms coalesce to produce voids. Such voids are shown in Figure B.15.23[27] in baffle bolts. These voids, as they coalesce, lead to strains that cause stresses and distortions.

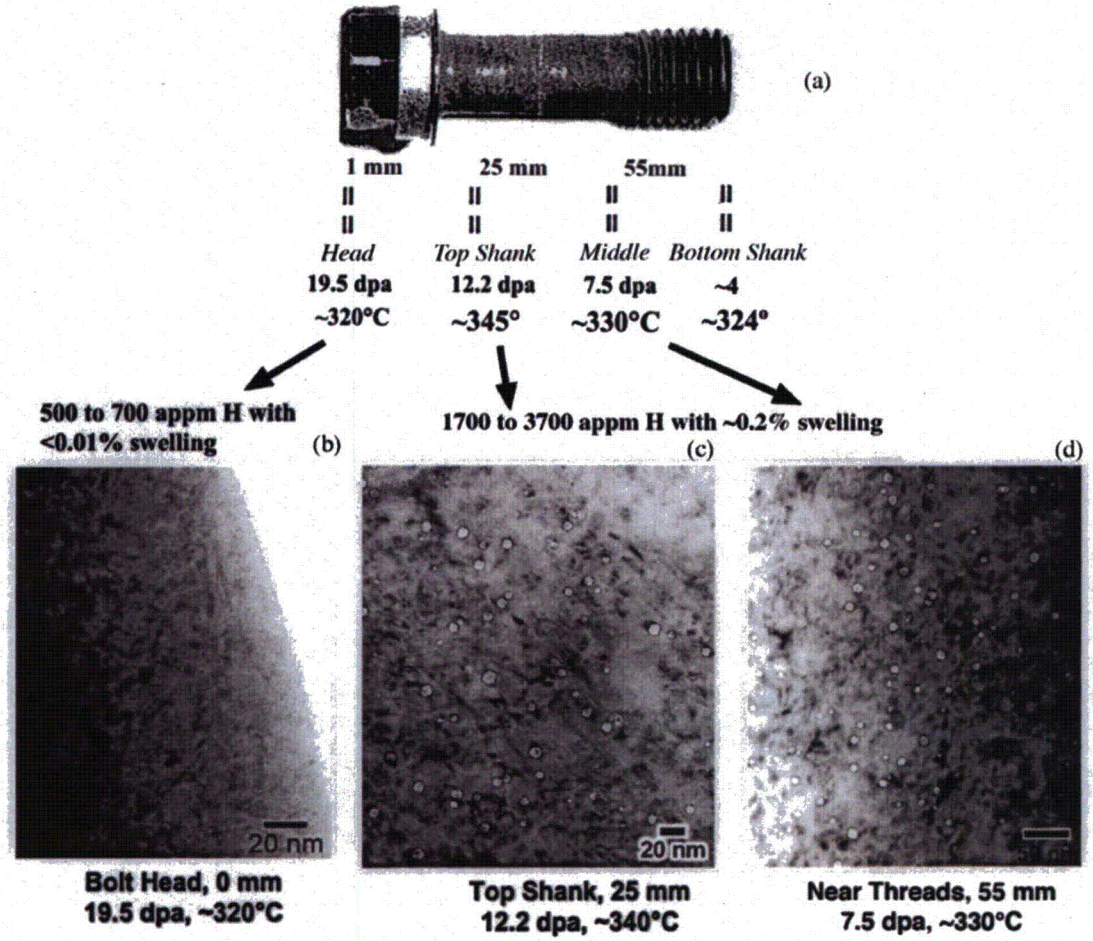

Figure B.15.23 Bolt connecting former and baffle from Tihange-1 PWR shown in terms of neutron dose giving concentration of He and swelling at locations along a bolt. From Garner et al.[27] Reprinted with permission from TMS.

Neutron flux, change composition of grain boundaries

A third example of a microprocess in the global domain is neutron flux, as it leads to changes of chemistry at grain boundaries. Figure B.15.24[28], from the work of Bruemmer, shows such a change of Cr in stainless steel after up to 13.3 dose per atom. These alterations affect the reactivity of the grain boundaries as well as changing the mechanical properties and diffusivity of environmental species such as oxygen.

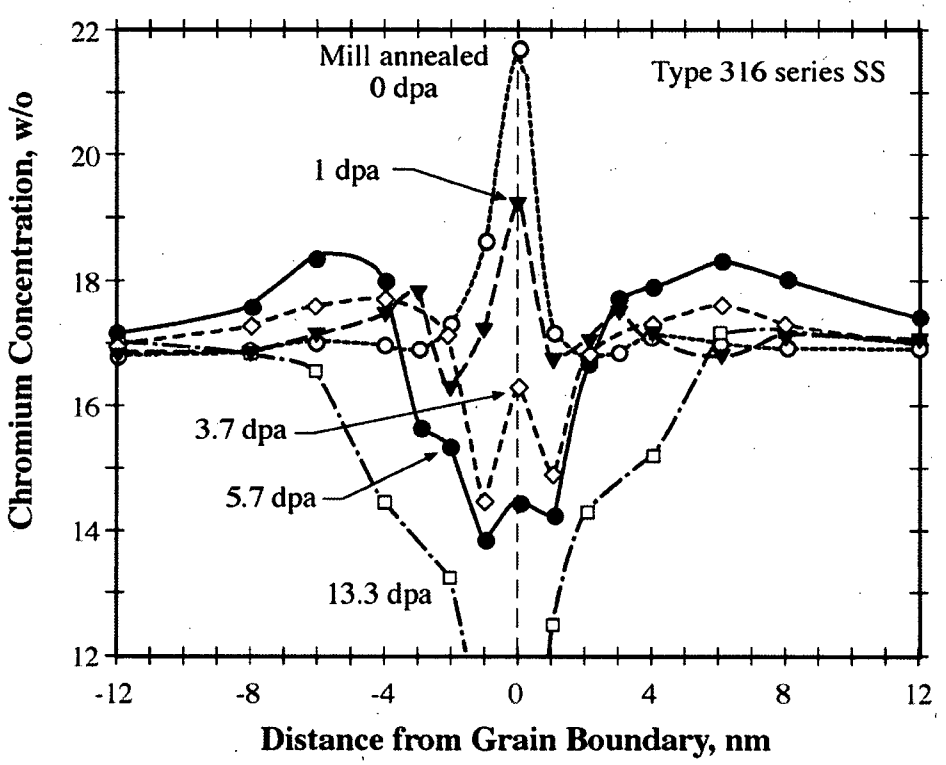

Figure B.15.24 Concentration of Cr across a grain boundary of mill-annealed Type 316 stainless steel as a function of dose up to 13.3 dpa. From Bruemmer.[28] © NACE International 2002.

4.2 Bulk Environment Domain

A schematic view of the Bulk Environment Domain is shown in Figure B.15.17, where several microprocesses are identified. This section gives two examples of such microprocesses.

Hydrazine (N_2H_4) reduces sulfate to sulfide

Hydrazine (N_2H_4) is added to the secondary side of SGs in order to reduce the concentration of oxygen that is assumed to promote SCC in crevices. As an aside, it is not clear that such an effect is important; and second, the very low hydrogen on the secondary side raises the potential, regardless. Whether hydrazine significantly counters this effect of low hydrogen is not clear.

Work by Daret, et al.[29] shows that the occurrence of sulfide produces SCC in Alloy 600MA, as shown in Figure B.15.25; further, this work is linked to the reduction of sulfate in secondary systems by hydrazine as shown in the reactions of Figure B.15.25. Work by Sakai et al.,[30] Sala et al.,[31] Allmon et al.,[32] and de Bouvier et al.[33] have shown clearly that N_2H_4 reduces SO_4^{2-} to S^{2-}.

Chloride inhibits dissolution

The rate of dissolution of high nickel alloys is very much affected by the anion as shown from work of Cullen in Figure B.15.26a[34]. Here, the dissolution of these alloys over a pH range from 1-6 is shown for several ratios of chloride and sulfate including the 100% compositions of each. These data show that the 100% chloride solution corrodes Alloy 600 about two orders of magnitude less than the 100% sulfate. In support of this trend, Figure B.15.26b[35] from Choi and Was, shows that the aspect ratio of pitting follows the same pattern. As the chloride-to-sulfate ratio increases, the pits become sharper, which is expected in view of the inhibitive effect of Cl^- as suggested in Figure B.15.26c from Staehle.[36]

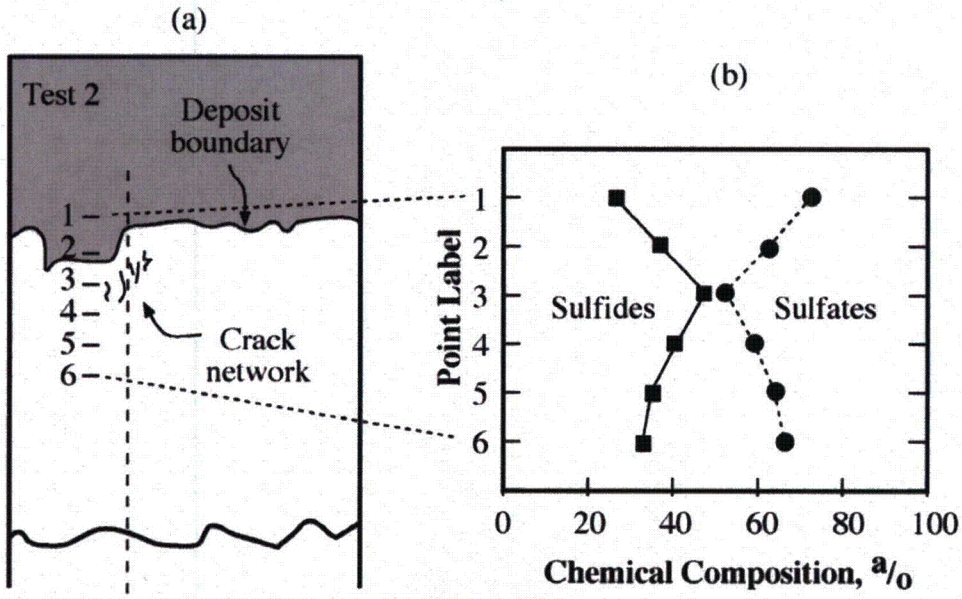

Sulfate is reduced to S^{2-} by hydrazine

$$2(SO_4)^{2-} + 18H^+ + 12e^- \rightarrow 2(HS^-) + 8H_2O$$

Hydrazine is oxidized

$$3(N_2H_4) + 12OH^- \rightarrow 3N_2 + 12H_2O + 12e^-$$

Figure B.15.25 Results from model boiler experiments with primary temperature in range of 330 to 350°C and secondary side temperatures in the range of 290 to 295°C with AVT chemistry. Sodium sulfate was added at 0.5 mg/kg in makeup water, and hydrazine was in the range of 10-50 µg/kg. Dissolved oxygen less than 1 µg/kg. (a) Location of SCC, boundary of deposit, and locations of analysis for sulfates and sulfides (1-6) for Alloy 600MA. (b) Atomic percent of sulfates and sulfides vs. distance from the boundary of the deposit into the metal and through the SCC zone. From Daret et al.[29] Reprinted with permission from TMS.

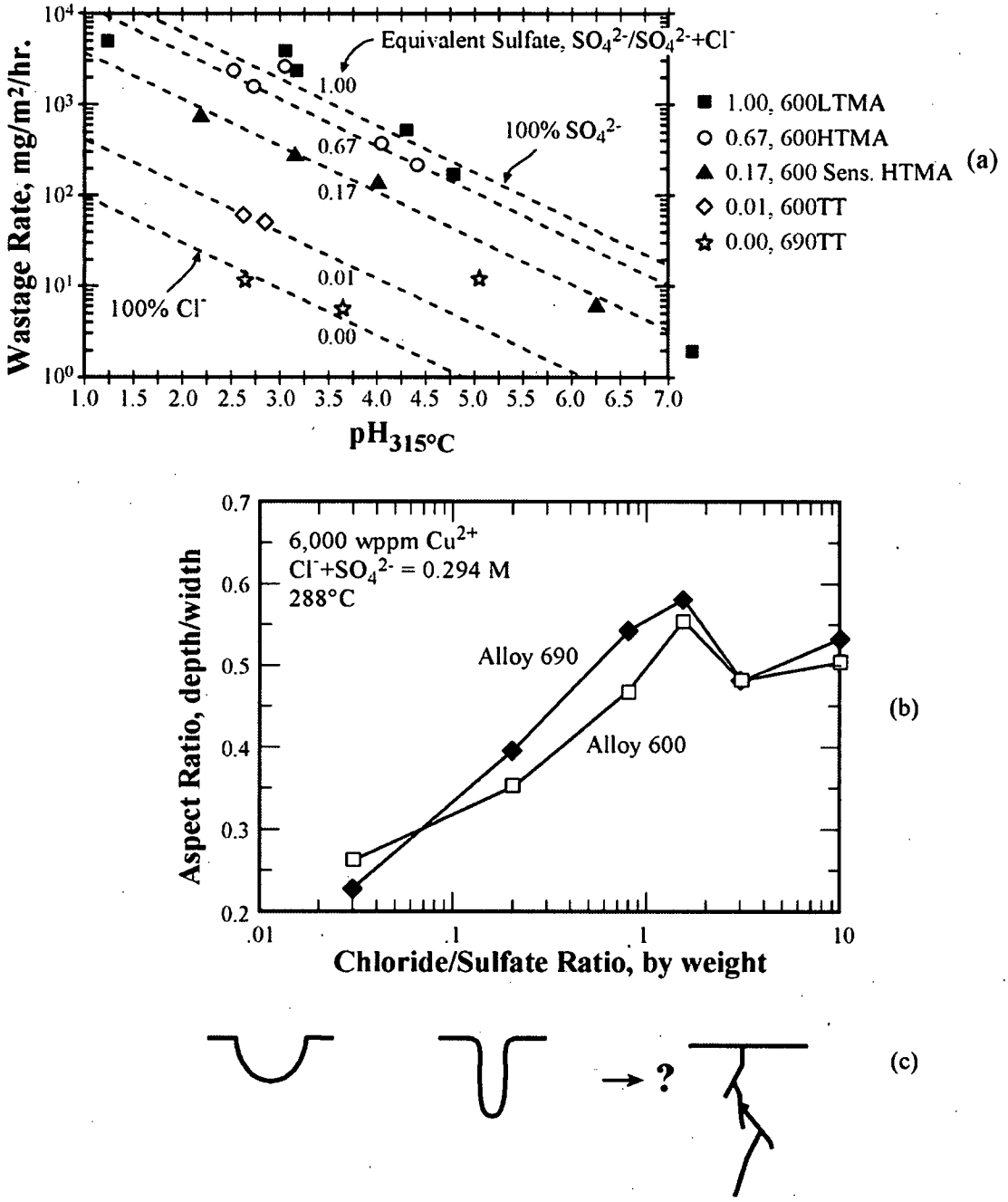

Figure B.15.26 (a) Wastage rate vs. pH for retort tests using Alloys 600 and 690 in various heat treatments in concentrated acidified sulfate and chloride solutions at a test temperature of 315°C. Arrows point to top and bottom dotted lines corresponding to 100% sulfate and 100% chloride solutions. Column of numbers in the middle corresponds to the ratio of equivalent sulfate as $SO_4^{2-}/(SO_4^{2-} + Cl^-)$; value of 1.0 is all SO_4^{2-} and value of 0.0 is all Cl^-. From Cullen.[34] © NACE International 1996. (b) Aspect ratio for pits vs. Cl^-/SO_4^{2-} ratio for Alloys 600 and 690 exposed in 6000 wppm Cu^{2+} at 288°C for $Cl^-+SO_4^{2-}$ = 0.294M. From Choi and Was.[35] © NACE International 1990. (c) Schematic view of implications of increasing acuity. From Staehle.[36] © NACE International 1996.

4.3 Near-Surface Environment Domain

A schematic view of the Near-Surface Environment Domain is shown in Figure B.15.18 as a part of the overall array of domains in Figure B.15.5. Examples from this domain are the following:

Heat transfer crevice

While the heat transfer crevice has been changed in the new generation of SGs, from the comprehensive envelopment of drilled holes, the occurrence of conditions for concentrating impurities persists as deposits continue to accumulate in line-contact geometries, although the resulting concentrations of species in these geometries have not been studied. Figures B.15.27a, b, c[37] show the nature of the chemical crevice in its complexity of chemistry, phases and gradients. Figures B.15.27d and e[1] show a schematic view of accumulation of deposits at egg crate line-contact crevices. These near-surface environments are substantially different from bulk environments in concentrations as well as in ratios of elements. Further, their chemistry changes in time. Such concentrating capacities of these crevices enable concentrating Pb, (e.g. from the ppt range to the low percentage range), at the metal-environment surfaces. It is likely that the line-contact accumulations will produce different chemistries from the drilled holes in view of the differences of geometry as these affect the concentration of species.

Accumulation of deposits and cells

Deposits accumulate with time due to superheat at the surfaces of tubes at tube supports and at the top of the tubesheet, as shown in Figures B.15.28a, b, c.[1] Such accumulations vary with locations. These deposits lead to the formation of electrochemical cells.

Deposit expansion and forces

Aside from the chemical and electrochemical aspects of deposits, as well as their heat transfer resistance; deposits also produce large forces in constrained geometries. Figure B.15.29, from the work of Pickering et al.,[23] shows a stainless steel specimen that was exposed in the non-stressed conditions with a stainless steel insert. The corrosion products that accumulated in the crevice between the specimen and the insert produced stresses, which caused SCC to start at the bottom of the crevice. After this SCC had propagated some distance, the insert was removed as part of the experimental program, and the corrosion products in the propagating SCC exerted sufficient force to cause the SCC to continue. These forces are produced by the larger specific volume of the oxide compared with the metal as reported in 1923 by Pilling and Bedworth.[24]

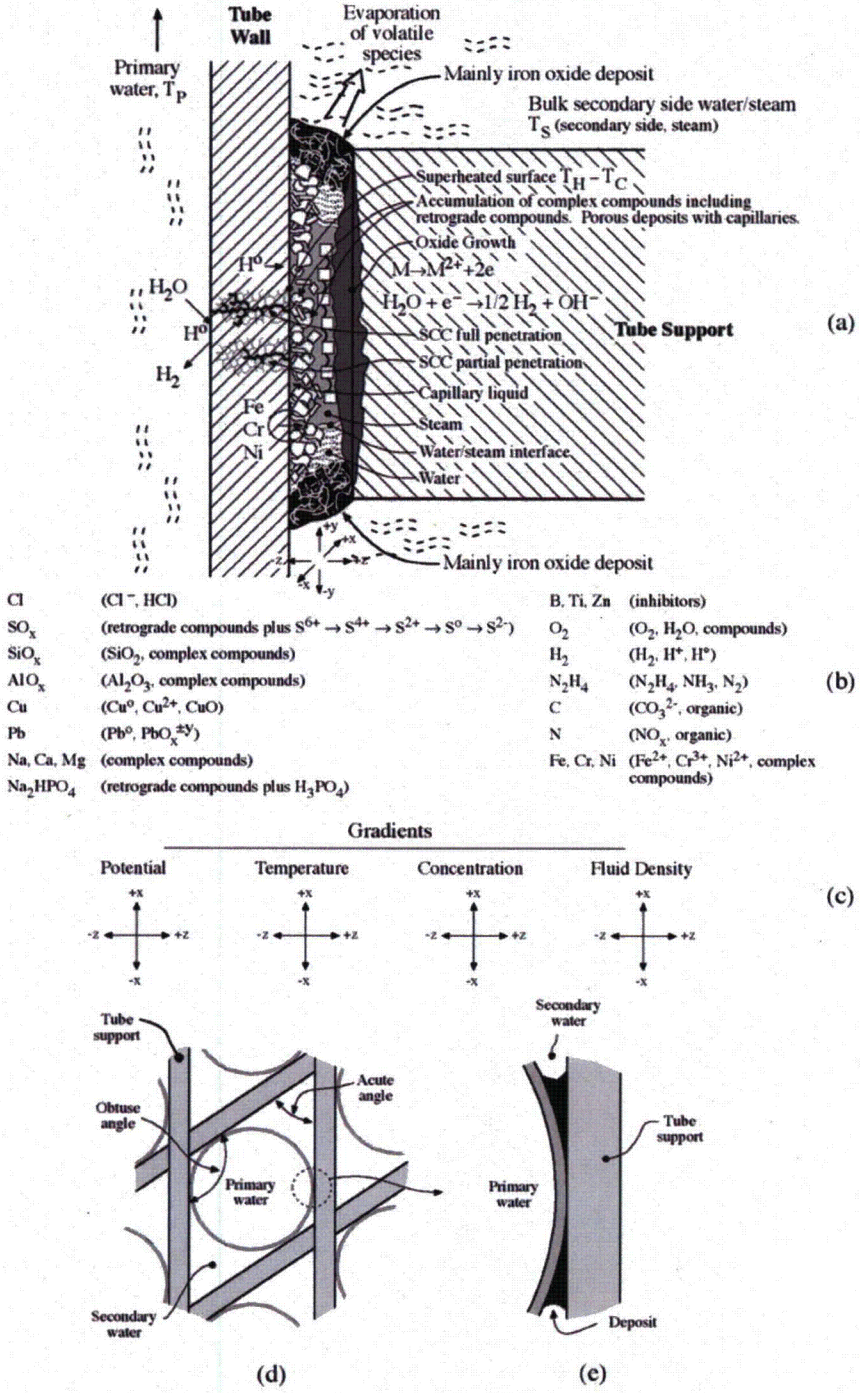

Figure B.15.27 Schematic view of heat transfer crevice at a tube support. (a) Geometry. (b) Chemicals that accumulate and transform. (c) Types of gradients inside the heat transfer crevice. From Staehle.[37] (d) Egg crate design of tube support and (e) schematic view of accumulation of deposits in line-contact geometry, based on direct observations. From Staehle and Gorman.[1] © NACE International 2003/2004.

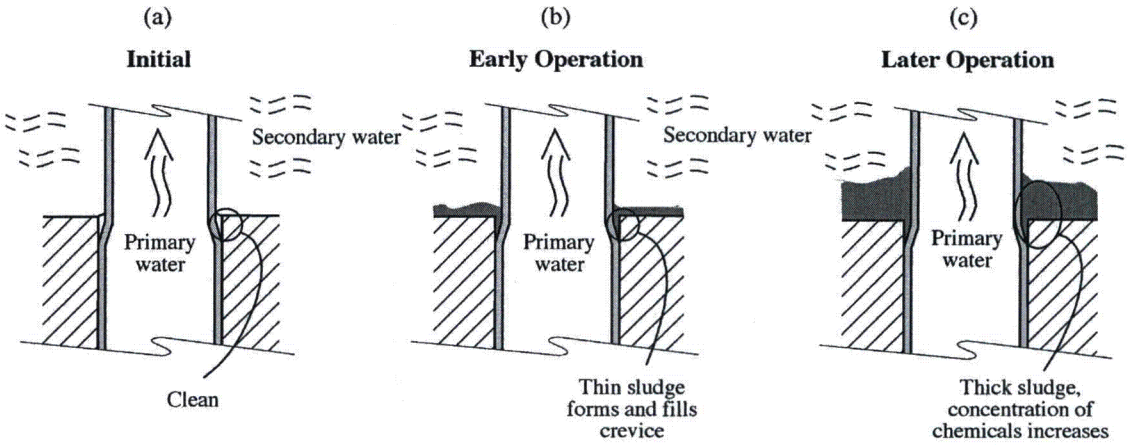

Figure B.15.28 Accumulation of deposits on top of the tubesheet with time. From Staehle and Gorman.[1] © NACE International 2003/2004.

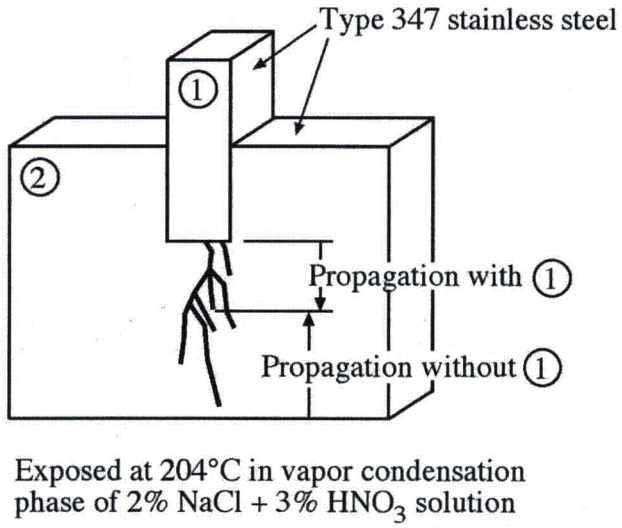

Figure B.15.29 Demonstration of forces produced by corrosion products. Stainless steel block and insert exposed at 204°C in vapor condensation of 2% NaCl+3%HNO_3 solution; no applied stress. SCC propagates with corrosion product forces between block and insert. Insert removed and cracks propagate due only to corrosion products in initial cracks. From Pickering et al.[23]

4.4 Protective Film Domain

Properties of protective films dominate much of the corrosion behavior of metals. Further, this film interacts with slip processes in the metal and through its normal epitaxial connection to the metal, produces stresses in the substrate. Also, the defect concentration in the film catalytically affects oxidation and reduction reactions. The relative position of the protective film in the domains is shown in Figure B.15.5, and examples of important related microprocesses are shown in Figure B.15.19.

Epitaxial film growth

Epitaxial protective films grow with time according to various rate laws and following influences of alloy, pH, and potential. Figure B.15.30[38] shows the effect of potential and alloy composition on the thickness of protective films on iron base alloys. These films affect the catalytic influence on electrochemical reactions and the overall rate at which the alloy dissolves, as it is controlled by the properties of these films.

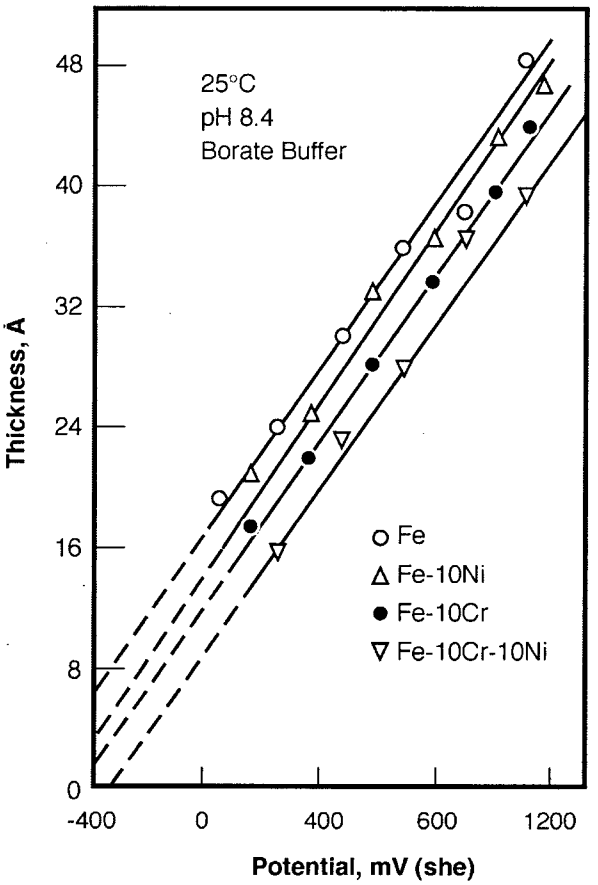

Figure B.15.30 Film thickness vs. electrochemical potential for Fe, Fe-10Ni, Fe-10Cr, and Fe-10Ni-10Cr alloys after one hour of polarization at 25°C measured in a pH 8.4 borate buffer solution. From Goswami and Staehle.[38] Reprinted with permission from Elsevier.

Slip as affected by protective films

Figure B.15.31[39] shows the effect of epitaxial films on the single slip of a nickel single crystal. The protective film increases the work hardening, therefore increasing the slope, on the surface as shown by the work of Latanision and Staehle; whereas, the absence of the protective film permits the non-inhibited single slip. In the former, the slip steps are dispersed and finely divided; whereas, for the non-filmed surface, the slip is coarse and sharp. The presence of such films, then, affects the mechanical properties.

Brittle film rupture

Figure B.15.32[40,43] illustrates the process by which SCC proceeds as related to the formation of a brittle reaction product on the surface. Such a brittle surface might develop from the formation of an epitaxial reaction product such as is assumed for copper alloys in ammoniacal solutions. The periodic breaking of such a brittle film has been often suggested as the means of propagation of some SCC. The rate of crack propagation, then, is related to the growth rate of the brittle film.

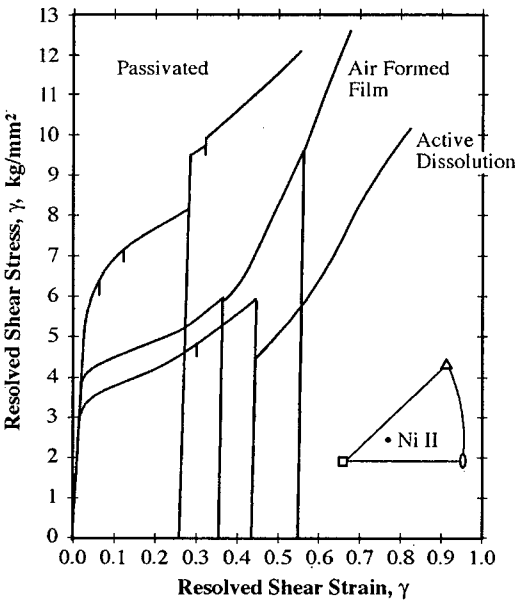

Figure B.15.31 Flow curves illustrating the effect of interruptions in tensile tests under active and passive conditions. About 3-4 μm were removed from the crystal surface before deformation under dissolution conditions at a steady state current density of approximately 4 mA/cm^2. From Latanision and Staehle.[39] Reprinted with permission from Elsevier.

4.5 Near-Surface Metal Domain

Enrichment and depletion

As some alloys dissolve, the atoms may dissolve as "alloy atoms," so that they appear to be essentially the same atom, although of different chemistries.[41] Alternatively, in an alloy, especially where one atom is more electrochemically active than the other, (e.g. Cr in a Ni base or Zn in a Cu base), preferential loss of the more active Cr or Zn is expected, especially in the ranges of pH where the active species are also relatively soluble and in ranges of potential above the solution potentials for the more active species. Figure B.15.33a[41] shows data from Staehle based on work of Rockel; and Figure B.15.33b[42] shows data from Lumsden and Stocker. Figure B.15.33 shows that the surfaces of materials change with time from the original composition of the alloy due to the loss of Cr. Such a change affects the electrochemistry and the mechanical properties of the surface. These depletions and enrichments change the chemical composition of the surface, and thereby change the catalytic and mechanical properties of the near surface—sometimes producing a brittle layer similar to the one described in connection with Figure B.15.32.

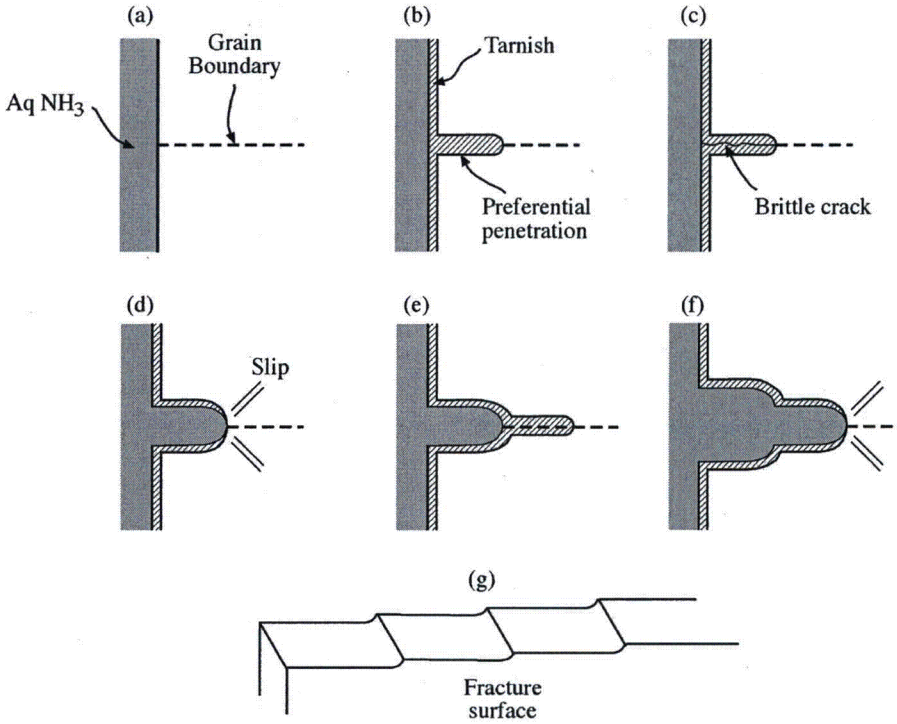

Figure B.15.32 Formation of brittle film on surface followed by successive breaking thereby producing SCC. From Pugh et al.[40] © NACE International 1969 and Forty and Humble.[43]

Preferential dissolution of phases

In the same environment, the phases in a multiphase structure may dissolve differently. These differences depend on the pH and potential of the dominating environments. Figure B.15.34[44] shows that the relative dissolution of pearlite, Fe_3C and α-Fe, depends on the pH and potential as well as species. Four modes of dissolution are observed: general dissolution independent of the phase, preferential dissolution of the α-Fe, preferential dissolution of the Fe_3C, and preferential dissolution of the interface between the Fe_3C and α-Fe. Each of these modes could affect initiation and propagation of SCC.

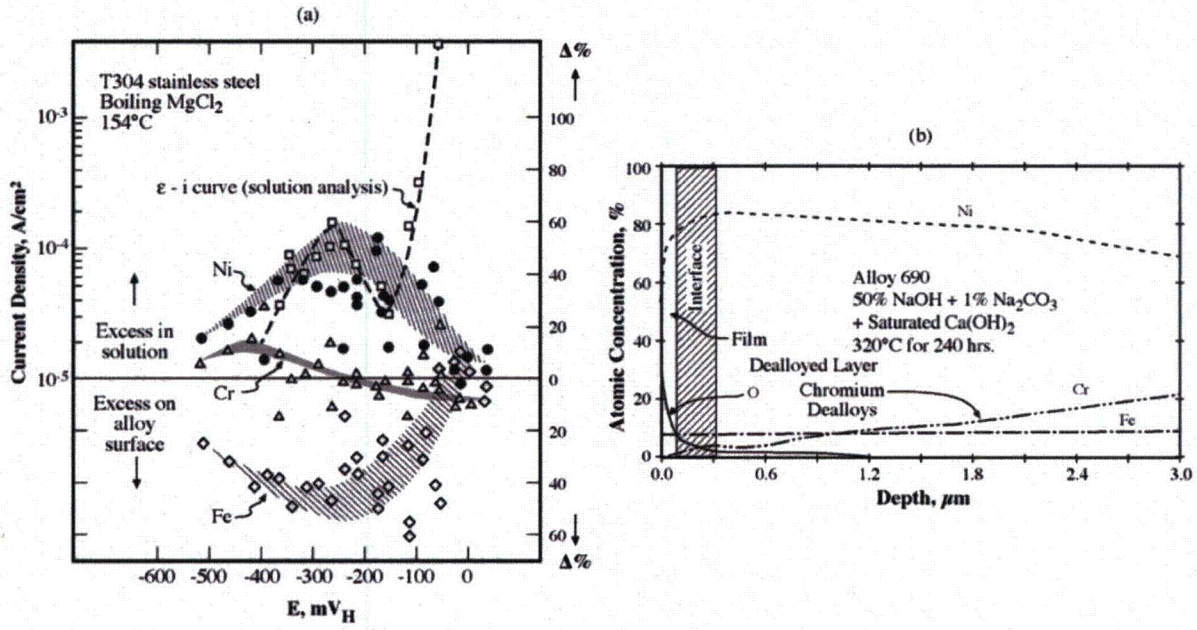

Figure B.15.33 (a) Surface enrichment/impoverishment, Δ, of Fe, Cr and Ni on Type 304 steel in $MgCl_2$ at 154°C as a function of applied potential. From Staehle.[41] © NATO-SCREC 1971. (b) Composition profile of Alloy 690 after exposure to 50% NaOH+1%Na_2CO_3+saturated $Ca(OH)_2$ at 320°C for 240 h from depth analysis using Auger spectroscopy. From Lumsden and Stocker.[42] © NACE International 1988.

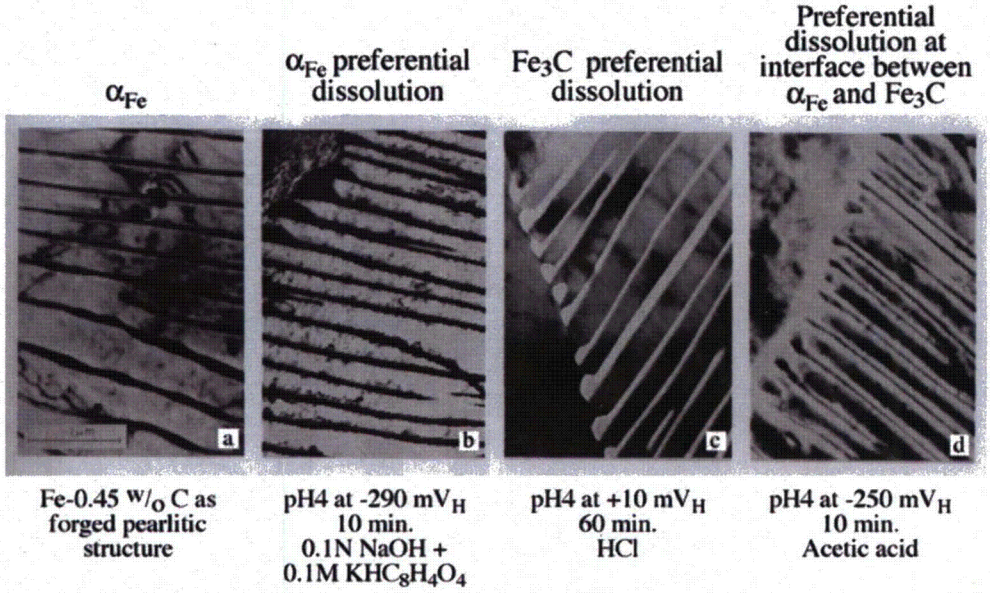

Figure B.15.34 TEM micrographs of pearlite (1045 steel) foils exposed to various pH and potentials and species showing preferential dissolution of three types. From Payer and Staehle.[44] © NACE International 1974.

Slip trenches and tunnels

When dislocations move and intersect a passive surface, the passive film is broken; a transient dissolution event occurs, the metal initially dissolves, and then repassivates. Such events are shown in Figure B.15.35a.[45,46] In Figure B.15.35a, a thin foil has been exposed to a corrosive environment and stressed, after which it was examined in a transmission electron microscope. The image shows that parallel dissolution events have occurred within a single grain and that dissolution has occurred on both sides of the foil as shown by parallel dissolution traces. In this case, such parallel dissolution traces occur on intersecting slip planes. Figure B.15.35b[47] shows, by examining an oxide film, which was removed from the surface, that tunnels can emanate from the slip trenches observed in Figure B.15.35a. Conditions that support the transient dissolution of Figure B.15.35 depend on pH, potential and species in the environment. It is likely that environments that support transgranular SCC also support both the trenches and the tunnels of Figure B.15.35.

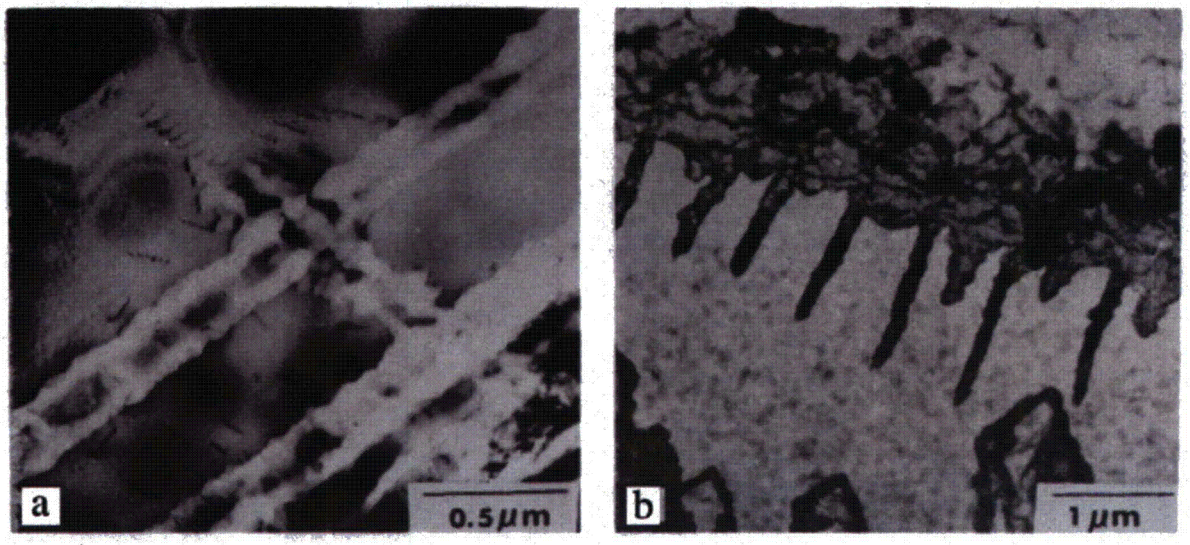

Figure B.15.35 Two similar modes of corrosion at surfaces, which is associated with moving dislocations breaking the surface and protective film. (a) TEM image of thin Fe-Cr-Ni alloy foil stressed in a corrosive medium at RT and then examined in the TEM. Parallel thinned regions indicate preferential dissolution at both sides of the foil. Two slip systems are identified. From work of Smith[45] and Davis.[46] T.J. Smith, Master's Thesis at The Ohio State University 1965 and J.A. Davis, Ph.D. Dissertation at The Ohio State University 1968. (b) An oxide film removed from the surface of stainless steel after exposure in a stressed condition to a corrosive environment. The thick region corresponds to the slip dissolution trenches shown in (a) and the protrusions are "tunnels" that have penetrated from the base of the dissolution trench. From Long.[47] Master's Thesis, The Ohio State University, 1973.

4.6 Bulk metal domain

Stacking fault energy

Much of stress corrosion cracking and corrosion fatigue depend critically on the movement and relative coplanarity of movement of dislocations as they react to local stresses. There are two main patterns of dislocation movement that affect corrosion processes, as well as other aspects of deformation or fracture that are not considered here. Slip is important to SCC as it relates to breaking protective films, either during the slip process as shown in Figure B.15.35, or as the pile-up of dislocations at internal barriers intensifies local stresses at grain boundaries that interact with a corrosive environment.

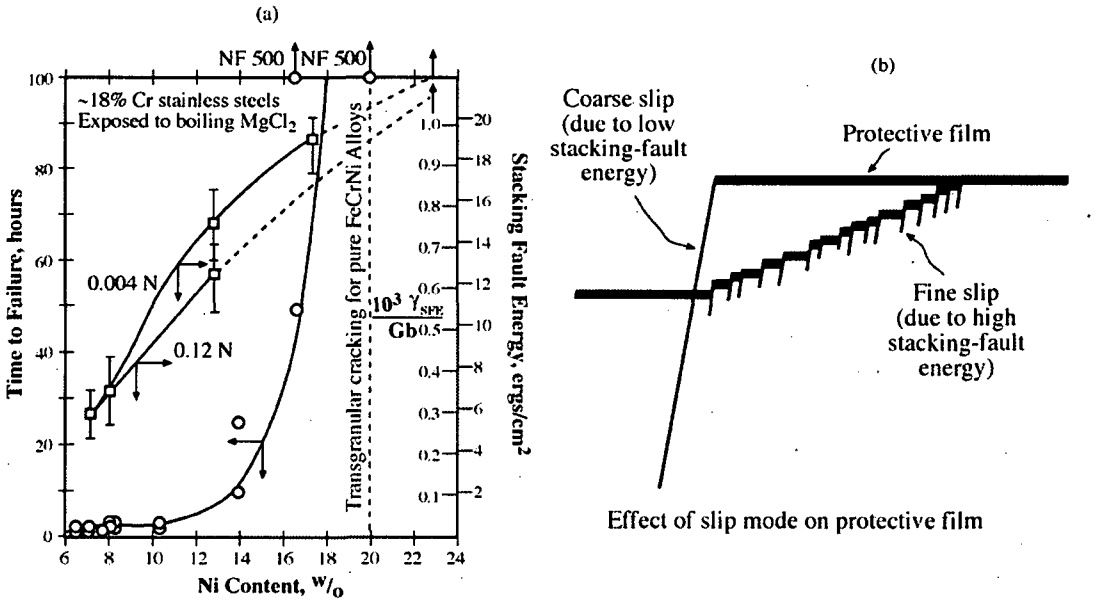

Figure B.15.36 (a) Time-to-failure for 18%Cr stainless steels exposed to boiling $MgCl_2$ compared with stacking fault energies for the same materials. (b) Nature of slip as affected by relatively high and low stacking fault energies.

Both roles, single slip and cross slip, of dislocation movement are related to whether the slip remains generally on single slip planes to intensify local stresses and the sharpness of slip step at the surface or can cross slip to relieve the intensification of local stresses as well as producing distributed slip at the surfaces. Dislocations can be generally constrained to remain on single slip planes once nucleated. On the other hand, the dislocations might "cross slip" out of the single plane and thereby relieve the local pile-up stresses. These two tendencies depend on the "stacking fault energy." A high stacking fault energy stimulates cross slip, and a low stacking fault energy stimulates single slip. Thus, a high stacking fault energy would mitigate against SCC related to internal barriers; whereas, a low stacking fault energy would promote SCC. Figure B.15.36 shows how the stacking fault energy relates to SCC and to the nature of surface slip.

Composition of grain boundaries

The composition of grain boundaries is affected in two ways and according to somewhat different dimensional scales as shown in Figure B.15.37. Figure B.15.37a[7] refers to the formation of precipitates, such as chromium carbide, in stainless steel. The dimensions here are on the order of μm. Three conditions result from this process. First, the precipitate forms with a concentration of the metal typically greater than in the metal matrix. In the case of stainless steels, the compound is in the range of $Cr_{22}C_7$ or Cr_7C_3. This high concentration of chromium renders the alloy corrosion resistant in neutral solutions; but, in alkaline solutions the chromium is quite soluble relative to iron. Adjacent to the precipitate is a depleted zone from which the chromium has been taken to form the Cr_xC_y compound. Such a zone, when depleted of chromium, is more prone to corrosion in neutral to acidic solutions but is more resistant to alkaline solutions. In addition, there is usually a narrow zone at the interface between the precipitate and the depleted zone where impurities are concentrated. Such interfaces have rarely been studied; but results, such as those in Figure B.15.34d, suggest that they could be prone to preferential corrosion depending on what species have been attracted or reflected during the formation of pearlite. Figure B.15.37c[7] shows the relative polarization rates for alloys across the range of alloy compositions.

In Figure B.15.37b,[7] the case of adsorption and desorption of species is shown for impurities and for alloying species. For the case of impurities, concentrations at the grain boundaries have been observed to be up to 10^6 greater than in the grain matrix. The dimensions of these highly concentrated regions are in the range of nm. Such concentrations, although narrow, provide a reactive path for corrosion. Figure B.15.37d shows the effect of such adsorption on the cracking behavior of Ni with sulfur segregated at the grain boundary.[48,49]

Much of the preferential IGC and IGSCC is related to cases where such changes in concentration occur at grain boundaries as shown in Figure B.15.37.

5. Development of Scenarios

Developing a scenario is the essential process of predicting failures that occur after long times as shown in Figure B.15.1. A schematic illustration of developing a scenario is shown in Figure B.15.6. The scenario begins with the start of a power plant or from a suitable reference time, and identifies the components in the precursor as shown in Figure B.15.6. The components of the scenario are taken from the domains and their microprocesses, as described in Sections 3.0 and 4.0. Quantifying the microprocesses provides a basis for estimating the time before an SCC process can start. The times consumed by the developing microprocesses depend on the kinetic process that occur in the range of operating conditions of the plant. Further, it is likely that some of the microprocesses occur in sequence, thereby requiring the completion of one before the onset of the next. Finally, at the end of the precursor stage, the chemistry and configuration must lead to a viable SCC or other damage process.

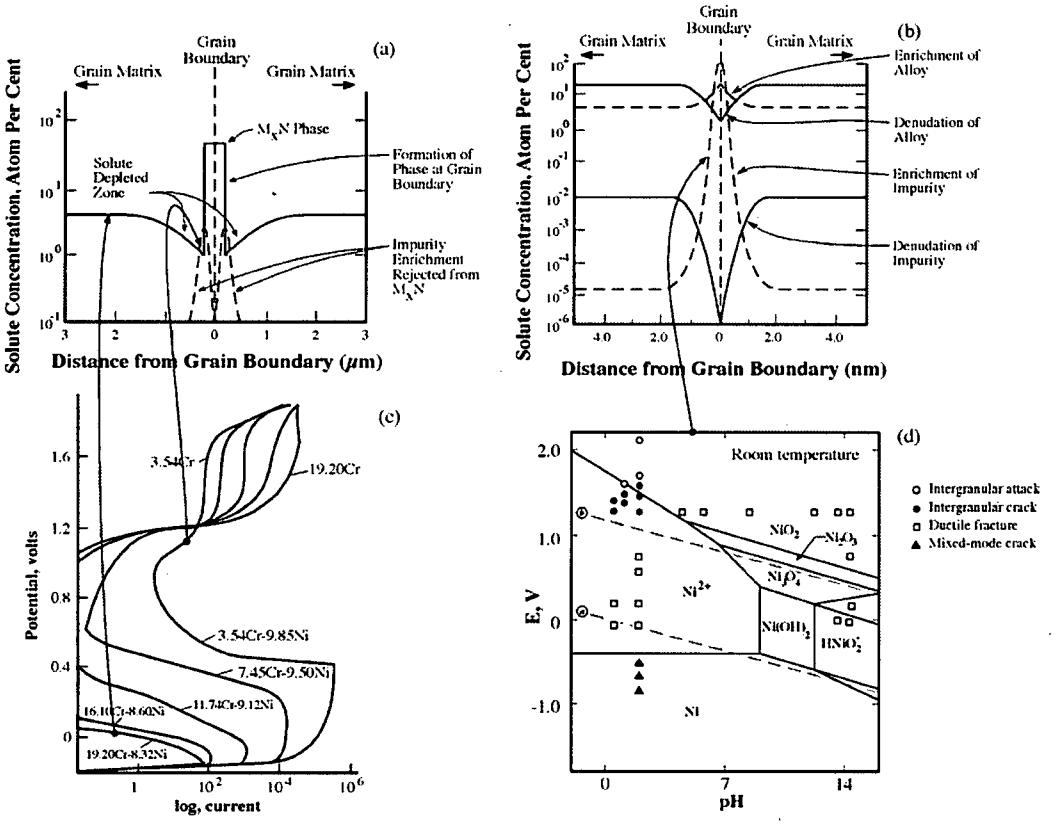

Figure B.15.37 (a) Distribution of species at grain boundary for the case of precipitation. (b) Distribution for the case of adsorption. (c) Polarization behavior in sulfuric acid at RT for alloys across the grain boundaries. From Staehle.[7] Courtesy of John Wiley & Sons, New York. (d) Cracking behavior for a Ni-base alloy with sulfur segregation as a function of pH and potential. From Chaung et al.[48,49] Reprinted with permission from TMS.

Selecting the domains and microprocesses, as shown schematically in Figure B.15.6, requires expert experience. More than a single scenario would probably be considered.

Figure B.15.38 shows the overall process for selecting a scenario, evaluating the important rates upon which the length of the precursor stage is based, and applying the result to the starting point for the SCC.

6. Target

The goal of developing scenarios is to identify conditions under which SCC or some other important damage process will start according to the pattern of Figure B.15.1, Case III. For such a target to be achieved, the target itself needs to be identified. One might be LPSCC or PbSCC as shown in Figure B.15.22. However, there may be others. There is a task, then, of quantifying possible targets, which embody conditions initiating SCC, some of which have not occurred in the past but can reasonably be identified for possibly occurring in the future.

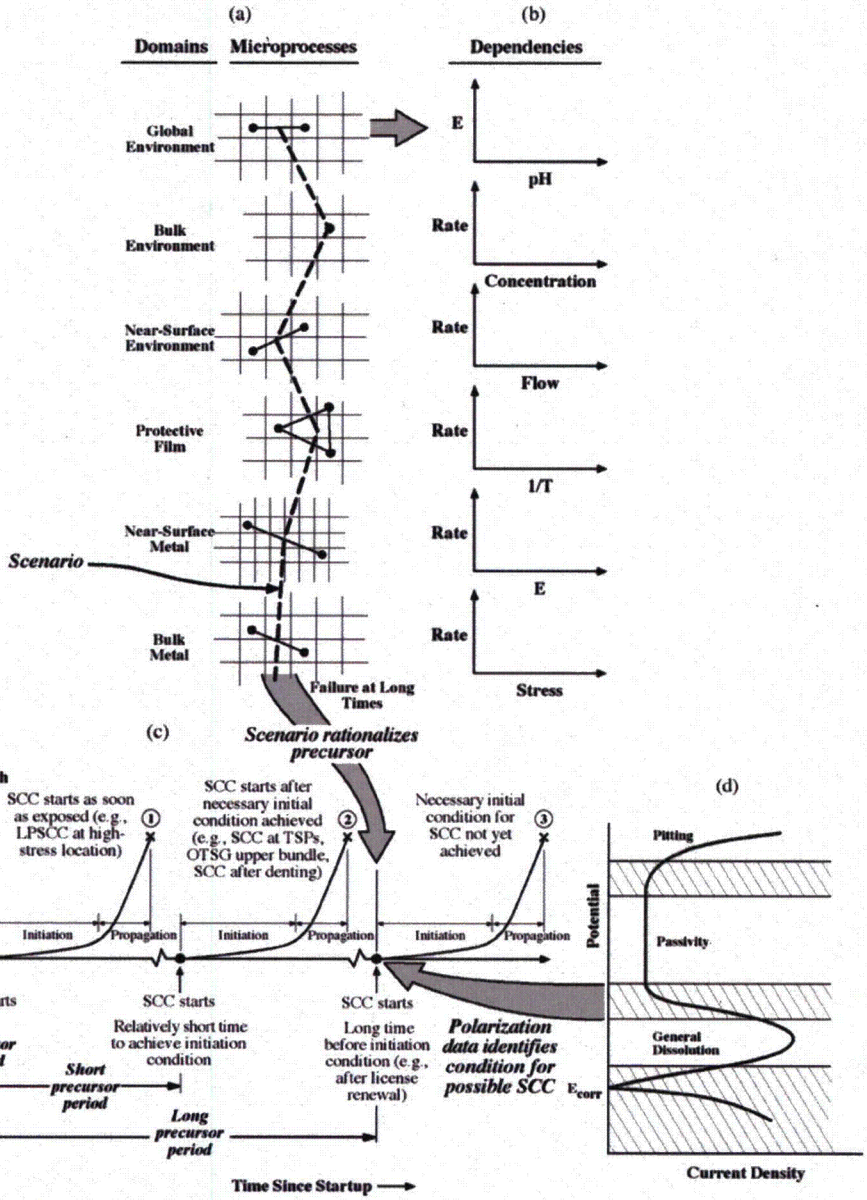

Figure B.15.38 Schematic view of overall process of prediction. (a) Scenario including microprocesses from various domains; scenario connects microprocesses from various domains. (b) Hypothetical rates associated with microprocesses to be used for estimating length of precursor period. (c) Three cases for SCC with precursor times identified. (d) Possible location of target for SCC initiate.

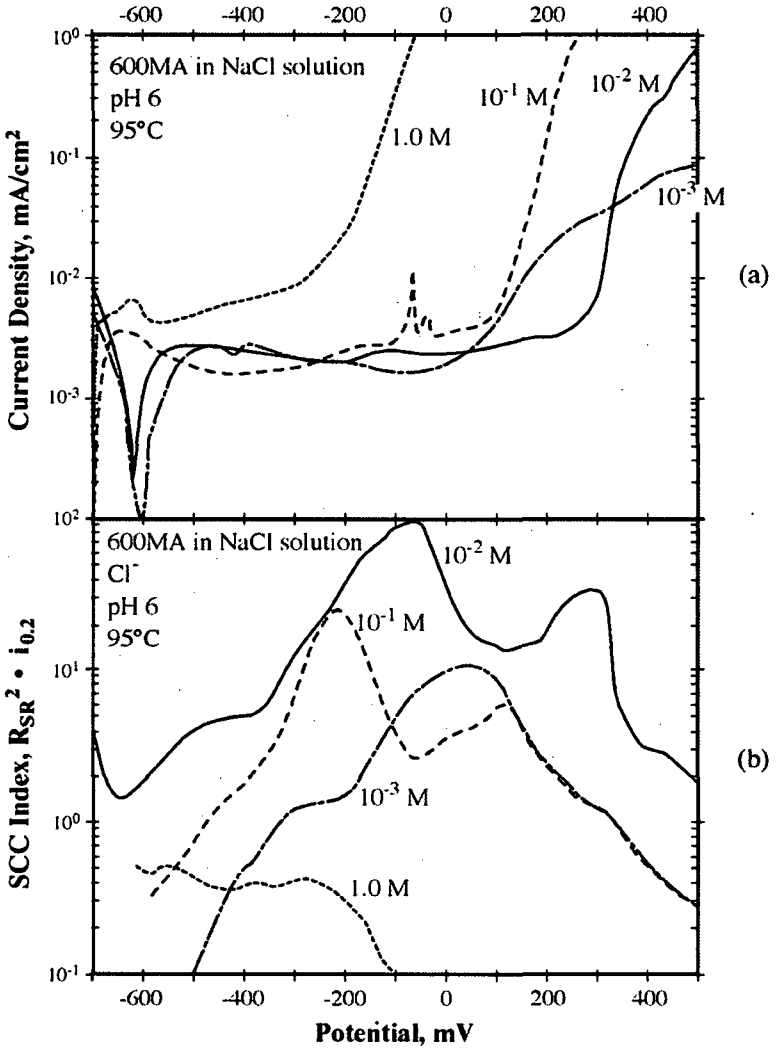

Figure B.15.39 Current density and SCC parameter vs. potential for Alloy 600MA in NaCl solutions at pH 6 and 95°C for concentrations from 10^{-3} to 1.0 M. From Staehle and Fang.[50] Courtesy of SFEN.

Where some SCC is suspected to occur, but for which no information is available, there are several survey approaches that can be used and have been successful in the past. Figure B.15.39 suggests that locations for the initiation of SCC often occur at potentials near regions of kinetic instability. Such regions can be evaluated using electrochemical methods, either by identifying regions of transition such as in Figure B.15.38d, or regions where there are large differences between slow and fast scans. Figure B.15.39 shows polarization curves for Alloy 600MA in 95°C NaCl solutions. Figure B.15.39b shows a SCC parameter, which has been developed by Staehle and Fang[50] vs. potential. This parameter is based on the differences in currents between fast and slow potentiodynamic scans. Peaks in Figure B.15.39b identify potentials where SCC is likely.

Another approach for identifying regions of possible SCC has involved CERT tests that are conducted as functions of potential. Such data are shown in Figure B.15.40 from experiments by Parkins[51] and others.

There are other well-known methods for identifying targets of the scenarios suggested in Figures B.15.6 and B.15.38. The principal point here is that surveying possible future targets for scenarios is an important part of prediction. Such approaches can rely on the fact that the boundaries and domains of SCC are generally orderly, as suggested by Figure B.15.41, which shows the zone of SCC for stainless steel in acid chlorides at room temperature from the work of Morin and Staehle.[52,57]

7. Predictions

Using the approach described in Sections 3.0 and 4.0 and Figures B.15.1, B.15.6, and B.15.38 some predictions are possible, and examples of these are described in this section.

Transport of low valence sulfur to turbine

Figure B.15.42 shows a sequence of events involving the microprocesses described in Sections 3.0 and 4.0. The essence of prediction as shown in Figure B.15.42 is the following:

a. Sulfate impurities are reduced in steam generators by hydrazine to a low valence sulfur species (M-1) such as HS^-.

b. The low valence sulfur species is transported (M-2) to the turbine.

c. This low valence sulfur species deposits (M-3) on surfaces of the turbine where the materials are generally high strength alloys.

d. High strength alloys are prone to SCC and failure occurs after sufficient accumulation of the low valence sulfur species (M-4).

Such a possible sequence of events can be evaluated by:

a. Analyzing surfaces in turbines.

b. Evaluating the SCC behavior of turbine alloys in such environments as are found on surfaces.

LPSCC of Alloy 690 occurs as chromium is depleted from the surface

Figure B.15.43 shows a sequence of events whereby Alloy 690TT can sustain LPSCC as follows:

a. Chromium dissolves preferentially in the environment at moderately alkaline pH as shown in (M-1).

b. The surface, as it is depleted, (M-2), becomes an alloy like Alloy 600, as at (M-3), and sustains LPSCC as shown in (M-4).

This sequence implies that the LPSCC will propagate as rapidly as the chromium is depleted from the surface. This surface eventually becomes the crack tip; the tip of the crack then advances as rapidly as the chromium is preferentially dissolved. Such a possible sequence can be evaluated with ATEM and by evaluating the pH of solutions inside advancing SCC.

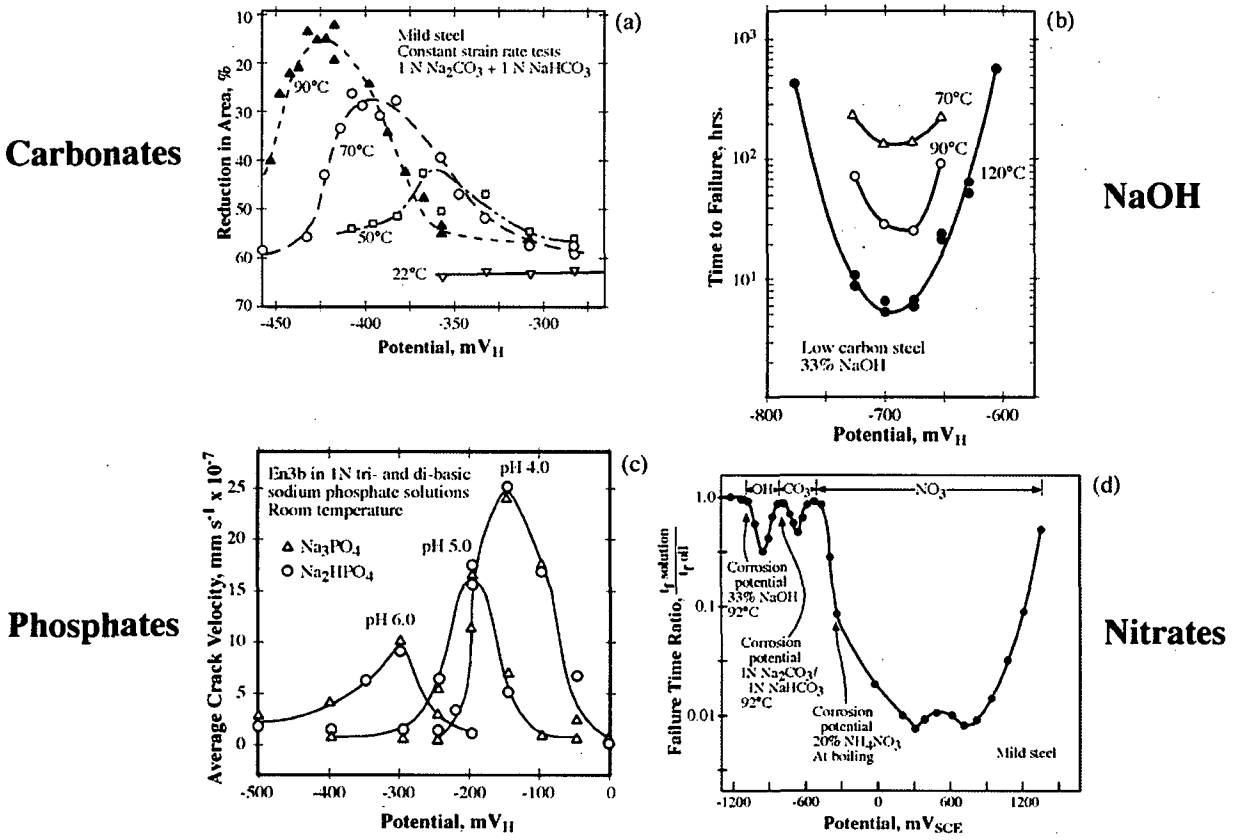

Figure B.15.40 (a) Reduction in area vs. potential for mild steel exposed to carbonate-bicarbonate solutions at various temperatures and tested in CERT. From Sutcliffe et al.[53] © NACE International 1978. (b) Time-to-failure vs. potential for three temperatures for a low carbon steel in 33% NaOH. From Singh[54] (Courtesy of Steel India) reporting on Bohnenkamp.[55] © NACE International 1969. (c) Average crack velocities vs. potential for (plain carbon steel) En3b (w/o C 0.12, Si 0.05, Mn 0.81, S 0.029, P 0.008) steel in Na_3PO_4 and Na_2HPO_4 tested at RT function of pH. From Holroyd.[56] N.J.H. Holroyd PhD Dissertation 1977. (d) Ratio of time-to-failure in solution to time-to-failure in oil vs. potential for NaOH, Na_2CO_3 + $NaHCO_3$ and $NaNO_3$ solutions. From Parkins.[51] Courtesy of Inst. of Mat., Minerals & Mining 1972.

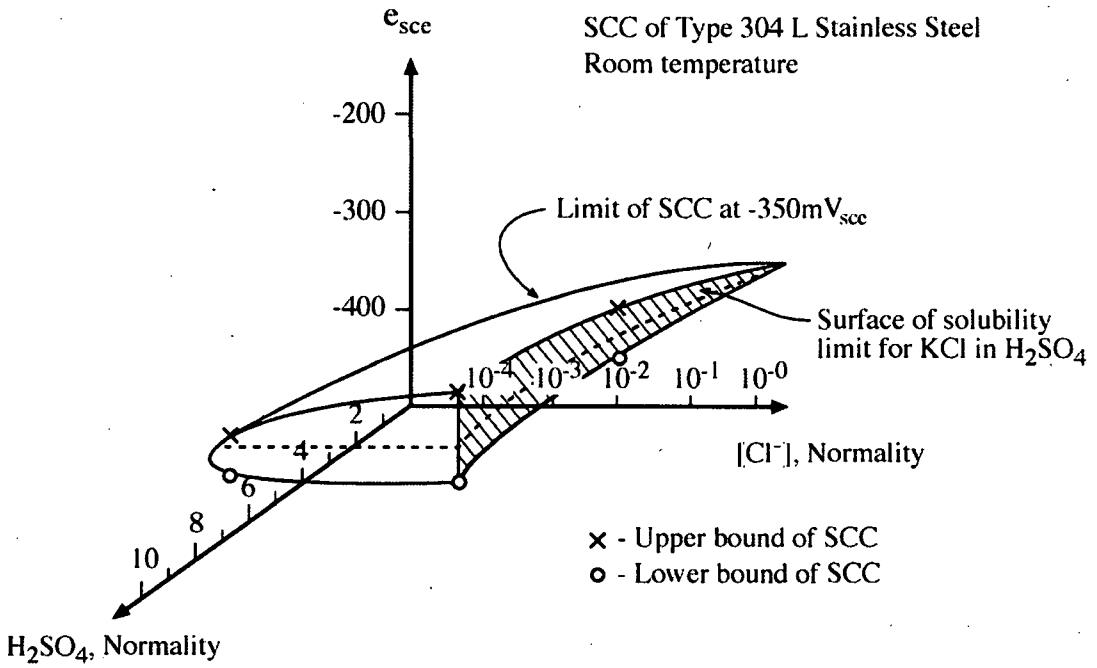

Figure B.15.41 Zone for the occurrence of SCC in stainless steels as a function of potential, H_2SO_4, and KCl at room temperature. From Morin[57] C.R. Morin Master's Thesis, The Ohio State University 1972 and used by Staehle.[52] Reprinted with permission from TMS.

PbSCC occurs as Pb is released from sequestering compounds

One of the as yet unexplained observations in the performance of SGs is why massive PbSCC is not occurring despite the relatively large amount of Pb present in crevices and also known to be present in some stress corrosion cracks that have been examined. Further, Pb has been shown to produce SCC at relatively low concentrations of Pb. It also appears that PbSCC occurs readily in Alloy 690TT.

Thus, understanding why PbSCC does not occur when the threshold for concentration is so low and the PbSCC is so rapid, is an important question. The answer to why PbSCC does not occur seems related to the fact that the activity of Pb is lowered by the formation of Pb-containing compounds. Such compounds could include silicates, phosphates, sulfates, carbonates, or chlorides separately or as multiple component compounds.

Since the compounds that form in crevices are in some equilibrium with the species in the bulk water, reducing such species might raise the activity of the Pb making it available for producing PbSCC.

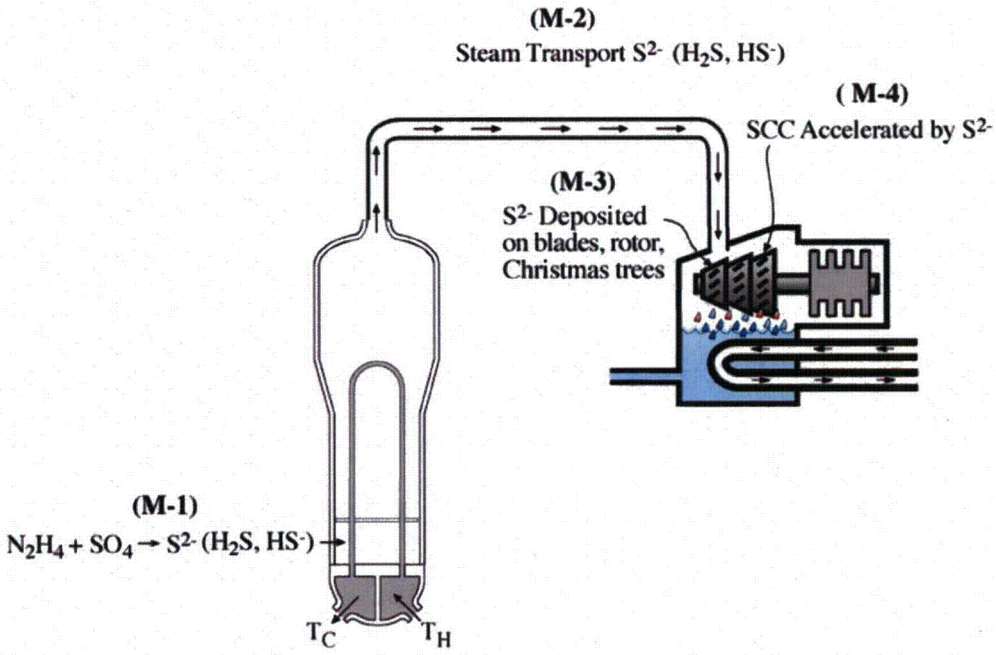

Figure B.15.42 Reduction of SO_4^{2-} by N_2H_4 in the SG and transport of reduced sulfur to the surfaces of the turbine where accelerated SCC is possible especially in view of high strength alloys from which the blades and rotors are constructed.

Figure B.15.44 shows a sequence of events associated with raising the activity of Pb by reducing the available compound-forming species.

a. Heat transfer crevices concentrate chemicals from feed water (M-1).

b. Lead enters heat transfer crevices (M-2).

c. A deposit forms containing Pb (M-3).

d. Pb concentrates on the hot surface as is observed from direct analysis (M-3).

e. Increasing the Pb activity is known to increase the intensity of PbSCC (M-4).

f. The activity of Pb will increase when the activity of compound forming species in the bulk water decreases (M-5).

Thus, it is possible that PbSCC will occur if the secondary water is further purified.

Such a process as described in Figure B.15.44 can be assessed by determining what compounds and chemical processes can immobilize the Pb. Such work has not yet been undertaken but it could predict the course of PbSCC.

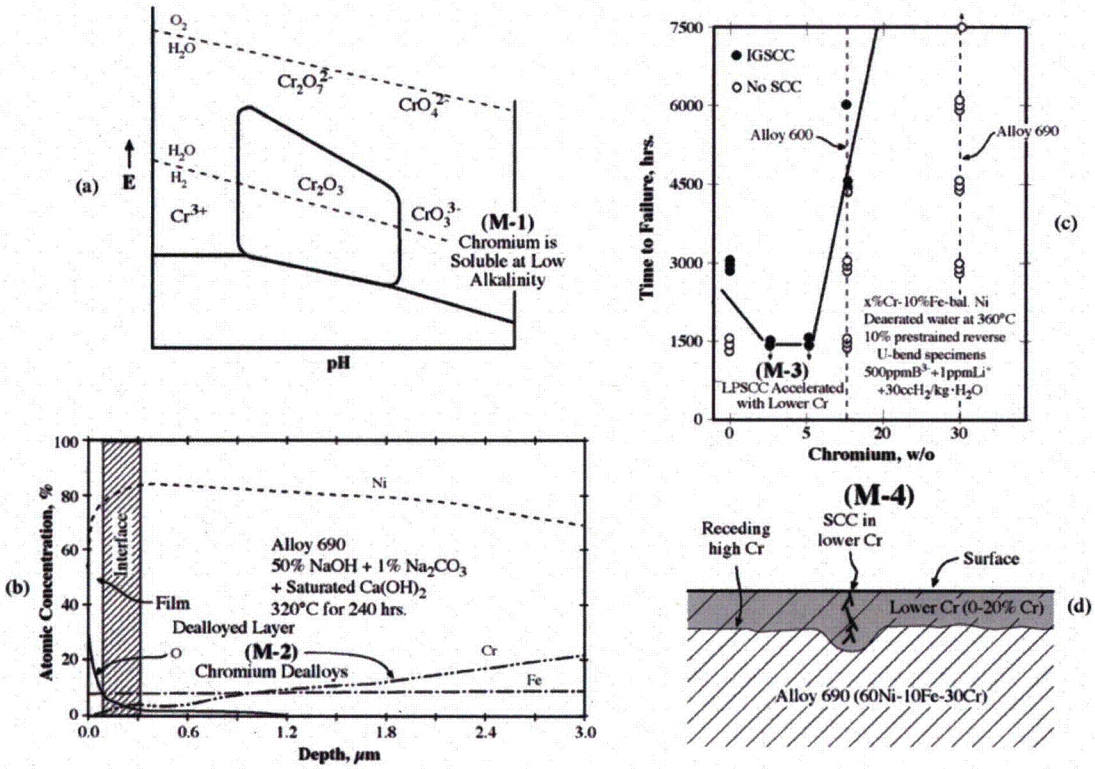

Figure B.15.43 The Cr of Alloy 690 is soluble in mildly alkaline solution and dissolves to give a lower Cr surface and is more prone to LPSCC.

SCC of low alloy steels in FAC type environments

SCC is known to occur episodically in low alloy steels when exposed to FAC type environments as well as to other environments. The episodic nature of the SCC suggests that the high velocity of coolant is, in fact, removing the initiating events, and only initiating events whose velocities that exceed the recession rate of the FAC can actually become growing SCC. Such a pattern suggests that lowering the FAC rate may increase susceptibility to SCC according to the following sequence as shown in Figure B.15.45.

a. The rate of recession of a surface is greater than the rate of penetration of SCC initiation (M-1), (M-2).

b. The initial material is replaced with one having a lower rate of FAC; however, the rate of recession is less than the penetration rate during initiation. (M-3)

c. The rate of initiation now exceeds the rate of recession (M-4).

At this point SCC can initiate and propagate.

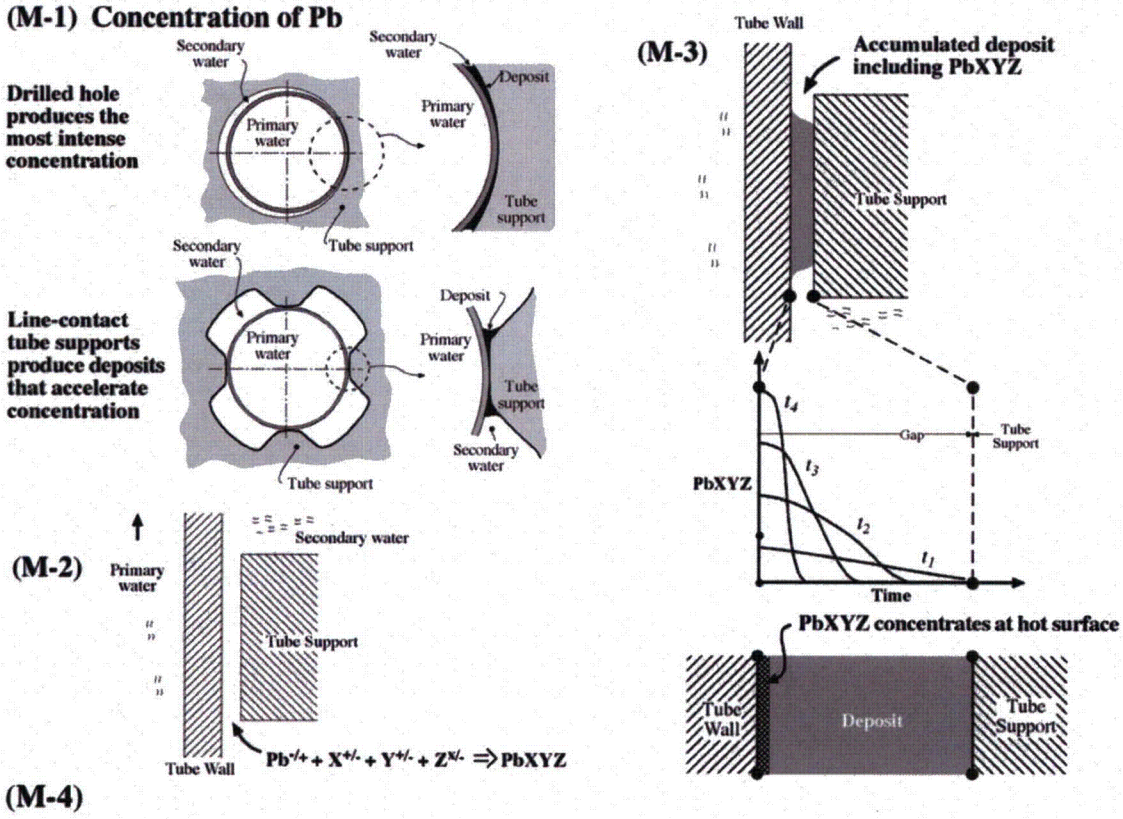

PbSCC increases when Pb activity [a_{Pb}] increases at metal surface [$a_{Pb,\,s}$]

1. **Pb activity increases when activity of compound-forming species decreases**

$$\text{e.g., } [a_{Pb,\,s}] \uparrow \text{ when } [a_{X,\,s}], [a_{Y,\,s}], [a_{Z,\,s}] \downarrow$$

2. **Activity of compound-forming species decreases on metal surface when these activities decrease in the bulk solution**

$$\text{e.g., } [a_{X,\,s}] \downarrow \text{ when } [a_{X,\,B}] \downarrow$$

(M-5)

PbSCC increases when activity of compound-formers (X,Y,Z) decreases in bulk

Figure B.15.44 Pb is concentrated in heat transfer crevices and accumulates at the surface. Initially, Pb is immobilized by forming compounds. When the activity of these insolubilizing species is reduced, Pb is released and PbSCC occurs.

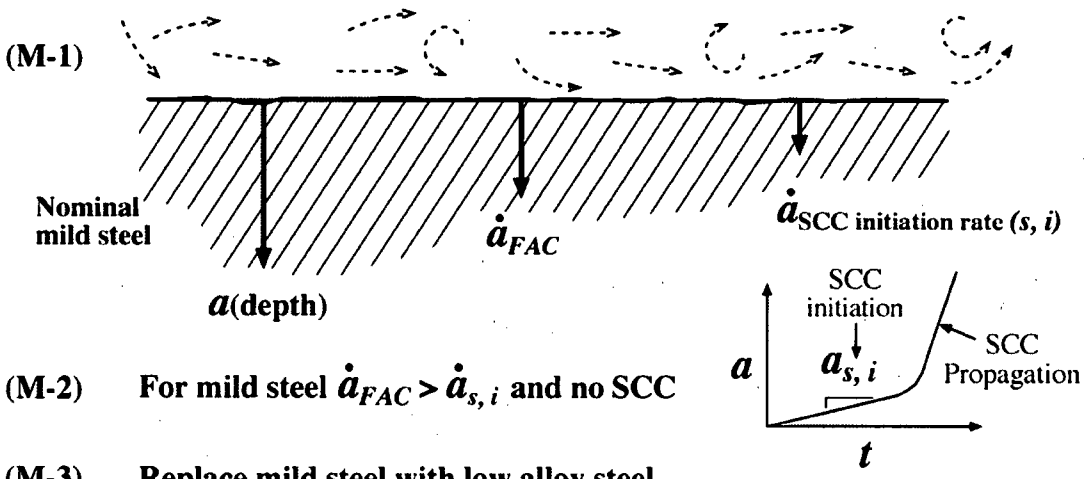

Figure B.15.45 Sequence of events for reduction in rate of FAC and then permitting the SCC initiation process to accelerate and perforate.

8. Conclusions

1. In order to assure reliability for long time performance, methods for predicting corrosion failures that have not yet occurred should be considered. Such methods include the Microprocess Sequence Approach (MPSA).

2. The essence of predicting corrosion failures that occur after long times of service is recognizing that such processes as SCC will not proceed monotonically from the beginning of operation to a failure many tens of years later. Rather, predicting the occurrence of failures after long times most likely results from a multi-step analysis. First, there are some processes that develop conditions that are favorable to the later occurrence of SCC. The first steps are "precursors." Second, once the necessary conditions for SCC coalesce, then the SCC proceeds according to processes that produce failures in times between a month and ten years.

3. Thus, the long times which are necessary for failures to occur depend mainly on the times for precursors to develop.

4. Quantifying the precursor step can be approached by identifying microprocesses that require some time for maturing to produce the conditions necessary for SCC. In general, there might be multiple microprocesses acting in series or in parallel or both.

5. Organizing the microprocesses into a precursor stage is most effectively accomplished by recognizing that there are six domains that influence conditions for initiating SCC after some long time: global, bulk environment, near surface environment, protective film, near surface

metal, and bulk metal. Within each of these domains are microprocesses that are already known.

6. The quantitative development of a precursor scenario involves selecting a sequence of microprocesses that become logical constituents of a scenario. Multiple scenarios might be developed. Once such scenarios are identified, the time required for conditions to occur for SCC to initiate can be calculated. Such hypotheses can then be tested experimentally.

7. In addition to developing scenarios for precursors, it is necessary to identify what conditions must be met for SCC to occur. An array of such specific conditions can be assessed using various survey methods already well known.

8. The total time for failure to occur, then, involves the time for the precursor step to produce conditions necessary for SCC and the time for the SCC, once initiated, to propagate to failure.

9. Acknowledgements

The development of the ideas in this paper is based on many discussions with my colleagues in the corrosion community. Among these are Masatsune Akashi, Peter Andresen, Sam Armijo, Allen Baum, Ted Beck, John Bockris, Floyd Brown, Steve Bruemmer, H.E. Chaung, Pierre Combrade, John Congleton, Jacques Daret, Jim Davis, David Douglass, Zhi Fang, (the late) Mars Fontana, Bob Frankenthal, Rick Gangloff, Jack Gilman, Jeff Gorman, Mac Hall, John Hirth, (the late) Sam Hoar, Bill Hocking, Xiangchun Jiang, Rob Kelly, Jerry Kruger, Ronald Latanision, Bill Lindsay, Mike Long, Jesse Lumsden, Al McIlree, Charlie McMahon, Bruce Miglin, Peter Millett, Joe Muscara, Roger Newman, (the late) Peter Paine, (the late) Redvers Parkins, Joe Payer, Neal Pessall, Howard Pickering, (the late) Marcel Pourbaix, Neville Pugh, Bob Rapp, Peter Rhodes, Norio Sato, Steve Sawochka, Peter Scott, John C. Scully, John R. Scully, Masahiro Seo, Bill Shack, Toshio Shibata, Tetsuo Shoji, Karl Sieradski, Ed Simonen, Susan Smialowska, Tom Smith, Bill Smyrl, Markus Speidel, Narasi Sridhar, Norm Stoloff, Peter Swann, Bob Tapping, Larry Thomas, Gary Was, Jack Westbrook, Bert Westwood, Mike Wright, and many others.

I particularly appreciate the stimulation by Dr. Joe Muscara of the NRC to think about the subject in this report through his persistently advocating a proactive approach to predicting corrosion processes. I also appreciate the support of both Dr. Joe Muscara and Dr. Bill Shack of ANL for my research into predicting early SCC failures in steam generators.

I appreciate also the stimulating discussions of my colleagues in the PMDA group. Again, I thank Joe Muscara for bringing this project into being and for assembling such a group of outstanding colleagues.

Also, I greatly appreciate the careful reviews of this manuscript by Robert Tapping, William Shack, and Jack Westbrook.
Finally, as always, I thank my office staff who individually and as a group exhibit such high standards of professionalism in their attention to details and their refusal to compromise on lesser quality work. Specifically, I appreciate Julie Daugherty who prepared the manuscript in its final form and who resolved the many questions associated with sometimes inscrutable details; I also appreciate the talent and diligence that John Ilg brings to the preparation of my graphics. Marcia Parrish-Siggelkow and Erin Kate Rediger also assisted.

References for B.15

[1] R.W. Staehle , J.A. Gorman, "Quantitative Assessment of Submodes of Stress Corrosion Cracking on the Secondary Side of Steam Generator Tubing in Pressurized Water Reactors," Corrosion, Part 1 Vol. 59 No. 11 November 2003, Part 2 Vol. 60 No. 1 January 2004, Part 3 Vol. 60 No. 2, NACE, February 2004.

[2] D.O. Harris, E.Y. Lim, D.D. Dedhia, "Probability of pipe fracture in the primary coolant loop of a PWR plant," NUREG/CR-2189, Vol. 5, U.S. Nuclear Regulatory Commission, August 1981.

[3] D.O. Harris, D.D. Dedhia, S.C. Lu, "Theoretical and User's Manual for PC-PRAISE: A Probabilistic Fracture Mechanics Computer Code for Piping Reliability Analysis," NUREG/CR-5864, U.S. Nuclear Regulatory Commission, 1992.

[4] J.W. Provan, Probabilistic Fracture Mechanics and Reliability, Dordrecht, Boston, Massachusetts, 1987.

[5] T.L. Dickson, et al., "Pressurized Thermal Shock Probabilistic Fracture Mechanics Sensitivity Analysis for Yankee Rowe Reactor Pressure Vessel," NUREG/CR-5782, U.S. Nuclear Regulatory Commission, 2004.

[6] J.M. Bloom, J.C. Ekvall, Probabilistic Fracture Mechanics and Fatigue Methods: Applications for Structural Design and Maintenance – A Symposium, ASTM Committee E-9 on Fatigue; ASTM Committee E-24 on Fracture Testing, STP 798, American Society for Testing and Materials, Philadelphia, Pennsylvania, 1983.

[7] R.W. Staehle, "Lifetime Prediction of Materials in Environments," Uhlig's Corrosion Handbook, 2nd edition, pp. 27-84, Ed. R.W. Revie, John Wiley and Sons, New York, 2000.

[8] R.W. Staehle, "Approach to Predicting SCC on the Secondary Side of Steam Generators," presented at Fontevraud 5, Contribution of Materials Investigation to the Resolution of Problems Encountered in Pressurized Water Reactors, SFEN, Paris, September 23-27, 2002.

[9] R.W. Staehle, "Predicting the First Failure," presented at Corrosion 2003, San Diego, March 16-20, NACE, Houston, Texas, 2003.

[10] R.T. Begley, A.W. Klein, R.E. Gold, "Investigation of ID Stress Corrosion Cracking in Field and Laboratory Programs," Contribution of Materials Investigation to the Resolution of Problems Encountered in PWR Plants: International Symposium, French Nuclear Energy Society, Paris, 1985.

[11] R.W. Staehle, et al., "Application of Statistical Distributions to Characterizing and Predicting Corrosion of Tubing in Steam Generators of Pressurized Water Reactors" Life Prediction of Corrodible Structures, R.N. Parkins, ed., NACE, Houston, 1994.

[12] Private communication courtesy of R. Eaker of Duke Power, Charlotte, North Carolina.

[13] G. P. Airey, Optimization of Metallurgical Variables to Improve Corrosion Resistance on Inconel Alloy 600, EPRI NP-3051, Electric Power Research Institute, 1983.

[14] M.O. Speidel, R. Magdowski, "Stress Corrosion Crack Growth of Cold Worked Nickel Base Alloy 600," International Conference on Corrosion-Deformation Interactions; CDI '92, p. 107, Electricite de France, Paris, 1992.

[15] C.H. Shen, P.G. Shewmon, "A Mechanism for Hydrogen-Induced Intergranular Stress Corrosion Cracking in Alloy 600," Metallurgical Transactions Vol. 21A, p. 1261,1990.

[16] H.M. Chung, "Formation of Microcavities in BWR Core Shroud Welds," Proceedings of the Tenth International Conference on Environmental Degradation of Materials in Nuclear Power Systems – Water Reactors, P. Ford, G. Was, L. Nelson, eds., NACE, 2002.

[17] A. Kimura, "Dependence of Susceptibility to IGSCC on the Location of HAZ of Welded SUS304 Core Shroud for BWR," Proceedings of the Tenth International Conference on Environmental Degradation of Materials in Nuclear Power Systems – Water Reactors, P. Ford, G. Was, L. Nelson, eds., NACE, 2002.

[18] J. Hickling, et al., "Characteristics of Crack Propagation Through SCC Under BWR Conditions in Stainless Steels Stabilized with Titanium or Niobium," Proceedings of the Ninth International Conference on Environmental Degradation of Materials in Nuclear Power Systems – Water Reactors, p. 299-308, S.M. Bruemmer, F.P. Ford, G.S. Was, eds., TMS, 1999.

[19] K. Matocha, J. Wozniak, "Stress Corrosion Cracking Initiation in Austenitic Stainless Steel in High Temperature Water," Proceedings of the Ninth International Conference on Environmental Degradation of Materials in Nuclear Power Systems – Water Reactors, S.M. Bruemmer, F.P. Ford, G.S. Was, eds.,TMS, Warrendale, Pennsylvania, 1999, p. 383-388.

[20] E.D. Eason , L.M. Shusto, Analysis of Cracking in Small Diameter BWR Piping, EPRI NP 4394, Electric Power Research Institute, Palo Alto, 1986.

[21] T.M. Angeliu, et al., "Intergranular Stress Corrosion Cracking of Unsensitized Stainless Steels in BWR Environments," Proceedings of the Ninth International Conference on Environmental Degradation of Materials in Nuclear Power Systems – Water Reactors, p. 567, S.M. Bruemmer, F.P. Ford, G.S. Was, eds., TMS, 1999.

[22] M.O. Speidel , R. Magdowski, "Stress Corrosion Cracking of Stabilized Austenitic Stainless Steels in Various Types of Nuclear Power Plants," Proceedings of the Ninth International Conference on Environmental Degradation of Materials in Nuclear Power Systems – Water Reactors, p. 567, S.M. Bruemmer, F.P. Ford, G.S. Was, eds., TMS, 1999.

[23] H.W. Pickering, F.H. Beck, M.G. Fontana, "Wedging Action of Solid Corrosion Product During Stress Corrosion of Austenitic Stainless Steels," *Corrosion, 18*, p. 230-239, NACE, 1962.

[24] N.B. Pilling, R.E. Bedworth, "The Oxidation of Metals at High Temperatures," *Metals V, 29*, p. 529-582, 1923.

[25] D.P. Rochester, "Laboratory Investigation of Free-Span Axial Corrosion in Oconee Nuclear Station's Once Through Steam Generators," Water Chemistry of Nuclear Reactor Systems 8, British Nuclear Energy Society, London, 2000.

[26] D.P. Rochester , R.W. Eaker, "Laboratory Examination Results from Oconee Nuclear Station Once Through Steam Generator Tubes," Proceedings of the Ninth International Conference on Environmental Degradation of Materials in Nuclear Power Systems - Water Reactors, p. 639, S.M. Bruemmer, F.P. Ford, G.S. Was, eds., TMS, 1999.

[27] F.A. Garner, L.R. Greenwood, D.L. Harrod, "Potential High Fluence Response of Pressure Vessel Internals Constructed from Austenitic Stainless Steels," Proceedings of the Sixth International Conference on Environmental Degradation of Materials in Nuclear Power Systems – Water Reactors, R.E. Gold and E.P. Simonen, eds., TMS, 1993.

[28] S.M. Bruemmer, "New Issues Concerning Radiation-Induced Material Changes and Irradiation-Assisted Stress Corrosion Cracking in Light-Water Reactors," Proceedings of the Tenth International Conference on Environmental Degradation of Materials in Nuclear Power Systems – Water Reactors, P. Ford, G. Was, and L. Nelson, eds., NACE, 2002.

[29] J. Daret, et al., "Evidence for the Reduction of Sulfates under Representative SG Secondary Side Conditions, and for the Role of Reduced Sulfates on Alloy 600 Tubing Degradation," Proceedings of the Ninth International Conference on Environmental Degrada-

tion of Materials in Nuclear Power Systems – Water Reactors, p 567, S.M. Bruemmer, F.P. Ford, and G.S. Was, eds., TMS, 1999.

[30] T. Sakai, et al., "Effect of Reduced Sulfur on High Temperature Aqueous Corrosion for Alloy 600," Proceedings of the Fourth International Symposium on Environmental Degradation of Materials in Nuclear Power Systems - Water Reactors, p. 12/37, D. Cubicciotti, ed., NACE, 1990.

[31] B. Sala, et al., "Chemistry of Sulfur in High Temperature Water Reduction of Sulfates," Proceedings of the Fifth International Symposium on Environmental Degradation of Materials in Nuclear Power Systems - Water Reactors, American Nuclear Society, 1992.

[32] W.E. Allmon, P.L. Daniel, S.J. Potterton, "Conditions for the Chemical Reduction of Sulfates in an Aqueous Environment," Proceedings: Workshop on the Role of Sulfur Species on the Secondary-Side Degradation of Alloy 600 and Related Alloys, p. 10/1, EPRI NP-6710-SD, U.E. Gustafsson, ed., Electric Power Research Institute, 1990.

[33] O. de Bouvier, et al., "Influence of High Reducing Conditions on IGA/SCC of Alloy 600 in Neutral Sulfate Environments," 11th International Conference on Environmental Degradation of Materials in Nuclear Power Systems – Water Reactors, Stevenson, Washington, August 1-14, 2003.

[34] W.H. Cullen, "Review of IGA, IGSCC and Wastage of Alloys 600 and 690 in High Temperature Acidified Solutions," Control of Corrosion on the Secondary Side of Steam Generators, p. 273, R.W. Staehle, J.A. Gorman, and A.R. McIlree, eds. NACE, 1996.

[35] D. Choi, G.S. Was, "Pit Growth in Alloy 600/690 Steam Generator Tubes in Simulated Concentrated Environments (Cu2+, Cl- and SO42-)," *Corrosion, 46*, p. 100, 1990.

[36] R.W. Staehle, "Occurrence of Modes and Submodes of SCC," Control of Corrosion on the Secondary Side of Steam Generators, p. 135, R.W. Staehle, J.A. Gorman, and A.R. McIlree, eds., NACE, 1996.

[37] R.W. Staehle, "Bases for Predicting the Earliest Penetrations Due to SCC for Alloy 600 on the Secondary Side of PWR Steam Generators," NUREG-CR-6737, U.S. Nuclear Regulatory Commission, 2001.

[38] F.N. Goswami, R.W. Staehle, "Growth Kinetics of Passive Films on Fe, Fe-Ni, Fe-Cr, Fe-Cr-Ni Alloys, *Electrochimica Acta 16*, pp. 1895-1907, 1971.

[39] R.M. Latanision, R.W. Staehle, "Plastic Deformation of Electrochemically Polarized Nickel Single Crystals," *Acta Metallurgica, 17*, pp. 307-319, March, 1969.

[40] E.N. Pugh, J.V. Craig, A.J. Sedriks, "The Stress-Corrosion Cracking of Copper, Silver, and Gold Alloys," Proceedings of Conference Fundamental Aspects of Stress Corrosion Cracking, p. 118, NACE-1, September 11-15, 1967.

[41] R.W. Staehle, "Stress Corrosion Cracking of the Fe-Cr-Ni Alloy System," NATO Science Committee Research Evaluation Conference, from The Theory of Stress Corrosion Cracking in Alloys, edited by J.C. Scully, 1971.

[42] J.B. Lumsden, P.J. Stocker, "Inhibition of IGA in Nickel Base Alloys in Caustic Solutions," Corrosion '88, Paper 252, NACE, March 21-25, 1988.

[43] A.J. Forty and P. Humble, *Phil.Mag., 8*, 247, 1963.

[44] J.H. Payer , R.W. Staehle, "Dissolution Behavior of Carbides in Aqueous Environments," Localized Corrosion, NACE-3, Eds. R.W. Staehle, B.F. Brown, J. Kurger and A. Agrawal, NACE, 1974, conference held at Williamsburg, Virginia, December 6-10, 1971.

[45] T. Smith, "Relationship of Defect Structure to the Corrosion Behavior of Some Austenitic Stainless Steels," M.S. Thesis, The Ohio State University, 1965.

[46] J.A. Davis, "Local Dissolution Phenomena Occurring on Iron-Chromium-Nickel Alloys: An Electron Microscopic Study," Ph.D. Dissertation, The Ohio State University, 1968.

[47] M. Long, "The Polarization Behavior of Iron-Nickel-Chromium Alloys in Caustic Solutions," M.S. Thesis, The Ohio State University, 1973.

[48] H.E. Chaung, Z. Szklarska-Smialowska, R.W. Staehle, "The Effects of Heat Treatment on Surface Segregation in Inconel 600," *Scripta Metallurgica, 13,* 1979.

[49] H.E. Chaung, J.B. Lumsden, R.W. Staehle, "Effect of Segregated Sulfur on the Stress Corrosion Susceptibility of Nickel," Metallurgical Transactions 10A, 1979.

[50] R.W. Staehle , Z. Fang, "SCC of Alloys 600 and 690 in the Mid-Range of pH," presented at the International Symposium Fontevraud IV, Contribution of Materials Investigation to the Resolution of Problems Encountered in Pressurized Water Reactors, September 14-18, 1998.

[51] R.N. Parkins, et al., "Stress Corrosion Test Methods," *British Corrosion Journal, 7*, p. 154, 1972.

[52] R.W. Staehle, "Development and Application of Corrosion Mode Diagrams," Parkins Symposium on Stress Corrosion Cracking, pp. 447-491, Eds. S.M. Bruemmer, E.I. Meletis, R.H. Jones, W.W. Gerberich, F.P. Ford, and R.W. Staehle, Cincinnati, Ohio, October 21-24, 1991, TMS (The Minerals, Metals and Materials Society), 1992.

[53] J.M. Sutcliffe, et al., "Stress Corrosion Cracking of Carbon Steel in Carbonate Solutions," *Corrosion, 28*, p. 313, 1978.

[54] V.K. Singh, "Stress Corrosion Cracking of Low-Carbon and Low-Alloy Steels," *Steel India, 11*, p. 53, 1988.

[55] K. Bohnenkamp, "Caustic Cracking of Mild Steel," Fundamental Aspects of Stress Corrosion Cracking, p. 374, NACE-1, R.W. Staehle, A.J. Forty, and D. van Rooyen, eds., NACE, 1969.

[56] N.J.H. Holroyd, "Environmental Aspects of Stress Corrosion Cracking of Ferritic Steels," Ph.D. Thesis, University of Newcastle-upon-Tyne, 1977.

[57] C.R. Morin, "Potential Dependent Stress Corrosion Cracking of Type 304-L Stainless Steel in H2SO4 + KCl at 25°C," Thesis presented in partial fulfillment of the requirement for degree of Master of Science, The Ohio State University, 1972.

B. 16 "Microbiologically Influenced Corrosion (MIC)," by Robert L. Tapping and Roger W. Staehle

Introduction

The objective of this topical discussion is to describe the subject of Microbiologically Influenced Corrosion (MIC) as applied to LWRs.

"Microbiologically Influenced Corrosion (MIC)" refers to corrosion that results from the presence and activities of microorganisms. MIC can result from microbial processes that produce corrosive environments such as organic acids or lower valence sulfur. The modes of corrosion, which can result from microbiologically produced local environments, include general corrosion (GC), pitting (PIT), crevice corrosion, de-alloying, galvanic corrosion, intergranular corrosion (IGC), stress corrosion cracking (SCC), and corrosion fatigue (CF).

Generally, the environments produced in the process of MIC are of three types:

- Formation of colonies, which are sometimes of substantial size, within which additional transformations beyond the initial metabolic processes can occur. Such colonies also have some of the features of "crevices" with the additional feature of dynamic changes of internal chemistry.

- Reactions between microorganisms and nutrients, e.g. nitrite oxidized to nitrate, or sulfuric acid/reduced sulfate compounds generated by sulfate-reducing bacteria, with a change in the corrosion modes thereby enabled.

- Corrosion directly on metal surfaces.

The term "microorganisms" includes bacteria and fungi. Both produce metabolic products that are acidic, as well as other byproducts, including sulfides. Some of the byproducts can react with the immediate environment to form corrosive species, acids, etc. The range of temperatures for vitality or growth and metabolic activity of the two are different, with fungi having a lower temperature tolerance limit than bacteria. Bacteria and fungi also differ with respect to the ranges of optimal growth in the sense that fungi and bacteria can survive different ranges and sets of unfavorable conditions. The intensity of MIC and the associated products of the microorganisms depend mainly on the following influences:

- Temperature, with there being a narrow optimum temperature for growth of each species of organisms.

- Water is necessary to the metabolic processes of all microorganisms. Bacteria require liquid (e.g. a thin surface film of liquid on which a biofilm can grow) for growth, but fungi can grow at relative humidity of 60% or higher.

- Oxygen is the electron acceptor for aerobic organisms, but anaerobes can use a variety of other terminal electron acceptors, e.g., SO_4^{2-}, NO_3, Fe(III), Mn(IV), Cr(VI).

- Nutrients including carbon, sulfur, phosphorous, nitrogen, are required. Such nutrients must include the capacity for electron exchange involving oxidation and reduction reactions. In some cases where nutrient availability is limited, secondary metabolic byproducts may be involved in the overall microbiological process and sustain the corrosion.

- Flowing, especially slowly flowing, environments tend to favor the growth of microbes by providing a ready supply of nutrients (in particular, periodically flushed systems). Stagnant areas adjacent to flowing areas are particularly susceptible to MIC (e.g., dead legs in piping).

- Microorganisms can grow in natural and processed waters including marine, potable, distilled, and fresh.

- Some species, e.g. boric acid, are toxic to microbes in high concentrations.

General Features of Microorganisms Relative to MIC

The following general properties concerning microorganisms as applied to nuclear applications are taken from Pope:[1]

- Individual microorganisms are small (from less than two-tenths to several hundred micrometers (□m) in length by up to two or three μm in width) a quality which allows them to penetrate crevices, etc., easily. Bacterial and fungal colonies can grow to macroscopic proportions.

- Bacteria may be motile, capable of migrating to more favorable conditions or away from less favorable conditions, e.g., toward food sources or away from toxic materials.

- Bacteria have specific receptors for certain chemicals, which allow them to seek out higher concentrations of those substances, which may represent food sources. Nutrients, especially organic nutrients, are generally in short supply in most aquatic environments; but surfaces, including metals, adsorb these materials, creating areas of relative plenty. Organisms able to find and establish themselves at these sites will have a distinct advantage in such environments.

- Microorganisms can withstand a wide range of temperatures (at least -10 to 99°C), pH (about 0 - 10.5) and oxygen concentrations (0 to almost 100% atmospheres).

- Microorganisms grow in colonies, which help to cross-feed individuals and makes survival more likely under adverse conditions.

- Microorganisms can reproduce very quickly if field conditions are particularly favorable

- Individual cells can be widely and quickly dispersed by wind and water, animals, aircraft, etc., and thus the potential for some of the cells in the population to reach more favorable environments is good.

- Many can quickly adapt to use a wide variety of different nutrient sources. For example, *Pseudomonas fluorescens* can use well over 100 different compounds as sole sources of carbon and energy including sugars, lipids, alcohols, phenols, organic acids, etc.

- Many form extracellular polysaccharide materials (capsules or slime layers). The resulting slimes are sticky and trap organisms and debris (food), resist the penetration of some toxicants (e.g., biocides) or other materials (corrosion inhibitors) and hold the cells between the source of the nutrients (the bulk fluid) and the surface toward which these materials are diffusing.

- Many bacteria and fungi produce spores, which are very resistant to temperature (some even resist boiling for over 1 hour), acids, alcohols, disinfectants, drying, freezing, and many other adverse conditions. Spores may remain viable for hundreds of years and germinate on finding favorable conditions. In the natural environment, there is a difference between survival and growth. Microorganisms can withstand long periods of starvation and desiccation. If conditions are alternating wet and dry, microorganisms may survive dry periods but will grow only during the wet periods.

- Microorganisms are resistant to many chemicals (antibiotics, disinfectants, etc.) by virtue of their ability to degrade them or by being impenetrable to them (due to slime, cell wall or cell membrane characteristics). Resistance may be easily acquired by mutation or acquisition of a plasmid (essentially by naturally-occurring genetic exchange between cells, i.e., genetic engineering in the wild).

Applications to LWRs

MIC is relatively common in LWR systems such as fire water, service water and low temperature cooling water systems and components, and typically occurs in light water plants in two general locations. One is on external surfaces where there is moisture and other materials, such as organic debris buildup; deposits containing animal droppings, and slimes; secretions; etc. which contain nutrients suitable for bacterial or fungal growth. The second occurs on internal surfaces in low temperature components; primarily those where water is flowing slowly or is periodically flushed; both situations provide a good supply of nutrients for microbiological activity and growth. This is particularly true for systems where deposits can build up, and where these deposits could accumulate bacterial or fungal populations by exposure to water that has been air-exposed.

Truly stagnant systems with no replenishment of nutrients (e.g. not exposed to air) are not favorable for significant MIC activity. Vertical deadlegs, with water flowing by the end of the deadleg, are areas particularly at risk for bacterial growth. It should be noted that periodic flushing, by introducing nutrients and bacteria, is one of the major factors in promoting MIC in piping and tanks. Usually this flushing is carried out for testing purposes and consideration should be given to reducing the frequency of such testing to minimize the risk of MIC. Chemicals that are common in LWR waters can affect the growth of microorganisms, for instance hydrazine and boric acid. MIC is often associated with fouling, the fouling being a combination of bacterial colonies and associated corrosion products, and the MIC damage found under the deposits. These deposits can be significant, resulting in blockage of piping and much reduced water

flows MIC and MIC-related fouling have been found in a wide range of systems, from fire protection and service water systems to ECC storage systems and spent fuel pools.

There are several key chemistry-related factors that may affect microbial activity in LWRs:

1. Temperature and pH

Hyperthermophiles (bacteria that can extend their temperature range above that typically found in most water systems) can grow up to a temperature of 110°C. In effect this defines the upper limit for MIC activity, although in practice MIC is rarely found at temperatures above 60°C. Bacteria can grow over the pH range from 0 to about 10.5, in effect the entire spectrum of pH found in LWR systems. Thus the temperature and pH ranges that can sustain microbial activity cover most of the conditions found in LWR low temperature systems.

2. Boric acid

Many LWR systems are borated, and thus are sometimes regarded as protected against microbial activity. The acute boron toxicity level for bacteria is between 8-340 mg/L. Bacteria have a low sensitivity to boron. Metabolism of boric acid is thermodynamically unfavorable. There are no known bio-transformations of borate. Thus borated systems at low temperature may be able to sustain microbial activity at boron concentrations below a few hundred mg/L.

3. Hydrazine

There is relatively little literature concerning the effect of hydrazine on bacterial growth under LWR conditions. Addition of hydrazine to low temperature systems, while common, is not an effective protection against rapid changes in oxygen concentration because the reaction of hydrazine with oxygen at low temperatures is slow, but nevertheless some low temperature recirculated systems do contain hydrazine as an oxygen scavenger. Based on limited data, then, hydrazine sulfate at 1mM is known to be an inhibitor for bacterial utilization of amino acids, although some growth was observed. Hydrazine can be metabolized to nitrogen gas by some nitrifying bacteria or reduced to ammonia by nitrogenase isolated from a nitrogen-fixing bacterium. Only concentrations below 1 mg/liter were completely degraded. Higher concentrations were inhibitory. It seems likely therefore that low temperature systems in LWRs containing a few mg/L (ppm) of hydrazine would be protected against microbial activity and corrosion, whereas for LWR systems containing less than this level of hydrazine, microbial activity would be possible.

Overall it appears, based on limited data, that in LWRs MIC is possible in systems operated with stagnant or intermittent flows and at temperatures less than 100°C, and containing low levels of hydrazine (less than a few ppm). Low levels of boric acid or borate appear to inhibit MIC, and thus systems containing boric acid are likely protected against MIC.

Over the past 5 to 10 years there has been an increase in reported incidences of MIC-related degradation, especially of underground systems and systems which have been flushed regularly as part of a testing program (for instance fire water systems and safety-

related systems), a practice that renders carbon steel piping susceptible to MIC. This has led to leakage of underground piping, plugging of heat exchangers and fire protection piping, plugging of strainers with bacterial growth, failure of tensioning cables, etc. In short, in any low temperature location where deposits and bacteria can build up, and especially where periodic replenishing of nutrients can occur, as with flushing of piping, carbon steel components can degrade through the action of MIC. This experience has led to the increasing use of plastic or epoxy piping in low temperature, low pressure systems. Such piping is immune to MIC degradation, although it may still be susceptible to buildup of deposits caused by microbial activity.

Acknowledgements

RLT and RWS acknowledge the contributions and assistance of Dr. Brenda Little of Stennis Space Center and Dr. Peter Angel of AECL.

References for B.16

[1] D. Pope, "A Study of Microbiologically Influenced Corrosion in Nuclear Power Plants and a Practical Guide for Countermeasures," EPRI Report NP-4582, Electric Power Research Institute, May 1986.

[2] ND Luchini, GA Broderick and DK Combs, "In Vitro Determination of Ruminal Protein Degradation Using Freeze-Stored Ruminal Microorganisms," *J Animal Science 74*, 1996.

B. 17 "Flow-Accelerated Corrosion,"
by Robert L. Tapping

Background

Flow-accelerated corrosion (FAC, sometimes termed flow-assisted corrosion) is a degradation mechanism affecting metallic materials that do not form tightly adherent passive surface films when the materials are exposed to fluid flow environments in power reactor systems, and thermal power plants. In reactor coolant/heat transfer systems where materials are exposed to flowing water this degradation mechanism typically affects only carbon steels and copper alloys. Sometimes the FAC results in sufficient wall loss that catastrophic piping failure occurs (Figure B.17.1), although more frequently leakage is the consequence, without rupture. It is important to note the distinction between FAC and erosion corrosion (EC). FAC is an electrochemical corrosion process dependent on pH, temperature, electrochemical potential and fluid mass transfer (velocity and turbulence). FAC is a flow-accelerated increase in the corrosion rate of a material; the increase in corrosion rate, which can be very large, can be simplistically thought of as a flow-induced increase in mass transfer of dissolving and reacting (corrosive) species at a high flow or highly turbulent location. Under low flow conditions, the corrosion rate of carbon steel is an electrochemically-coupled reaction and is a function of the rate of dissolution of the substrate (Fe for carbon steels) and the oxide formed by reaction of some of the dissolved iron with water and water-borne oxidants, and the rate of formation of a surface oxide. Under FAC conditions the rate of Fe/ iron oxide dissolution exceeds the rate of formation of the oxide that would be expected under low flow conditions. This coupled oxidation/dissolution reaction is best described as an electrochemical process, determined by the concentration of electrochemically active species at the metal-fluid interface, in particular those controlling the pH and oxidants.

Erosion corrosion is properly described as the abrasive or cavitation-induced (mechanical) removal of surface material; either the protective film or the underlying material for systems that do not form protective surface layers. A common form of EC in LWRs is related to entrainment of abrasive material in a fluid flow, for instance sand entrainment in water intake flows, and both FAC and EC may occur simultaneously, depending on the flow conditions. Typically, power plant cooling and heat transfer systems do not contain abrasive materials in quantities sufficient to cause EC, although condenser cooling water systems may contain abrasive debris. Under very high flow conditions, best described as water jetting or steam jetting, the abrasive wear or cutting of the material can take place without abrasive materials being present. Typical examples are steam cutting/wear in condenser inlets and the use of high pressure (typically 5000 to 10 000 psi) water lances to cut concrete. It should be noted that the term "erosion-corrosion" has been frequently used as a synonym for FAC, which can be confusing and is incorrect.

Factors Influencing Material Susceptibility

There are several factors affecting susceptibility to FAC:

- pH
- Temperature
- Water chemistry
- Material properties (alloy content)
- Mass transfer (flow, turbulence, steam quality)

For carbon steels, the pH should be controlled in the range 7 to 10, preferably between 9 and 10 (room temperature pH) to minimize corrosion in water. For copper alloys the pH should be between 7 and 9; thus in mixed metal systems pH control is a compromise between corrosion of carbon steels and copper alloys, and pH is typically in the range 8.8 to 9.4. Most nuclear plants have now switched to all-ferrous piping systems, primarily to protect steam generators from degradation, and thus there is little concern for corrosion of copper alloys. In all-ferrous systems the pH is typically maintained >9.4, often as high as 9.8 to 10.0. Note that in two-phase systems, such as in steam generators, it is the liquid phase pH that is important and pH control agents should be chosen such that preferential partitioning to the steam phase does not occur, or does not lower the liquid phase pH below an acceptable level. So-called "alternative amines" have been used to ensure that such partitioning is limited and thus the high temperature pH of the liquid phase remains in an acceptable range.

Water temperature significantly affects FAC, with the maximum FAC rates occurring, all else being equal, at about 130°C in single-phase flow, and at about 180°C in two-phase flow. Thus the feedwater systems are at significant risk of FAC, and these systems are typically inspected on a routine basis to ensure that wall thinning is monitored. FAC in these systems can result in wall loss rates of >10 mm/year in unfavorable situations, and in a few cases has resulted in deaths as a consequence of pipe rupture when the wall thickness decreased sufficiently that mechanical failure occurred. Typically FAC rates decrease at temperatures on either side of the peak temperature, all other factors being equal, but given that FAC is often very localized because of mass transfer effects, the rate may still be sufficient to result in wall thinning and piping failure in thin-walled pipes.

Water chemistry is an important variable for FAC. The conditions leading to increased FAC rates are reducing chemistry (low electrochemical potential) and low dissolved iron concentrations in the water. Steam generators are an example of how FAC can occur under the highly reducing conditions that are typically used to protect the SG tube bundle. In several instances (Bruce NGS and Gravelines, for example) carbon steel support plates have disintegrated as a consequence of FAC, where it was concluded that a significant factor was the use of high hydrazine concentrations (>100 to 200 ppb). The sensitivity of FAC to low dissolved iron concentrations is a consequence of the dependence of FAC on the solubility of iron, and to the local potential. In fundamental terms this dependence relates to the liquid layer at the steel surface, which becomes more difficult to measure and predict in two-phase flows. In feedwater systems this iron solubility dependence is most obvious in systems such as the moisture separator reheater drain lines, where steam has been condensed and relatively iron-free water is flowing. Many cases of FAC have occurred in such lines. Note also the use of alternative amines to ensure appropriate high temperature pH in two-phase flows (see Secondary Water Chemistry Topical Report) also mitigates these effects of iron concentration and potential on FAC.

Material properties have a significant impact on FAC rates, and typically the plant operator has no control over this unless replacement of piping is an option. The most important alloy variable affecting FAC is chromium (Cr) content of the alloy. Although copper and molybdenum content have also been suggested to have beneficial effects, the effects are typically small and not clearly related to plant experience. It is generally regarded that in single phase piping subject to FAC, a Cr content >0.1 wt. % is recommended. Plant and laboratory data suggest that Cr contents below about 0.04 wt. % are insufficient to provide any useful protection against FAC, and concentrations above 0.05 to 0.08 wt. % are necessary to show significant improvement. Many experts now recommend a Cr content >0.2 wt. % to provide optimal resistance. The

beneficial effect of Cr on FAC is thought to be related to the formation of a Cr-rich oxide at the oxide-metal interface, and that this oxide confers resistance to FAC. In two-phase flows, which are typically very much higher velocity than single phase flows, it is probably expedient to use Cr-Mo steels or, preferably, stainless steels. Many feedwater system components are now fabricated from these materials to minimize FAC degradation.

Mass transfer effects relate to areas where locally high turbulence is created, usually by geometric factors. Elbows, bends, orifices, valves, etc., all cause local turbulence which significantly increases FAC rates in or immediately downstream of the component. This turbulence increases the FAC rate by increasing the transport of dissolving iron away from the surface and, by increasing mechanical stresses on the oxides formed at the site of the corrosion, which can be significant under very high velocities.

Typical Occurrences of FAC in Power Plants

Most of the FAC degradation in power plants has occurred in feedwater, extraction steam, and drains systems. However, there have been observations of FAC in steam generators and in primary side piping in CANDU™ (Canadian Deuterium Uranium) PHWR (Pressurized Heavy Water Reactor) power plants. In these systems, FAC has been found in most parts of the system, and is often associated with areas of high mass transfer, such as downstream of welds and valves, reducers, orifices, and in elbows and tees. The SG FAC has been typically found in two-phase flow areas, including upper support plates, steam separators and blowdown piping. In the CANDU heat transport system (310°C, velocity 15 to 18 m/s), the FAC has occurred at bends in carbon steel outlet feeder piping. The FAC rates there are much lower than in the feedwater and SG systems, but still can impact the integrity of the thin-wall feeder piping.

In condensers, steam impact erosion has occurred on the outer tube bundle where the steam inlets are located, a degradation phenomenon similar to that found in turbines, and has been resolved using stainless steels in this area and changes to the inlet flow distribution. This degradation occurs because the steam, by the time it reaches the condenser, is sufficiently wet that droplet impingement occurs, in addition to FAC (depending on the tube material and its susceptibility to FAC). On the water side of condensers made with copper alloy tubing, in particular Admiralty Brass, significant FAC and erosion occurs, usually resulting in tube leakage and the need to replace the condensers after about 15 years or so.

Inspection and Remediation Strategies

The most effective management strategy for FAC of feedwater systems is to employ a FAC prediction code such as EPRI's CHECWORKS code, or an equivalent, to predict locations most susceptible to FAC, and then to focus inspections on those locations predicted to be most at risk. Without use of this code, or an equivalent, it is difficult to predict and prioritize the many locations that could suffer FAC. Usually the Cr content of the steel is unknown, so it is not possible to restrict inspections to only one train of a given system, regarding it as a "lead" train. It is generally known that all high mass transfer areas are susceptible to FAC, but some may degrade at much slower rates than others, depending on hydraulic and chemistry conditions, and thus an inspection prioritization plan is needed. Note that the recent Mihama-3 pipe failure (see Figure B.17.1), caused by FAC, was in a line predicted by CHECWORKS to be at risk, but never inspected.

For steam generators, visual inspection for internal secondary side carbon steel components is usually necessary; this inspection, based on in-service experience so far, can be limited to upper support plates and separators.

The most effective remediation strategies are to replace all degraded material with stainless steel, or with Cr-Mo material if the post-weld heat treatment requirements are feasible. Typically as feedwater system carbon steel components have failed, replacements have been with FAC-resistant material. For new systems, analysis of the system can identify locations at risk of FAC and these are fabricated from austenitic stainless steels (Qinshan CANDU plants, for example). Some plants have essentially all-stainless steel feedwater systems (KWU Konvoi plants, for example). All new SGs have stainless steel support plates and other internals susceptible to FAC. For condensers, most plants have now replaced any copper-alloy condensers with Ti-tubed units (seawater cooling), with appropriate baffles to prevent inlet steam erosion of the outer row Ti tubing, or with stainless steel units (seawater and freshwater cooling).

Remediation by chemistry modification has limited application given that most plants now employ an effective feedwater chemistry control designed to minimize FAC and other degradation mechanisms. For SGs with carbon steel secondary side internals, reducing hydrazine to <100 ppb is recommended.

Life Management Issues

Current industrial practice is to routinely inspect for FAC-induced wall thinning, usually using a predictive tool such as CHECWORKS in order to minimize the number of critical locations, as well as to generate a database of at-risk locations, the inspection history, and the wall thinning rate. Where piping failures occur, replacement of a failed component should be with a more-resistant material. It is cost-effective to reduce inspection by replacing carbon steel with stainless steel in at-risk areas. Chemistry control should be monitored to ensure that it is compatible with reduced FAC risk; operation of feedwater systems at very low dissolved oxygen (<5 ppb), for instance, can place the system at increased risk compared to slightly higher oxygen (5 to 10 ppb).

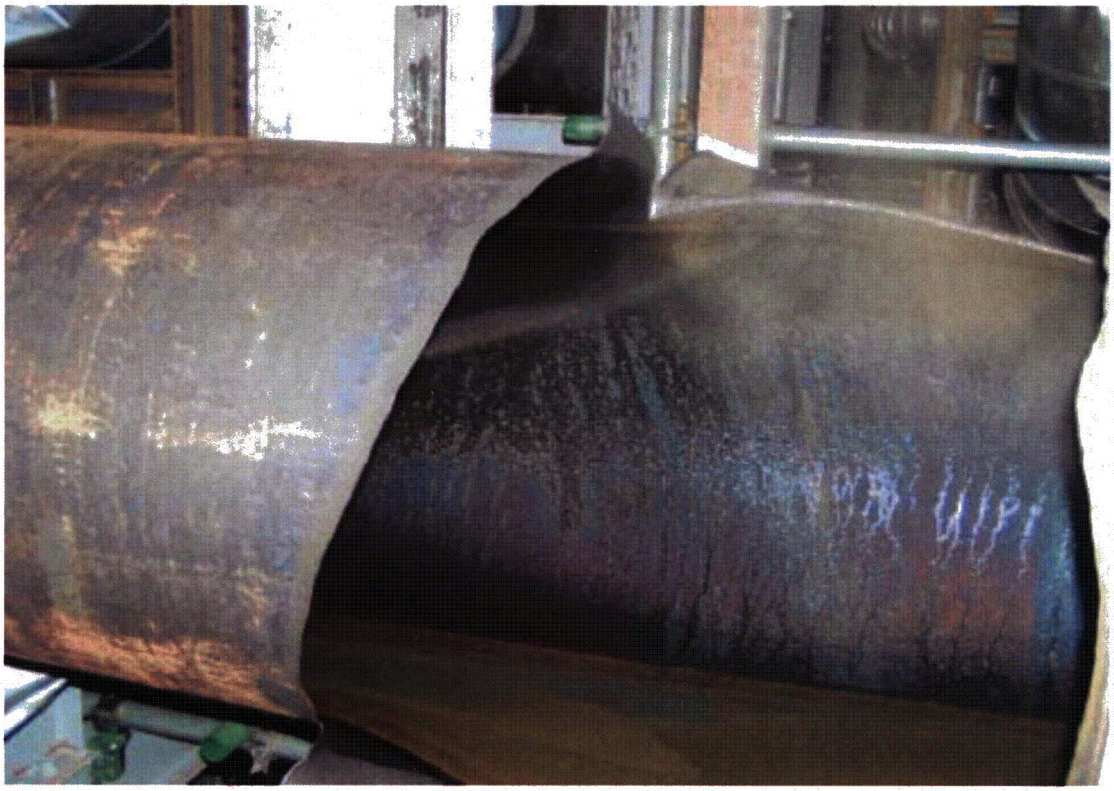

Figure B.17.1 Failed steam line at Mihama-3.

References for B.17

[1] B. Chexal et al, "Flow-Accelerated Corrosion in Power Plants," EPRI TR-06611-R1, Electric Power Research Institute, 2001.

[2] "Erosion/Corrosion in Nuclear Plant Steam Piping: Causes and Inspection Program Guidelines", EPRI NP-3944, Electric Power Research Institute, 1985.

[3] I.S.Woolsey, "Erosion-Corrosion in PWR Secondary Circuits," CEGB (Central Electricity Generating Board; UK) Report TPRD/L/3114/R67, 1987.

[4] V.N. Shah and P.E.Macdonald, eds., "Aging and Life Extension of Major Light Water Reactor Components," Elsevier, Amsterdam (1993); ISBN 0 444 89448 9.

B.18 "Topical Report on Boric Acid Corrosion (BAC)," by Robin L. Jones and John Hickling

Understanding of BAC prior to the 2002 Davis Besse Incident

Corrosion of carbon and low-alloy steel (C&LAS) components by leaking borated water has posed significant maintenance problems for many PWR plants[1]. Two incidents illustrate the potential importance of this problem. In 1980, leakage from the gaskets of two reactor coolant pumps at one plant resulted in severe corrosion to seven coolant pump flange studs. The diameter of the worst-case stud was reduced from its original 3.5 inches (89 mm) to 1.0-1.5 inches (25-38 mm). This represents a reduction to less than 20% of the original stud cross-sectional area. In 1986, leakage from a valve body-to-bonnet gasket at another plant resulted in corrosion that extended two-thirds of the way through the wall thickness of a low-alloy steel nozzle in the main coolant piping system.

Subsequent to these and other significant events, the NRC issued Generic Letter 88-05,[1] requiring operators of PWR-type power plants to develop and implement a plan to ensure that there is an extremely low probability of abnormal leakage, rapidly propagating failure, or gross rupture as a result of boric acid corrosion (BAC) of primary coolant loop components.

EPRI efforts to provide assistance to utilities in addressing the requirements of NRC GL 88-05 and BAC issues in general have centered around the *Boric Acid Corrosion Guidebook,* originally published in 1995 and updated in 2001,[2] which summarized the extent of the BAC problem as recognized at the respective times, as well as compiling and assessing data from previously performed BAC test programs.

Background

Borated water is used in the primary systems of PWR plants to control reactivity during normal plant operation and refueling and under potential accident conditions. This is accomplished by adding boric acid to the primary side water. In some cases, boric acid is also injected into the secondary side of PWR plants at low concentrations to reduce the potential for corrosion of Alloy 600 steam generator tubing at crevice locations.

In general, there is little concern with general corrosion inside the primary and secondary systems since the concentrations of boric acid and oxygen in these systems are low, and corrosion rates are typically less than 0.001 inches per year (in/yr) (0.025 mm/yr). Although C&LAS are not normally exposed directly to PWR primary water, the use of high-alloy materials in contact with the coolant is for reasons of chemistry (including radiation protection) and cleanliness, rather than the avoidance of C&LAS corrosion. In fact, LAS is sometimes exposed as a result of a "half-nozzle" repair to component penetrations and this has been deemed acceptable by the U.S. regulator from a corrosion standpoint.[3]

Exceptions to this generally good experience for materials in intended direct contact with PWR operating media include 1) stress corrosion cracking of some stainless steel pipes containing stagnant, high-concentration boric acid solutions, 2) cracking of stainless steel cladding in some components that leads to galvanically driven stress corrosion cracking (SCC) of the low-alloy steel base materials, and 3) primary water stress corrosion cracking of Alloy 600 nozzle penetrations and welds (considered in a separate topical report).

If borated water leaks from primary and secondary systems through gasketed joints, valve packing, mechanical seals, etc., significant corrosion problems can develop. Specifically, the water can become oxygenated and the boric acid can concentrate as the water boils off or evaporates. These factors can increase the corrosion rate of exposed carbon steel to several inches per year.

The reported plant incidents prior to 2002 ranged in severity from minor corrosion of parts, which can be accepted without evaluation or repair, to major incidents involving plant shutdowns and significant loss of material on major components (see Fig. B.18.1).

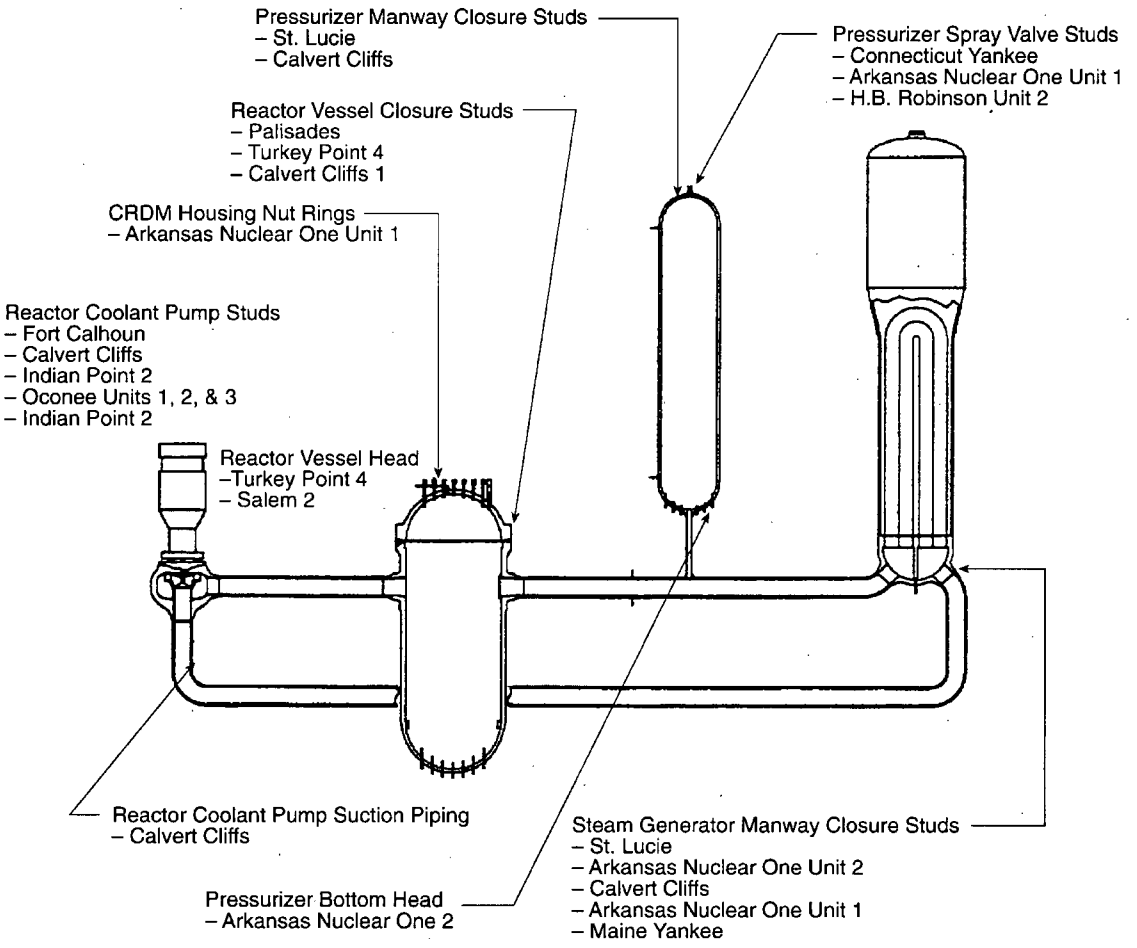

Figure B.18.1 Locations of boric acid corrosion experienced in primary loop[2] *Used by Permission of EPRI.*

Reference 1 required that utilities develop and implement programs to identify leaks and take corrective action to prevent recurrence. All plants have developed programs that respond to this generic letter. Fig. B.18.2 gives some information on the identified sources of leakage.

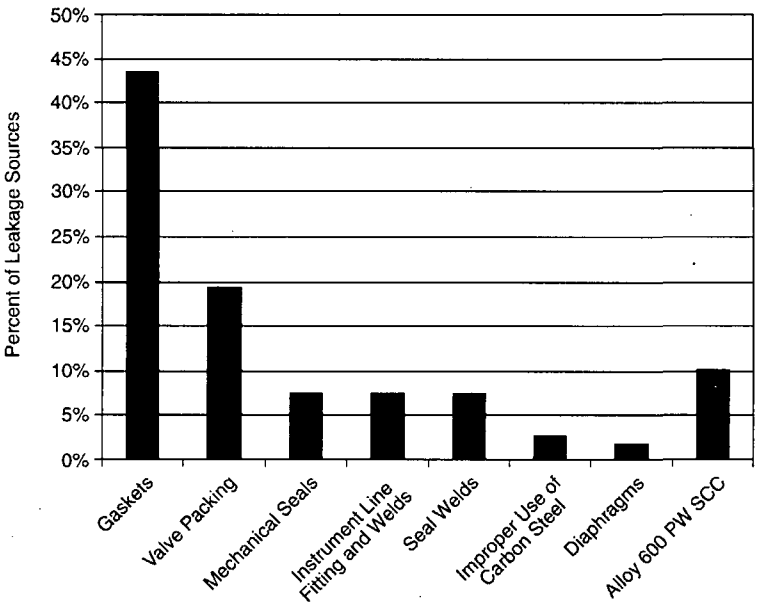

Figure B.18.2 Distribution of reported leakage incidents (US prior to 2002) by source[2]
Used by Permission of EPRI

Main type of boric acid corrosion observed

Overall, the mode of corrosion of greatest concern due to leakage of borated water is uniform corrosion, often referred to by plant engineers as "wastage," of C&LAS. Boric acid in water can result in an aggressive environment that uniformly attacks the surface of the metal. Although boric acid is considered a "weak" acid when compared to acids such as hydrochloric or nitric acid, boric acid in water will still increase the concentration of hydrogen ions (H) and lead to a drop in pH. In reality, the process of surface attack is further accelerated by what amounts to miniature galvanic cells, whereby small areas of the metal surface behave cathodically or anodically due to slight changes in the alloy composition (for example, higher chromium or nickel in steel), surface imperfections or defects, or surface strain. In addition, the corrosion product itself may be cathodic to the surrounding base metal. The anodic/cathodic areas on the metal surface can shift with time, resulting in an essentially uniform rate of attack over the entire metal surface. One of the reasons that the rate of attack of the unprotected, exposed steel can be so great is that the exposed area of the cathodic surfaces often exceeds that of the anodic material.

Surfaces which are corroded generally often exhibit some increase in texture as a result of small differences in the rate at which different areas of the surface are attacked. It is sometimes difficult to detect general corrosion of a surface because there is no clear reference point for assessing the amount of material loss, particularly if the rust is continually solubilized by, or entrained into, the fluid stream.

General corrosion is usually the easiest form of corrosion to predict using experimental data. However, as with all modes of corrosion, the rate can be affected significantly by factors that were not included in the experiments used as the basis for the predictions. Some of these factors are discussed in the following paragraphs.

Effect of Impurities on General Corrosion

When impurities are present in the metal, they may act as the source of local anodes/cathodes and thus accelerate corrosion. If impurities are present in the corrosive medium, they can have a variety of effects on the corrosion rate. Impurities may act to increase the conductivity of the aqueous solution, thereby often increasing corrosion rates, and can also cause increased corrosion rates by affecting or destroying the protective layer of hematite (rust) or other metal oxide that builds up on the exposed surface of the metal, helping to protect it from further damage. In other cases, impurities in the fluid stream can actually help retard corrosion by acting as inhibitors. In any event, the effect of impurities is generally complex and non-linear and must be determined through experiments designed to simulate the actual metal/environment combination.

Effects of Oxygen and pH on General corrosion

The corrosion of most steels which are soluble in acids depends on pH similar to the pattern shown in Figure B.18.3. In the middle pH range of 4 to 10, the corrosion rate is generally controlled by the rate of diffusion of oxygen to the surface and the insolubility of oxides in oxidizing systems, which increases with increasing electrochemical potential. At lower pH, the uniform corrosion rate increases owing to the progressive increase of oxide solubility in acidic solutions and the increased availability of hydrogen ions for reduction in the cathodic areas. At intermediate pH values, both the rate itself, and the extent to which corrosion becomes non-uniform, are still affected by the concentration of dissolved oxygen (the other main cathodic reactant).

Effect of Temperature on Wastage

In most cases of corrosion in acids, corrosion rates increase with increasing temperature and high enough temperatures also boil the water away, leaving more concentrated acid and thus even higher corrosion rates. However the concentration of dissolved oxygen in the water decreases with increasing temperature, so that the situation is more complex with a weak acid such as that resulting from leakage of primary water. Furthermore, as the temperature continues to increase, the water may be boiled off completely, leaving dry boric acid crystals that are not very corrosive at all.

Effect of Flow Velocity on Wastage

In many of the field reports, general corrosion is accelerated by the impingement of borated water, or steam with boric acid carryover, onto hot metal surfaces. This impingement has the dual effect of removing protective corrosion films from the surface of the metal and replenishing the corrodent with fresh, oxygenated acid. Both of these factors can markedly increase the corrosion rate.

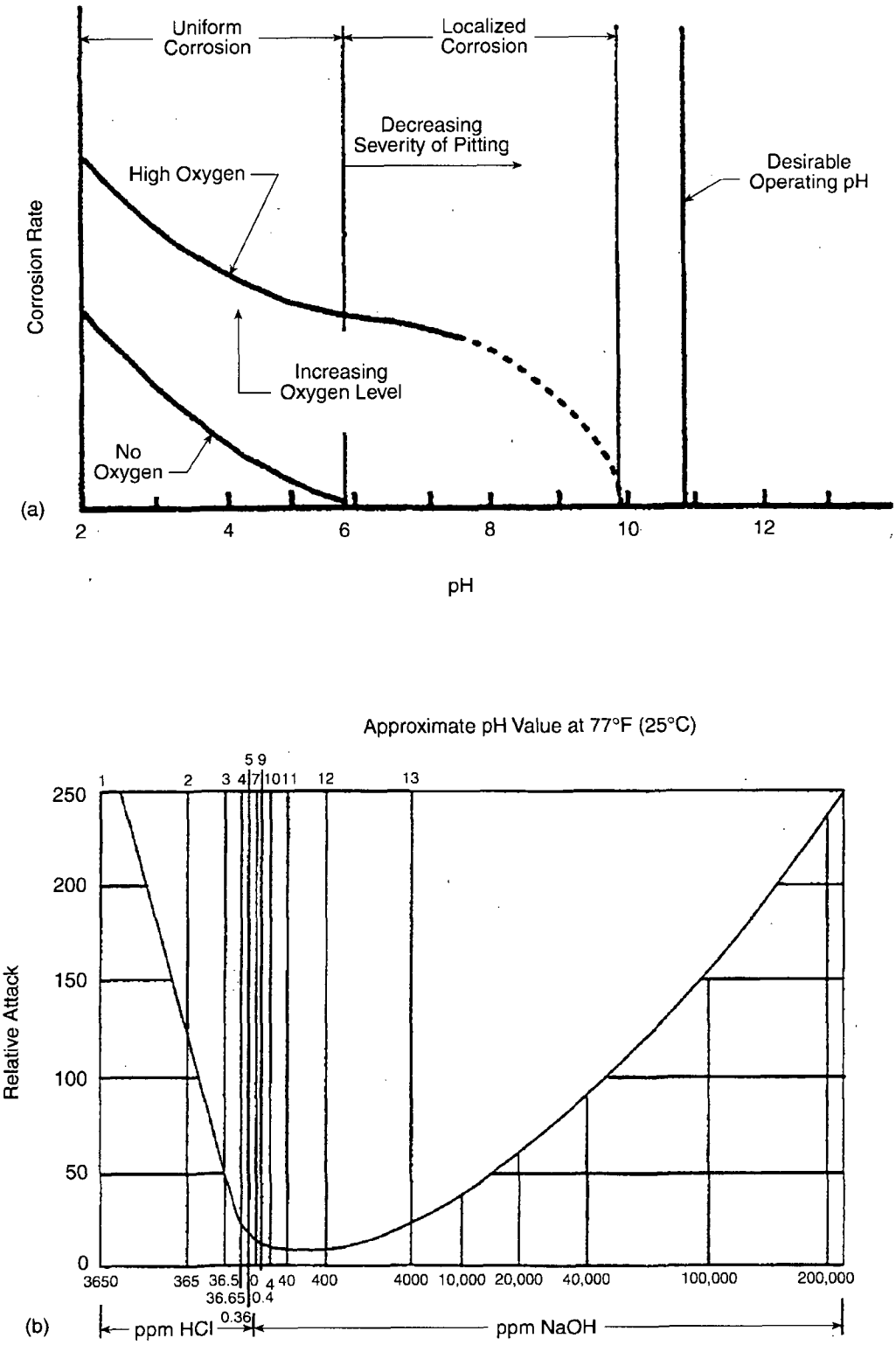

Figure B.18.3 Summary of oxygen and pH effects on general corrosion of iron[4] *Used by Permission of EPRI.*

Secondary Types of Boric Acid Corrosion

In addition to general corrosion (the predominant type of boric acid corrosion), there have been isolated reports of other types of corrosion, such as galvanic corrosion, crevice corrosion, pitting, intergranular attack, and stress corrosion cracking.

Galvanic Corrosion

A practical example of such a condition in an aerated, borated water environment in a PWR plant would be a weld between a low-alloy steel pipe and a stainless steel pipe. The stainless steel is the more noble material, and the low-alloy steel is the more active material. Field experience and laboratory test results both indicate that a galvanic couple between carbon steel and stainless steel can accelerate the local corrosion rate in the carbon steel, typically by about 1.5 times. Therefore, the galvanic effect for BAC can be significant, but is not usually overwhelming and will depend upon pH, boric acid concentration and dissolved oxygen level. It is not expected to be a major factor in deaerated primary water of nominal composition.[3]

Crevice Corrosion

Environmental conditions in a crevice can be significantly different than on adjacent bare metal surfaces. Under many conditions, the environment in the crevice can be more aggressive than outside the crevice, and accelerated local corrosion can take place. Typical crevice locations on the outside surfaces of PWR pressure boundary parts include bolts, washers, and gaskets. Crevice corrosion has not generally been reported to be a significant practical problem in borated water environments on the outside surfaces of PWR components. However, this may not always be the case if the part or component includes crevices.

Both galvanic and crevice effects can become significant in the case of C&LAS exposed to boric acid via a crack or other such defect in a stainless steel or nickel base cladding.

Pitting

Pitting has not generally been reported to be a significant problem in borated water environments on the outside surfaces of PWR components, probably because the conditions under which it might be expected (see Fig. B.18.3) involve higher pH values than would normally be expected for BAC and because boric acid is a buffer that does not support local acidification within an incipient pit.

Intergranular Corrosion

Intergranular corrosion is localized attack along the grain boundaries of a metal or alloy and is most common with stainless steels or nickel-base alloys that are generally resistant to BAC. There are no reports of intergranular corrosion being a significant contributing factor to problems associated with C&LAS corrosion due to leakage of borated water.

Stress Corrosion Cracking

Stress corrosion cracking in the presence of borated water leakage has been reported to be a problem only in the case of highly loaded steam generator manway studs that have been coated with lubricants containing sulfur and is not thought to be associated with boric acid itself. The most celebrated case occurred at Maine Yankee where 6 of 16 studs were found to have failed

after disassembly, and 5 more were found to be cracked. The stress corrosion cracking in this case was attributed to interaction between the leaking borated water, leak sealant, and sulfur-containing thread lubricant. This experience identified the need to minimize the use of sulfur-containing compounds around pressure boundary parts.

Summary of Corrosion Rates for Various Situations

Figure B.18.4 summarizes the results for all of the corrosion tests reported in reference 2 and points out the main areas of interest. Briefly summarizing the key points:

Corrosion rates for immersion in deaerated, dilute boric acid solutions are usually quite low regardless of temperature. Moderate corrosion rates, between 0.02 and 0.05 in/yr (0.5 and 1.3 mm/yr), have typically been measured[a] during immersion in deaerated, concentrated boric acid solutions.

For cases involving immersion in aerated borated water, corrosion rates are in the range of 0.001–0.01 in/yr (0.025–0.25 mm/yr) for low concentrations at room temperature and increase to a maximum of 1–10 in/yr (25–254 mm/yr) for high concentrations at 200–220°F (93–104°C).

The main problem regarding borated water dripping on hot metal surfaces is that the solution can concentrate as the water boils off and the boiling can lower the local metal temperature to the boiling point (212–230°F [100–110°C]) of the concentrated boric acid solution, thus avoiding dry-out. Therefore, the typical situation is to have concentrated boric acid at around 212–220°F (100–104°C), which is the point of the maximum corrosion rate. However, if the metal surfaces are hot and the leakage rate sufficiently low, the water evaporates rapidly, leaving dry boric acid crystals that cause essentially no corrosion. Lower corrosion rates are expected when the surfaces onto which the borated water is dripping are below the boiling point of the borated water.

If borated steam impinges on hot metal surfaces, the corrosion rates can be very high as a result of the combination of high concentration, local metal temperatures near the boiling point of the borated water, and some mechanical effects due to the flow impingement. This condition can be highly damaging as evidenced by several cases involving rapid stud corrosion.

Laboratory results suggest that borated water leaking from a PWSCC-type crack should not cause corrosion deep in the annular clearance gap to the vessel shell since there is little oxygen at this location. However, tests with upward-pointing nozzles suggest that corrosion rates exceeding 1 in/yr (25 mm/yr) are possible. It is not yet clear if these test data are directly relevant to CRDM penetrations in the RPV head.

---

[a] Note, however, that ongoing work referred to later in this topical paper appears to suggest that these values can be exceeded under certain circumstances.

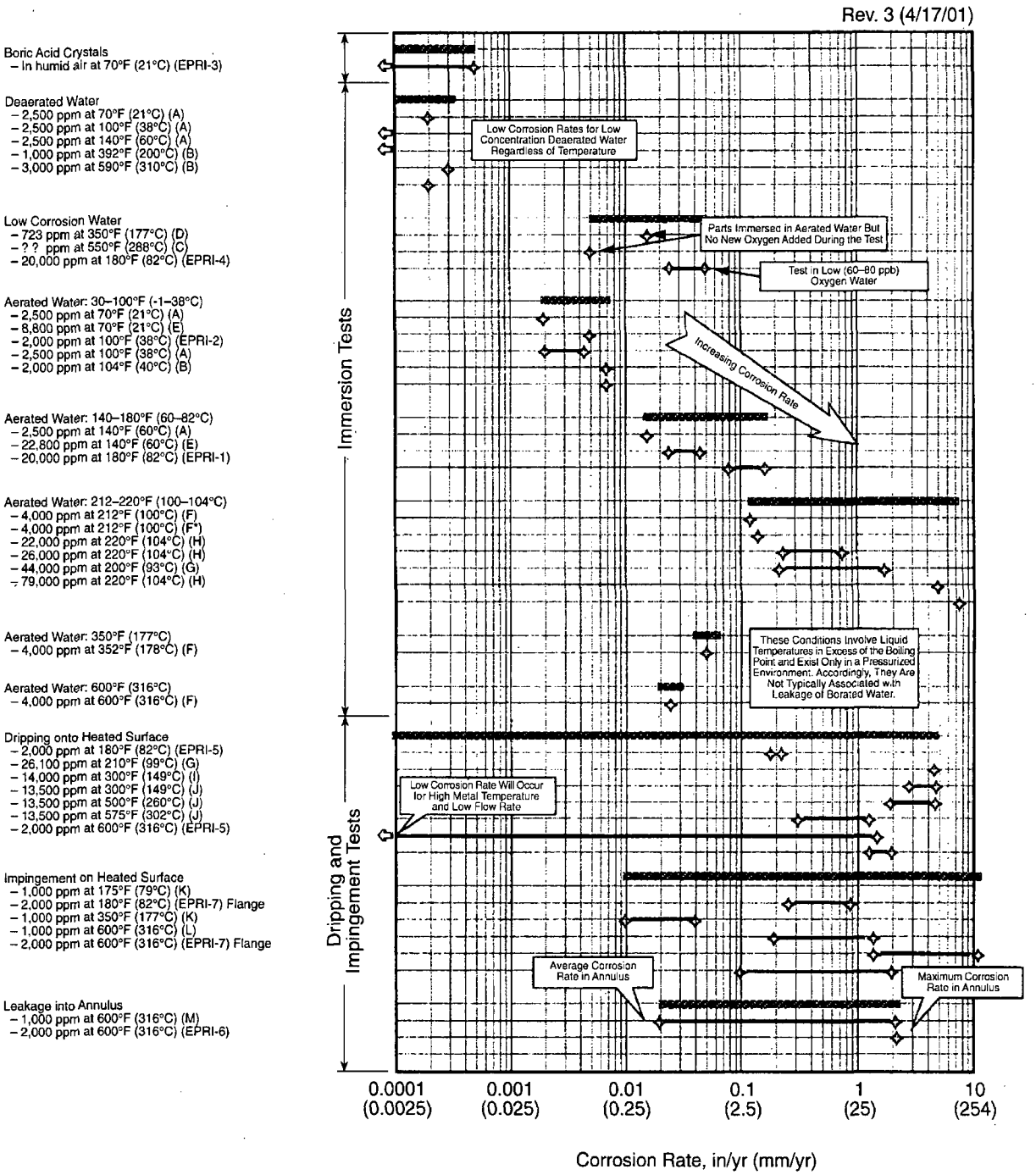

Figure B.18.4 Summary of corrosion tests on BAC of C&LAS prior to 2002[2] *Used by Permission of EPRI.*

BAC management programs at U.S. PWRs

The first level of protection against boric acid corrosion should be to prevent leaks from occurring in the first place. If there is no leakage, there will be no boric acid corrosion.

Detecting and preventing leakage

The requirements of the Code of Federal Regulation, the NRC, and the ASME Boiler and Pressure Vessel Code are remarkably similar as they apply to leakage from reactor coolant systems. The common themes in these requirements are:

- Closures should be designed to have a low risk of leakage.
- Closure designs and materials should be such that there is a low risk of rupture or abnormally high leakage.
- Closures should be fabricated and assembled to have a low risk of leakage.
- Inspection programs should be developed and implemented to find leakage and to determine other areas where the leakage could have flowed or accumulated.
- Corrective action should be implemented to correct situations where leakage has occurred.

The NRC is prepared to grant relief from the ASME Code requirements to remove insulation during the final VT-2 inspections of insulated flanges. However, several reasonable concessions have to be made to obtain the relief.

In most cases, the technical means for reducing leakage are not difficult. However, developing an effective program for reducing leakage risk from the many possible sources requires concerted effort by both plant management and staff. A major key to cost effective leakage reduction is to start with state-of-the-art procedures and materials that are capable of developing high-integrity joints and then train craft personnel to follow the procedures and identify adverse conditions.[5] EPRI sponsors a Fluid Sealing Technology Working Group where utilities meet on a regular basis to review the results of relevant research, discuss plant-specific leakage problems, obtain complementary information on current areas of research from sealing technology vendors, and establish priorities for further leakage reduction activities.

A more problematic source of leakage is through-wall cracks which can develop under certain circumstances in reactor components themselves. For example, there have been many reported cases of leakage of primary water from primary water stress corrosion cracks (PWSCC) in Alloy 600 nozzles attached to pressure boundary parts by partial penetration J-groove welds.[6,7] Another major source of leakage of primary coolant above the RPV has been transgranular SCC in stainless steel canopy welds.[8]

Preventing Degradation If Leaks Occur

The consequences of leakage in both joint fasteners themselves and adjacent components can often be reduced by replacing the carbon steel or low-alloy steel parts with more corrosion-resistant materials or diverting any leakage to areas where it will not cause damage (e.g., by installing protective shrouds).

The primary emphasis should always be on preventing leakage from occurring in the first place and then stopping leaks when they are found by retightening joints, injecting sealants, and other similar procedures. In some cases, however, it may be necessary to continue operating a plant with leakage and/or continuing degradation. A prime reason is that leakage may be discovered during plant operation, and it may be desirable to defer maintenance until the next scheduled refueling outage so that the repairs will not result in a power decrease or plant shutdown. In other cases, it may be desirable to defer repairs for problems discovered during a refueling outage due to a lack of parts, or for other reasons. In either case, a justification for continued operation (JCO) with the leakage and/or degradation must be prepared and Reference 2 describes a recommended methodology for this. The level of effort in developing the JCO will depend upon the criticality of the affected parts. Preparation of a JCO for operation with a small leaking valve in an isolable line requires significantly less effort than a JCO for continued operation with a leaking reactor coolant pump flange gasket.

Condition monitoring

A key factor in a successful boric acid corrosion management program is sound condition monitoring. This includes both equipment condition assessment and leakage detection. Information on equipment condition can lead to improvements that can reduce the potential for leakage. For example, potentially detrimental effects of smooth flanges, gouged flanges, out-of-flat flanges, misalignment, damaged valve stems, damaged or corroded bolts, etc., can be rectified and, thereby, reduce the potential for leakage. Similarly, low levels of plant leakage and a good leakage detection system can improve the ability to detect leaks early enough to take corrective action before more drastic measures are required. Enhanced monitoring for leakage may be advisable under certain circumstances and various systems are now available for this purpose.[9]

Ongoing BAC activities following the 2002 Davis Besse incident

Background

Between November 2000 and April 2001, leaks were discovered from reactor vessel top head penetrations at Arkansas Nuclear One-1 and Oconee 1,2: and 3. The leaks were discovered by visual inspections of the heads, which showed small amounts of boric acid crystal deposits ("popcorn" – see Fig. B.18.5) that were determined to have come from the annulus between the nozzles and the vessel head. The CRDM nozzle leaks were traced to predominantly axial PWSCC cracks in the Alloy 600 material of the head penetrations.

In August 2001, the NRC issued Bulletin 2001-01 requesting that PWR licensees provide information related to the structural integrity of the RPV head penetration nozzles, including the extent of nozzle leakage and cracking found. In response to this NRC bulletin, PWR licensees performed bare metal visual inspections of the RPV head looking for boric acid deposits adjacent to RPV head penetrations. An extensive safety analysis was also carried out to demonstrate that structural integrity was maintained, even with leaking CRDM penetrations.[10] The extent and way in which head penetrations of PWR vessels are inspected to detect boric acid leakage have also now been refined and details of current practices are contained in Reference 11.[11]

Figure B.18.5 Typical appearance of boric acid deposits (without wastage) at a leaking Alloy 600 CRDM penetration in a RPV head. *Used by Permission of EPRI*

In March 2002, in conjunction with an earlier inspection regime, the Davis-Besse (D-B) plant discovered evidence of significant wastage of the low alloy steel head contiguous to CRDM nozzle #3 (see Figs. B.18.6 & 7) and much less substantial wastage adjacent to other CRDM nozzles. The extent of the corrosion at nozzle #3 was completely unanticipated given the results of previous head inspections there and at other plants which had shown small volumes of leakage from a few nozzles, but little evidence of corrosion of the low-alloy steel head.

Figure B.18.6 Cavity in RPV head at D-B after removal of CRDM nozzle #3

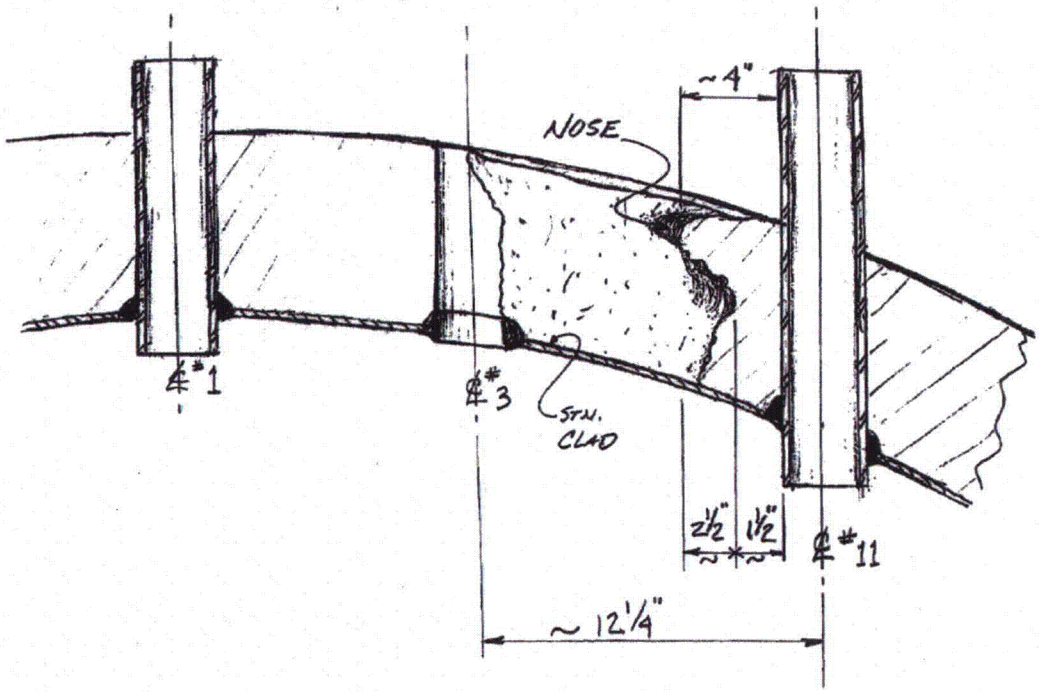

Figure B.18.7 Sketch of D-B RPV head degradation between nozzles 3 and 11

In response to the findings at D-B, the NRC issued Bulletin 2002-01 focusing on the integrity of the reactor coolant pressure boundary including the reactor pressure vessel head and the extent to which inspections have been undertaken to identify corrosion of the RPV head.

Analysis carried out to understand the severe BAC in the D-B RPV head

Reference 2 is a relatively comprehensive source document with regard to managing boric acid corrosion issues at PWR stations. Care is needed, however, in interpreting its content with regard to the way in which PWR primary coolant might attack the LAS of the vessel head if it leaks from a through-wall SCC crack in an adjacent Alloy 600 penetration tube. At the point in time where a tight, highly-branched, intergranular crack in the Alloy 600 material (or interdendritic crack in the J-groove weld) first intersects the outer surface of the high-alloy material, the leakage rate will be extremely low, irrespective of the annulus geometry (i.e. interference fit or radial gap). Thus the pressure drop to saturated vapor pressure will occur within the stress corrosion crack itself and the environment immediately above the J-weld is likely to be hydrogenated, superheated steam. As the leakage rate into the annulus from SCC of the high-alloy material increases, boiling (and possible concentration) of primary water will occur within the annulus itself, i.e. external to the crack or cracks. The exact location of the boiling transition and the extent of concentration near the liquid/vapor interface will be a complex function of the crack and annulus geometries.

In considering the composition of the liquid formed with regard to its propensity to initiate OD SCC of the CRDM penetration, the MRP Expert Panel on PWSCC considered that it would most likely to be buffered to a pH close to that of normal PWR primary water [12] as a result of precipitation of various boron compounds (including iron metaborate arising from corrosion of the LAS). It was agreed that back diffusion of oxygen into the crevice environment could be disregarded for a number of reasons (steam counterflow, hydrogen concentration, etc.), even without taking into account the gettering effect of corrosion at the LAS crevice wall. This scenario would appear to describe the situation at most leaking CRDM nozzles (including those at D-B apart from #3), where little or no wastage corrosion of the RPV head material has been observed.

To account for the development of the cavity found at D-B adjacent to leaking nozzle #3, a large number of potential BAC mechanisms (and their complex interaction over time) have been postulated,[13] as illustrated by the preliminary analysis shown in Figs. B.18.8 and 9.

The initial industry model ("top-down" corrosion – see Appendix C of Reference 14[14]) concentrated on the formation of a pool of highly concentrated boric acid on the top of the RPV head adjacent to nozzle #3 due to the ready supply of boric acid (from pre-existing deposits on the head) and local cooling of the metal so as to maintain an acidic pool of aerated liquid, despite the high temperature of the rest of the head. Independent thermohydraulic analyses confirmed that such a scenario is indeed viable, once the leakage rate of primary water through a cracked nozzle is sufficiently high, although some of the assumptions made in the calculations (e.g. with regard to the effective cross-sectional area of the PWSCC cracks in the nozzle material) require experimental verification. However, it was considered likely that flow and impingement effects adjacent to the liquid exiting the SCC cracks might also be involved. Furthermore, a possible role of LAS corrosion in "molten" boric acid within the deposits was recognized.

PRELIMINARY

Rough Progression of Mechanisms	Extent of Wastage: Initial Tight Annulus	Enlarged Annulus	Small Cavity	Large Cavity
Low-Oxygen Boric Acid Corrosion Conc. Boric Acid Corrosion but $DO_2 \approx$ 0-10 ppb	Low rates	Low rates	Low rates	Low rates
Dry BA or Boric Oxide Crystal Corrosion Corrosion in Contact with Dry Crystals and Humidity	Low rates	Low rates	Low rates	Low rates
Steam Cutting Single-Phase Erosion	Yes for high leak rates	Less likely than for tight	Less likely than for tight	Large flow area
Flow Accelerated Corrosion (FAC) Low-Oxygen Dissolution through Surface Oxides	Possible if liquid velocities high enough	Possible if liquid velocities high enough	Possible if liquid velocities high enough	Oxygen stabilizes films
Impingement / Flashing-Induced Erosion Droplet and Particle Impact Opposite Crack Outlet	Possible if droplets right size and momentum	Possible if droplets right size and momentum	Possible if droplets right size and momentum	Possible if droplets right size and momentum
Crevice Corrosion Liquid Ionic Path from Top Head Surface	Possible if liquid at mouth	Possible if liquid at mouth	Possible if liquid at mouth	No crevice geometry
Galvanic Corrosion Corrosion Driven by EMF Between Dissimilar Metals	Possible if liquid at mouth	Possible if liquid at mouth	Possible if liquid at mouth	No crevice geometry
"Molten" Boric Acid Corrosion Corrosion in Pure or Nearly Pure Melted BA Crystals	Possible on top head surface	Possible on top head surface	Possible	Possible
Boric Acid Corrosion (BAC) with Oxygen Concentrated Boric Acid Solution with Oxygen	No oxygen in crevice	Unlikely	Possibly	1-5 inches per year

Figure B.18.8 Preliminary analysis of possible BAC mechanisms to cause D-B cavity[13]

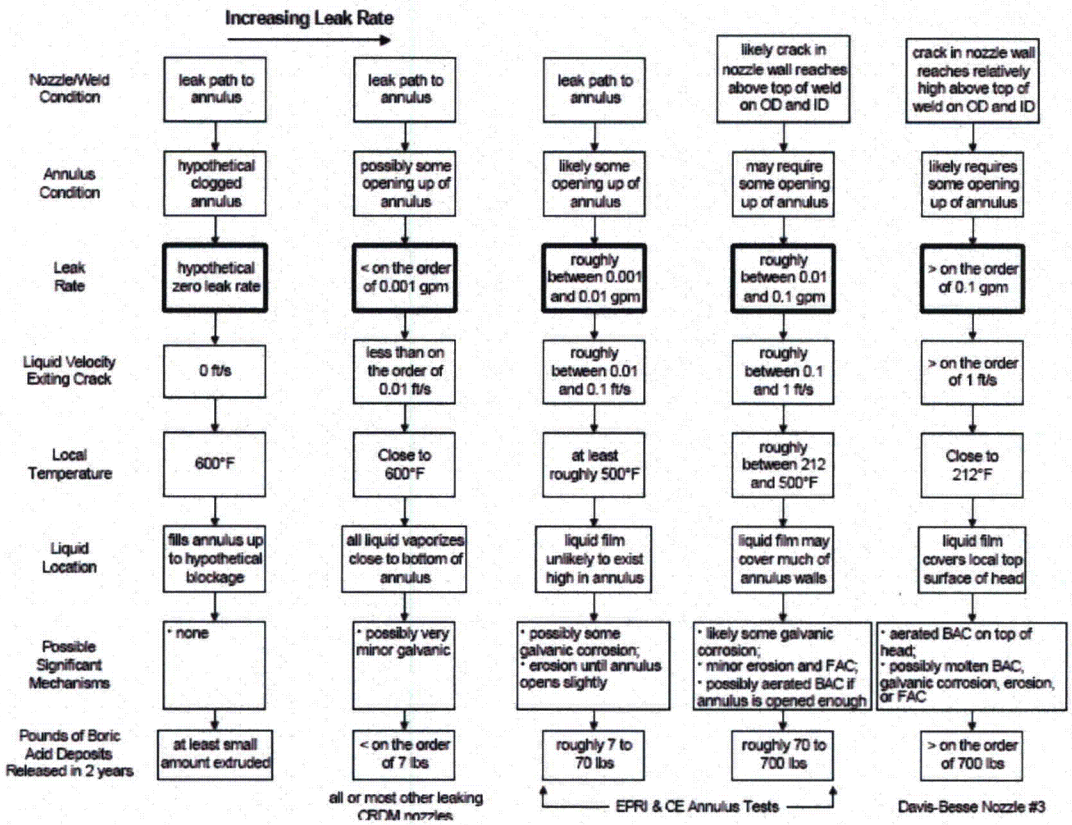

Figure B.18.9 Postulated progression of degradation with leak rate as main parameter[13]

Additional experimental work on BAC following the D-B incident

- Both the US PWR industry and NRC Research have initiated major programs on BAC since 2002, the results of which have yet to be fully reported.[b] The EPRI-managed program is structured to
  - improve understanding of the progression of boric acid wastage at RPV head penetrations,
  - identify the influence of plant specific parameters on wastage, and
  - support development of required inspection intervals for PWR plants with various penetration designs.

It consists of 4 main tasks, as shown schematically in Fig. B.18.10, culminating in an instrumented, full-scale RPV head penetration mock-up test (due to start in 2005):

Task 1: Corrosion tests in stagnant and low flowing (<0.005 gpm) primary water, simulating early stages of CRDM penetration degradation.[15]

Task 2: Corrosion tests in flowing primary water, with measurement of real time corrosion rate and ECP under laminar and impact flow.[16]

Task 3: Testing focused on a matrix of laboratory immersion corrosion, autoclave chemistry, and electrochemical polarization curve tests for concentrated boric acid and wetted molten boric acid environments.[15]

Task 4: Full-scale mockup tests for CRDM nozzles (planned examination of synergies considering the detailed results from Tasks 1, 2, and 3).

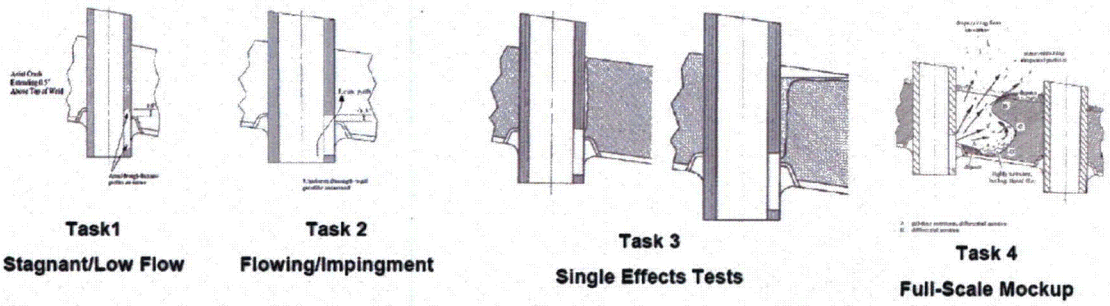

Figure B.18.10 Schematic of additional industry BAC testing program started in 2003

[b] Since the initial preparation of this paper, the NRC research results have been reported in NUREG/CR-6875 "Boric Acid Corrosion of Light Water Reactor Pressure Vessel Materials," by J.H. Park, O.K. Chopra, K. Natesan, and W. J. Shack, July 2005.

At the time of writing (March 2005), some initial results from Task 3 have been publicly reported[17] with the following preliminary conclusions:

- Corrosion rates up to about 6 inches/yr were observed for the laboratory conditions tested.
- Corrosion was significantly slowed by the presence of lithium, with the effect being most apparent at high temperatures.
- Corrosion was greatest at intermediate temperatures and boric acid concentrations (50%, versus 1% or 90%).
- For high boric acid concentrations, no large reduction in corrosion rate due to deaeration was observed for the laboratory conditions tested
- pH measurements will be used to verify that this is due to low pH.
- Corrosion rates under deoxygenated conditions were about half to two-thirds of the rate under the corresponding oxygenated conditions.
- No significant acceleration was noted due to galvanic coupling or crevices.

The NRC experimental program at ANL has been completed and preliminary results, together with a survey of BAC plant experience and some analysis of the most likely scenario at D-B, are given in reference.[18] The authors conclude, "The galvanic difference between A533 Grade B steel, Alloy 600, and 308 stainless steel is not significant enough to consider galvanic corrosion as a strong contributor to the overall boric acid corrosion process." In addition, the NRC test program has found that the corrosion rate of A533 Grade B steel in contact with molten salts of the H-B-O system at 150°C to 170°C can be as great as that of A533 Grade B steel in contact with an aqueous, aerated solution of boric acid at temperatures near the boiling point, although the MRP test program suggests that this situation may not be applicable to operating plants.[17]

Finally, it should be mentioned that a full-scale destructive examination of the D-B RPV head cavity has now been carried out. These results were recently reported.[19]

Improvements to plant BAC management programs

Subsequent to the D-B incident, considerable attention has been paid to the way in which monitoring for BAC leakage is actually being carried out at operating plants [20] and revised "best practice" guidance is currently being put into effect within the industry.[21] The American Society of Mechanical Engineers (ASME) has also approved a 7/5/05 Code Case N-722 "Additional Examinations for PWR Pressure Retaining Welds in Class 1 Components Fabricated with Alloy 600/82/182 Materials."

References for B.18

[1] "Boric Acid Corrosion of Carbon Steel Reactor Pressure Boundary Components in PWR Plants," NRC Generic Letter 88-05, U.S. Nuclear Regulatory Commission, March 17, 1988.

[2] Boric Acid Corrosion Guidebook, Revision 1: "Managing Boric Acid Corrosion Issues at PWR Power Station, Electric Power Research Institute, 2001.

[3] "Low-Alloy Steel Component Corrosion Analysis supporting Small Diameter Alloy 600/690 Nozzle Repair/Replacement Programs," NRC SER on CE NPSD 1198-P, U.S. Nuclear Regulatory Commission, Feb. 2002.

[4] Handbook of Corrosion Engineering, McGraw-Hill, 1999.

[5] "Establishing an Effective Leak Management Program," TR-114761, Electric Power Research Institute, December 2000.

[6] " PWSCC of Alloy 600 Materials in PWR Primary System Penetrations," TR-103696 Electric Power Research Institute, July 1994.

[7] "PWSCC of Alloy 600 Type Materials in Non-Steam Generator Tubing Applications - Survey Report Through June 2002 Part 1 PWSCC in Components Other than CRDM/CEDM Penetrations" (MRP-87), Electric Power Research Institute, 2002.

[8] C. M. Pezze, I. L. W. Wilson, "Transgranular Stress Corrosion Cracking of 304 Stainless Steel Canopy Seal Welds in PWR Systems," Proceedings of the Fourth International Symposium on Environmental Degradation of Materials in Nuclear Power Systems–Water Reactors, pp. 4-164–4-179, Jekyll Island, GA, August 6–10, 1989.

[9] "Survey of On-Line PWR Coolant Leak Detection Technologies" (MRP-94), Electric Power Research Institute, 2003.

[10] "Reactor Vessel Closure Head Penetration Safety Assessment for US PWR Plants" (MRP-110), Electric Power Research Institute, 2004.

[11] "Materials Reliability Program Inspection Plan for Reactor Vessel Closure Head Penetrations in U.S. PWR Plants" (MRP-117), Electric Power Research Institute, 2004.

[12] " Crack Growth Rates for Evaluating Primary Water Stress Corrosion Cracking (PWSCC) of Thick-Wall Alloy 600 Materials" (MRP-55, Rev. 1), Electric Power Research Institute, 2002.

[13] G. White, C. Marks, S. Hunt, "Technical Assessment of Davis-Besse Degradation," NRC ADAMS Accession No. ML021420150, U.S. Nuclear Regulatory Commission, May 5, 2002.

[14] "PWR Reactor Pressure Vessel (RPV) Upper Head Penetrations Inspection Plan, Revision 1" (MRP-75), Electric Power Research Institute, 2002.

[15] A. McIlree et al., "MRP Boric Acid Corrosion Testing, Tasks 1 & 3," EPRI/MRP Alloy 600 PWSCC Workshop," Tamaya Resort, New Mexico, March 2005.

[16] J. Pongpuak et al., "Corrosion of Reactor Pressure Vessel Steel by an Impinging Jet of PWR Coolant: Status Report on an EPRI/MRP Experimental Study," EPRI/MRP Alloy 600 PWSCC Workshop," Tamaya Resort, New Mexico, March 2005.

[17] EPRI/MRP Boric Acid Corrosion (BAC) Testing Program: Immersion Test Results, NRC/ANL/MRP meeting, Argonne, IL, January 2005.

[18] S. Crane, W. Cullen, "Survey of Boric Acid Corrosion Events" (Rev. 9), Materials Engineering Branch, Office of Regulatory Research, US NRC; ADAMS Accession No. ML0430002740, U.S. Nuclear Regulatory Commission, October 22, 2004.

[19] S. Fyfitch, "Boric Acid Corrosion of the Davis-Besse Reactor Pressure Vessel Head," EPRI/MRP Alloy 600 PWSCC Workshop," Tamaya Resort, New Mexico, March 2005.

[20] "Materials Reliability Program: EPRI Boric Acid Corrosion Workshop," (MRP-77), Electric Power Research Institute, July 25-26 2002.

[21] T. Satyan Sharma, "WCAP-15988, Revision 1: Generic Guidance for an Effective Boric Acid Corrosion Control Program for Pressurized Water Reactors," EPRI/MRP Alloy 600 PWSCC Workshop," Tamaya Resort, New Mexico, March 2005.

B. 19 "Variability in the Corrosion of Materials in LWR Environments," by Roger W. Staehle

Introduction

Regardless of the mode or intensity of corrosion, failures in identical components exposed to identical conditions in the same or different plants do not occur simultaneously. There is always a "first failure" in a set of identical components; and, when failures can occur, the first failure is followed by others. This first failure is frequently, and erroneously, attributed to a "bad heat" or to some carelessness in manufacturing or operation. As failures of the same mode accumulate, it is common to accept the inevitable trend, rather than having accepted the inevitability of subsequent failure at the earliest failure. Sometimes, the first failure may occur several orders of magnitude in time earlier than the mean value as determined by later testing or much later failures in the field. As used in this paper, the term failure means the initiation of degradation, its progression to detectable size, eventual propagation through the component wall, or any combination of these.

The objective of this discussion is to describe the reality of the nature and scope of variability in the occurrence of corrosion damage in operating LWR plants as well as in the laboratory testing that is intended to elucidate the nature of such failures in applications. A further objective here is to alert regulators, designers, and operators to the inevitability of the statistical nature of corrosion failures.

Statistical Distributions

Variability in the corrosion of materials has been described by Staehle and co-workers in several references [1-6]. In order to discuss the variability in corrosion of materials, a brief review of the statistical methodology and terminology is useful. For the purposes of this discussion, the statistical methodology is described in terms of the Weibull distribution [7-9]. Of the several distributions, which are available for correlating failure data, the Weibull distribution usually fits failure phenomena the best. However, there are several useful distributions that are widely used as described in texts by Nelson and others [10-13]. The background of applying statistical distributions to corrosion is described by Staehle [1] and by Shibata [14].

The principal relationships used to describe the distribution of data in the Weibull framework are shown in Equations 1-8

where:

$$f(t)=\left[\frac{\beta}{(\theta-t_o)^{\beta}}\right](t-t_o)^{\beta-1}\exp\left[-\left(\frac{t-t_o}{\theta-t_o}\right)^{\beta}\right], t>t_o \quad (1)$$

$$F(t)=P\{t\le t\}=\int_0 f(t)dt \quad (2)$$

$$F(t)=1-\exp\left[-\left(\frac{t-t_o}{\theta-t_o}\right)^{\beta}\right] \quad (3)$$

$$\ln\left[\ln\left(\frac{1}{1-F(t)}\right)\right]=\beta\left[\ln(t-t_o)-\ln(\theta-t_o)\right] \quad (4)$$

$$R(t)=P\{t>t\}=\int_t^{\infty} f(t)dt=1-F(t)=\exp\left[-\left(\frac{t-t_o}{\theta-t_o}\right)^{\beta}\right] \quad (5)$$

$$h(t)=\frac{f(t)}{1-F(t)} \quad (6)$$

$$h(t)=\left(\frac{\beta}{\theta-t_o}\right)\left(\frac{t-t_o}{\theta-t_o}\right)^{\beta-1}=\frac{\beta}{(\theta-t_o)^{\beta}}(t-t_o)^{\beta-1} \quad (7)$$

$$F_T(t)=1-\left[1-F_1(t)\right]\left[1-F_2(t)\right]\bullet\bullet\bullet\left[1-F_n(t)\right] \quad (8)$$

where:

t	=	Time
t_o	=	Location parameter, sometimes called, erroneously, the "initiation time."
θ	=	Scale parameter or the Weibull characteristic which is evaluated at $t = \theta$ where the probability is 0.632.
β	=	Shape parameter or often called the "Weibull slope" as is evident from the linearized version in Eqn. (4). β is also called the "dispersion."
$f(t)$	=	Probability density function, pdf.
$F(t)$	=	Cumulative distribution function, cdf, also the probability of failure in time.
$F_T(t)$	=	Total probability including the i^{th} element.
$F_i(t)$	=	Probability for the i^{th} element.
$R(t)$	=	Reliability
$R_T(t)$	=	Total reliability
$R_i(t)$	=	Reliability of i^{th} element
$h(t)$	=	Hazard function

Until about ten years ago, it was common to evaluate only the scale parameter, θ and the shape factor, β, owing to the difficulty of evaluating the three parameters including the location parameter, t_o; further, it was mistakenly thought that a phenomenon that started at the beginning of component life would have a t_o=0. Now, with a number of good computer programs [15], all three parameters are customarily evaluated giving a "three parameter fit" of the data rather than a "two parameter fit."

Eqn. (1) and Figure B.19.1a show the "probability density function (pdf)," which gives the probability of occurrence, *f(t),* (of corrosion failure in this discussion) in the interval *dt.* This is a familiar form, and in normal statistics the pdf gives the widely recognized "bell shaped curve."

Of more use is the "cumulative distribution function (cdf)," which gives the cumulative failures or probability of failure, *F(t)* vs. time. *F(t)* vs. time is obtained by integrating the pdf from zero to "t" as shown in Eqn. (2) and Figure B.19.1b. The result of this integration is Eqn. (3); and Eqn. (3) is usually linearized for the Weibull distribution as Eqn. (4) by taking the natural log of both sides twice. The result is a relationship of the form, y=mx+b, where the shape parameter, β, is the slope. This shape parameter is often called the "dispersion" since it describes how broadly the data are distributed. The probability of failure, *F(t),* which is the probability of failure at time, *t*, is 1-*R(t),* where *R(t)* is the "reliability" or the probability that the components will not fail by time, *t*. *R(t)* is given in Eqn. (5).

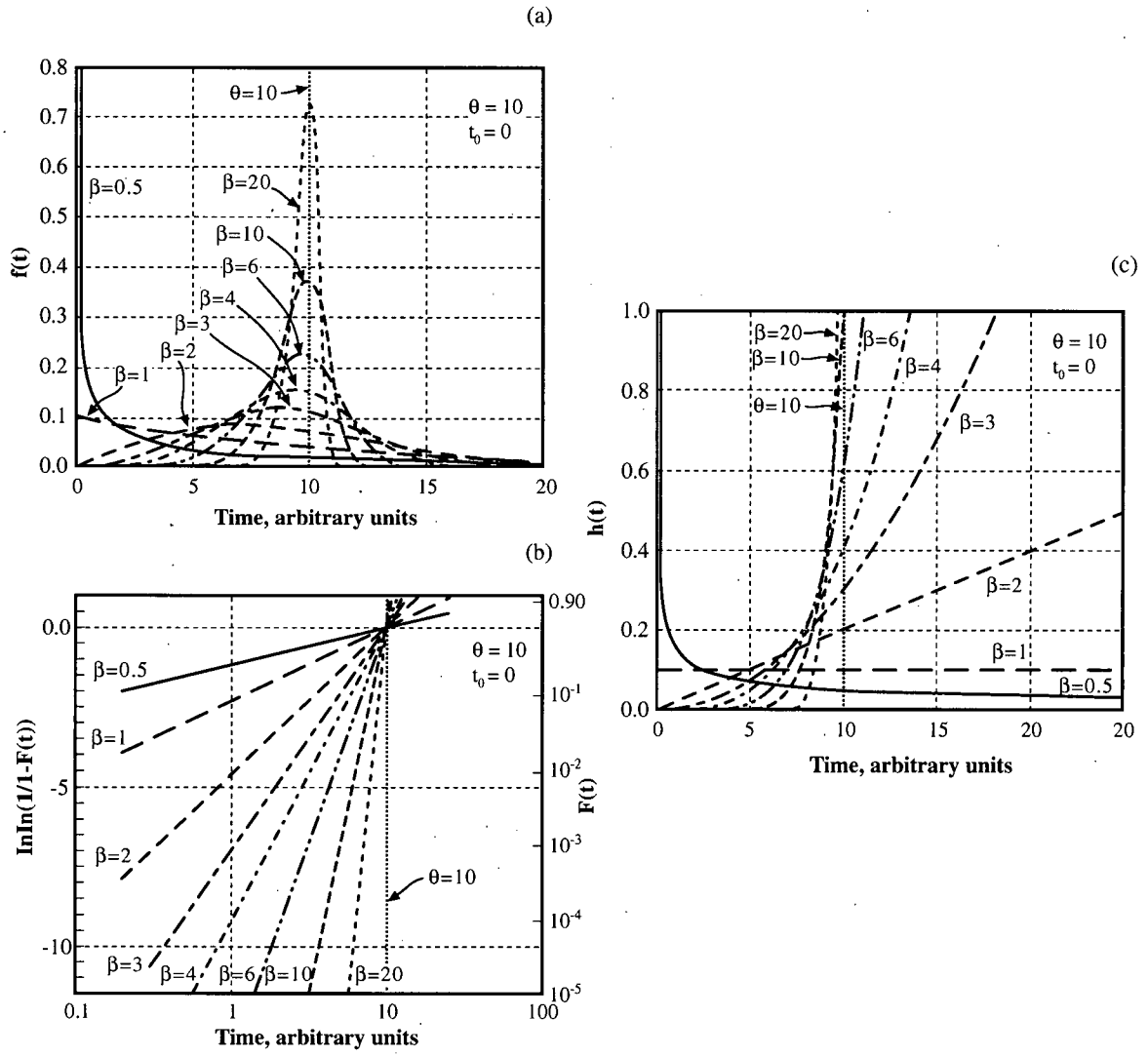

Figure B.19.1 (a) *f(t)* vs. time for constant *θ*. (b) *F(t)* vs. time for constant *θ*. (c) *h(t)* vs. time for constant *θ*. From Staehle [3]. © NACE International 2003.

Finally, another useful relationship is the "hazard function (hf)," *h(t)*, which is the probability of failure of components that have not yet failed. The hazard function is given in Eqn. (6) and Figure B.19.1c. The hazard function has the interesting property that, when β=1 the probability of failure is independent of time as is evident in Eqn. (7) and is shown in Figure B.19.1c. A shape factor of β=1 is commonly observed in field failures, thereby indicating that the probability of failure for components, which have not yet failed, is independent of time.

Often, failures of components result from multiple modes of failure as has been common in the tubes of steam generators, which are described by Staehle and Gorman.[i] Thus, the total probability of failure can be evaluated using Eqn. (8). Here, the separate $F_i(t)$ are evaluated for multiple modes of failure and then inserted into Eqn. (8) where the total probability of failure, $F_T(t)$, is evaluated. Eqn. (8) assumes that the multiple failure modes do not interact.

Interpretation of Distributions

Figure B.19.2 shows the commonly used cumulative distribution from the Weibull distribution shown in Figure B.19.1b. Figure B.19.2a shows the probability of failure vs. time for two values of the shape parameter, β, where β =1.0 and β =4.0; these values, as well as the range between them, are commonly observed in failures that occur in nuclear applications.

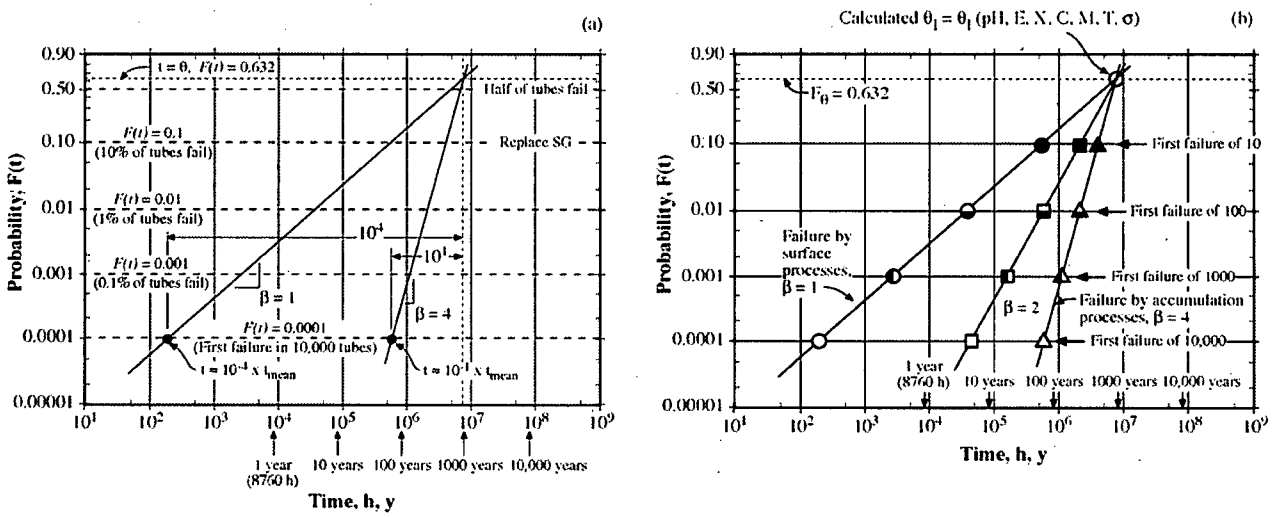

Figure B.19.2 (a) Cumulative distribution function with two values of b shown together with relationship between the failure time at F(t)=0.0001 and the mean failure time.. (b) Schematic view of probability vs. time for a calculated θ and three options for slopes within the range of engineering experience. Locations of the earliest failures noted for various populations according to three values of β. From Staehle [3]. © NACE International 2003.

Figure B.19.2a shows how the cumulative distribution is commonly used and interpreted:

- The ordinate is the probability, *F(t)*, of failure and the abscissa is time-to-failure, usually in seconds, hours, or years. Sometimes, in nuclear applications, the time is given as EFPH (equivalent full power hours).

- The ordinate is shown for the range of 0.00001 (1/100,000) to 0.90. This range applies to the failure or plugging of tubes in steam generators. Commonly, there are about 4000 tubes in a single steam generator, and, with up to four steam generators, there may be 12,000 to 16,000 tubes total. The failure or plugging of one tube in 10,000 is a failure probability of 0.0001.

- A horizontal dotted line is shown at *F(t)*=0.632 which is the value of *F(t)*when $\theta = t$. This "Weibull" characteristic is nearly the same as the mean value where *F(t)*=0.5. The location of *F(t)*=0.5 is also shown.

- Two straight lines are shown for slopes of β=1.0 and β=4.0 with both lines having the same time for *F(t)*=0.632.

- Also shown are dotted horizontal lines for $F(t)$=0.1, 0.01, 0.001, and 0.0001 or, respectively 10%, 1%, 0.1% and 0.01% failures as these horizontal lines intersect the lines for β=1.0 and β=4.0. Black dots are shown at 0.01% failures indicating a point for the first failure of one tube in a population of 10,000 tubes.

- Also, at $F(t)$=0.0001 (0.01%) probability there are notes that the first failure or tube plugging in 10,000 is some fraction of the mean. Thus, for β=1.0 the first failure in 10,000 tubes occurs at about 10^{-4} of the mean time-to-failure; whereas, at β=4.0 the first failure at $F(t)$ =0.0001 occurs at about 10^{-1} of the mean time-to-failure.

- Note also that Figure B.19.2, as well as Figure B.19.1b, emphasizes early failures or tube plugging as the scale is expanded at low probabilities. Other types of distributions emphasize failures in the high range.

- Data points are placed on the plot in terms of the fraction of the total failed or plugged at a given time; i.e. the first tube failed in 10,000 would be plotted as 0.0001 at the time of failure. After 100 tubes fail, this would be plotted as 0.01 after failures of the first 100 are observed.

Figure B.19.2b shows the same information as in Figure B.19.2a in more detail for three values of β and shows the times-to-failure of the first failure for various populations from 10 to 10,000.

With respect to the performance of steam generators, it is common that an SG is considered failed when about 10% of the tubes have been plugged. On Figure B.19.2, this is a probability of 10% or 0.1.

Plotting the occurrence of failures on such plots is described in detail by Abernethy [13]. There are several computer programs for preparing such plots [15].

Applications of Distributions

The application of a cumulative distribution of the type shown in Figures B.19.1b and 2 by incorporating actual data is described stepwise in Figure B.19.3 with plots of Figures B.19.3a, b, c. Figure B.19.3 also shows how the accumulating data are used to reach conclusions of future performance in terms of progressively more refined projections based on progressively improved values of the shape factor, β. As data are successively accumulated, it becomes possible to predict when some critical fraction of failures can occur, e.g. 10% of tubes in an SG.

Figure B.19.3a shows a black dot where the first failure of 10,000 tubes is plotted. This first failure is shown to occur at about 5 time units (hours, years) and is plotted at a probability of 0.0001 or one tube of 10,000. At this point, straight lines are drawn through this point using values of β= 1.0 and 10.0 which include a reasonable range of expected shape factors or dispersions of data.

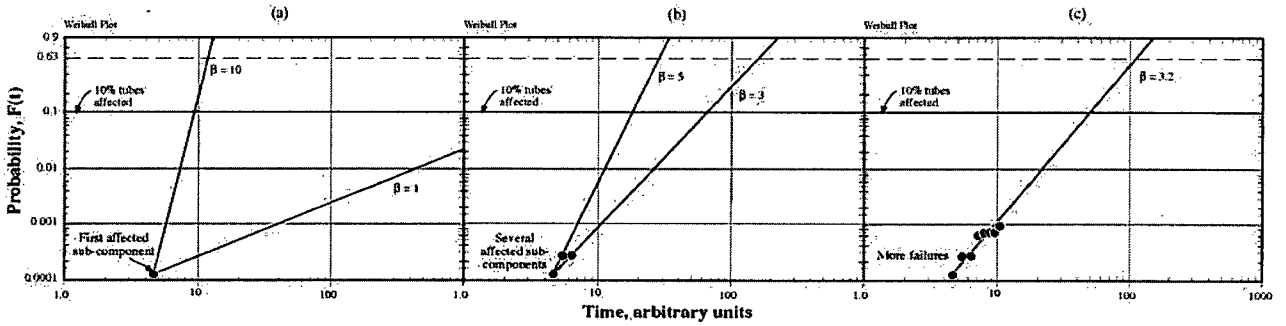

Figure B.19.3 (a), (b), (c) Schematic Weibull plots for cdfs and the evolution of failure points together with expected slopes for prediction. From Staehle.[3] © NACE International 2003.

With only one point, more precision is not possible. With these values of β= 1.0 and 10.0, failure of the SG (e.g. 10% of tubes failed) might occur as early as 10 units or as late as about 10,000 units of time. Further precision is not possible with a single first point.

After more failures occur, the range of slopes can be estimated more precisely as suggested in Figure B.19.3b. Here, a range of β=3.0 to β=5.0 is suggested showing that the SG failure point for 10% or 0.1 of the tubes failed might occur between 20 to 70 time units.

As more early failures occur, as shown in Figure B.19.3c, an even more precise value of β can be estimated, which is shown as a β=3.2. Now the time for 10% failure of tubes can be estimated to be about 50 time units. This is a basis for a nuclear utility to take action to purchase a new steam generator at some time (e.g. 3-4 years) before SG failure is predicted to occur. In the meantime more data points would be accumulated at successive inspections.

Note that each point plotted gives the total number of failures to time, *t*, divided by the population, giving the fraction failed in a given time. As shown in Abernethy [13], there are some adjustments to the data used in plotting to take account of sample size, but these are not useful to discuss here.

Weibull Distributions for Corrosion Failures in LWRs.

Cumulative corrosion failures of various components in LWRs have been dealt with using cumulative distributions and procedures as described for Figures B.19.1b, 2, and 3 [16-19]. This section describes some typical examples from operating systems and laboratory experiments.

Corrosion failures in welds from BWR pipes are plotted in Figure B.19.4 based on data from Eason and Shusto [18]. Figure B.19.4 shows the probability of failure of welds in 2" and 4" pipes in BWR applications vs. time. In both cases the β is about unity or a little less. It is interesting that about 100,000 welds are included in the 2" group and 10,000 welds in the 4" group. The fact that so many welds from different plants follow consistent Weibull behavior indicates the usefulness of the Weibull correlation and the coherence of the data.

Figure B.19.5 from Bjornqvist and Gorman [20] show data from the failures of SG tubes in Ringhals-4 PWR. Such data are taken at successive shutdowns using various NDE methods

including eddy current. These data show seven different modes of failure; and the failure data from the seven modes are combined using Eqn. (8) to produce an "aggregate all mechanisms." This aggregate probability can then be extrapolated to 10% failure in order to define when new SGs should be purchased. This method and such plots have been widely used for estimating the time when steam generators should be replaced and thereby defining when such SGs should be purchased.

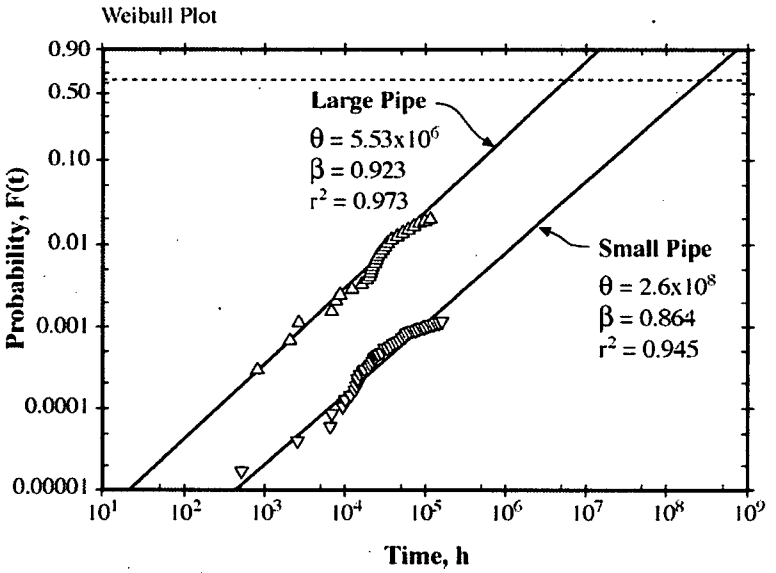

Figure B.19.4 Probability vs. time since startup for SCC failure of welded stainless steel pipes from piping used in boiling water nuclear reactors (BWR).
"Large pipe" refers to 4-inch diameter. "Small pipe" refers to 2-inch diameter.
Adapted from Eason and Shusto.[18]

In addition to pipes and SG tubes, the failures of bolts, as affected by nuclear radiation, have been analyzed by Scott as shown in Figure B.19.6 [19]. Again, this correlation shows good agreement with the Weibull distribution, noting the values of r^2, and shows clearly the dependence on neutron dose. The displacements of the Weibull correlations for different locations of formers seems related to the differential thermal expansion effects on bolt loads at these locations.

The SCC of Zircaloy-2 exposed to iodine gas as a function of stress was investigated by Shimada and Nagai, as shown in Figure B.19.7, [17] where the data are summarized in a Weibull format. Here the value of the space parameter θ decreases with stress as does the location parameter, t_o. The shape parameter, β, is unusually high and increases, as expected, with increasing stress. These experiments are relevant to the effect of iodine, which is released during fission, on the integrity of fuel cladding.

Figures B.19.4 through B.19.7 show four different applications of Weibull cdfs to LWR applications, e.g. piping, SG tubes, bolts and fuel cladding. Clearly, the Weibull correlation is useful and permits carrying forward trends as shown in Figure B.19.3. There are many more examples, especially in Staehle,[1] as well as in private and non-published sources.

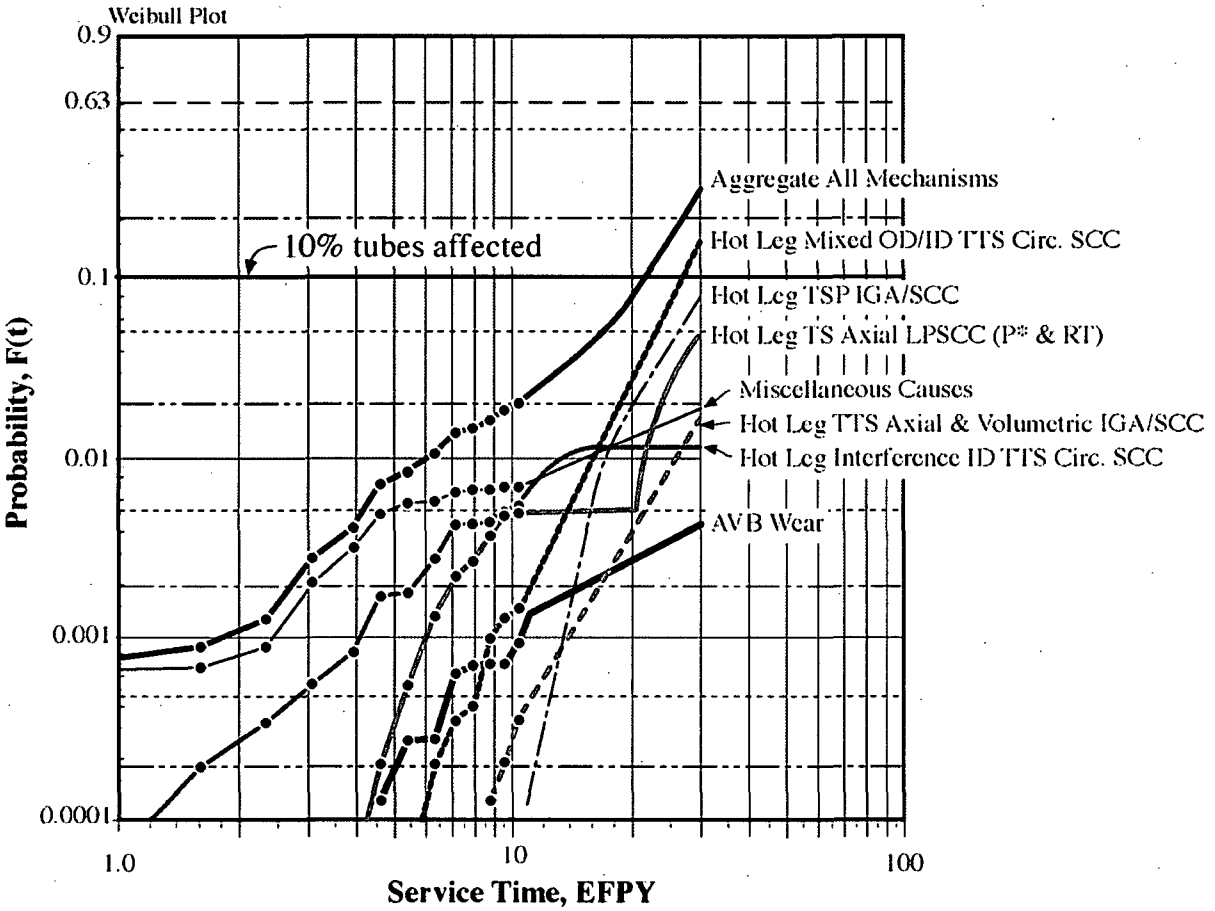

Figure B.19.5 Probability vs. equivalent full power years (EFPY) for failures of tubing from a set of SGs in the Ringhals 4 PWR. Designations: TTS = "top of tube sheet." TS = "tubesheet." Circ. SCC = "circumferential SCC." P* = special location where SCC is not serious. RT = "roll transition." AVB = "antivibration bars."[20]

Background for Random Occurrences of Corrosion Failures

It would seem that experiments could be carried out with such care that there would be no variability in the results. This is a frequent aspiration of both design and materials engineers. However such an aspiration cannot be achieved even from the most careful work. Corrosion, and particularly SCC, involve multiple events in their evolution as illustrated in Figure B.19.8. Here, the sequence of events from the earliest stage of initiation to final fast fracture is shown to include nine segments. Within each of these are micro-options that affect the courses of initiation and propagation. With such an array of macro and micro options, single deterministic times-to-failure for a corrosion process, e.g. SCC, are not possible even under the best of circumstances.

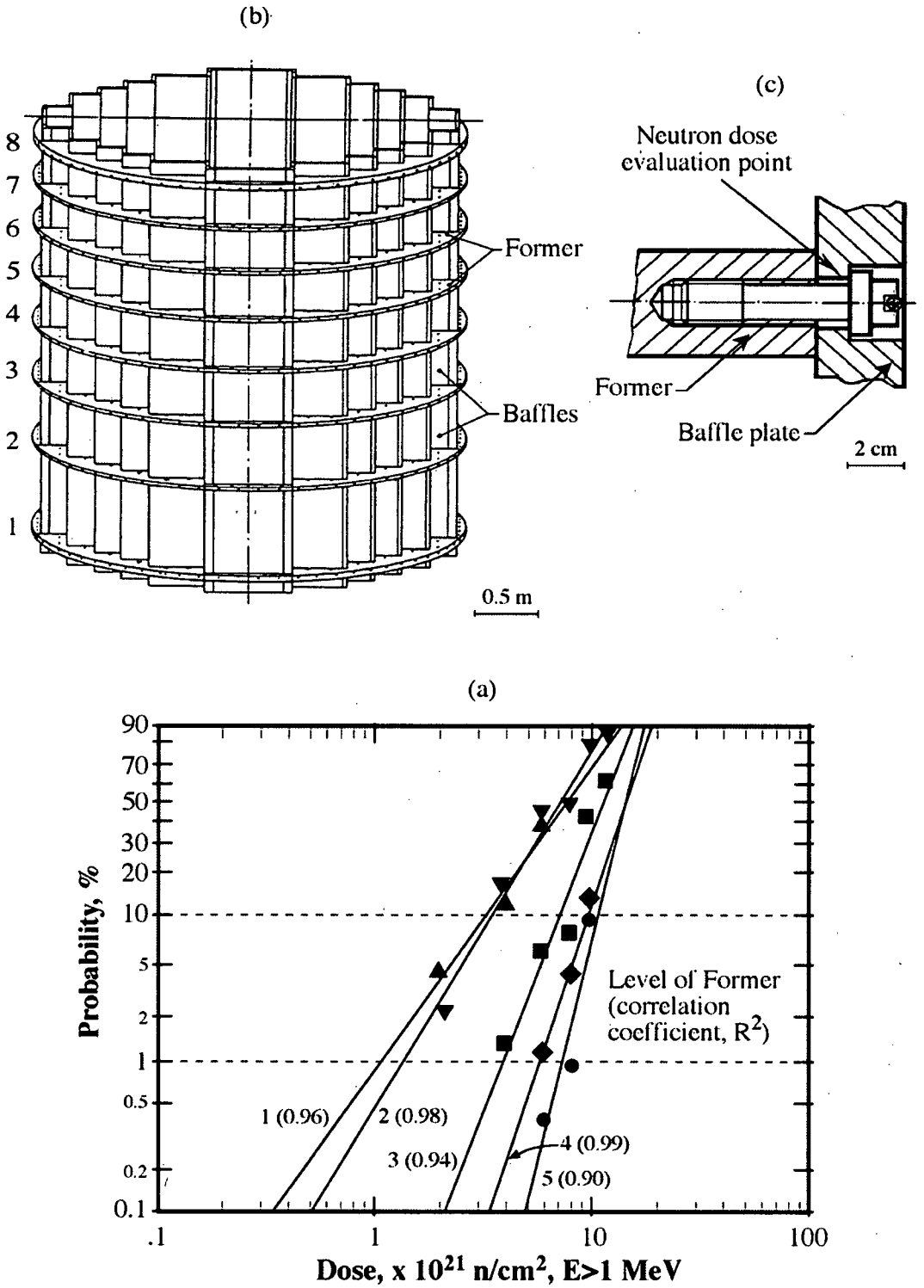

Figure B.19.6 (a) Probability of defective bolts at the joints between the formers and baffles vs. neutron dose based on data for all inspections for Bugey-2 plant. (b) Arrangement of formers and baffles. (c) View of bolts and location of neutron dose used for (a). Adapted from Scott et al.[ii] ©ASTM International.

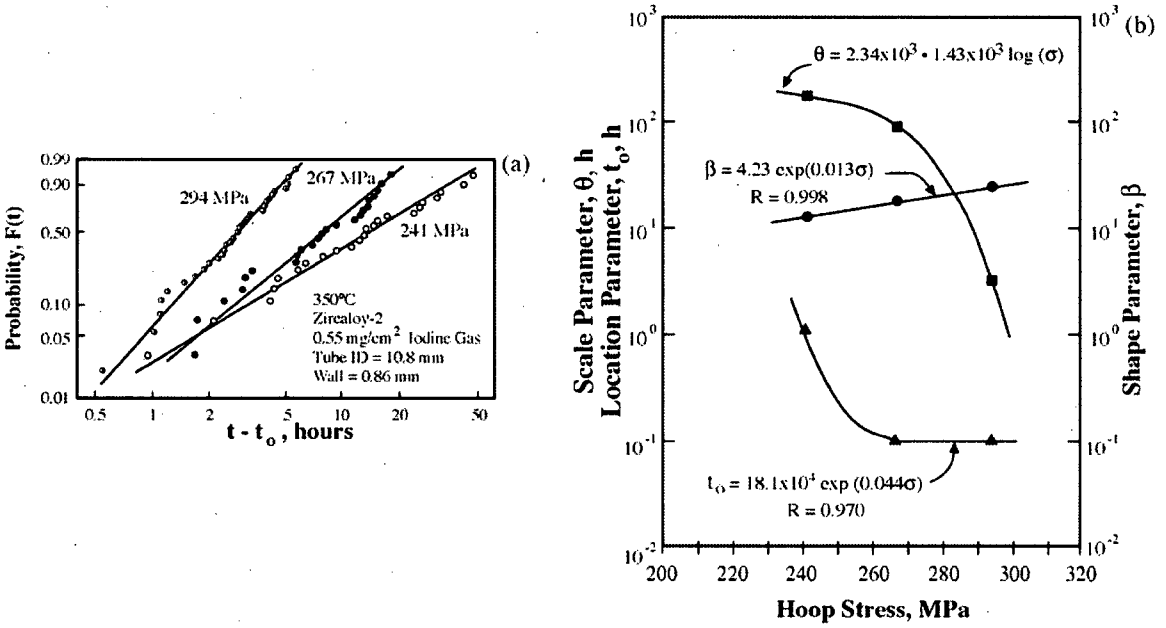

Figure B.19. 7 (a) Probability vs. time-to-failure for Zircaloy 2 fuel cladding material exposed at 350˚C to iodine gas. (b) Weibull parameters vs. hoop stress. Adapted from Shimada and Nagai.[17] Reprinted with permission from Elsevier. Calculated dependencies by Fang and Staehle.

The discussion of Figure B.19.8 concentrates generally on the metallurgical aspects of the variability. In addition, another kind of variability is related to environments as illustrated by Figure B.19.9a,[iii] which shows schematically aspects of environments in heated crevices at tube supports on the secondary side of SGs. Here, dilute chemicals are concentrated by the local heat transfer conditions, and the resulting environments are variable as implied by the distribution of chemicals inside the heat transfer crevice, which is shown in Figure B.19.9b.[iv]

Figures B.19.8 and 9 show some of the reasons for the variability of the time-to-failure shown in Figure B.19.5.

The large variability of corrosion data in general and in SCC in particular is not so widely appreciated; but such variability exists and is sometimes extensive. Scott, in his Speller Lecture [19] reported results from his study of failure indications of SG tubes. Figure B.19.10 shows results from his study of tubes with NDE indications (not necessarily plugged) from both primary and secondary sides of two different SGs after relatively long times; 40,000 hours for the primary side and 75,000 hours for the secondary side. Figure B.19.10a for the primary side shows 41 vertical bars that correspond to 41 separate heats that were used to produce tubes for the same SG. These heats all manufactured by the same company, are arranged in order of the dates of melting. At the top of each bar is the number of tubes that were used in the respective SG from the respective heat. The height of each bar indicates the percentage of tubes in that heat with NDE indications. All the tubes were exposed to the same secondary or same primary environments in the applicable steam generator.

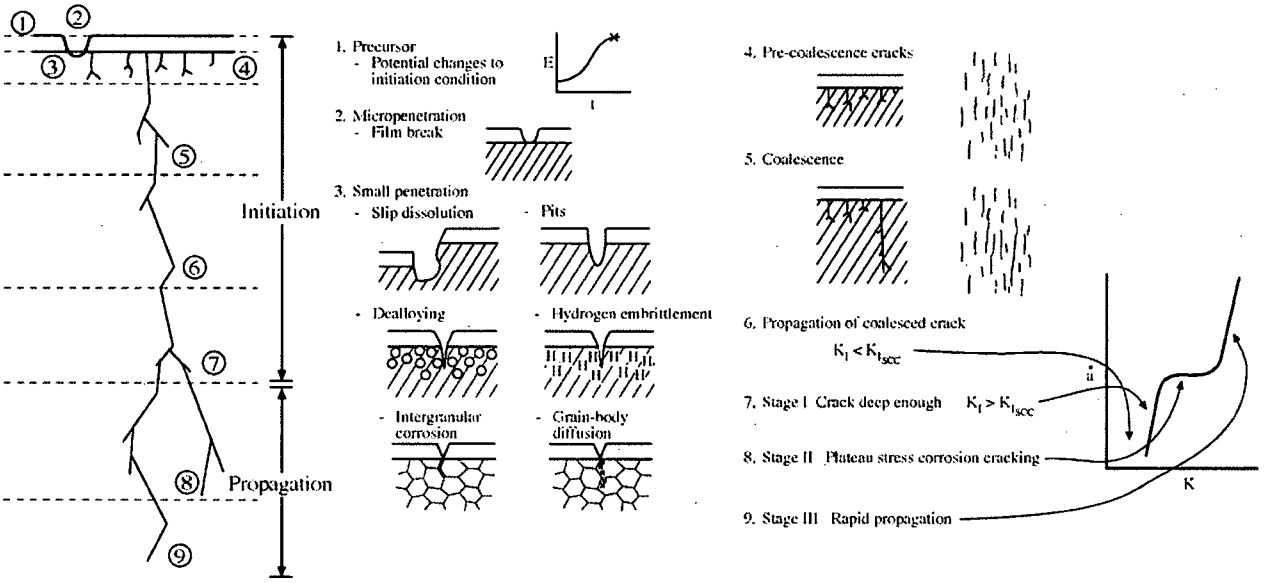

Figure B.19.8 Nine sequential segments of SCC. Practical transition from initiation to propagation shown. Protective film adjusts to the environment. From Staehle.[3] ©NACE International 2003.

Despite all the factors that were constant for the heats in Figure B.19.10a, the fraction of the tubes, which failed on the primary side, varied from zero to 41%. A similar pattern occurs on the secondary side after 75,000 hours. Note that these data for the primary and secondary sides were taken from different SGs.

Supposing that one of the heats with a high failure rate, as identified in Figure B.19.10, was chosen for an experimental program; then, it would be concluded that a high failure rate is characteristic—and vice versa. In fact, nearly all the experimental programs have used heats that were known to be very susceptible. One can only conclude that there is large variability in the failure rate of SG tubes despite the best efforts to assure similar conditions—such a pattern can be expected for all materials. The patterns of Figure B.19.10 indicate that attention that should be given to selecting a suitable array of materials with which to conduct tests.

Similar implications, to those in Figure B.19.10 from Scott, have been shown by Jiang and Staehle [24] from evaluating the SCC of stainless steels in boiling $MgCl_2$; and the results are shown in Figure B.19.11. Data are shown for the time-to-failure for specimens exposed over a ranges of temperatures, Figure B.19.11a, and ranges of stresses, Figure B.19.11b. The data for effects of temperatures in Figure B.19.11a includes experiments by 23 different investigations and for stress in Figure B.19.11b from 40 different investigations. Figures B.19.11c and 11d show the range activation energies from the data of Figure B.19.11a; Figures B.19.11e and 11f show the ranges of stress exponents from the data in Figure B.19.11b.

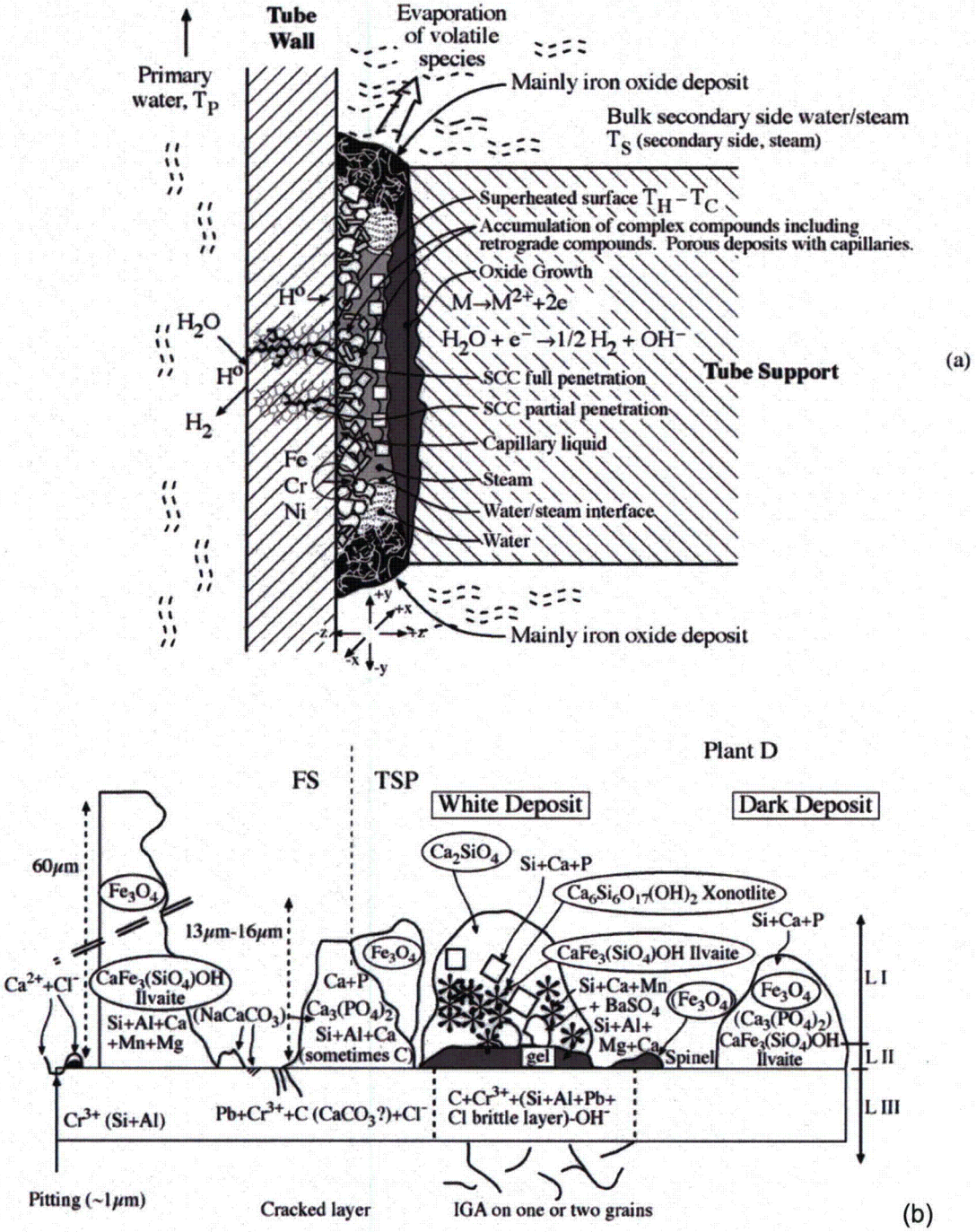

Figure B.19.9 (a) Schematic view of chemical conditions inside a heat transfer crevice on the secondary side of PWR SGs. From Staehle [22]. Reprinted with permission of John Wiley & Sons, Inc.
(b) Schematic view of an OD tube surface inside the tube support and outside on the free surface. The condenser was titanium and the water conditioning was NH_3. The tube was examined after 81,900 hours. From Cattant et al. [23]. © SFEN 1994.

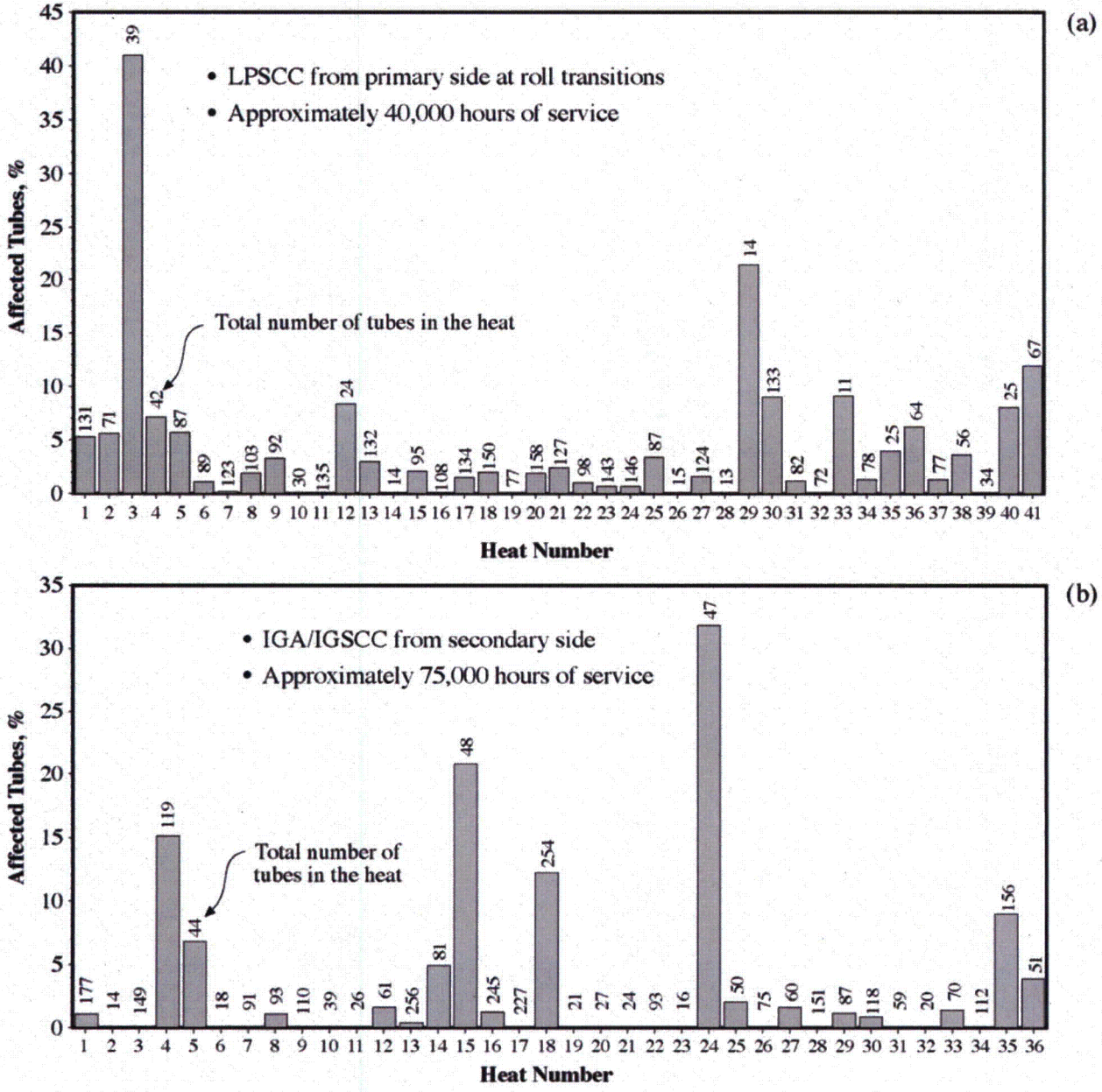

Figure B.19.10 (a) Percent of tubes affected by LPSCC (i.e. with NDE indications) from the primary side of a PWR steam generator vs. heat number determined at roll transitions after approximately 40,000 hours of service. Primary surface temperature at this location is about 310°C. Environment is primary water as identified in Figure 4. (b) Percent of tubes affected by IGA and IGSCC (i.e. with NDE indications) vs. heat number from the secondary side of a PWR steam generator in heat transfer crevices after approximately 75,000 hours of service. From Scott.[19] © NACE International 2000.

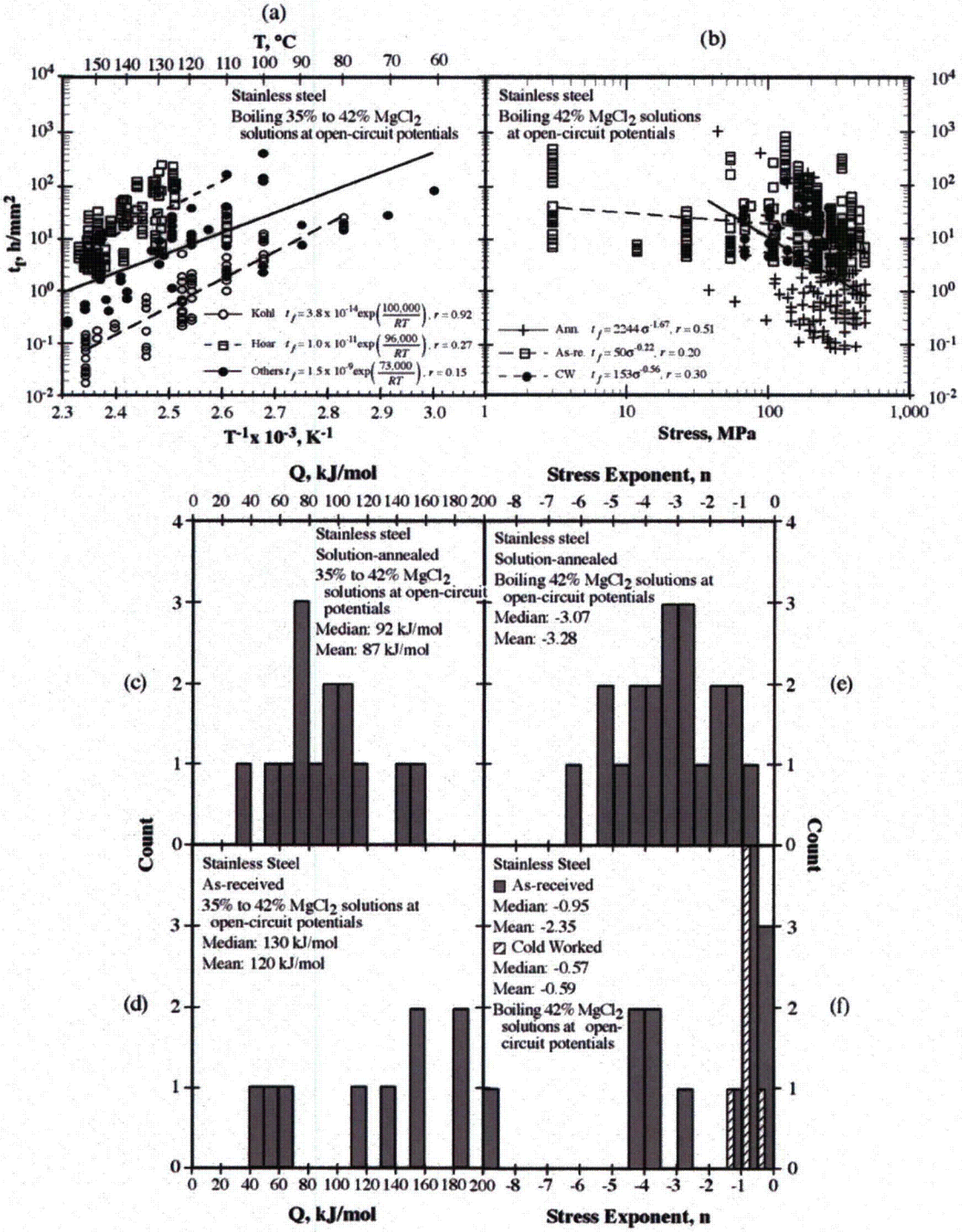

Figure B.19.11 Time-to-failure vs. temperature (a) vs. stress (b) for stainless steel in boiling $MgCl_2$. The units of time-to-failure have been normalized by a cross-sectional area of specimens used by different investigators. (c), (d), (e), and (f) show the array of activation energies and stress exponents from the various studies which were analyzed. Adapted from Jiang and Staehle.[24]

The data of Figure B.19.11 are equivalent to using different manufacturers where the materials are exposed, as components, to essentially the same environments. These data are prototypic of corrosion in crevices, such as in Figure B.19.9, where the solutions are concentrated by heat transfer. It is likely that the boiling $MgCl_2$ environments, even those used in multiple laboratories, are more uniform than the environments that occur in heat transfer crevices. The data in Figure B.19.11 exhibit ranges of failure times of about 10^4. The implications here are similar to those of Scott in Figure B.19.10.

Implications of the variability in SCC of SGs are shown in Figure B.19.12, from Staehle and Gorman [16] where they plot the replacements of SGs vs. time. These did not all fail at the same time despite their general similarity of design--again, an indication of the variability of the corrosion phenomena that produce failures.

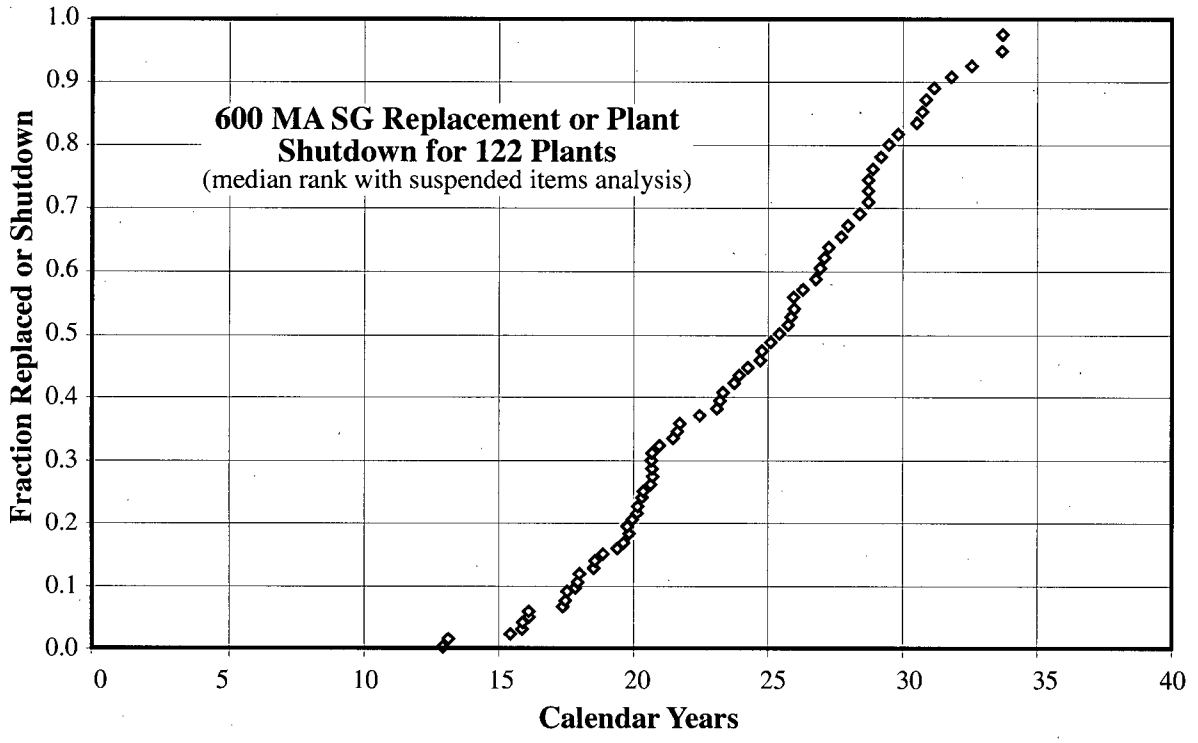

Figure B.19.12 Fraction of replaced or shutdown steam generators vs. calendar years for Alloy 600MA plants in the world. From Staehle and Gorman.[16] © NACE International 2003/2004.

Finally, a further contributor to the variability of corrosion that produced the results shown in Figure B.19.12 was the variety of modes of failures and the multiple locations where corrosion failures occurred as shown in Figure B.19.13 [16]. Thus, in addition to the variability in a single SCC, which is implied in Figure B.19.8, there is further variability in corrosion failures owing to multiple modes of failure and multiple locations of failures. . Multiple failures are dealt with as shown in Figure 5 and through the use of Eqn. (8).

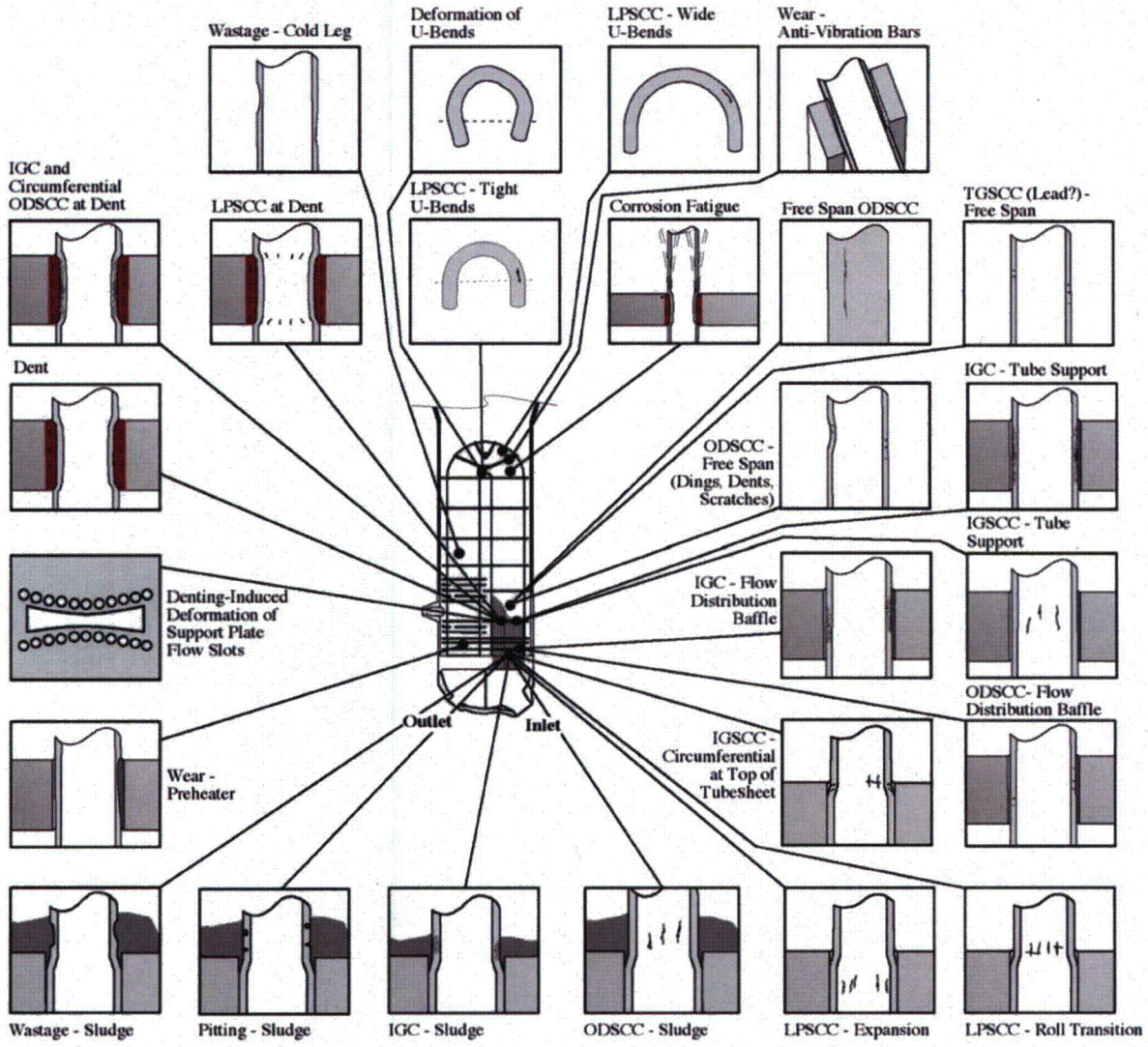

Figure B.19.13 Array of modes of failure at various locations (mode-location cases) that have occurred in recirculating steam generators. From Staehle and Gorman.[16] © NACE International 2003/2004.

The Physical Meaning of Statistical Parameters

The statistical correlations as illustrated in Eqn. (1) through (8) and in Figures B.19.1, 2, 3, 4, 5, 6, and 7 are nominally pure correlations without having been derived from physical experience; although Weibull developed his distribution based on his interest in modeling the failures of ball bearings [7]. Nonetheless, in the paper by Staehle [25] it was shown that statistical parameters could be extrapolated and interpolated using activation energies and stress exponents.

In a detailed analysis by Staehle [1], it was shown that the statistical parameters could be correlated according to generally regular dependencies on temperatures, stresses, and concentrations. For example, Figure B.19.14 shows two separate cumulative distributions in

Figures B.19.14a and 14b for SCC of Type 304 stainless steel tested at 288°C in high purity oxygenated water. One study was conducted by Clark and Gordon [26] in the United States and the other was conducted by Akashi and Ohtomo[27] in Japan. The dependence of statistical parameters on stress is compared in Figure 14c. The results are quite similar for the dependencies of θ, β, and t_o. Such regular dependencies were found by Staehle[1] for other alloys in various environments and for the variables of temperature, stress, and concentration of solutions. Such regular dependencies suggest that statistical distributions could be extrapolated over ranges of temperature, stress, and concentration as well as over other variables that control corrosion such as pH, potential, alloy composition, and alloy structure as has been described by Staehle.[6]

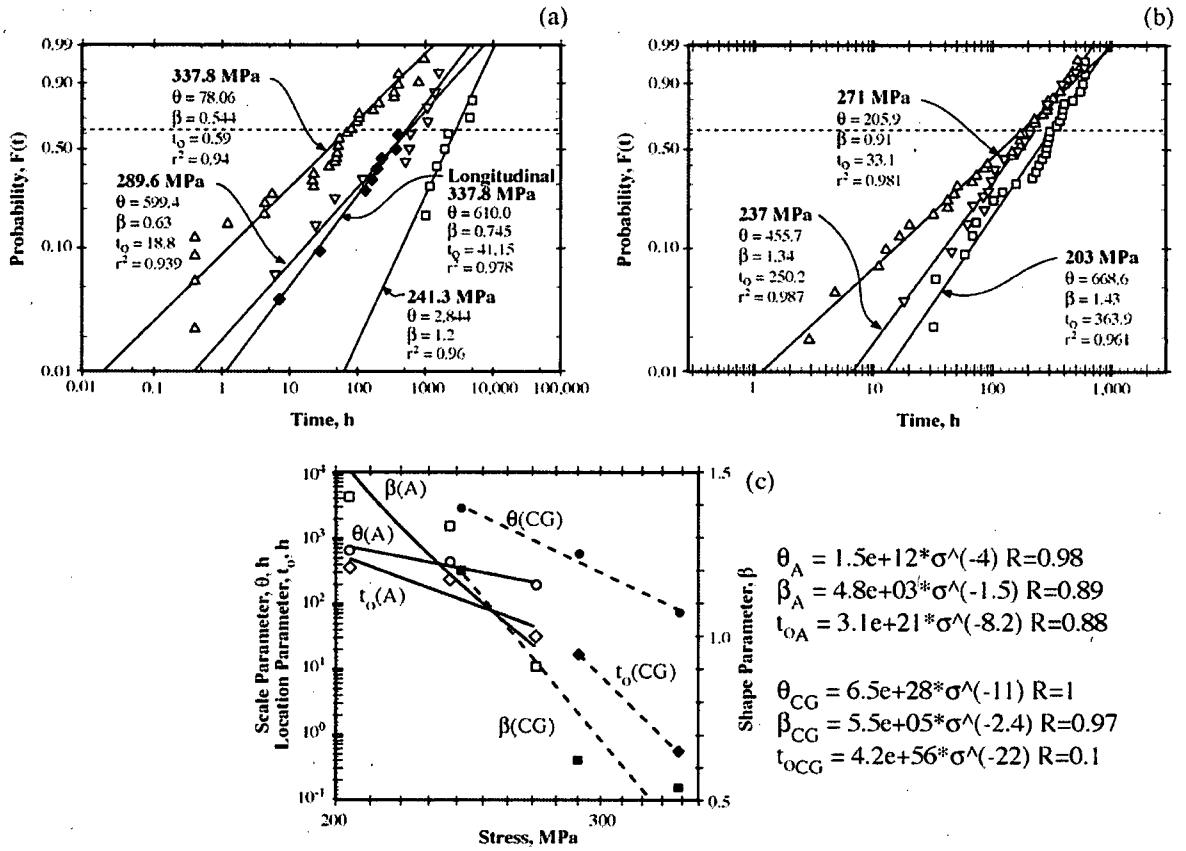

Figure B.19.14 a) Probability vs. time for sensitized Type 304 stainless steel tested at 288°C in high purity oxygenated water. Adapted from Clarke and Gordon.[26] © NACE International 1973. (b) Probability vs. time for sensitized Type 304 stainless steel tested at 288°C in high purity oxygenated water. Adapted from Akashi and Ohtomo.[27] (c) Weibull parameters vs. stress from both the Clarke and Gordon (CG) (dotted lines) and Akashi (A) (solid lines) distributions.

From the analyses by Staehle,[1,6] it appears that the values of β in many cases are directly related to physical conditions. Figure B.19.15 shows a cdf and hf for the cases where β=1.0 and 4.0, together with schematic illustrations of their physical significance. As shown in Figures B.19.1b and 2, the slope of the *F(t)* vs. time for β=1.0 is lower than that for β=4.0 which means that the first failure occurs at a much shorter time relative to the mean for β=4.0 than for β=1.0. In Figure B.19.15b the hf is independent of time for β=1.0 whereas, the hf increases sharply around the value of θ for β=4.0.

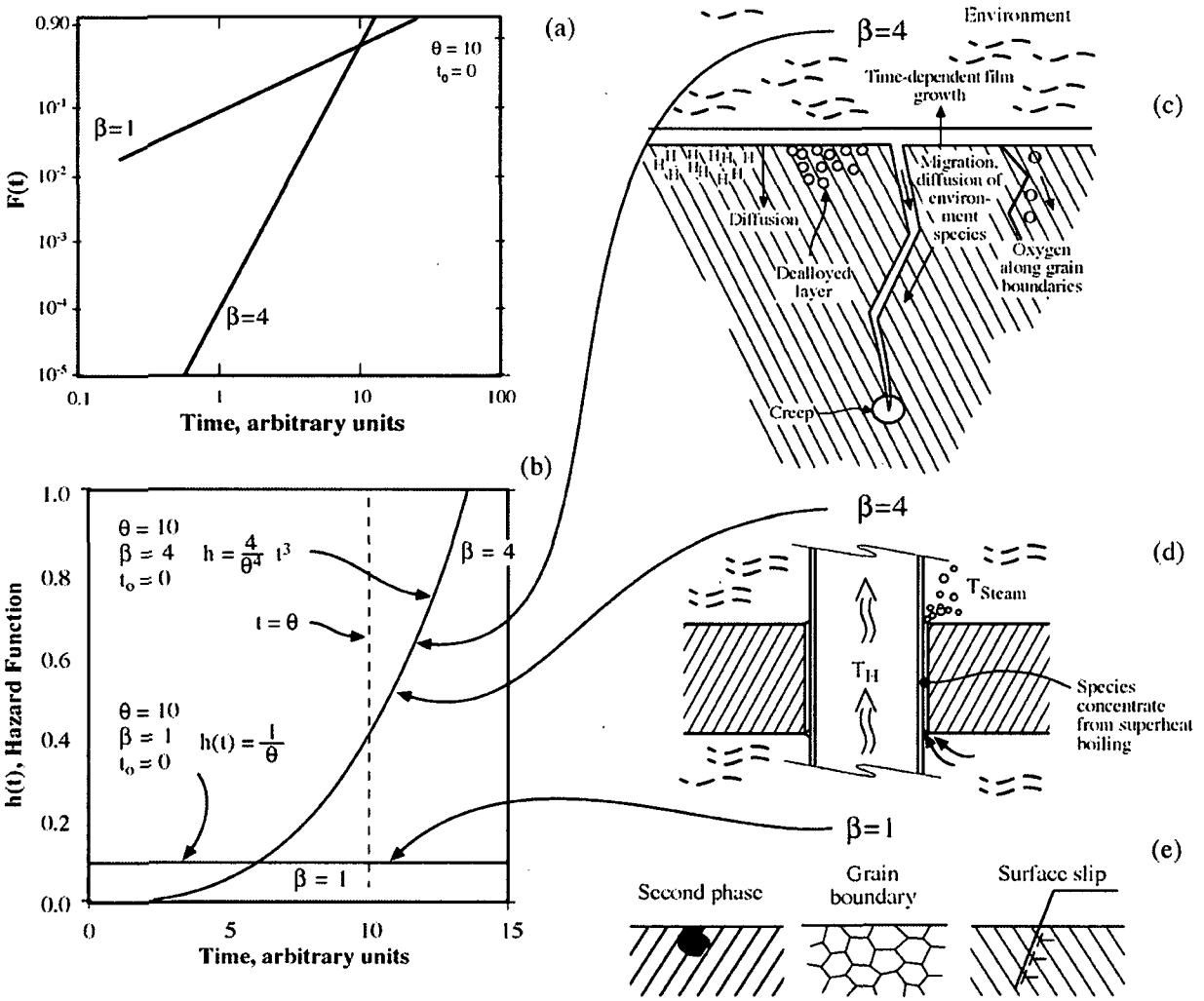

Figure B.19.15 a) cdf for β=1 and β=4 vs. time. (b) hf vs. time for β=1 and β=4 cases at θ=10 and t_o=0. (c) Possible contributions in the metal substrate, for a growing SCC, to the accumulation case for β=4. (d) Possible contributions to the accumulation case β=4 from a superheated tube support geometry. (e) Possible contributions to the β=1 case from surface processes. From Staehle.[3] © NACE International 2003.

A reasonable interpretation of the tendencies in Figure B.19.15b is suggested in the schematic illustrations of Figures B.19.15c, 15d, and 15e. It has been well known that lower values of β e.g. a β=1.0 are related to surface processes and the initiation stages of pitting and SCC. Such morphologies for surface reactions are illustrated in Figure 15e. On the other hand, the relatively rapid rise in the hf for β=4.0 after an initial quiescence suggests that some time or pre-condition is required before SCC can occur; but, when the necessary conditions are present, SCC can proceed relatively rapidly. Such pre-conditions may be associated with critical early diffusive or migration processes as illustrated in Figure 15c or geometrical conditions, which present an impeded diffusion path, as illustrated in Figure 15d.

The validity of the implication in Figure 15b, as related to the comparison between the initiation stage of Figure 15e and the propagation of Figure 15c, is shown in Figure B.19.16 from work by Shibata and Takeyama.[28] Here, the β for initiation is consistently unity; whereas, that for propagation increases with applied stress following the trend with stress in Figure B.19.7.

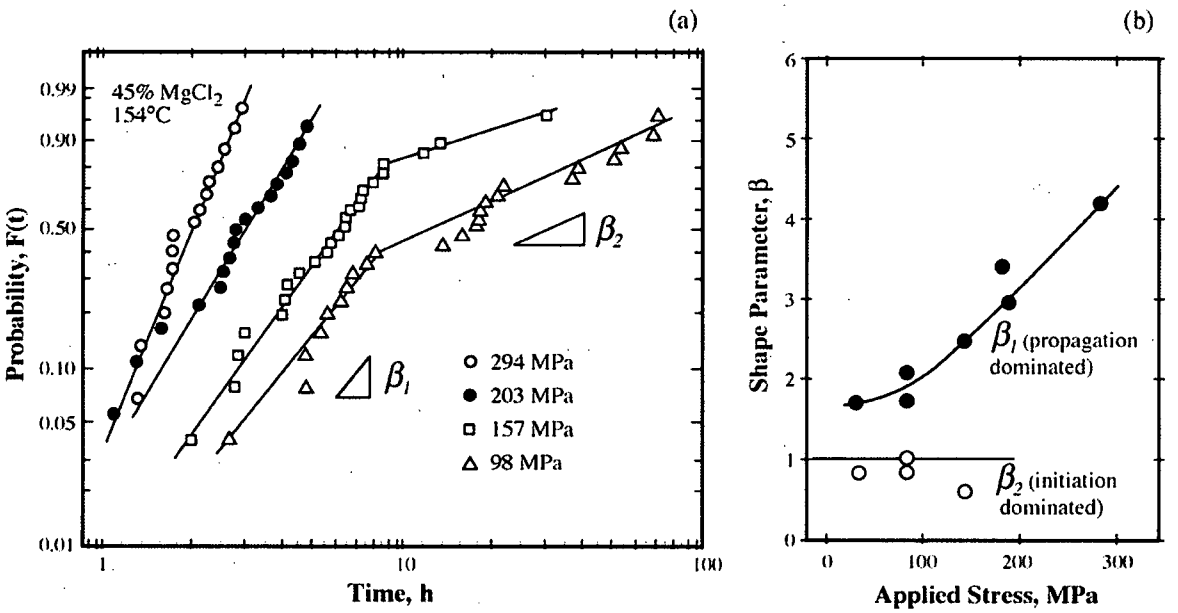

Figure B.19.16 (a) Probability vs. time for Type 304 stainless steel exposed to boiling $MgCl_2$ at 154°C at various stresses. (b) Values of β for upper and lower segments vs. stress from (a). From Shibata and Takeyama [28].[28] Reprinted with permission from The Iron & Steel Institute of Japan.

Accelerated Testing and Pitfalls

Testing is often accelerated in order to predict the occurrence of performance in the future. Thus, one could hope that successful performance after some length of time could be predicted by short term testing that is accelerated along vectors of temperature, stress, solution concentration, or some other variable.

It is common to conduct accelerated testing to determine some mean time-to-failure that can predict the mean time-to-failure at longer operating times at conditions that are less severe. An acceleration of about 100 may be about the best to expect. However, such testing is usually

conducted to predict mean times-to-failure notwithstanding the implications of Figures 1, 2, and 3 as well as Figures 4, 5, 6, and 7.

In general, the real problem of prediction is not predicting the mean time-to-failure since, by the time 50% have failed, the application has long since failed. What needs to be predicted is the first failure or the first 0.1% of failures. While it would be convenient to assume that the acceleration for the mean time is the same as that for 0.1%, such an assumption cannot be justified *a priori*. For the data from an accelerated test to apply at the 0.1% or 0.001 probability would require that the expected values of β for failures in the field would be the same as the β for failures in tests.

Figure B.19.17 shows schematically a typical plot of field failures with β=1.0 and a schematic plot of hypothetical (but typical as in Figure B.19.4) data from an accelerated test with β=5.0. Here, while the mean value of the accelerated test is about 100 times less than that of the field failures (and thereby being a good acceleration), there is no acceleration at a 0.001 probability. The value of β=5.0 is chosen for this schematic since β is generally increased as the stressors are increased and as the material chemistries are more homogeneous.

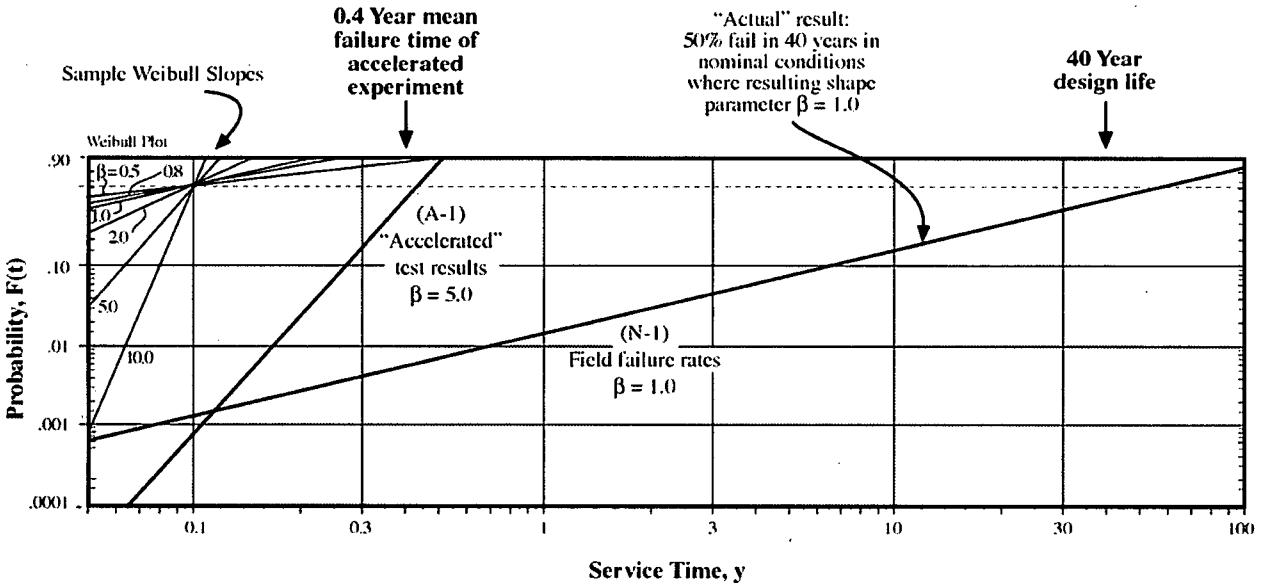

Figure B.19.17 Schematic plot of probability of failure vs. time for field data and accelerated tests based on Weibull coordinates. N-1 corresponds to assumed field results; A-1 corresponds to assumed accelerated testing. From Staehle.[3] © NACE International 2003.

Figure B.19.17 shows that "accelerated testing" may not provide acceleration for the early failures, and such a result cannot be assumed without directly measuring the statistical parameters in the accelerated testing.

Conclusions

1. Corrosion data in the field and in laboratory testing are statistically distributed under the most well-controlled circumstances. There are no bases for assuming that even well conducted testing or well-controlled field performance will produce failures at identical times.

2. In choosing materials for laboratory testing, it is necessary to choose multiple sources of testing materials that are typical of applications since a choice of a single heat could misrepresent either the mean, the most rapid, or the least rapid rates of relevant modes of corrosion.

3. The occurrence of early failures are not likely to result from "bad heats" or carelessness but are more likely to be the early failures in a regular distribution of failures.

4. Knowing the shape parameter for various mode-location cases is important. For example, for a set of 10,000 elements, e.g. steam generator tubes, it is possible for the ratio of the times-to-failure for the Weibull characteristic, θ□ (close to the mean) and the first failure to be 10^4 for 10,000 tubes if the Weibull shape parameter, β, is unity; whereas, this ratio would be about 10 if the shape factor were 4. Thus, knowing the shape parameter early is important to anticipating the occurrence of failures. Note that Weibull shape parameters of 1 through 4 and somewhat greater are common in nuclear components, depending on the component and the mode of corrosion.

5. There is clear evidence that the shape parameter depends on the physical conditions of SCC. For example, where the critical conditions for SCC are associated with surface processes, such as pitting or surface corrosion, the shape factor tends to be in the range of unity. One the other hand, when the critical conditions relate to diffusion processes, the shape parameter tends to be in the range of 2-10.

6. A clear question was identified for conducting and applying the results of accelerated testing. Whereas the mean value of test results may provide the necessary acceleration as a result of using accelerating variables as stress, temperature, and pH, these accelerations may not relate to the early failures, which are the most important. Results of accelerated testing must be evaluated for the early failures such as at 0.001 or 0.0001 probabilities. It can be shown from practical data that a useful acceleration may apply to comparing mean values of field and laboratory tests, but there may be no acceleration for the low probabilities owing mainly to the usually higher values of the shape parameter for accelerated testing that result from using single heats and more intense testing conditions.

Acknowledgements

I am indebted to my hard working staff for helping with the preparation of this paper; especially Julie L. Daugherty, Marcia Parrish-Siggelkow, and John Ilg. For the work in this paper, I relied on past collaborations with Jeffrey Gorman of Dominion Engineering and Robert Abernethy of Weibull Risk & Uncertainty Analysis. I appreciate also the timely help from Peter Scott of Framatome and Robert Tapping of AECL. Finally, I appreciate the intellectually challenging discussions with my colleagues in the PMDA group.

References

[1] R.W. Staehle, "Bases for Predicting the Earliest Penetrations Due to SCC for Alloy 600 on the Secondary Side of PWR Steam Generators," NUREG/CR-6737, ANL-01/20, RWS-151, U.S. Nuclear Regulatory Commission, September, 2001.

[2] R.W. Staehle, "Bases for Predicting the Earliest Failures Due to Stress Corrosion Cracking." Chemistry and Electrochemistry of Corrosion and Stress Corrosion Cracking: A Symposium Honoring the Contributions of R. W. Staehle, pp. K1-K92, Ed. Russell Jones, TMS (The Minerals, Metals and Materials Society,) 2001.

[3[R.W. Staehle, "Predicting the First Failure," presented at Corrosion 2003, San Diego, NACE, March 16-20, 2003.

[4] J.A. Gorman, R.W. Staehle, K.D. Stavropoulos, "Statistical Analysis of Steam Generator Tube Degradation," EPRI NP-7493, Electric Power Research Institute, September 1991.

[5] M. Bruemmer, E.I. Meletis, R.H. Jones, W.W. Gerberich, E.P. Ford, and R.W. Staehle, Eds., Parkins Symposium on Fundamental Aspects of Stress Corrosion Cracking, TMS (The Minerals, Metals and Materials Society), 1992.

[6] R.W. Staehle, "Approach to Predicting SCC on the Secondary Side of Steam Generators," presented at Fontevraud 5, Contribution of Materials Investigation to the Resolution of Problems Encountered in Pressurized Water Reactors, SFEN, Paris, September 23-27, 2002.

[7] W. Weibull, "A Statistical Distribution Function of Wide Applicability," *Journal of Applied Mechanics 10*, p. 293, 1951.

[8] E.J. Gumbel, "Statistical Theory of Extreme Values and Some Practical Applications," *Applied Mathematics 33*, p.1, National Bureau of Standards, 1954.

[9] E.J. Gumbel, Statistics of Extremes, Columbia University Press, New York, 1958.

[10] W. Nelson, "Weibull Prediction of a Future Number of Failures," *Quality and Reliability Engineering International 16*, p. 23, 2000.

[11] K.T. Chang, "Analysis of the Weibull Distribution Function," *Journal of Applied Mechanics 49*, p. 450, 1982.

[12] R.K. Reeves, D.W. Hoeppner, "A Weibull Analysis of Center Cracked Panel Crack Growth Data of a 0.40/0.50 Carbon Steel," *Engineering Fracture Mechanics 10*, p. 571, 1978.

[13] R.B. Abernethy, The New Weibull Handbook; Fourth Edition, R.B. Abernethy Publisher, North Palm Beach, Florida, 2000.

[14] T. Shibata, "1996 W.R. Whitney Award Lecture: Statistical and Stochastic Approaches to Localized Corrosion," *Corrosion 37*, 11, p. 813, 1996.

[15] WINSMITH (TM) Weibull 3.0U.

[16] R.W. Staehle, J.A. Gorman, "Quantitative Assessment of Submodes of Stress Corrosion Cracking on the Secondary Side of Steam Generator Tubing in Pressurized Water Reactors," *Corrosion*, Part 1 Vol. 59 No. 11 November 2003, Part 2 Vol. 60 No. 1 January 2004, Part 3 Vol. 60 No. 2, NACE, February 2004.

[17] S. Shimada, N. Nagai, "Variation of Initiation Time for Stress Corrosion Cracking in Zircaloy-2 Cladding Tube," *Reliability Engineering 9,* p. 19, 1984.

[18] E.D. Eason, L.M. Shusto, Analysis of Cracking in Small Diameter BWR Piping, EPRI NP 4394, Electric Power Research Institute, 1986.

[19] P.M. Scott, "2000 F.N. Speller Award Lecture: Stress Corrosion Cracking in Pressurized Water Reactors – Interpretation, Modeling, and Remedies," *Corrosion 56*, p. 771, 2000.

[20] Unpublished data provided by L. Bjornkvist of Vattenfall and J. Gorman of Dominion Engineering.

[21] P.M. Scott, et al., "An Analysis of Baffle/Former Bolt Cracking in French PWRs," Environmentally Assisted Cracking: Predictive Methods for Risk Assessment and Evaluation of Materials, Equipment and Structures, ASTM 1401, R.D. Kane, Ed., American Society for Testing and Materials, 2000.

[22] R.W. Staehle, "Lifetime Prediction of Materials in Environments," Uhlig's Corrosion Handbook; 2nd Edition, p. 27, R.W. Revie, ed., John Wiley and Sons, New York, 2000.

[23] F. Cattant, et al., "Analyses of Deposits and Underlying Surfaces on the Secondary Side of Pulled Out Tubes From a French Plant," Contribution of Materials Investigation to the Resolution of Problems Encountered in Pressurized Water Reactors; Proceedings of the International Symposium, p. 469, Fontevraud III, F. de Keroulas, chair., French Nuclear Energy Society, Paris, 1994.

[24] X.C. Jiang, R.W. Staehle, "Effects of Potential and Stress on Stress Corrosion Cracking of Austenitic Stainless Steels in Concentrated Chloride Solutions," *Corrosion Journal 53*, No. 8, pp. 631 – 643, August 1997.

[25] R.W. Staehle, et al., "Application of Statistical Distributions to Characterizing and Predicting Corrosion of Tubing in Steam Generators of Pressurized Water Reactors," Presented at the 3rd International Relations Committee Symposium, Life Prediction of Corrodible Structures, Cambridge, UK, NACE, 1991.

[26] W.L. Clarke, G.M. Gordon, "Investigation of Stress Corrosion Cracking Susceptibility of Fe-Ni-Cr Alloys in Nuclear Reactor Waste Environments," *Corrosion, 29*, p. 1, 1973.

[27] M. Akashi, A. Ohtomo, "Evaluation of the Factor of Improvement for the Intergranular Stress Corrosion Cracking Life of Sensitized Stainless Alloys in High-Temperature, High-Purity Water Environment," *Journal of the Society of Materials Science of Japan 36*, p. 59, 1987.

[28] T. Shibata, T. Takeyama, "Probability Distribution of Failure Times of Stress Corrosion Cracking of 17Cr-11Ni Stainless Steel," Tetsu-To-Hagane Vol. 66, p. 693, 1980.

Appendix C – Panel Members

Dr. Peter L. Andresen

Dr. Andresen received his B.S. in Materials Engineering (Cum Laude) in 1972, his Ph.D. and M.S. in Materials Science in 1978 and 1974 from the same institution Rensselaer Polytechnic Institute.

Dr. Andresen's expertise is in the area of corrosion and environmental effects on mechanical properties and integrity of materials. His research has focused on corrosion and environmental fracture of iron- and nickel-base alloys under conditions of interest to the energy and plastics industries. He also studied corrosion fatigue of Cu-Al alloys and has published and consulted widely on pitting, general corrosion, erosion and polarization behavior in aqueous and organic media. In addition to numerous presentations of his research, Dr. Andresen has given many invited lectures at technical and educational symposia.

Prior to GE, Dr. Andresen worked as an independent consultant specializing in corrosion and metallurgical failure analysis. Dr. Andresen is the author of over 250 publications. He holds twenty-five patents, is a Fellow of the American Society for Metals and the National Association of Corrosion Engineers, on the Board of Directors of NACE, and is a member of the International Cooperative Groups on Irradiation Assisted Stress Corrosion Cracking and on Environmentally Assisted Cracking. He has served in many capacities in professional societies, including as Chairman of the Corrosion/93 Research-in-Progress Symposium; Board of Editors for Corrosion Journal; Chairman of the NACE Research Committee; NACE Awards Committee, Advisory Panel / Quick Response Team for Halden, Norway and MIT test reactor programs; Committee and Symposia Chairman of the NACE Group (T2) and Unit Committees on Corrosion in Nuclear Systems (T2A) and SCC / CF (T3E); Chairman of the Data Analysis and Round Robin Committees for the International Cooperative Group on Irradiation Assisted SCC; Executive Committee of the International Cooperative Group on Environmentally Assisted Cracking; and Chairman of the Eastern NY Chapter of ASM. He has served on several DOE Expert Review Panels for Fusion Energy and Radioactive Waste Disposal, as acting (5 months) technical administrator for the Inorganic Materials Laboratory, on RPI Trustees Committees for Faculty and Staff Compensation and Presidential Search, and on several thesis committees. He has received two Whitney Gallery of Achievers Awards and the Dushman Award from GE, the Speller Award from NACE, and was selected as one of "50 Stars to Watch" by Industry Week in 1996 and one of "2000 Outstanding Scientists of the 20th Century" by Int. Biographical Center of Cambridge, England.

Dr. Peter Ford

Peter Ford received his bachelors and doctoral degrees from Cambridge University, UK and his master's degree from the Rensselaer Polytechnic Institute, USA. These degrees concentrated on metallurgy and corrosion science.

After finishing an apprenticeship with the turbine manufacturer, British Thomson Houston in the UK, he joined the staff of the Olin Mathieson Chemical Corporation in the US, developing and fabricating advanced corrosion-resistant aluminum–magnesium alloys. Following these early experiences he concentrated on mitigating corrosion problems in the power generation business, initially as a group leader at the Central Electricity Research Labs in the UK, and then for 25 years as a manager of the corrosion and coatings program at the General Electric Global Research Center (formally the GE Corporate Research and Development Center). During that latter time much of the efforts of the program were focused on developing prediction methodologies for environmental degradation of BWR materials (stress corrosion cracking, irradiation assisted SCC, corrosion fatigue, etc). Based on this fundamental understanding, the group was instrumental in the formulation, qualification and implementation of various mitigation strategies (noble metal coating and cladding processes, underwater weld repair, etc) as well as defining sound materials and water chemistry specifications.

He has been the recipient of various awards from GE and from technical societies, including the Whitney Award from the NACE International for "contributions to corrosion science and especially life prediction methodologies for light water reactors (LWRs)." He has also been a member and chairman of various technical societies/cooperative organizations including the International Cooperative Group on Environmentally Assisted Cracking that covers the work of 86 organizations in 16 countries in the area of materials degradation in LWRs

Since retiring from General Electric he has been a member of the Advisory Committee on Reactor Safeguards to the USNRC.

Dr. Karen Eleanor Gott

Dr. Gott studied metallurgy and materials science at Imperial College, London.

During the more than 20 years she has worked in Studsvik Dr. Gott studied many aspects of the environmental effects on structural materials in nuclear power plants, both through contract research projects and failure analysis. She has held a number of different types of position whilst at Studsvik including project manager, marketing manager and manager of the reactor chemistry group. She was also on periodic loan to a US subsidiary in Richland, WA, to help them establish laboratory support for their decontamination services.

The main areas of her research activities were

- Creep crack formation in stainless steels (mechanical testing, electron and light optical metallography)
- Fracture mechanics (corrosion fatigue, residual stress measurement, non-destructive testing)
- Reactor chemistry (PWR and BWR chemistry, activity build-up including field measurements, decontamination)
- Reactor materials (surveillance testing, failure analysis, metallography of Inconel 182)

In her current position at the Swedish Nuclear Power Inspectorate she has continued to work in the field of environmental degradation of nuclear power plant structural materials. The work covers both the regulatory and the research aspects. On the regulatory side she is involved in the development of regulations, inspection and safety evaluations that form the basis for decisions based on Swedish law and regulations. One of her responsibilities includes the management of the materials and chemistry research area for the Inspectorate. In addition she has built a database covering operationally induced failures and damage to mechanical components in the Swedish nuclear fleet and is responsible for its maintenance and the associated analysis of failure cases. In 2003 she was on a six-month job rotation to the Materials Engineering Branch of NRR working amongst other things on primary water stress corrosion cracking problems.

She is a member of the international conference committee, which arranges the regular water chemistry conferences in the nuclear field, and has also acted on the international committee for the Fontevraud conference in France. She serves as chairperson of the steering committees of two large international projects concerning irradiation assisted stress corrosion cracking and the establishment of a pipe failure database.

Dr. Robin L. Jones

Dr. Jones received his B.A. (1962) and M.A. in Natural Sciences (1965), and Ph.D. in Metallurgy (1966) from the University of Cambridge, UK.

Dr. Jones is Technical Executive, Materials Science & Technology, at the Electric Power Research Institute (EPRI). He has more than 35 years of experience and achievement in materials-related contract research and R&D management, and is a recognized expert on corrosion-related materials integrity problems in nuclear power plants. Since joining EPRI in 1978, his assignments have included leadership of EPRI's materials R&D programs that address high-impact materials issues, industry-wide programs on BWR pipe cracking, PWR steam generator reliability, and BWR vessel and internals degradation, which have attracted worldwide participation by nuclear utilities. Dr. Jones has been responsible for managing the Nuclear Power Sector's Major Component Reliability, Fuel Reliability, Storage & Disposal, and Low-Level Waste, Chemistry & Radiation Control programs. He has made keynote presentations on materials performance and degradation at many international conferences and symposia, as well as invited lectures on these subjects.

Prior to joining EPRI, Dr. Jones was the Manager of the Metallurgy Program at SRI International, where he developed and directed contract R&D activities on materials and corrosion issues in fields ranging from aerospace to energy. Earlier, he was with Franklin Institute Research Laboratories, where he was principal investigator on several large R&D contracts on aerospace materials.

A member of ASME, TMS and NACE, Dr. Jones has made keynote presentations on materials performance and degradation at many international conferences and symposia and has presented invited lectures on these subjects at major universities such as MIT, Stanford and the University of California.

Dr. Peter Scott

Peter Scott received his B.Sc. in chemistry from the University of Sheffield in England in 1965 and his Ph.D. in physical chemistry from the same university in 1968. He spent two years as a Post Doctoral Fellow in the Department of Applied Chemistry of the National Research Council of Canada before starting his career in the nuclear industry in the Materials Development Division at the Harwell Laboratory of the UKAEA. During 18 years at Harwell, he became a section head and a recognized expert in corrosion of metallic materials, particularly concentrating on the phenomena of corrosion fatigue and stress corrosion cracking in thermal and fast reactor systems. He entered the Framatome Group in 1989 and was named 'Expert Principal' (or Senior Corrosion Consultant) in 1993. In this capacity, he represents the company on several international working groups dealing with problems of stress corrosion cracking of materials in light water reactors. He is also a member of the editorial board of the NACE Corrosion Journal. He received the 2000 F. N. Speller Award from the NACE for outstanding contributions to the practice of corrosion engineering. He is the author or co-author of over 80 scientific publications.

Dr. Scott's work areas include stress corrosion cracking and corrosion fatigue of pressure vessel steels and piping of nuclear power stations and other non-nuclear structures, areas in which he directed research work on safety and reliability during his period with the UKAEA.

Stress corrosion cracking of steam generator components, reactor core internals and other components of both PWRs and BWRs are topics on which he has contributed in establishing, presenting and defending dossiers justifying the continued operation of nuclear power plants as well as directing research work on these topics. He assists the Fuel Division resolve corrosion problems in fuel assemblies.

Dr. Scott's network of contacts include EDF, CEA, ENS des Mines de Paris et St. Etienne, FTI, EPRI, NRC, Westinghouse, General Electric, PNNL, University of Michigan, AECL, AEA Technology, Rolls Royce, British Energy (Nuclear Electric), Laborelec, Tractebel, Vattenfall, SKI, Studsvik, Mitsubishi, Kansai Electric, Hitachi, Toshiba, TEPCO, NHI, JAERI, China Institute of Atom Energy, and the Shanghai Research Institute of Materials.

Dr. Tetsuo Shoji

Dr. Shoji received his Bachelor's (1970), Master's (1972) and Doctoral degrees (1975) from school of Engineering, Tohoku University, Japan.

His current position at Tohoku University is Executive Director and Vice President since April 1, 2005. He also worked as Director of the Center for Mechanical Science Based on Nanotechnology. After receiving his doctoral degree from Tohoku University, he was appointed as a Research Associate in 1975, Associate Professor in 1983, and full Professor in 1989 of Tohoku University. During that time, he also served as a Visiting Scientist in the Department of Metallurgy and Materials Engineering at the University of Newcastle Upon Tyne, UK, from May 1982 to August 1983 and as a visiting professor in the Department of Nuclear Engineering at Massachusetts Institute of Technology, USA, from April to September, 1994.

He led the Center of Excellence Program on the Physics and Chemistry of Fracture and Failure Prevention under Combined Environments as a Program leader from1998 to 2003. He is also serving as program leader of the 21st Century Center of Excellence Program on the Exploration of the Frontiers of Mechanical Science Based on Nanotechnology from October 2003 to March 2008. Since November of 2002, he has been serving as an acting committee member of the Nuclear and Industrial Safety Agency, METI, Ministry of Economy, Trade and Industry regarding the Integrity Assessment of Nuclear Power Plants, Evaluation of Codes and Standards Work Group, and the Inspection Technology Advancement Work Group.

His research area covers mechanistic study of environmentally assisted cracking in LWR environments with a combination of mechanics and mechanisms. Among the honors he has received are the A. B. Campbell Award for Young Authors from the National Association of Corrosion Engineers, USA (1977), Honorary member of the Russian International Academy of Engineering (1995), the W. R. Whitney Award, NACE International (1998), the ASTM Division Award for Annual Best Paper published in JTEV (Journal of Testing and Evaluation), ASTM International (2001), and the First Prime Award during the competition on fundamental investigations from the Institute of Theoretical and Applied Mechanics SB, Russian Academy of Science (2003).

Dr. Roger Washburne Staehle

Dr. Staehle received his bachelor's and master's degrees from Ohio State University in 1957, attended Westinghouse Reactor Engineering School in 1959, and received his Ph.D. from Ohio State University in 1965.

Currently a resident of North Oaks, Minnesota, Dr. Staehle has served as a Naval Officer and Nuclear Engineer with the U.S. Navy and the U.S. Atomic Energy Commission (with Vice Admiral H.G. Rickover) Naval Nuclear Reactor Development, 1957-1961. From 1965 to 1970 he was an Associate Professor at Ohio State University, was Director and Founder of the Fontana Corrosion Center from 1975 to 1979, Dean of the University of Minnesota Institute of Technology from 1979-1983, and a Professor of that University's Chemical Engineering and Materials Science Department from 1983 to 1988. From 1984 to 1986, he was President and Chairman of Automated Transportation Systems, Inc. (now Taxi-2000).

Dr. Staehle currently serves as an Adjunct Professor at the University of Minnesota (since 1988) and as an Industrial Consultant (since1986). Among the honors he has received are as a Le Hsun Lecturer, Institute of Metals Research, Shenyang, China, October 2004, as a Plenary Lecturer, Corrosion 2004 in New Orleans, the Electrochemical Society (ECS) Fellow Award, 2000, the TMS Meeting, "Chemistry and Electrochemistry of Corrosion and Stress Corrosion," held in his honor, New Orleans, February 2001, the NACE Fellow Award (first group of fellows), 1993, the NACE T.J. Hull Award, Corrosion'92, Nashville, TN, the Distinguished Alumnus, The Ohio State University; College of Engineering, April, 1989, the Willis Rodney Whitney Award from NACE for Outstanding Contributions to Corrosion Research, 1980, the Research in Progress meeting of NACE special award (1979) for organizing the first conference. He was elected to the National Academy of Engineering in 1978, was named International Nickel Professor of Corrosion Science and Engineering, 1971-1976, was named ASM Fellow (first group of fellows), 1975, received three awards for achievement (1966, 1969 and 1970) from the College of Engineering, received the Ohio ASEE Award for Innovative Teaching, 1975, and has given Plenary Lectures at International Congresses (quadrennial) on Metallic Corrosion in Amsterdam (1968), in Sidney (1972) and in Tokyo (1976).

He has published numerous edited volumes, major review articles and technical reports, served as Editor of *Corrosion Journal* 1971-1979, and as Editor of *Advances in Corrosion Science and Technology.* He has served on the Board of Directors of such organizations as Data Card Corporation, Donaldson Company, Inc, Teltech, Inc., Great Northern Iron Ore Properties, and Taxi 2000.

Dr. Robert L. Tapping

Dr. Tapping received a B.Sc. (Hons) in Chemistry, and a PhD in Physical Chemistry, from the University of British Columbia, in Vancouver, Canada, in 1968 and 1972, respectively. Dr. Tapping's specialty was in the areas of magnetic resonance spectroscopy and in electron spectroscopy of surfaces and surface reactions, and he pursued this line of research whilst doing two post-doctoral fellowships.

In 1976 Dr. Tapping joined Alcan Research in Kingston, Ontario, Canada, where he specialized in applications of electron spectroscopy to aluminum corrosion, and provided inputs into corrosion consulting and new alloy developments for aluminum alloys. In 1979 Dr. Tapping joined Atomic Energy of Canada's Chalk River Laboratories as a corrosion specialist, focusing on aluminum alloy corrosion in research reactors, and also on heat exchanger materials corrosion, including condenser degradation issues. Over the next 10 years Dr. Tapping took over the R&D programs related to steam generator materials degradation, and later, on zirconium alloy corrosion in-reactor. He was also involved in applications of plastics and elastomers in reactor systems, and in maintaining awareness of new materials applications, and ensuring that AECL's corrosion-related R&D programs were complementary to that elsewhere. Part of this focus was to ensure that electrochemical and surface science capabilities and applications to corrosion R&D at AECL were "state-of-the-art." More recently Dr. Tapping has focused on carbon steel corrosion, particularly flow-accelerated corrosion and cracking of carbon steels under CANDU reactor conditions. Currently Dr. Tapping is Acting Director of the Components and Systems Division within AECL, responsible for a wide range of chemistry, materials and engineering applications of relevance to CANDU reactor technology. Dr. Tapping acts as a corrosion consultant for AECL on a wide variety of materials and chemistry issues.

Dr. Tapping has published more than 250 papers and reports on corrosion and surface science, and has made many presentations to external groups. He represents AECL on many national and international committees, and has won a number of awards for his work, most notably election as a Fellow of the Chemical Institute of Canada. He is also a member of ASTM and NACE. Dr. Tapping currently focuses on plant life management and health monitoring technologies, attempting to integrate AECL's many years of chemistry and materials R&D knowledge into practical guidelines and technologies for plant applications.

NRC FORM 335
(9-2004)
NRCMD 3.7

U.S. NUCLEAR REGULATORY COMMISSION

BIBLIOGRAPHIC DATA SHEET

(See instructions on the reverse)

1. REPORT NUMBER
(Assigned by NRC, Add Vol., Supp., Rev., and Addendum Numbers, if any.)

NUREG/CR-6923

2. TITLE AND SUBTITLE

Expert Panel Report on Proactive Materials Degradation Assessment

3. DATE REPORT PUBLISHED

MONTH	YEAR
February	2007

4. FIN OR GRANT NUMBER

Y6868

5. AUTHOR(S)

Expert Panel: P.L. Andresen, F. P. Ford, K. Gott, R. L. Jones, P. M. Scott, T. Shoji, R. W. Staehle, R. L. Tapping
BNL: M. Subudhi, D. J. Diamond
NRC: J. Muscara

6. TYPE OF REPORT

7. PERIOD COVERED *(Inclusive Dates)*

8. PERFORMING ORGANIZATION - NAME AND ADDRESS *(If NRC, provide Division, Office or Region, U.S. Nuclear Regulatory Commission, and mailing address; if contractor, provide name and mailing address.)*

Brookhaven National Laboratory, Upton, NY 11973-5000

9. SPONSORING ORGANIZATION - NAME AND ADDRESS *(If NRC, type "Same as above"; if contractor, provide NRC Division, Office or Region, U.S. Nuclear Regulatory Commission, and mailing address.)*

Division of Fuel, Engineering and Radiological Research
Office of Nuclear Regulatory Research
U.S. Nuclear Regulatory Commission
Washington, DC 20555-0001

10. SUPPLEMENTARY NOTES

11. ABSTRACT *(200 words or less)*

This study is part of the NRC's Proactive Materials Degradation Assessment (PMDA) program. The main objective was to identify materials and components where future degradation may occur in specific light water reactor (LWR) systems. The approach was to use a structured elicitation drawing on the knowledge of a panel of eight experts and the use of a Phenomena Identification and Ranking Table (PIRT) process. The international panel was given information on the materials, fabrication process, and operational environment for hundreds of different parts of systems in a Westinghouse four-loop design pressurized water reactor and a BWR-5 design boiling water reactor. They considered extensions to other designs as well. The panel developed metrics and used them to evaluate the susceptibility of given parts to different degradation mechanisms as well as the level of understanding for the varying degradation mechanisms for the given part. Inherent in arriving at these judgments of future behavior was an understanding of the prediction methodologies for the various degradation phenomena, calibrated by the component failures that have occurred in the past in the global LWR fleet. Also taken into account were the successes and limitations of mitigation/control approaches that have been used to date.
This report includes not only the panel's scoring and their rationale for it, and the conclusions derived from the process, but also considerable documentation of the relevant issues, the latter being found in the appendices.

12. KEY WORDS/DESCRIPTORS *(List words or phrases that will assist researchers in locating the report.)*

aging, degradation, damage, corrosion, failure, reactor safety, mechanisms, proactive, PMDA, PMDM, PIRT, fracture, materials, cracking, MIC, alloy 600, PWSCC, lead, PbSCC, IGSCC

13. AVAILABILITY STATEMENT

unlimited

14. SECURITY CLASSIFICATION

(This Page)
unclassified

(This Report)
unclassified

15. NUMBER OF PAGES

16. PRICE

Federal Recycling Program